

International Conference

MARIDV

Marine & River Dune Dynamics

4th-6th April 2016 • North Wales, UK

Book of Abstracts

Editors:

K. Van Landeghem, T. Garlan and J. Baas

French Hydrographic &
Oceanographic Office



PRIFYSGOL
BANGOR
UNIVERSITY

maridv.bangor.ac.uk

MARID V

Marine and River Dune Dynamics 2016

Caernarfon, North Wales, United Kingdom
4th - 6th April 2016

Organising committee

Chair: Katrien Van Landeghem (Bangor University, United Kingdom)
Co-chair : Thierry Garlan (French Hydrographic Office, France)
Co-chair : Jaco H. Baas (Bangor University, United Kingdom)
Suzie Jackson (Bangor University, United Kingdom)
Emmer Litt (National Resources Wales, United Kingdom)
Guy Springett (Bangor University, United Kingdom)
Martin Austin (Bangor University, United Kingdom)
Dei Huws (Bangor University, United Kingdom)
Connor McCarron (Bangor University, United Kingdom)
Edward Lockhart (Bangor University, United Kingdom)
Megan Baker (Bangor University, United Kingdom)

Scientific committee

Thierry Garlan (French Hydrographic Office, France)
Suzanne Hulscher (University of Twente, The Netherlands)
Dan Parsons (University of Hull, United Kingdom)
Vera Van Lancker (Royal Belgian Institute of Natural Sciences, Belgium)
Katrien Van Landeghem (Bangor University, United Kingdom)
Sophie Le Bot (University of Rouen, France)
Alain Trentesaux (University of Lille, France)
Jim Best (University of Illinois, United States of America)
Marc Roche (Federal Public Service Economy, Belgium)

This publication should be cited as follows:

*Van Landeghem, K.J.J., Garlan T. and Baas, J.H. (Eds), 2016. **MARID 2016. Fifth International Conference on Marine and River Dune Dynamics**, Caernarfon, United Kingdom, 4 – 6 April 2016. Bangor University and SHOM. 216 pp. ISBN 978-2-11-128417-3*

MARIDV is organised by...

Bangor University

School of Ocean Sciences
Bangor, Gwynedd, LL57 2DG, United Kingdom
www.bangor.ac.uk/oceansciences



SHOM

French Naval Hydrographic and Oceanographic Office

Oceanographic Center/Sedimentology
13, rue du Chatellier - CS 92803, 29228 Brest Cedex 2, France
www.shom.fr



... in collaboration with

National Resources Wales

Maes y Ffynnon, Penrhosgarnedd,
Bangor, Gwynedd, LL57 2DW, United Kingdom
<https://naturalresources.wales/splash?orig=>



SEACAMS a development to integrate research and business opportunities in the marine sector in Wales.
<http://www.seacams.ac.uk>



The MARIDV team is grateful to its sponsor:

Reynolds International Ltd.

Suite 2 Broncoed House, Broncoed Business Park,
Wrexham Road, Mold, CH7 1HP United Kingdom
<http://www.reynolds-international.co.uk>



Preface & Welcome

Welcome to North Wales, welcome to the fifth conference on Marine and River Dune Dynamics (MARIDV)!

Under the aegis of the North Sea Hydrographic Commission, a workshop on marine sand wave dynamics was organised by the French Naval Hydrographic and Oceanographic Office (SHOM) and the University of Lille 1 (France) back in 2000. This workshop was then succeeded by conferences covering marine and river dune dynamics in 2004 (University of Twente, Enschede, The Netherlands), in 2008 (University of Leeds, United Kingdom) and in 2013 (Royal Belgian Institute of Natural Sciences, Belgium). Now known by the acronym MARID, these conferences provide state-of-the-art overviews in fundamental and applied knowledge of marine and river dunes.

Dunes form as a result of turbulent shear generated by the interaction of a fluid flow with underlying mobile sediment. This interaction is complex, with dunes having varying dimensions, geometries and degrees of mobility. The processes governing dune dynamics have still not been unravelled adequately and the MARIDV delegates will outline progress across a wide number of disciplines, including hydrography, fluid dynamics, oceanography, earth sciences, sedimentology, laboratory experimentation, numerical modelling, and field quantification. The science programme will outline our current understanding of marine and river dune dynamics, and identify areas for future investigation and cross-disciplinary collaboration.

Marine and River Dune Dynamics V (MARIDV) is held in Caernarfon in beautiful North Wales, organised by the School of Ocean Sciences at Bangor University and the French Naval Hydrographic and Oceanographic Office (SHOM). The science conference takes place in Galeri Caernarfon on the 4th and 5th of April 2016. On the 6th April we host a field trip on the island of Anglesey.

We hope that MARIDV will lead to fruitful and productive discussions, which in turn should help guide future collaborations to further investigate marine and river dunes. The smaller, focussed format of the MARID conferences has proven to be ideally suited for such networking activities. Long may it continue!

Katrien Van Landeghem, Thierry Garlan & Jaco H. Baas.

Table of Contents

Keynotes

M. Colombini Università di Genova, DICCA, Genova, ITALY	Stability of river bed forms	41 - 48
J.M. Reynolds North Wales Tidal Energy and Coastal Protection Co. Ltd & Reynolds International Ltd UNITED KINGDOM	Managing the issue of seabed sediment in offshore renewable energy projects	155 - 158
C. Winter Center for Marine Environmental Sciences, MARUM, Bremen, GERMANY	Properties of active tidal bedforms	205 - 208

Oral Presentations

A.W. Baar, M.G. Kleinhans, J.C. de Smit, W.S.J. Uijttewaai	Influence of bedforms on the transverse bed slope effect	5 - 8
N. Bristow, G. Blois, W. Anderson, Z. Tang, J. M. Barros, J. L. Best, K. T. Christensen	Measurements of flow dynamics associated with interacting, subaqueous barchans: Exploring bedform asymmetry and three-dimensionality in a novel flume environment	21 - 24
G.H.P. Campmans, P.C. Roos, S.J.M.H. Hulscher	Modelling the influence of storm-related processes on sand wave dynamics: a linear stability approach	25 - 28
H.Q. Cheng, D.M. Wang, T.Y. Wei, W. Chen, Z. Y. Yang, J. F. Li	Formation of estuarine subaqueous dunes in coarse silt and very fine sand in resuspension-dominated tidal flow conditions	31 - 32
K. Choi, J. Jo	Morphodynamics, hydrodynamics and stratigraphic architecture of intertidal compound dunes on the open-coast macrotidal flat in the south of Ganghwa Island in Gyeonggi Bay, Korea	33 - 36

J. Cisneros, J. Best	Low-angle dunes in big rivers: morphology, occurrence and speculations on their origin	37 - 40
J.M. Damen, T.A.G.P. van Dijk, S.J.M.H. Hulscher	Spatial variations in sand waves superimposed on sand banks: an automated analysis method	49 - 52
N. Debese, J. J. Jacq, K. Degrendele, M. Roche	Ripple filtering and ridge enhancement applied to morpho-dynamical tracking of sand dunes	57 - 60
R. Durán, J. Guillén, J. Rivera, A. Muñoz	Holocene evolution of sand ridges in a tideless continental shelf (Western Mediterranean)	61 - 64
D. Frank, A. Penko, J. Calantoni	High-speed phase-separated PIV over laboratory sand ripples	65 - 68
E. Gallagher	A Self-Organization Model for Multi-Scale Bedforms in Tidal Inlets and Bedform-Induced Roughness	69 - 72
T. Garlan, E. Brenon, E. Marchès, O. Blanpain	From regional variability of the morphology of dunes to a new method of their classification	73 - 76
Q. Guerrero, J. Guillén, R. Durán, R. Urgelés	Contemporary subaqueous dune-field development off an abandoned river mouth in the Ebro Delta (NW Mediterranean)	77 - 80
I. Hennings, D. Herbers	Suspended sediment dynamics above submerged compound sand waves observed during a tidal cycle	81 - 84
C.M. Herbert, J. Alexander	Unit bars formed by dune stacking in a recirculating flume	85 - 88
F.J. Hernández-Molina, G. Ercilla, D. Casas, C. Roque, D.A.V. Stow, MOWER Cruise team	Larger morphological sea-floor features and bedforms associated to the Mediterranean Outflow Water in the Gulf of Cadiz	89 - 92
Z. Fu, W. Huang, F. Chen, Z. Yue, J. Yan, J. Geng, F. Yang	Application of artificial dunes to shoal protection in waterway regulation practice	99 - 102

Marine and River Dune Dynamics – MARID V – 4 & 5 April 2016 – North Wales, UK

C.E. Keevil, D.R. Parsons, P.J. Ashworth, J.L. Best, A.P. Nicholas, E.W. Prokocki, S.D. Sandbach, G.H. Sambrook Smith, C.J. Simpson	Dune migration around a bar within a tidal system	103 - 106
M. Kubacka, S. Rudowski, R. Wróblewski, K. Szeffler, Ł. Gajewski	Giant Subaqueous Dunes on a Tideless Sea Bottom, Rozewie Bank, Southern Baltic	111 - 114
A. Lefebvre, A. J. Paarlberg, C. Winter	Influence of complex bedform morphology on flow and shear stress	115 - 118
I.D. Lichtman, P.D. Thorne, J.H. Baas, L.O. Amoudry, COHBED team	Bedform migration in an intertidal environment influenced by cohesion	119 - 122
E. Litt	Newborough Sand Dune Rejuvenation Project	123 - 126
X. Ma, J. Yan	Geometry and internal structures of dunes in the bedload convergence regions in Beibu Gulf, northwest South China Sea	127 - 132
C. McCarron, N. Howard, K. Van Landeghem, J. Baas, L.O. Amoudry	Sediment transport and bedform morphodynamics in sand-gravel mixtures	137 - 140
E.W. Prokocki, J.L. Best, P.J. Ashworth, D.R. Parsons, G.H. Sambrook, A. Nicholas, S. Sandbach, C.J. Simpson, C. Keevil, M.M. Perillo, S. Constantine, M. Marti	Bedform morphology across the fluvio-tidal-marine hydraulic transitions: Lower Columbia River, USA	145 - 148
A.J.H. Reesink, D.R. Parsons, P.J. Ashworth, J.L. Best, S.E. Darby, R.J. Hardy	Visualizing bed deformation and sediment dispersal across dune fields	149 - 154
N. Terseleer, K. Degrendele, M. Roche, D. Van den Eynde, V. Van Lancker	Dynamics of very-large dunes in sandbank areas subjected to marine aggregate extraction, Belgian continental shelf	173 - 176
P. D. Thorne, A.G. Davies	Measurements and analysis of suspended sediment particle size sorting above bedforms under waves	177 - 180
R. Toodesh, S. Verhagen	First steps towards developing a risk-based hydrographic surveying policy	181 - 184

Marine and River Dune Dynamics – MARID V – 4 & 5 April 2016 – North Wales, UK

V. Van Lancker, F. Francken, L. Kint, G. Montereale-Gavazzi, N. Terseleer, D. Van den Eynde	Large dunes hosting hotspots of biodiversity: Testing proxies of occurrence and habitat change	189 - 192
K.J.J. Van Landeghem, H. Niemann, P.F. Croker, D.G. Huws, L. Steinle, S.S. O'Reilly	Methane-rich glacial clays on top of a large sediment wave?	193 - 196
J. J. Warmink	Adapting the Coleman et al. (2005) time-lag approach for application under unsteady discharge	197 - 200
T. Wever, S. Papili	New strategy for predictions bedform migration	201 - 204
L. Ye, D.R. Parsons, A.J. Manning, COHBED Project Team	Bedform development and morphodynamics in mixed cohesive sediment substrates: the importance of winnowing and flocculation	213 - 216

Poster Presentations

A. Abdulkade, P. Carling, Q. Zong, J. Leyland, C. Thompson	Temporally dynamic, spatially static, cobble bedforms in reversing subtidal currents	1 - 4
J. Baas, J. Best, J. Peakall	Predicting bedforms and primary current stratification in cohesive mixtures of mud and sand	9 - 12
Z. Babiński, M. Habel	Value of bedload movement in alluvial rivers using analysis of sand bar migration	13 - 16
O. Blanpain, X. Demoulin, T. Garlan, P. Guyomard	Measurement and modelling of bedload self-generated noise on a sandy dune	17 - 20
P. Carling, C. Bristow, A. Litvinov	Ground Penetrating radar stratigraphy and dynamics of megaflood gravel dunes	29 - 30
J.H. Damveld, B.W. Borsje, P. C. Roos, S.J.H.M. Hulscher	Smart and sustainable design for offshore operations in a sandy seabed – the SANDBOX programme	53 - 56

Marine and River Dune Dynamics – MARID V – 4 & 5 April 2016 – North Wales, UK

H. Hu, D.R. Parsons, A. Ockelford, R.J. Hardy, P.J. Ashworth, J. Best	The response of bedforms and bed elevation to sudden hydrodynamics changes	93 - 98
K. Krämer, C. Winter	Field measurements of small scale bedform dynamics in tidal environments in the German Bight	107 - 110
A. Maspataud, T. Schmitt, L. Biscara, R. Créach	High resolution coastal DEM of the Dover Strait: managing dynamic bedforms	133 - 136
J. Ogor, B. Zerr	Towards the automation of sand dune detection in the bathymetry	141 - 144
O. Schloemer, J. Herget	Physical modeling of fluvial obstacle marks at a sediment layer of limited thickness	159 - 162
T. Schmitt, N.C. Mitchell	Multibeam survey of a tidal banner bank: morphology of dunes in eroding partially compacted sands?	163 - 166
A. Slooman, M.J.B. Cartigny, P.L. de Boer, A. Moscariello	Depositional character of submarine dunes on a Pleistocene distally steepened carbonate ramp (Favignana Island, Italy)	167 - 172
I. Turki, S. Le Bot, N. Kakeh, C. Michel, R. Lafite	Changes in migration of intertidal dunes: from observation to modelling. Case of Somme Bay (NW France)	185 - 188
X. Wu, J.H. Baas, D.R. Parsons, D. Mouazé, S. Mclelland, L. Amoudry, J. Eggenhuisen, M. Cartigny, G. Ruessink	Wave-induced ripples development in mixed clay-sand substrates	209 - 212

Temporally dynamic, spatially static, cobble bedforms in reversing subtidal currents

A. Abdulkade *Geography & Environment, University of Southampton, UK – aa12g12@soton.ac.uk*

P. Carling *Geography & Environment, University of Southampton, UK – P.A.Carling@soton.ac.uk*

Q. Zong *College of Water Conservancy & Architectural Engineering, Shihezi University, Shihezi, Xinjiang, China - quanli1871@gmail.com*

J. Leyland *Geography & Environment, University of Southampton, UK – J.Leyland@soton.ac.uk*

C. Thompson *Ocean and Earth Science, National Oceanography Centre Southampton, UK - celt1@noc.soton.ac.uk*

ABSTRACT: Flow-transverse cobble bedforms are exposed at extreme low-water Spring tides on an inter-tidal bedrock shelf in the macro-tidal Severn Estuary, UK. Near-bed flow velocities during Spring tides can exceed 1.5ms^{-1} , with water depths varying from zero to in excess of 10m. The bedform geometry tends to be weakly asymmetric; orientated down-estuary with the ebb current. Bedload transport and hydrodynamic data have been measured during both flood and ebb over the crests. The bulk hydraulic data are supplemented by particle tracer studies and laser-scanning of bed configurations between tides. The results of this study explain the interactions between flow characteristics, bedform mechanics, and sedimentological processes of coarse estuarine sediments.

1. INTRODUCTION

Dunes are one of the bedforms commonly found in many rivers as well as tidal and marine environments (Allen, 1984). The existence of dunes effects flow resistance primarily through hydraulic form roughness (Carling et al., 2006; Wilbers, 2004). The size of dunes is considered with respect of the height and length and a wide range of sizes has been reported (Wilbers, 2004). The form resistance produced by dunes initiates turbulence in downstream which in turn is related to dune development, especially size and shape. Apart from effects on flow resistance, dunes are responsible for channel depth limitations. All of these effects are significant in several aspects, such as the design of engineering structures, dredging strategies and storm tide prediction. Moreover, the changes in bedform morphology and the internal structures are useful in the process of interpreting ancient sedimentary assemblages which is believed to be of tidal origin (Carling et al., 2006).

Several studies have described and observed physical characteristics and processes of dunes,

both in fluvial and marine environments (e.g. Allen et al., 1994; Kostaschuk and Best, 2005; Choi and Jo, 2015). Only a few researchers have studied and explained the processes of fine-gravel dune formation, such as Dyer (1971), Dinehart (1992a, 1992b), Carling (1996), Carling et al. (2006), Williams et al. (2006). However, coarse-gravel dunes, as well as cobble dunes, are not well researched. There are no studies focused on intertidal dunes developed in coarse gravels. Therefore, this study will address the hydrodynamics, dunes dynamics, and sedimentary structure of coarse gravel (cobble) dunes.

The main goal of this research is to understand the behaviour of subaqueous dunes developed in coarse gravel which are found in the intertidal zone of River Severn, United Kingdom (Figure 1). The specific objectives of the study are: (a) to observe cobble dune movements by comparing the data of dune positions and shape measured in the field site, (b) to collect quantitative flow data and investigate flow hydrodynamics which will provide bulk flow parameters, (c) to examine the

interaction between flow hydrodynamics, sediment transport and morphology of cobble dunes to gain an understanding of flow interacts with the bedform, and (d) to study both external and internal structure of dunes developed in coarse sediments.

2. STUDY SITE

Hill Flats, located at approximately 51° 40.45'N: 2° 33.24'W (Carling et al. 2006), is in an intertidal zone in the Severn Estuary, landward of the Bristol Channel (Allen & Fulford 1996; Uncles 2010). The site is on the left bank of the estuary in Southwest Britain and consists of a rock platform 3 km long and 650 m wide approximately and lies in a north-east to south-west direction. The surface of this location is uneven with varied elevation, from c. 0 Ordnance Datum to a few meters above. The highest elevation is towards the landward where there is an artificial sea bank along the shoreline of the Severn. The elevation declines seaward, which elevation is varied by the sea bank, salt marsh, small near-vertical marsh cliffs, mudflats and finally the bedrock platform. The lowest area of Hill Flats extends toward the river in the north-west direction (Allen & Fulford 1996; Carling et al. 2006).

3. METHODOLOGY

In order to understand the processes of dune development, the key factors having effects on dune dynamics were investigated. Data used in this study are derived from fieldwork during the lowest spring tides from February 2012 to September 2015. A repeated footwork survey with dGPS and Total Station provides the locations of the dune crestlines in planform and the distance between each dune through time. A series of dune survey data were overlaid and used to compute migration rates and planform changes through time. Vertical cross-sectional profiles detail dune form in section. For flow conditions, up to three Valeport electromagnetic current meters, model 808, were deployed in the vertical to collect flow data across the dune field. The data consisted of local water depth, velocity profile, flow direction, shear stress, bed roughness, and wind-wave climate. Bedload and suspended load transport rates and grain

size variations were also determined using field data to provide detail of the sediment transport environment. Impact sensors recorded bedload intensity and duration. Moreover, coarse-gravel particle tracer studies and terrestrial laser-scanning (Leica P20) of bed configurations between tides were also completed to supplement the sediment transport and morphological data.

4. PRELIMINARY RESULTS

The dunes migrate slightly up or down estuary with each flood or ebb tide respectively during Spring tides. During Neap tides the dunes are mainly immobile. When exposed, the bedform geometry tends to be locally symmetric or more generally asymmetric; orientated down estuary with the ebb current. During Spring tides, impact plate and trap data record vigorous bedload transport of gravel (including large cobbles) during both flood and ebb over the crests and yet, despite this temporal dynamism, the bedforms remain spatially static over long time-periods or show weak down-estuary migration. Stasis implies that the tidal bedload transport vectors are essentially in balance.

Near-bed flow velocities during Spring tides can exceed 1.5ms^{-1} , with water depths varying from zero to in excess of 10m. Near-bed shear stress and bed roughness values vary systematically with the Spring-tide current speeds and the predicted grain-size of the bed load using the Shields criterion is in accord with observed coarser grain-sizes in transport. Coarse gravel is transported in apparently equal quantities on both flood and ebb tides. The particle tracer studies showed that tracers placed on the bedrock troughs between dunes rapidly congregated in the bedforms, whereas tracers placed on the bedform crests tended to remain there indefinitely. Laser scanning at low water showed localized erosion on the up-estuary sides and deposition in the down-estuary sides. The high-energy environment, with effectively *in situ* sorting results in two forms of armouring. (1) Pronounced steep imbrication of platy-cobbles occurs on the steep up-estuary sides of dunes and probably is disrupted during flood tides leading to rapid reworking during flood tides of the toe deposits facing up-estuary. The steep

down-estuary sides usually lack distinct imbrication and gravels appear readily entrainable. (2) In contrast, some crest and leeside locations have been stable for prolonged periods such that closely-fitted fabrics result; these portions of the bedforms are static and effectively are ‘armour-plated’. Ebb-tide deposits of finer, ephemeral sandy-units also occur over gravel on the down estuary side of the bedforms. Sandy-units (although not observed at low tide) presumably also are deposited on the up estuary side during flooding tides but these deposits are destroyed by ebb flows.

5. CONCLUSIONS

During neap tides the bedforms are not exposed, and sediment is calculated to be of limited mobility. Geometry measurement of dunes shows that the dunes tend to be asymmetric and ebb orientated. Bedload transport of gravels and coarser grains occurs over the dunes during both flood and ebb tides. However, the dunes rarely show significant changes over several tidal cycles. Although there is temporal dynamism existing in the process, the dunes remain spatially static over long periods or have weak down-estuary migration implying a near balance in bedload transport in flood and ebb tides. The hydrodynamic data, delimited by estimates of the threshold of motion, and integrated over either flood or ebb tides, explain the apparent stability of the bedforms. The high-energy environment results in two forms of armouring. The two forms of armouring in this high-energy environment reflect the presence of a static core to dunes below the crests and more dynamic lee-sides consisting of different components of sediment. The relationship of sediment transport processes and the stratification of the bedforms (as yet undefined) is to be considered further.

6. ACKNOWLEDGMENT

The author is grateful to The Royal Thai Government for financial support. The National Oceanography Centre Southampton is thanked for the loan of the Valeport current meters.

7. REFERENCES

- Allen, J. R. L. 1984. Sedimentary structures: their character and physical basis. Amsterdam: Elsevier Scientific Publishing Co.
- Allen, J. R. L., Friend, P. F., Lloyd, a., & Wells, H. 1994. Morphodynamics of Intertidal Dunes: A Year-Long Study at Lifeboat Station Bank, Wells-Next-the-Sea, Eastern England. Philosophical Transactions of the Royal Society A: Mathematical, Physical and Engineering Sciences, 347, 291–344.
- Carling, P. A. 1996. A preliminary palaeohydraulic model applied to late Quaternary gravel dunes: Altai Mountains, Siberia, pp 165-179 In J. Branson, A. G. Brown, & K. J. Gregory (Eds.), Global Continental Changes: The Context of Palaeohydrology.
- Carling, P. A., Radecki-Pawlik, A., Williams, J. J., Rumble, B., Meshkova, L., Bell, P., & Breakspear, R. 2006. The morphodynamics and internal structure of intertidal fine-gravel dunes: Hills Flats, Severn Estuary, UK. Sedimentary Geology, 183, 159–179.
- Choi, K., & Jo, J. 2015. Morphodynamics and stratigraphic architecture of compound dunes on the open-coast macrotidal flat in the northern Gyeonggi Bay, west coast of Korea. Marine Geology, 366, 34–48.
- Dinehart, R. L. 1992a. Evolution of coarse gravel bedforms: Field measurements at flood stage. Water Resources Research, 28, 2667–2689.
- Dinehart, R. L. 1992b. Gravel-bed deposition and erosion by bedform migration observed ultrasonically during storm flow, North Fork Toutle River, Washington. Journal of Hydrology, 136, 51–71.
- Dyer, K. R. 1971. The distribution and movement of sediment in the Solent, southern England. Marine Geology, 11, 175–187.
- Kostaschuk, R., & Best, J. 2005. Response of sand dunes to variations in tidal flow: Fraser Estuary, Canada. Journal of Geophysical Research: Earth Surface, 110, 1–11.
- Langhorne, D. N., Heathershaw, A. D., & Read, A. A. 1986. Gravel Bedforms in the West Solent , Southern England, 225–230.
- Wilbers, A., 2004. The development and hydraulic roughness of subaqueous dunes: Volume 323 of Netherlands geographical studies, Royal Dutch Geographical Society, Utrecht University.

Williams, J. J., Carling, P. a., & Bell, P. S. 2006.
Dynamics of intertidal gravel dunes. *Journal of Geophysical Research: Oceans*, 111(C6), p.C06035.

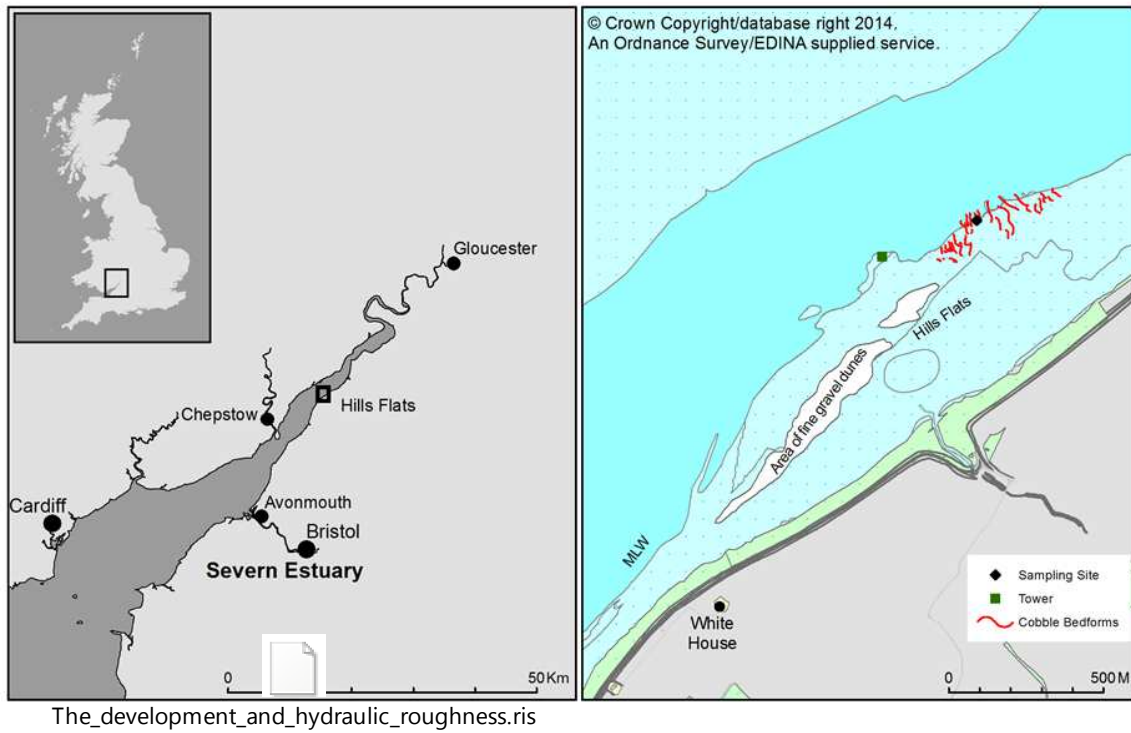


Figure 1. Location of study site, Hill Flats, Severn Estuary, UK.

Influence of bedforms on the transverse bed slope effect

A.W. Baar *Utrecht University, Utrecht, The Netherlands – a.w.baar@uu.nl*

M.G. Kleinhans *Utrecht University, Utrecht, The Netherlands – m.g.kleinhans@uu.nl*

J.C. de Smit *Utrecht University, Utrecht, The Netherlands – j.c.desmit@students.uu.nl*

W.S.J. Uijttewaal *Delft University of Technology, The Netherlands – w.s.j.ujttewaal@tudelft.nl*

ABSTRACT: the deflection of sediment transport on a transverse slope due to gravity determines the large scale morphology by influencing bar dimensions and bifurcation dynamics. However, existing transverse bed slope predictors in morphodynamic models are based on a small range of flow conditions and sediment sizes, and do not account for the presence of bedforms. The objective of the current research is to quantify the transverse slope effect for a large range of flow conditions and sediment sizes, using an annular flume. Preliminary results show that the transverse slope is related to helical flow intensity and sediment size. Also, different bed form types developed during the experiments and appear to have a large influence on flow patterns. In order to quantify the effects of bed forms on the transverse slope, a Large Eddy Simulation model of the annular flume is needed.

1. INTRODUCTION

A crucial part of morphodynamic models is the transverse bed slope effect, which determines the deflection of sediment transport on a transverse sloping bed due to gravity (Fig. 1). Overestimating this effect leads to flattening of the morphology, while underestimating leads to unrealistic steep bars and banks (Fig. 2). Thus an incorrect estimation of the transverse bed slope effect could also have major consequences for the predicted large-scale morphology, as it influences the development of river bifurcations, meander wave length and the degree of braiding in rivers and estuaries.

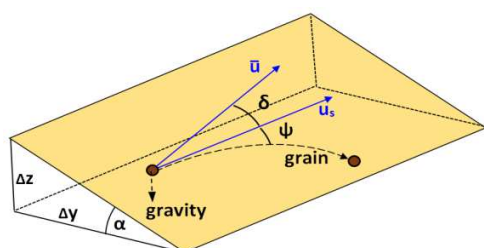


Figure 1. Transverse bed slope effect (after Sekine & Parker, 1992)

In current models, the prediction of the magnitude of sediment transport is based on a situation of a flat bed with a single grain size, and

only the direction is afterwards corrected for transverse gradients (e.g. Ikeda, 1982; Talmon et al., 1995). However, in reality sediment transport is also affected by bedforms, grain size distribution and suspension rate. Therefore, in current modelling practice the angle of sediment deflection needs to be calibrated on measured morphology afterwards.

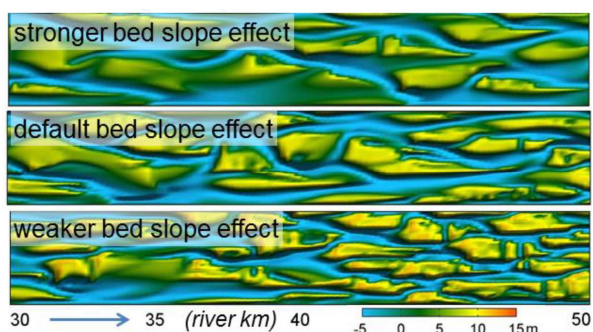


Figure 2. The effect of stronger and weaker transverse bed slope effect on channel morphology (Schuurman et al., 2013)

2. PREVIOUS RESEARCH

Current transverse bed slope predictors are based on theoretical model studies (e.g. Odgaard, 1981; Sekine & Parker, 1992) and laboratory experiments. Experimental studies focused on experiments with bended flumes (e.g. Zimmerman

& Kennedy, 1978; Struikma et al., 1985; Ikeda & Nishimura, 1986), or straight flumes initiated with a transversely sloped bed that relaxed to a horizontal bed, to reduce secondary currents (e.g. Ikeda, 1982; Talmon et al., 1995; Talmon & Wieseman, 2006). In bended flumes the transverse bed slope is also affected by helical flow, whilst in the experiments with a straight flume it is impossible to measure an equilibrium slope. Finally, existing predictors can only apply for a certain range of conditions as all previous transverse bed slope experiments were performed with a small range of flow conditions and mostly uniform grain sizes, varying from 0.09 mm (e.g. Talmon & Wieseman, 2006) to 0.79 mm (e.g. Talmon et al., 1995).

The effect of bedforms on the transverse slope that develops is not yet taken into account. Either the experimental conditions were chosen to avoid bedforms (Hasegawa, 1981; Engelund, 1995), or the presence of bedforms only resulted in a different calibration factor of the transverse slope predictor (Talmon et al., 1995, Wieseman et al., 2006). Wieseman et al (2006) observed that downslope sediment transport decreased when dunes were present, while Sieben & Talmon (2011) show that avalanching at lee sides of dunes slightly enhances the slope effect.

3. AIM AND METHODOLOGY

The aim of the current research is to experimentally quantify the bed slope effect for a large range of flow velocities, helical flow intensities and particle sizes (0.1 - 4 mm), while taking into account the effect of bed forms. The experiments are being executed in the annular flume of Delft University of Technology (Fig. 3). This flume functions as an infinitely long bended flume, which therefore avoids boundary effects. Flow is generated by rotating the lid of the flume, which can be controlled to create a large range of flow conditions. Also, the intensity of the helical flow can be controlled by counter-rotating the bottom of the flume (Booij & Uijtewaal 1999). The equilibrium transverse slope that develops during the experiments is a balance between the transverse bed slope effect, the bed shear stress caused by the helical flow and the centrifugal force caused by the rotation of the bottom of the flume

(Fig.4). This balance depends on particle size, size range and density, and the rotation velocities of the lid and the bottom of the flume. All these parameters are systematically varied during the experiments in order to determine the separate effect on the equilibrium slope. Also, the effect of bedforms and suspension can be studied by the large range in flow conditions and grain sizes. For the first set of experiments only uniform sediment is being used. At a later stage, also poorly sorted sediment will be used in order to focus on sediment sorting processes. By systematically varying all these parameters, we aim to develop a more physical based transverse bed slope predictor that is applicable in a wide range of model simulations.

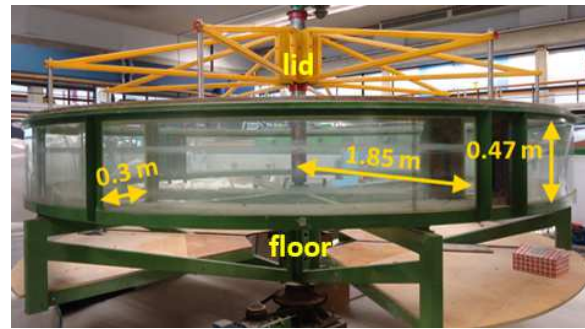


Figure 3. The annular flume at Delft University.

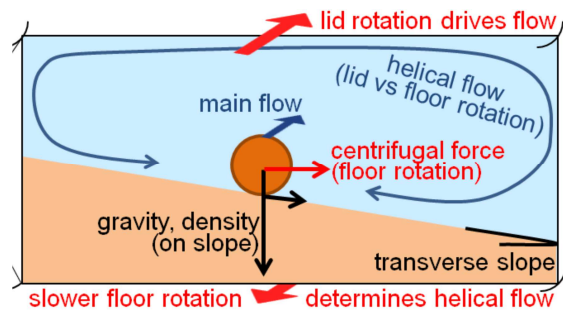


Figure 4. Forces acting on particles that can be controlled in the annular flume (after: Booij and Uijtewaal, 1999).

4. PRELIMINARY RESULTS

Fig 5 shows the morphology of several experiments with a grain size of 0.17 and 1 mm, as well as the corresponding maximum transverse bed slope that developed. During this set of experiments the rotation velocity of the lid of the flume (ω_l) is kept constant, while the rotation of

the bottom of the flume in the opposite direction (ω_b) increases. The average flow velocity therefore increases, as the difference between both rotation velocities increases. By increasing the bottom rotation, the centrifugal force on the sediment also increases, which counteracts the helical flow driving sediment inwards. Therefore, the transverse slope decreases with increasing centrifugal force. When the centrifugal force is larger than the helical flow intensity, a steep slope develops towards the outside wall of the flume.

Next to variations in transverse slopes, different bedforms are observed. Dunes developed during the experiments with grainsizes of 1 and 4 mm, of which the dune length varied with different flow velocities and helical flow intensities. During the experiments with finer sediment (0.17 and 0.37 mm), ripples were observed at experiments with a relatively low sediment mobility, while at higher sediment mobilities dunes were formed. In Figure 6 examples are shown of bedforms that occurred during the experiments with a D50 of 0.17 mm. During these experiments even the transition from dunes to an upper plane bed was observed at high flow velocities.



Figure 6 – Examples of bedforms that developed during the experiments. Sediment mobility increases from top (ripples) to bottom (upper plane bed).

In figure 7 the average equilibrium transverse slope (dz/dy) is plotted against the sediment mobility (Θ) for three different sediment sizes. For the experiments with a D50 of 0.17 mm also the bedform type that developed is indicated. As visible, the transverse slope increases with increasing mobility during the 4 mm experiments, while during the experiments with finer sediment the slope first increases and then locally decreases for intermediate Θ . This temporary decrease could be the result of changing bed form height, type (ripple/dune) and dune crest orientation.

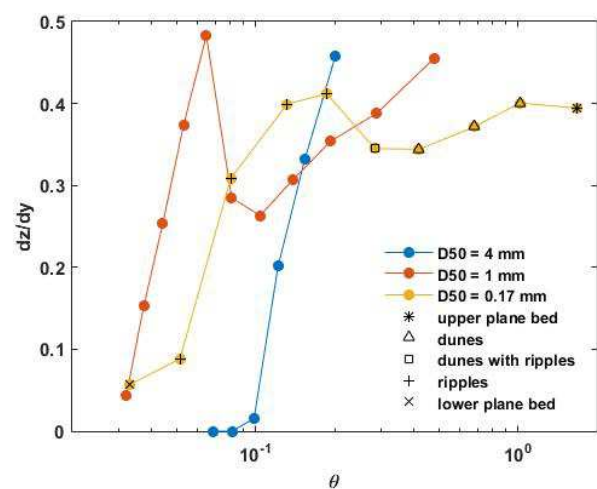


Figure 7 – Trend of the average transverse bed slope (dz/dy) with increasing sediment mobility (Θ) of three different sediment sizes. Sediment mobility was increased by higher lid rotation velocities.

5. FUTURE WORK

The resulting transverse bed slopes described above are based on average bed levels, while figure 5 shows a large variation in bed levels when dunes are present. Also, it is observed during the experiments that the dunes appear to have a large effect on the secondary circulation. We aim to use a Large Eddy Simulation model of the annular flume for idealized bed forms of varying height and orientation to quantify effects of bed forms on near-bed flow patterns and the resulting transverse slope.

6. REFERENCES

- Booij, R., Uijtewaal, W.S.J. 1999. Modeling of the flow in rotating annular flumes. *Engineering Turbulence Modeling and Experiments* 4:339–348.
- Hasegawa, K. 1981. Bank-erosion discharge based on a non-equilibrium theory. *Proc. JSCE, Tokyo*, 316:37–50.
- Ikeda, S., Nishimura, T. 1986. Flow and bed profile in meandering sand-silt rivers. *Journal of Hydraulic Engineering* 112: 562-579.
- Odgaard, A. J. 1981. Transverse bed slope in alluvial channel bends. *Journal of the Hydraulics Division* 107(12):1677-1694.
- Schuurman, F., Marra, W.A., Kleinhans M.G. 2013. Physics-based modeling of large braided sand-bed rivers: Bar pattern formation, dynamics, and sensitivity. *Journal of geophysical research: Earth Surface* 118.4:2509-2527.
- Sekine, M., Parker, G. 1992. Bedload transport on transverse slopes. *Journal of Hydraulic Engineering* 118:513–535.
- Sieben, J., & Talmon, A. M. 2011. Bed-load transport in obliquely dune-covered riverbeds. *Journal of Hydraulic Research*, 49(3): 317-324.
- Struiksma, N., Olesen, K.W., Flokstra, C., de Vriend, H.J. 1985. Bed formation in curved alluvial channels. *Journal of Hydraulic Research* 23:57-79.
- Talmon, A., Struiksma, N., van Mierlo, M. 1995. *Journal of Hydraulic Research* 33:495–517.
- Talmon, A., Wiesemann, J. 2006. Influence of grain size on the direction of bed-load transport on transverse sloping beds. *Proc. 3rd Int. Conf. on Scour and Erosion, Amsterdam, Netherlands*.
- Wieseman, J., Mewis, P., Zanke, U.C.E. 2006. Downslope transport (transverse sediment transport). *Third Chinese–German Joint Symposium on Coastal and Ocean Engineering, Tainan, Taiwan*.

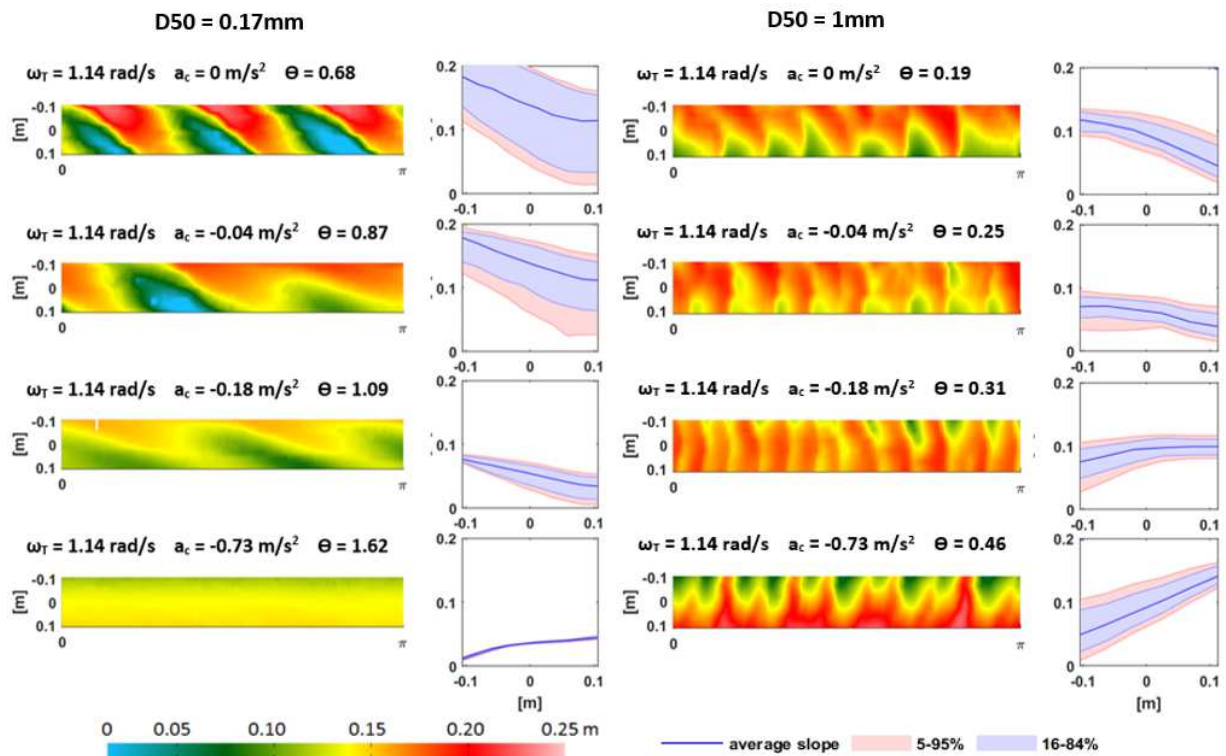


Figure 5. Resulting morphology (top view) of a series of experiments with a constant rotation velocity of the lid of the flume (ω_T) and increasing centrifugal acceleration (a_c), and corresponding transverse bed slopes. The width of the flume is measured relative to the average radius.

3. RESULTS

These experiments allow proposition of a model for flows that are transitional between a turbulent and laminar behaviour (Figure 2), and that is based on the changing nature of the velocity profiles and turbulence characteristics as volumetric clay concentration is increased. Five stages of turbulence modulation can be discerned:

1. Turbulent flow (TF)
2. Turbulence-enhanced transitional flow (TETF)
3. Lower transitional plug flow (LTPF)
4. Upper transitional plug flow (UTPF)
5. Quasi-laminar plug flow (QLPF)

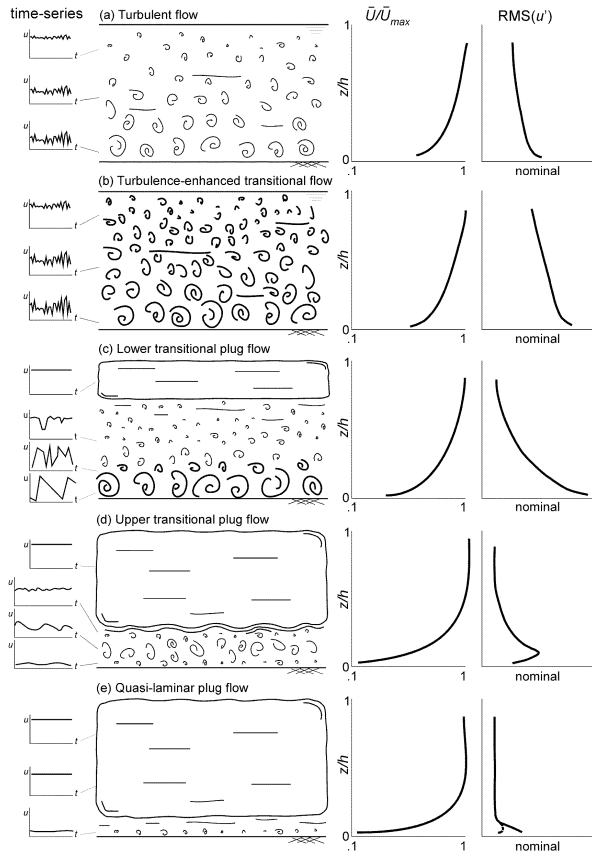


Figure 2: Schematic models of turbulent, transitional and quasi-laminar clay flows over a smooth, flat bed. Characteristic streamwise velocity time series at various heights in the flows are given on the left-hand side. The graphs to the right of the models represent characteristic vertical profiles of dimensionless downstream velocity (\bar{U} is maximum flow velocity) and $\text{RMS}(u')$ that are the root-mean-square values of the streamwise velocity fluctuations (after Baas and Best, 2002; Baas *et al.*, 2009)

Controls on Transitional Flows

This sequence of transitional flows has been found to be robust in flows of both kaolinite and bentonite, with the phase boundaries between the flows being produced at lower clay concentrations for bentonite. Higher mean velocities also require a greater clay concentration to produce a given transitional flow. Additionally, the phase boundaries are influenced by the presence of form/grain roughness that act to provide additional turbulence. *In summary, the balance between cohesive and turbulent forces favours the production of transitional flows: i) at higher clay concentrations, ii) with clays with a more viscous behaviour, iii) in the presence of lesser roughness, and iv) at lower shear stresses for a given clay concentration. Turbulence, whether generated by bed shear or grain/form roughness, creates local shear that acts to break up clay bonds and gels, and thus produces flows with a less laminar behaviour.* However, we have found that *irrespective* of roughness (Baas and Best, 2009) or shear stress, at some clay concentration this predictable sequence of transitional flows is generated.

A New Bedform Phase Diagram

Our mobile bed experiments allow proposition of a new bedform phase diagram for transitional flows (Figure 3). This diagram uses a grain-related mobility parameter, θ' , and the yield strength of the kaolin suspension, τ_Y , for the ordinate and abscissa axes respectively. Bedforms with a modified morphology, as compared to their clearwater counterparts, are produced (see Figure 4).

4. CONCLUSIONS

Transitional flows possess a predictable sequence of flow characteristics as clay concentration is increased, with the boundaries between flow types being dependent on the fluid shear, clay type and boundary roughness. These flows produce bedforms that may display a significantly different morphology to those produced in clear water flows. Ongoing research is investigating the boundary conditions of such flows with respect to flow salinity and extrapolymeric substances, and the nature/preservation of transitional flow deposits in the stratigraphic record.

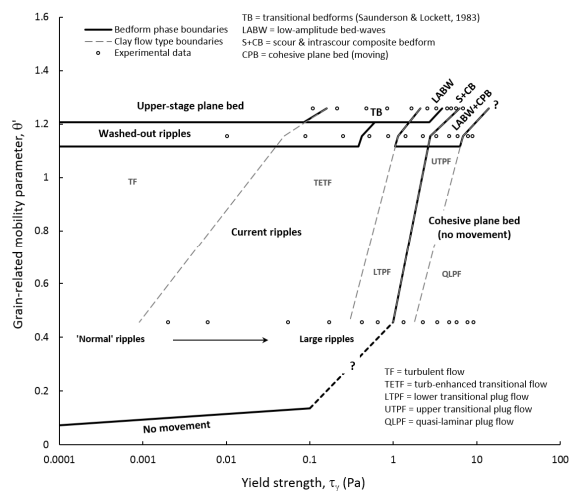


Figure 3: Bedform phase diagram for rapidly decelerated cohesive sand–mud flows, showing the stability fields for different bedform types. This diagram is valid only for poorly sorted sediment with $D_{50} = 0.085$ mm. At $\tau_T = 0$ (i.e. for clay-free sand), the boundaries between ‘normal’ ripples, washed-out ripples and upper-stage plane bed correspond approximately to those in the bedform phase diagram of van den Berg & van Gelder (1993) for a dimensionless grain size, $D^* = 2.15$. Radical changes in bedform type with increasing yield strength are evident, which are largely associated with changes in flow type. The question marks denote inferred boundaries (from Baas *et al.*, 2015).

5. ACKNOWLEDGMENTS

We are very grateful to the UK Natural Environment Research Council for grant NE/C514823/1 (TransFlow), which allowed this research to be initiated and undertaken at the Sorby Environmental Fluid Dynamics Laboratory while JHB and JLB were at Leeds with JP, and grant NE/I027223/1 (COHBED), which allowed JHB and JP to continue investigating bedform development in mixed cohesive mud and non-cohesive sand.

6. REFERENCES

Baas, J.H. & Best, J.L., 2002 Turbulence modulation in clay-rich sediment-laden flows and some implications for sediment deposition, *Journal of Sedimentary Research*, 72, 336-340.

Baas, J.H. & Best, J.L., 2009 On the flow of natural clay suspensions over smooth and rough beds, *European Research Community on Flow, Turbulence and Combustion (ERCOFTAC) Bulletin*, 78, 58-63.

Baas, J.H., Best, J.L. & Peakall, J., 2015 Predicting bedforms and primary current stratification in cohesive mixtures of mud and sand, *Journal of the Geological Society*, doi:10.1144/jgs2015-024.

Baas, J.H., Best, J.L., Peakall, J. & Wang, M. 2009 A phase diagram for turbulent, transitional and laminar clay suspension flows, *Journal of Sedimentary Research*, 79, 162–183.

Van den Berg, J.H. & van Gelder, A. 1993. A new bedform stability diagram, with emphasis on the transition of ripples to plane bed in flows over fine sand and silt. In: Marzo, M. & Puigdefabregas, C. (eds) *Alluvial Sedimentation*. IAS Special Publication, 17, 11–21.

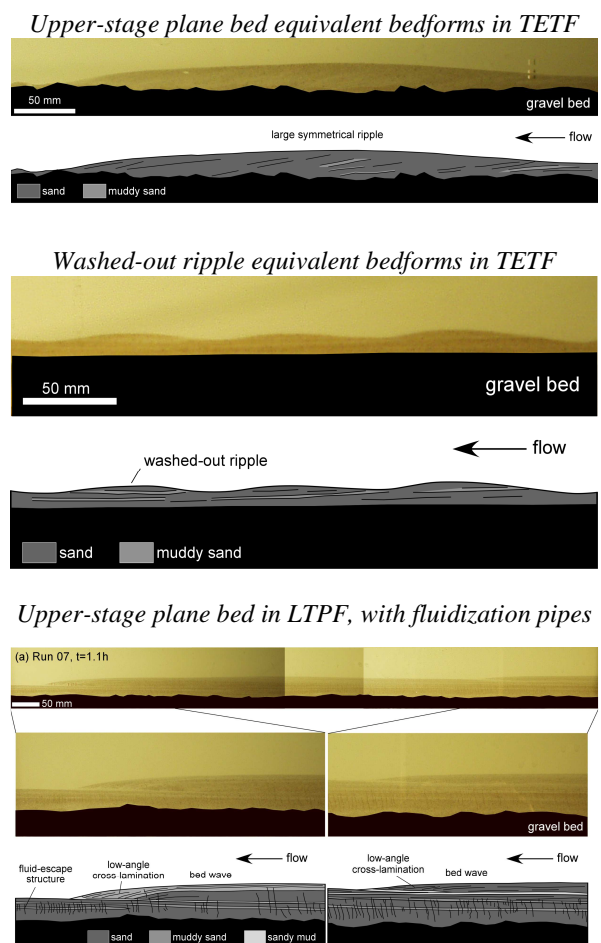


Figure 4: Examples of three distinct types of stratification formed under rapidly-decelerated transitional flow (from Baas *et al.*, 2015).

Value of bedload movement in alluvial rivers using analysis of sand bar migration

Z. Babiński *Kazimierz Wielki University, Bydgoszcz, PL – zygunt.babinski@gmail.com*

M. Habel *Kazimierz Wielki University, Bydgoszcz, PL – hydro.habel@ukw.edu.pl*

ABSTRACT: The channel mesoforms dynamics was conducted of the lower Vistula river (Poland). Movement of bars was determined on own measurements carried out at the three characteristic sections: unregulated channel, strong transformation channel below dam and regulated reach. Studies showed that each increase in flows corresponds to a proportional increase in the mesoforms dynamics. The size of bedload movement was determined based on the dynamics of bars, their movement rate and the layer thickness of these forms. Studies showed that bedload in the unregulated section on average amounted to nearly 2.2 million tons per year, whereas in the regulated section it did not exceed 1.0 million tons per year.

1. INTRODUCTION

Mesoforms are of major importance in the study of channel processes, defined by Popov (1977) as an unsteady continuous movement of the river channel bed under the influence of flowing water (Van Rijn, 1984). Kurpianov and Kopaljani (1979), suggest that the channel process is chiefly conditioned by a mechanism for fluvial transport and they establish certain relationships between them. These relationships have also been built up by Schumm (after Shen 1982) and by Winkley et al. (1984). From these data it can be inferred that a channel pattern (channel process) and an adequate system of mesoforms, depend on the quantity and quality of the bed-load transport. Continuous bed-load transport leads to the formation of dunes and sand ripple marks, i.e. microforms, whereas discontinuous transport results in central and lateral bars (islands), i.e. mesoforms (Carling et al., 2000; Rodrigues et al., 2014). The term channel mesoforms refers to forms, the size of which corresponds with the channel width and high stability of which is determined by hydraulic geometry of a stream. They usually comprise single large sand-gravel waves and fixed lateral bars, the surface of which lies in a zone of average

water stages although they are formed at high water stages (Babinski, 1987).

2. STUDY AREA AND METHODS

Research on channel mesoforms dynamics was conducted in the years 1981–2014 over a 200 km-long section of the lower Vistula (Northern Poland) (Babiński, 1992a). The research posts were located at specific sections of the river which is partially regulated and features a single dam. In recent years, the researchers constantly monitored pools located along the line of a new road bridge over the Vistula river near Toruń. Both horizontal and vertical movement of bars was determined on the basis of own measurement methods, including geodetic measurements carried out at the unregulated Vistula reach near Warsaw (Fig. 1), as well as at the section being subject to strong transformation caused by the dam in Włocławek (Habel 2013). The third selected reach had been regulated to a constant width in the second half of the 19th century (Babiński 1992b). Both cross- and longitudinal sections of the channel proved to be extremely helpful when preparing the bathymetric maps of the channel (bars and pools morphometry). The study was supplemented with

measurements of mechanical composition of the bars and pools.

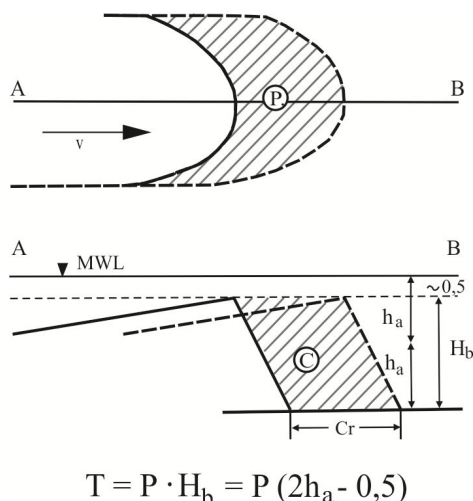


Figure 1. Ideogram of bed-load transport value (T) based on measurements of alternate sand bars dynamics at the regulated Vistula reach. Explanations: H_b – average thickness of sandbar, Cr – velocity of movement, P – surface rate of movement.

The following bars were identified on the lower Vistula in the course of field research and aerial photographs analysis: at the unregulated section of the Vistula – lateral sand bars and mid-channel bars, elevation of which corresponds with average annual water stages, linguoid bars, whose elevation coincides with average low water stages and occasionally (mostly at the regulated, straight section) diagonal bars that in terms of elevation fall between the abovementioned forms. The lateral and mid-channel bars are approximately 550 – 750 m long and 200 – 300 m wide, the linguoid bars reach an average length of 450 m and width of up to 200 m, whereas the diagonal bars reach on average 800 – 1200 m and 300 m respectively. Pools, erosion forms that can be found together with bars and which are at the same time commensurate with their size, reach a depth (measured at average water stages) of 4.0 – 4.5 m, 5.5 m locally in the case of braided channel, and 5-7 m with local depressions of up to 12 m at the regulated section of the lower Vistula.

3. RESULTS OF STUDY

Results analysis of the geodetic measurements of the bars and the channel sections against the Vistula river flows showed a dependence between the mesoforms dynamics and the hydrological regime of the river. The relation was the greater, the smaller was the impact of non-hydrological factors, such as channel morphology, ice phenomena and anthropogenic activity (bridges, channel regulation). Generally, each increase in flows corresponds to a proportional increase in the mesoforms dynamics and vice versa. The analysis of reaches featuring different channel development levels shows that the heads of bars of the same kind move at similar rate, however, this tends to change the more the bars differ in terms of, among others, elevation of their surfaces. Thus, the highest bars, i.e. lateral and mid-channel bars, have the lowest movement rate (Fig. 2), in the range of 0.2 – 1.27 m per day (on average 0.6 – 0.8 m per day), diagonal bars – alternate (occurring mostly at the regulated sections) – from 0.4 to 2.4 m per day (on average 1.1 – 1.2 m per day), whereas linguoid bars, being the lowest (corresponding to mean low water flows) and most dynamic forms (Fig. 2), move at a rate of 0.6 to 4.3 m per day (on average 1.7 – 1.8 m per day).

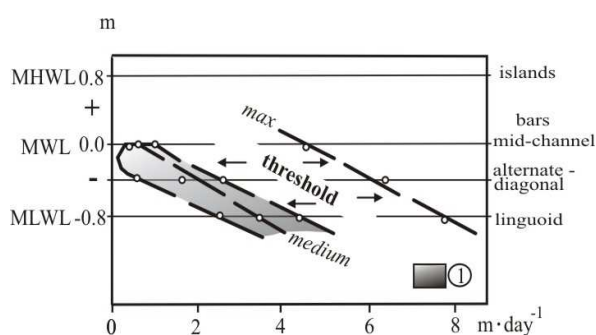


Figure 2. Mean diurnal rate of bar shifting on the unregulated and regulated sections of Vistula: 1 — zone of average velocities of bar shifting, MHWL — average high water stage, MWL — average water stage, MLWL — average low water stage.

4. CONCLUSIONS

The size of bedload movement was determined based on the dynamics of bars, their movement rate and the layer thickness of these forms. Studies showed that bedload in the unregulated section (reservoir backwater area) on average amounted to nearly 2.2 million tons, whereas in the regulated section, in the hydrological years of 1971/1995, it did not exceed 1.0 million tons. During a wet year 1975, the lower Vistula can transport up to 4 million tons of bedload at the braided and anastomosing section (unregulated channel) and more than 1.5 million tons at the regulated reach in the profile of Toruń, with the minimum of, respectively, nearly 1.0 and 1.5 million tons. The above data show that the smallest differences in bedload movement between these two sections occur in dry years (twofold), and the largest during wet periods (2.7 times). This spatial differentiation of bedload movement arises from: (a) the impact of the 19th century regulatory works, which transformed the braided and anastomosing channel (currently above the backwater of the Włocławek reservoir) into a straight, slightly winding one with a system of diagonal bars, and (b) limited capacity to collect bedload below the dam as a result of bed erosion (geological structure), which prevents the river from reaching the value of the section upstream of the water body (Babiński, 1992a). The bedload movement anomaly that occurs below the erosion zone is associated with the moment when the river becomes “saturated” with bedload (eroded from the bottom and banks), which is then temporarily discharged before entering into the regulated section of the Vistula (Figure 2 - Babiński, 1992a, 2002). The obtained results correspond to the findings of research conducted at the site of the road bridge construction in Toruń in the years 2011-2015 (Babiński, 1992a), albeit certain differences have been indicated. These involve a slight reduction in the rate of movement of pseudo-curved bars above the pillar of the bridge, and vice versa – the rate tends to increase down the river (Babiński et. al. 2014).

5. ACKNOWLEDGMENT

The research leading to these results has received funding from the People Programme (Marie Curie Actions) of the European Union's Seventh Framework Programme FP7/2007-2013/ under REA grant agreement n° [PIRSES-GA-2012-318969], acronym FLUMEN.

6. REFERENCES

- Babiński, Z. 1987. Morphometry and Morphodynamics of the Lower Vistula Channel Mesoforms, *Geographia Polonica*, vol. 53: 85—100.
- Babinski, Z. 1992a. The present-day fluvial processes of the lower Vistula River, IGI Polish Academy of Science in Warsaw, 210.
- Babiński, Z. 1992b. Hydromorphological Consequences of Regulating the Lower Vistula, Poland, *Regulated Rivers: Res. and Manag.*, John Wiley and Sons, 7: 337—348.
- Babinski, Z., Habel, M. & Chalov, S.R. 2014. Prediction of the Vistula channel development between Włocławek and Torun, *Questiones Geographicae*, 33(3): 5—13.
- Carling P.A., Gölz E., Orr H.G., Radecki-Pawlik A. 2000. The morphodynamics of fluvial sand dunes in the River Rhine, near Mainz, Germany. I. *Sedimentology and morphology. Sedimentology* 47: 227–252.
- Habel, M. 2013. Dynamics of the Vistula river channel deformations downstream of the Włocławek Reservoir, Copyright by UKW, Bydgoszcz, 214.
- Kurpianov V. V., Kopaliani Z. D., 1979, Resume of research into river channel changes conducted in the USSR, *Bulletin des Sciences Hydrologiques* 24, 345 — 349.
- Popov, I.V. 1977. *Zagadki rechnogo rusla*, Hidrometeoizdat, Leningrad, 356.
- Schumm, S.A. 1977. *The fluvial system*, John Wiley and Sons Ltd, New York.
- Shen, H.W. 1982. *The wandering rivers*, Water International Publications, IWRA by Elsev. Sequoia S. A., Lausanne 7, 10—17.
- Winkley, B.R., Schumm, S.A., Mahmood, K., Lamb, M.S. & Linder, W.M. 1984. New developments in the protection of irrigation, drainage and flood control studies on rivers, ICID, Symposium, Fort Collins, 69—111.
- Van Rijn L.C. 1984. Sediment transport, part II: bed forms and alluvial roughness. *Journal of Hydraulic Engineering* 110: 1733–1754.

Measurement and modelling of bedload self-generated noise on a sandy dune.

O. Blanpain *SHOM, HOM/Sedimentology, Brest, France* - olivier.blanpain@shom.fr

X. Demoulin *MAREE, Lorient, France* - xdemoulin@maree.fr

T. Garlan *SHOM, HOM/Sedimentology, Brest, France* - thierry.garlan@shom.fr

P. Guyomard *SHOM, HOM/Sedimentology, Brest, France* - patrick.guyomard@shom.fr

ABSTRACT: Passive acoustic method, based on hydrophones measuring self-generated noise due to inter-particle collisions, is relevant to study bedload processes: the signal intensity and the frequency spectrum are linked to bedload fluxes and grain size distribution. An experiment was conducted on a sandy dune subjects to high tidal currents. Signal processing has been adapted to distinguish the useful information, bedload self-generated noise, from other sound sources. Passive acoustic data proved to fit well with the intensity of bedload transport. A semi-empirical model is proposed to generate a simulated signal as a summation of individual shock signals. The latter is mainly affected by moving particle number and size. Thus, by minimizing the error between acoustic intensity simulated and measured, the optimized granulometry can be calculated.

1. INTRODUCTION

Bedload transport monitoring at sea still remains a challenge for sedimentologists and coastal engineers. Although such measurements are required to validate sediment transport models, data and instrumental techniques that establish a detailed link between boundary layer turbulence and sediment mixture dynamics are still scarce. Passive acoustic devices can offer this possibility when associated with high frequency velocity measurements in the nearbed. The method is based on the use of hydrophones recording self-generated noise due to inter-particle collisions during bedload transport. It presents numerous advantages: it is not disruptive to the flow field or the seabed, light, easy to handle and cost effective. The literature mainly describes developments made in controlled conditions with coarse particles (Thorne, 1985; Thorne, 1986). Few experiments took place in rivers (Belleudy et al, 2010; Geay, 2013) or marine environment (Thorne, 1986). It has been shown that the amplitude and the frequencies spectrum of the monitored signals are linked to bedload fluxes and grain size distribution. From laboratory studies, it has been shown that the observations could be explained in terms of rigid body radiation, which arises from the sudden

velocity change of the impacting particles (Thorne and Foden, 1988).

The present paper describes further developments in the prediction of the global self-generated noise level emitted by natural sand grains subject to tidal currents. Measurements on a sandy dune in the Iroise Sea are first briefly described and then an empirical model is proposed to generate a simulated signal as a summation of individual shock signals. Its intensity is mainly affected by the number of moving particles and their sizes. Thus, by minimizing the error between acoustic levels simulated and measured, the optimized grain size or the sediment fluxes can be calculated.

2. METHODOLOGY

2.1 In-situ measurements

The study area is located in the Four Channel (Iroise Sea, France) by 60 meters depth. The sea floor is covered by sandy dunes and influenced by strong tidal currents until 1 m/s. An instrumented frame was deployed on the sea bottom during 3 days of smooth to moderate sea state.

Passive acoustic data have been acquired with the use of one hydrophone located 40 cm above the bottom. Current velocity has been recorded with an upward-looking ADCP. No grab sediment sample

has been done during the deployment. But data acquired during previous surveys on the area allow the specification of the sedimentary characteristics: the median diameter is ranging between 0.4 mm and 1 mm.

Acoustic data and current velocities were recorded during fifteen minutes every half an hour. In order to reduce the background noise, the raw acoustic signal has been high-pass filtered with a 10 kHz cutoff frequency. The filtered signal is composed of short spikes (0,05 ms typical duration, 100 kHz dominant frequency) emerging from the background sound. Thus, the temporal signal can be considered as a combination of successive and numerous shocks due to sediment transport. A root mean square (rms) pressure has been calculated every minute. This P_{rms} is associated with a velocity measurement at the same time.

2.2 Model description

The model aims to estimate the total rms pressure generated by moving sand particles on the sea floor. In accordance with the observations, the temporal simulated signal is considered to be the combination of individual shock signals.

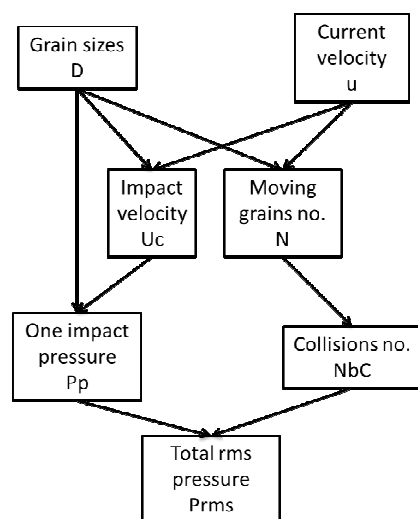


Figure 1. Diagram of the modeling strategy.

Figure 1 presents a diagram of the modeling strategy we used and highlights the different processes we need to quantify. For each current velocity u and grain size D , we first calculate the number of moving grains N and their velocity during the collision U_c . Then, the number of impacts N_bC and the pressure radiated from a pair

of impacting particles P_p are quantified. Finally, a total rms pressure level P_{rms} is obtained by the summation of each particle impact signal.

2.2.1 Collision number estimation

The Shields diagram (Shields, 1936; Soulsby (1997) is widely used to specify the critical thresholds for initiation of sand grain motion. Thus, for each current velocity and grain size values, the mobility parameter can be calculated and compared to the critical threshold for initiation of motion to determine if particles are moving.

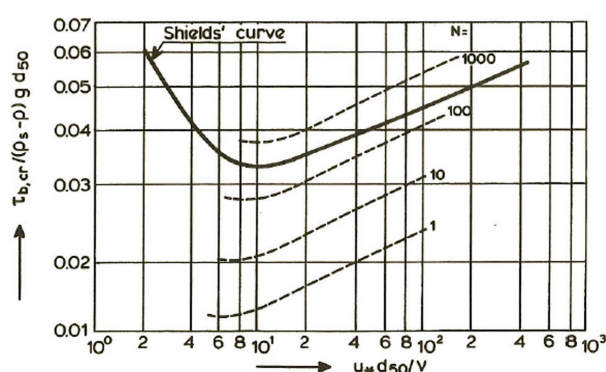


Figure 2. Number of particle moving per unit area (m^2).

Van Rijn (1993) plotted the Shields curve on a diagram with the aim of quantifying the number of sand grain moving per unit area (Figure 2).

It is noticeable that Shield's curve is included between the 100 and the 1000 moving particle curves. That seems to indicate that Shield criterion correspond to a global initiation of motion or to a permanent particle movement and not a single grain movement at one location.

Figure 2 allow us to evaluate the number of moving grains per unit of area as a function of particle diameter and current speed. During the measurement campaign, the Shields criterion corresponds to $N = 300$ moving particles. By fitting the number of moving particles versus the ratio between the mobility number for N particles, and the Shield criterion, we obtain the following expression:

$$N = 10^{5.33 - 2.78 \cdot \frac{u_*^2}{u_{*c,N}^2}} \quad (1)$$

The number of collisions N_bC between a moving particle and grains on the sea floor is estimated as:

$$NBC = N \cdot S \cdot P \quad (2)$$

With S the surface of sea floor where impacts contribute to the signal level recorded by the hydrophone (Figure 3) and P the probability of collision for each moving grain. According to Thorne (1986), $P = 10\%$. The distance a corresponds to the radius of the surface S . Assuming each impact of a pair of grains is considered as a dipolar source, $a = 2h$ (Demoulin, 2013) and thus:

$$S = 4 \cdot \Pi \cdot h^2 \quad (3)$$

Each particle collision is thus associated with an angle θ and a distance r to the hydrophone.

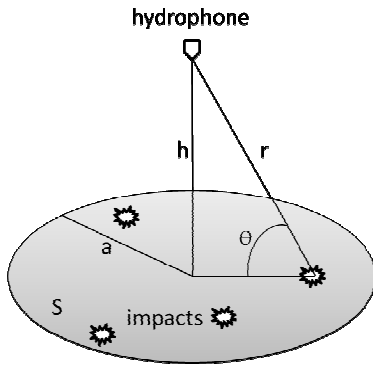


Figure 3. Geometry for the signal generation modeling.

2.2.2 Pressure radiated from a pair of impacting grains

Thorne and Foden (1988) described a theoretical framework for the generation of underwater sound by colliding spheres. Rigid body radiation theory has been adopted. The solution proposed considers that each sphere is an independent source which generates a transient that can be described by an impulse solution convolved with the acceleration time history during the collision. The impact process is assumed to be elastic so that a Hertzian acceleration description can be employed. The sound field is then obtained from the sum of the two signals. Thus, the total pressure radiated from a pair of impacting grains is formed by the contribution of each particle. The set of equations can be simplified if (i) the particles are the same (equivalent diameter and mass), (ii) their density is larger than half the water density and, (iii) the range distance r is larger than the particle radius. The impact velocity is considered equal to the current velocity at height D above the seabed.

2.2.3 Total rms pressure generation

The total pressure generated $Prms$ is the summation of pressure signals P_p radiated by each collision for each particle randomly scattered on the sea floor surface S during an integration time T split in x periods:

$$P_{rms} = \sqrt{\frac{1}{x} \sum_{i=1}^x \sum_{NBC} \sum_D P_p(t)^2} \quad (4)$$

3. RESULTS

Following the modeling strategy, the particle size is optimized by minimizing the error between acoustic pressure simulated and measured. A rms pressure is calculated for particle sizes varying from $D = 0.1$ mm to $D = 2$ mm by step of 0.1 mm. The root mean square deviation is minimized for particle size of 0.8 mm. This value is equivalent to the median diameter of sediment samples previously realized near the deployment site. The match with the measurements is shown on Figure 4. The model tends to underestimate measured $Prms$ and especially fails to reproduce the higher values which are recorded when current velocities are important. Under these strong hydrodynamic conditions, an important spreading of $Prms$ is noticeable for a same current speed value. This observation can be due to (i) the turbulent bursting phenomenon of sediment transport, or (ii) the grains hitting the instrument frame. In either case, model is not set up to simulate these processes.

Another model limitation can explain the underestimation of pressure: only impacts between two particles of the same diameter are taken into account. However, we can consider that the probability for a moving grain to impact a non-moving coarser one is higher, and then the induced pressure is higher.

These results are obtained for a single size diameter representative of well sorted sediment. A better error minimization can be reached by taking into account a grain size distribution. The measured curve has been manually fitted by several red straight lines delimiting four sections (Figure 4). That partition can be explained by the contribution of bigger grains set into motion with the increase of current velocity. A preliminary

analysis with four different grain sizes tends to better represent the shape of the curve.

4. CONCLUSIONS

A sea experiment has been undertaken to evaluate the feasibility of using passive acoustic for sand transport characterization. Measurements have shown that the recorded Prms evolves with current velocity fluctuations and, even for grain sizes as small as sand, self-generated noise due to inter-particle collisions can be relevant to identify bedload transport.

An empirical model has been set up in order to simulate the pressure signal due to moving grains. Governing parameters are the number of moving particles and their size. By fitting the pressure measured and calculated, a median grain size involved into the sediment transport has been evaluated. This value is consistent with the medium grain size observed on the area. First attempts made with several grain sizes tend to improve the simulated signal.

The validity of this inversion process depends on the model precision and the raw data processing. Major limitations can be overtaken by taking into account collision from two particles of different size. Data acquisition can be improved by using an hydrophone with a higher frequency sampling rate and a lower signal to noise ratio. A signal analysis

effort can be made on the detection of grain-frame impacts.

5. REFERENCES

- Belleudy, P., Valette, A., Graff, B. 2010. Passive Hydrophone Monitoring of Bedload in River Beds: First Trials of Signal Spectral Analyses. U.S. Geological Survey Scientific Investigations Report 2010-5091, 266–282.
- Demoulin, X. 2013. Vagues, bulles et sons, rapport MAREE.
- Geay, T. 2013. Mesure acoustique passive du transport par charriage dans les rivières. Thèse de doctorat de l'Université de Grenoble, 163p.
- Shields, A. 1936. Application of similarity principles and turbulence research to bedload movement. Hydrodynamics Laboratory, California Institute of Technology.
- Soulsby, R. 1997. Dynamics of marine sands. Thomas Telford Publication.
- Thorne, P.D. 1985. The measurement of acoustic noise generated by moving artificial sediments. *J.Acoust.Soc.Am.*, 78:1013-1023.
- Thorne, P.D. 1986. Laboratory and marine measurements on the acoustic detection of sediment transport. *J.Acoust.Soc.Am.*, 80, 899-910.
- Thorne, P.D. and Foden, D.J. 1988. Generation of underwater sound by colliding spheres. *J.Acoust.Soc.Am.*, 84:2144-2152.
- VanRijn, L. 1993. Principles of sediment transport in rivers, estuaries and coastal seas, Part 1.

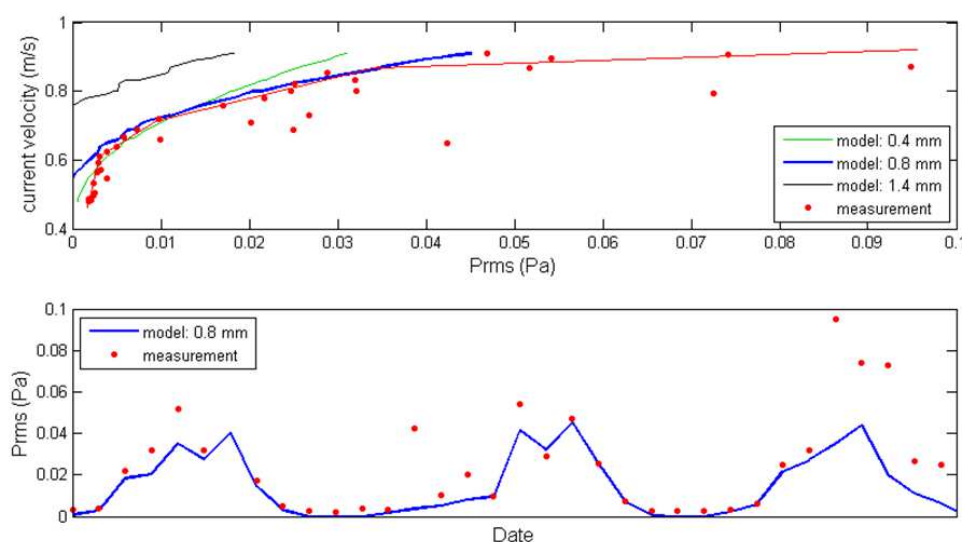


Figure 4. Comparison between model calculation and measurements.

Measurements of flow dynamics associated with interacting, subaqueous barchans: Exploring bedform asymmetry and three-dimensionality in a novel flume environment

N. Bristow *University of Notre Dame, Notre Dame, Indiana, U.S. – nbristow@nd.edu*

G. Blois *University of Notre Dame, Notre Dame, Indiana, U.S. – gblois@nd.edu*

W. Anderson *University of Texas at Dallas, Dallas, Texas, U.S. – William.anderson@utdallas.edu*

Z. Tang *Hebei University of Technology, Tianjin, China*

J. M. Barros *United States Naval Academy, Annapolis, Maryland, U.S. – barros@usna.edu*

J. L. Best *University of Illinois, Champaign, Illinois, U.S. – jimbest@illinois.edu*

K. T. Christensen *University of Notre Dame, Notre Dame, Indiana, U.S. – kchrist7@nd.edu*

ABSTRACT: While barchan dunes are traditionally associated with aeolian environments, recent efforts now highlight the emergence of barchans in subaqueous environments as well, particularly in rivers. To this end, herein the flow associated with interacting barchan dunes is quantified in the laboratory as a means of understanding a range of morphodynamic issues associated with their evolution. The interaction between barchans of different sizes produces complex processes such as collision, amalgamation and breeding. In this study, idealized, fixed physical models are utilized to permit accurate interrogation of the flow with both high-resolution planar and volumetric particle image velocimetry. Specific simplified geometrical configurations of two fixed barchan dunes in tandem reveal the flow modifications induced by dune proximity as compared to the baseline case of flow around an isolated dune. Initial measurements focused on the latter, followed by measurements of several tandem configurations replicating sequential stages in a dune-dune collision.

1. INTRODUCTION

Barchan dunes are three-dimensional (3D) topographic features generated by geophysical flows in the presence of a limited sediment supply over an underlying substrate, and are important in a number of engineering and geophysical applications (Lancaster, 1994). While barchan dunes are traditionally associated with aeolian environments, recent high-resolution maps of river bed topography using new methods (i.e. multibeam echosounding) have revealed the occurrence of such dunes in subaqueous environments. These observations, and ongoing research in aeolian environments, have sparked interest in these bedforms among the scientific river community, particularly for their geomorphological, environmental and engineering significance.

Barchans typically occur in fields with significant heterogeneity in dune size and migration rate. In this situation, the interaction between barchans of different sizes produces complex processes such as collision, amalgamation and breeding (Endo et al., 2004). While the morphology of barchan dunes has been widely studied, the interaction between turbulent flows and barchans is limited to a few recent studies (Palmer et al., 2012; Charru and Franklin, 2012). The number of direct flow measurements is even fewer with respect to the interaction mechanisms occurring when barchans are in close proximity. This lack of data is partially due to the geometric complexity of these bedforms that introduces significant challenges in high-resolution optical flow diagnostic techniques such as particle image velocimetry (PIV). As a result, the processes involved in the interaction and collision of barchan dunes remains poorly

understood, with the impact of turbulence not being incorporated in current numerical models.

In particular, models based on mean bed shear stress (Parteli et al., 2014) struggle to accurately predict the morphodynamics of barchans when they come in close proximity, including dune-dune collisions. This model deficiency is readily observed in the Figure 4 which compares the model results (a-e) (Parteli et al., 2014) of a smaller barchan approaching a larger one (barchan migration rate is inversely proportional to size) with a similar scenario observed in laboratory experiments (f-j) (Hersen et al., 2005). Figure 4 highlights the contrasting dynamics, with erosion of the downstream dune occurring prior to contact, indicating that models based solely on mean bed shear stress fail to capture the key flow physics associated with such interactions. Thus further experimental work is needed to inform these deficiencies and elucidate the role of unsteady turbulence in barchan morphodynamics.

In this paper, we study the flow field surrounding idealized, fixed physical models with high-resolution planar and volumetric PIV. Several different configurations of models are used, including a baseline isolated case and a number of dune-dune collision cases. Access to the flow field around these geometrically complex dunes is achieved using a refractive index matching (RIM) approach. Transparent models of barchan dunes, whose shape was based upon previous work (Palmer et al., 2012), were fabricated by casting urethane material into 3D printed molds. The models were fixed in a RIM flow tunnel that employs an aqueous solution of sodium iodide (~63% by weight) as the working fluid, and rendered invisible, thus facilitating unimpeded data collection around the entire bedform configuration. Planar measurements at high spatial and temporal resolution were conducted in both the x - z (i.e. wall-parallel) and the x - y (i.e. wall-normal) planes, at several different elevations and spanwise positions respectively, in order to reveal the 3D nature of the flow. An example of these measurements is shown in Figure 1, where the case of an *offset* collision is shown. In addition to planar measurements, volumetric measurements were performed using the TSI V3V PIV system to reveal the instantaneous 3D flow structures shed

from the barchan crests, as well as observe their evolution as they convect and impinge onto the downstream barchans (Lai et al., 2008). Figure 2 reports an example of such volumetric measurements. The measurements

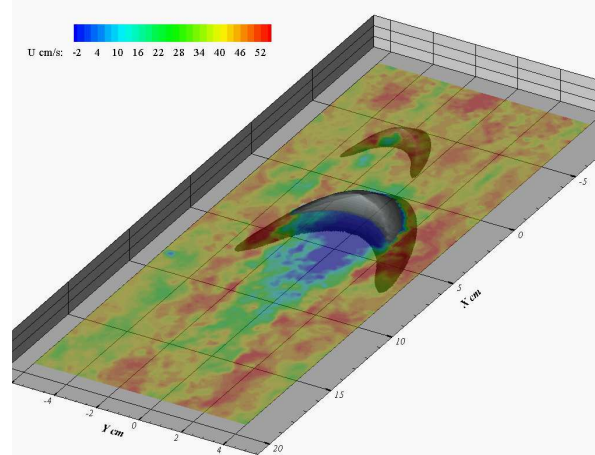


Figure 1. Instantaneous distribution of the streamwise component of velocity around two interacting barchan dunes in an offset collision configuration at $y = 0.5h$.

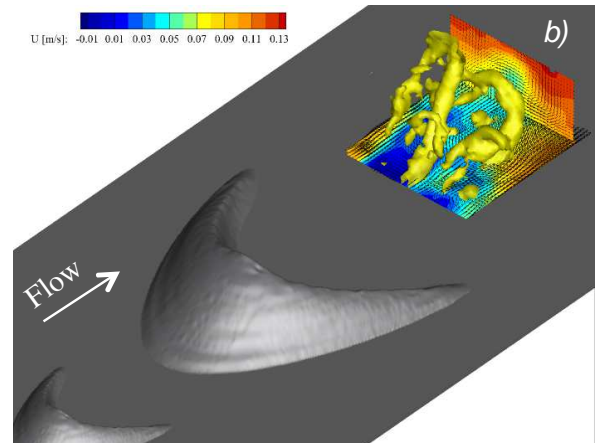


Figure 2. Instantaneous flow structures captured by the V3V system at two different streamwise positions downstream of the larger barchan dune for the inline collision configuration. Iso-surfaces are 3D swirling strength.

conducted in this work would be impossible in either a wind or water tunnel owing to laser blockage and/or aberration upon light interaction with the barchan models. In contrast, because the refractive indices of the fluid and solid models are matched precisely in the present experiments, no loss of laser energy or laser deflection is present as light passes through the solid models, while optical aberrations are also minimized.

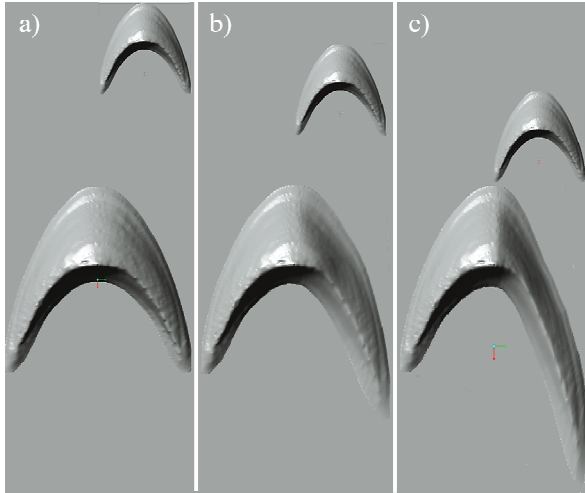


Figure 3. Barchan dune model configurations in a dune-dune offset collision sequence.

Each barchan offset collision configuration simulates a successive stage in the process of a dune-dune collision whereby a smaller, spanwise offset, upstream dune collides with a larger downstream dune, the two dunes having a 1:8 volumetric ratio. Inspired by the experimental work by Hersen et al. (2004), the final two stages in this collision involve asymmetric, deformed morphologies. The three stages in this dune-dune collision are shown in Fig. 3.

2. RESULTS

Analysis of the isolated barchan case shows that the flow separates at the crest of the barchan, producing a 3D shear layer that is suggested to present a symmetrical (in the spanwise direction) arc-like shape. The flow region behind the leeside is characterized by low momentum. Under such conditions in a mobile bed, a fraction of the sediment that was entrained upstream would be deposited, resulting in bedform migration. Our results indicate that the shear layer may have important morphodynamic implications, since it embodies a significant fraction of the Reynolds shear stress (RSS) and thus plays a central role in the erosion processes induced by barchans. These measurements are the first step towards linking, in a quantitative fashion, the energy dissipation due to turbulent mechanisms (i.e. shear layers) to localized erosion phenomena (i.e. erosion on the stoss side) that have been highlighted by previous

qualitative mobile bed experiments involving interacting bedforms (Endo et al., 2004).

While flow symmetry for an isolated barchan was confirmed, our results indicate that the presence of an upstream dune may break this symmetry around the downstream barchans, unless the two dunes are perfectly symmetrical and perfectly aligned. The in-line case studied shows that the symmetry of the mean flow is highly sensitive to dune alignment, and this can provide insight to understand the imperfect symmetry of barchans in natural environments. The offset cases enhance this flow asymmetry, as is particularly apparent in the single point statistics (turbulent kinetic energy (TKE) and RSS). The streamlines show an enhanced recirculation near the horn of the larger barchan dune that is closer to the smaller barchan in both of the offset cases. A reduction in TKE, that is spatially coincident with the enhanced recirculation, is also noted at the same location. RSS shows a contrasting behaviour, with enhancement for the case of offset collision and reduction in the case of offset ejection. Finally, the 3D flow fields obtained by extracting the iso-contour of the swirling strength from the V3V dataset, reveal the presence of horseshoe-like vortical structures that are shed from the crest of the barchan. For the in-line case considered herein, these vortices convect and impinge upon the larger downstream barchan dune. Their behaviour is consistent with recently published LES simulations using similar geometries.

3. CONCLUSIONS

This study provides accurate 2D and 3D flow measurements of the turbulent flow field surrounding fixed, interacting barchan dune models. Using both planar and volumetric PIV in conjunction with a refractive index matching technique, the instantaneous and mean flow structure around dunes in different configurations was measured and is presented here. This preliminary study is key to further experimental investigations that will consider a wider range of dune volumetric ratios and interacting configurations. Future work will focus on the morphodynamic implications of the turbulent events revealed using our unique experimental

approach as well as targeted numerical simulations using large-eddy simulation to explore a broader range of dune interaction scenarios.

4. REFERENCES

- Charru F. and Franklin, M. 2012. Subaqueous barchan dunes in turbulent shear flow. Part 2. *Fluid Flow. J. Fluid Mech.* 694:131-154.
- Endo, N., Taniguchi, K. and Katsuki, A. 2004. Observation of the whole process of interaction between barchans by flume experiments. *Geophys. Res. Lett.* 31.
- Hersen, P., Douady, S. 2005. Collision of barchan dunes as a mechanism of size regulation. *Geophys. Res. Lett.* 32.
- Lai W., G. Pan, R. Menon, D. Troolin and E. Graff. 2008. Volumetric three-component velocimetry: a new tool for 3D flow measurement. *Proceedings of the 14th Int. Symp. on Applications of Laser Techniques to Fluid Mechanics.*
- Lancaster N. 1994. Dune morphology and dynamics. *Geomorphology of Desert Environments.* Springer Netherlands: 474-505.
- Palmer J.A., R. Mejia-Alvarez, J.L. Best and K.T. Christensen. 2012. Particle-image velocimetry measurements of flow over interacting barchan dunes. *Exp. Fluids* 52: 809–829.
- Parteli, E., Duran, O, Bourke, M, Tsoar, H, Poschel, T, Herrmann, H. 2014. Origins of barchan dune asymmetry insights from numerical simulations. *Aeolian Research.* 12: 121-133.

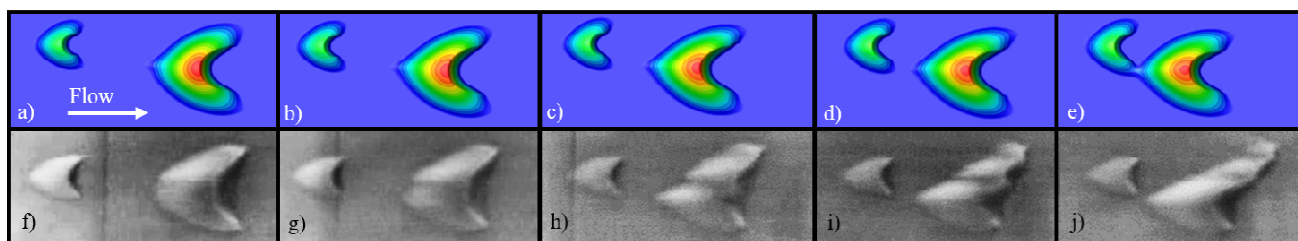


Figure 4. Comparison of (a-e) morphodynamic model and (f-j) mobile-bed flume experiments (Hersen et al., 2005), highlighting model deficiencies for a barchan collision. Code courtesy Parteli et al. (2014) (modified by us for this scenario).

Modelling the influence of storm-related processes on sand wave dynamics: a linear stability approach

G.H.P. Campmans *Water Engineering & Management, University of Twente, Enschede, The Netherlands, g.h.p.campmans@utwente.nl*

P.C. Roos *Water Engineering & Management, University of Twente, Enschede, The Netherlands*

S.J.M.H. Hulscher *Water engineering & Management, University of Twente, Enschede, The Netherlands*

ABSTRACT: Literature shows that storms play a significant role in sand wave dynamics. We present a 3D idealized sand wave model, capable of systematically investigating the influence of storm-related processes, i.e. wind-driven flow and wind waves, on the formation stage of sand waves. Model results show that wind-driven flow affects sand wave migration, and wind-waves affect the wavelength and growth rate of the fastest growing mode.

1. INTRODUCTION

Tidal sand waves are large-scale rhythmic bed forms observed in many tide-dominated shallow seas with a sandy seabed. The behaviour of sand waves is of practical interest because they tend to interfere with navigation, dredging, and pipelines. Process-based morphodynamic models have been developed to increase our understanding of sand wave dynamics (Besio et al. 2008; Van den Berg et al., 2012). In particular, sand waves have been explained as free instabilities of the system (Hulscher, 1996).

Limitations of existing sand wave models (overestimating sand wave heights and inaccurately predicting sand wave migration) suggest that some processes are either poorly represented or still missing. Observations show that storms, not included in the above models, play a significant role in sand wave dynamics (Terwindt, 1971; Harris, 1989; Houthuys et al., 1994). Németh et al. (2002) found that wind-driven flow affects sand wave migration. The effect of wind waves on sand wave growth dynamics has not yet been investigated.

In this study, we present an idealized sand wave model to systematically investigate the influence of storm-related processes on sand wave dynamics,

in the stage of formation. Moreover, we aim to identify potentially important storm-related processes, and restrict ourselves to linear stability analysis (e.g. Dodd et al., 2003). Our model adopts the linear stability analysis approach to investigate the fastest growing mode when including storm-related processes. This mode is assumed to be the dominant bed form. Sand wave properties obtained from this analysis are: growth rate, migration rate, wavelength and orientation.

2. METHODS

We present a 3D idealized sand wave model to investigate the influence of storm-related processes (see fig. 1). These processes are included in a schematised way in order to obtain a fast and relatively simple model that is capable of investigating the influence of storm-related processes on sand wave dynamics, and is also capable to identify the most important physical mechanisms.

2.1. Processes included

During fair weather, sand waves are subject to tidal flow; and bed load is the dominant sediment transport mode.

During storms, both wind-driven flow and wind-waves are generated. Larger flow velocities due to wind-driven flow and stirring due to wind-waves can initiate suspended load sediment transport.

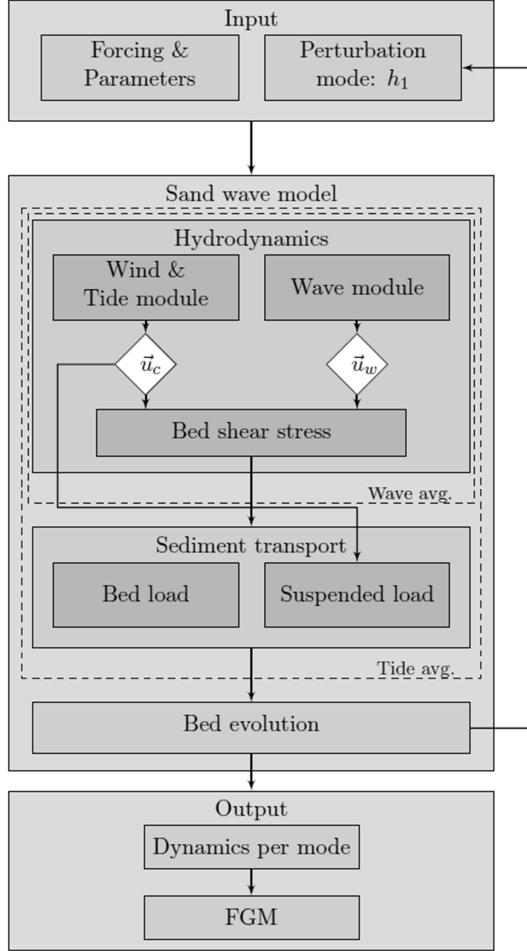


Figure 1. Schematic model overview.

2.2. Model formulation

Both wind-driven currents and tidal flow are described by the 3D nonlinear shallow water equations, including the Coriolis effect. These consist of two horizontal momentum equations and a continuity equation. Wind-driven flow is forced by a shear stress at the water surface. Tidal flow is forced by a horizontal oscillatory pressure gradient, which – in the case of a flat bed – produces a prescribed residual current, M_0 , and tidal ellipses of the M_2 , M_4 and higher-order harmonic components. Turbulence is described by a constant eddy viscosity, combined with a partial-slip condition near the bed.

Wind-waves are included via a separate wave module based on linear wave theory.

Both the currents module and the wave module generate near-bed velocities, which are translated to a combined bed shear stress.

Sediment transport consists of both bedload and suspended load. Bed load transport is assumed to respond instantaneously with changing bed shear stress, and is modelled as a power law including the bed slope effect. Suspended sediment transport is modelled via the advection diffusion equation. Near the bed, a reference concentration is prescribed as a power law function of the bed shear stress.

Finally, the bed evolution follows from (tidally averaged) sediment conservation.

2.3. Linear stability analysis

Using linear stability analysis, we investigate the stability of the flat bed subject to a spatially uniform tidal motion, called the basic state.

This is done by analysing the response of the system to small-amplitude sinusoidal perturbations:

$$\frac{h}{H} = \varepsilon h_1 = \varepsilon \cos(k_x x + k_y y). \quad (1)$$

Here, h is the bed level, H the mean water depth, $\varepsilon \ll 1$ a small expansion parameter, h_1 the perturbed bed level and k_x and k_y are the topographic wave numbers in x - and y -direction, respectively.

The unknowns of the system, symbolically represented as φ , are expanded in powers of ε :

$$\varphi = \varphi_0 + \varepsilon \varphi_1 + \mathcal{O}(\varepsilon^2). \quad (2)$$

Here, φ_0 is the basic state of the system, φ_1 is the perturbed state system response, and higher-order terms are neglected since ε is small. The solution of the bed evolution is written as follows:

$$h_1 = \cos\left(k_x x + k_y y - c_{mig} \sqrt{k_x^2 + k_y^2} t\right) e^{\omega t} \quad (3)$$

Here, c_{mig} is the migration speed in the direction perpendicular to the crest, ω is the growth rate, which results in exponential growth (or decay if it is negative). The system is linearly stable, when

$\omega < 0$ for all k_x and k_y . If $\omega > 0$ for at least one mode, the basic state is unstable. The mode with the maximum growth rate is termed to be the fastest growing mode (FGM). The properties of the FGM are: wavelength, orientation, growth rate and migration rate.

2.4. Solution method

Since the bed perturbations are described as Fourier modes, the horizontal structure of the response of the system according to this linear model also consists of Fourier modes. Additionally, the tidal current is assumed to be harmonic in time. Only in the vertical direction, numerical integration is required to solve the hydrodynamic perturbed state. The basic state can be solved analytically, because a constant eddy viscosity is chosen. As the numerical integration problem is just 1D, the model is fast.

3. RESULTS & DISCUSSION

For typical North Sea conditions, the flat seabed turns out to be unstable, so that some perturbation modes tend to grow. On an initially flat bed containing equally small perturbations of all modes, the FGM will soon dominate all other modes. The FGM is therefore assumed to be the most likely surviving bed form during the stage of formation.

Different storm processes, i.e. wind-driven flow and wind waves, yield different sand wave dynamics (see fig. 2). Wind-driven flow primarily affects sand wave migration, and wave action tends to increase wavelength and reduce the growth rate.

Processes are represented in a schematized way, hence the model results should be interpreted as qualitative indications of the influence of storm-related processes on sand wave dynamics. Note that the model is valid for small amplitudes only; higher-order amplitude effects are likely to yield different properties of fully grown sand waves.

4. CONCLUSIONS

The new idealized sand wave model is capable of qualitatively analysing the physical mechanisms

that cause sand wave formation. Additionally, the model is well suited to perform a sensitivity analysis for a large set of model parameters. Preliminary results show that wind-driven flow affects the migration rate of sand waves and wave action affects their wavelength and growth rate.

5. ACKNOWLEDGMENT

This research is supported by the Dutch Technology Foundation STW, which is part of the Netherlands Organisation for Scientific Research (NWO), and which is partly funded by the Ministry of Economic Affairs.

6. REFERENCES

- Besio, G. & Blondeaux, P. & Brocchini, M. & Hulscher, S. J. M. H. & Idier, D. & Knaapen, M. A. F. & Németh, A. A. & Roos, P. C. & Vittori, G. 2008. The morphodynamics of tidal sand waves: a model overview. *Coastal Engineering*, 55(7): 657-670.
- Dodd, N. & Blondeaux, P. & Calvete, D. & De Swart, H. E. & Falqués, A. & Hulscher, S. J. M. H. & Różyński, G. & Vittori, G. 2003. Understanding coastal morphodynamics using stability methods. *Journal of Coastal Research*, 19(4): 849-865.
- Harris, P.T. 1989. Sandwave movement under tidal and wind-driven currents in a shallow marine environment: Adolphus channel, northeastern Australia. *Continental Shelf Research*, 9(11): 981-1002.
- Houthuys, R & Trentesaux, A. & De Wolf, P. 1994. Storm influences on a tidal sandbank's surface (Middelkerke Bank, southern North Sea). *Marine Geology*, 121(1): 23-41.
- Hulscher, S.J.M.H. 1996. Tidal-induced large-scale regular bed form patterns in a three-dimensional shallow water model. *Journal of Geophysical Research* 101(C9): 20,727-20,744.
- Németh, A.A. et al. 2002. Modelling sand wave migration in shallow shelf seas. *Continental Shelf Research*, 22(18): 2795-2806.
- Terwindt, J.H.J. 1971. Sand waves in the southern bight of the North Sea. *Marine Geology*, 10(1): 51-67.
- Van den Berg, J. et al. 2012. Non-linear process based modelling of offshore sand waves. *Continental Shelf Research*, 37: 26-35.

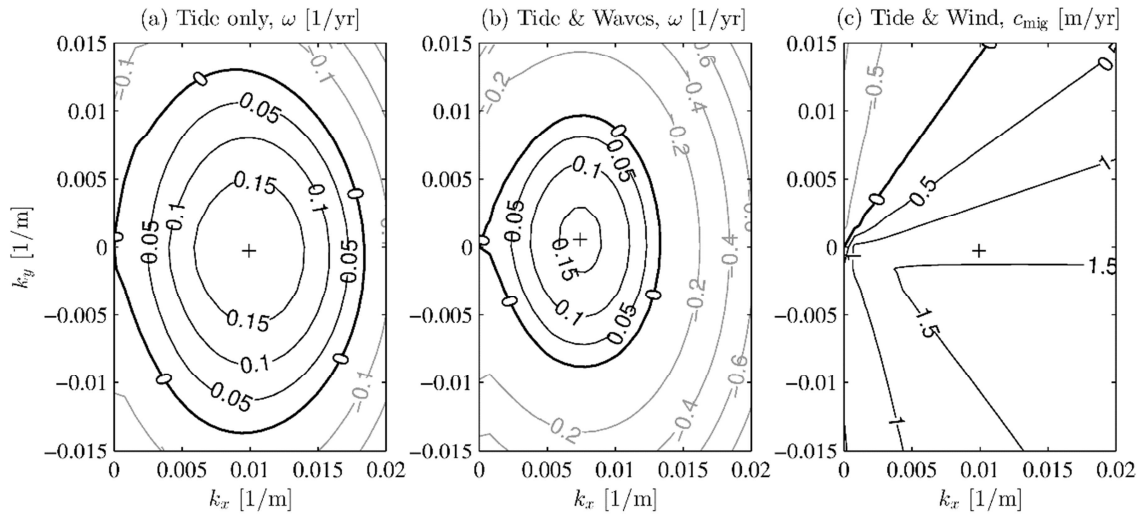


Figure 2. Model output as a function of topographic wave numbers k_x and k_y : (a) growth rates, ω for tide only, (b) growth rates, ω for tide and wind waves, (c) migration rate, c_{mig} for tide and wind forcing. In this example, the tide is symmetric (such that $c_{mig} = 0$ in cases a and b), the wind is parallel to the tidal flow direction and wind waves propagate orthogonal to the tidal flow direction. The growth rates for tide and wind forcing are nearly identical to the tide only case. The fastest growing mode is denoted with a +.

Ground Penetrating radar stratigraphy and dynamics of megaflood gravel dunes

P. Carling *Geography & Environment, University of Southampton, UK - p.a.carling@soton.ac.uk*

C. Bristow *Department of Earth & Planetary Sciences, University of London, London, UK*

A. Litvinov *Institute of Monitoring of Climatic and Ecological Systems, Siberian Branch of the Russian Academy of Sciences, Russian Federation*

1. INTRODUCTION

Ground-penetrating radar was used to elucidate the stratigraphy of Pleistocene gravel dunes in Kuray Basin of the Altai mountains, southern Siberia (Fig. 1). Dunes formed when the Kuray-Chuja lake emptied catastrophically due to ice-dam failure (Carling, 1996a & b). Lake drainage was rapid but with steady reduction in water level and flow direction (Bohorquez et al., 2015). GPR survey-lines acquired across five prominent dunes had a resolution of decimetres, with depth penetration of



Figure 1. Location of the Kuray Basin (K) and the Chuja Basin (C) in the Altai mountains of southern Siberia.

around 20m. The reflections are interpreted using seismic methodology in identifying bounding surfaces and radar facies supplemented by stratigraphic descriptions from excavated pits. Two significant classes of unconformities are identified: (i) a single erosional unconformity at

the dunes base; (ii) several steeply-inclined unconformities within the dunes which truncate underlying reflections but are also downlapped by overlying inclined reflections within the dunes.



Figure 2. View to the southwest across the dunefield with the pine forest of the Tetyo River immediately behind. Steep leeside dune slopes are shadowed.

We identify six radar facies:

Facies 1, basal sub-horizontal discontinuous discordant reflections; Facies 2, poorly-defined discordant reflections within the stoss-toes; Facies 3, planar inclined reflections; Facies 4, sigmoidal inclined reflections; Facies 5, trough fills; Facies 6, low- angle upstream inclined reflections.

The basal unconformity represents the surface cut by flood flows, across which the dunes migrated in a non-aggradational setting. The inclined unconformities may be interpreted in two ways: (a) As erosional surfaces induced by unsteady flow within one flood event, or (b) as erosional surfaces developed by a series of flood events reactivating dunes left stranded by previous floods. Arguments are presented in favour of the latter model, which interpretation is consistent with there having been several dune-forming events within the lake basin.

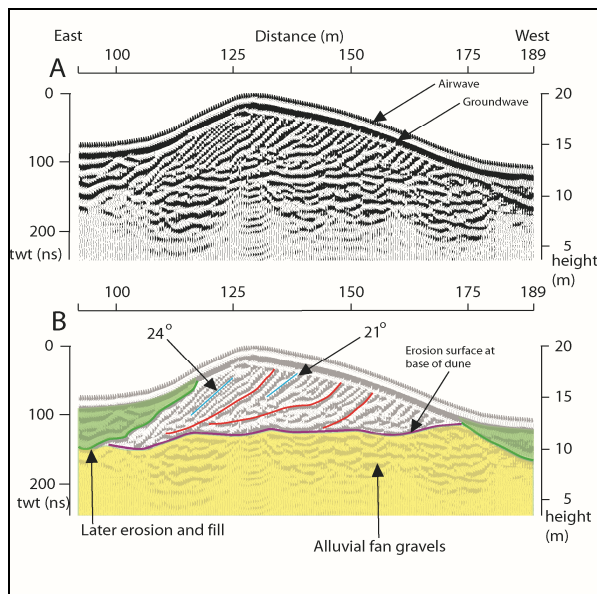


Figure 3. (A) 2012 Radar reflectors for Dune 4; (B) Interpretation of the 2012 radar facies for Dune 4. The well-defined cross-sets (e.g. blue curves) are relatively steep. The radar stratigraphy shows reactivation surfaces (red curves) and the unconformable interface (purple curve) with the underlying gravel deposits. Later fill in the dune troughs (green) has subdued the modern topography. Palaeoflow right to left.

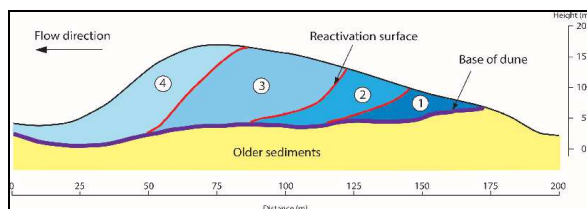


Figure 4. Cartoon interpretation of four packages (1 – 4) of cross-strata separated by bounding reactivation surfaces above a basal unconformity, down-lap and truncation of reflections are represented by small arrows. Package 1 consists of irregular stratification, in the upflow position, deposited as an incipient bedform against which steep cross-sets were deposited once steady flow and the bedform were established. Reactivation surface 1 represents cutting of the lee-side of package 1 during falling flow. RS2 and RS3 represent reactivation surfaces associated with two subsequent events. Packages 2, 3 and 4 represents renewed deposition of cross-sets in the lee of the

bedform stranded after three repeated floods to give a history due to four floods in total.

2. CONCLUSIONS

Large gravel dunes were formed by catastrophic rapid drainage of a Pleistocene ice dammed lake. GPR survey reflections highlight cross-sets due to dune progression in three to four flood events. Three to four unconformities represent reactivation surfaces that separate each cross-set package that developed when the dunes moved on each flood. During lake drainage the dunes migrated for short periods of time. During periods of lake refilling the dunes were submerged by the rising lake water and remained inactive on the lake bed.

3. REFERENCES

- Bohorquez, P., Carling, P.A., Herget, J., 2015, Dynamic simulation of catastrophic Late Pleistocene glacial-lake drainage, Altai Mountains, central Asia. *International Geology Review*, DOI: 10.1080/00206814.2015.1046956
- Carling, P.A. 1996a. Morphology, sedimentology and palaeohydraulic-interpretation of large gravel dunes: Altai Mountains, Siberia. *Sedimentology*, 43, 647-664.
- Carling, P.A. 1996b. A preliminary palaeohydraulic model applied to Late-Quaternary gravel dunes: Altai Mountains, Siberia. In: *Global Continental Changes: The Context of Palaeohydrology*. J. Branson, K.J. Gregory and A. Brown (Editors) *Geol. Soc. London Spec. Publ. No. 115*, 165-179.

Formation of estuarine subaqueous dunes in coarse silt and very fine sand in resuspension-dominated tidal flow conditions

H.Q. Cheng *State Key Laboratory of Estuarine and Coastal Research, East China Normal University, Shanghai 200062, China; Email: hqch@sklec.ecnu.edu.cn*

D.M. Wang *SKLECR, East China Normal University, Shanghai*

T. Y. Wei *SKLECR, East China Normal University, Shanghai*

W. Chen *Institute of Marine and Atmospheric Research, Utrecht University; Email: W.Chen4@uu.nl*

Z. Y. Yang *SKLECR, East China Normal University, Shanghai*

J. F. Li *SKLECR, East China Normal University, Shanghai*

ABSTRACT: We investigated the influence of resuspension on dune formation in coarse silt and very fine sand in the Yangtze estuary focusing on explaining why dunes occur in tidal estuaries with fine sediment ($0.063 < D_{50} < 0.125$ mm) in contrast to what the models suggest. We simultaneously measured dune length and height and flow and suspended sediment concentration (SSC) and analyzed the data to assess the importance of resuspension with periodicity ranging from a few seconds to a few minutes. Equations for the influence of SSC on dune shape in fine sediment were derived using a more complex approach with the same scale level of time-variable SSC as the reference SSC. Results show that subaqueous dune formation is highly correlated with longer periodical resuspension (2–4 min) instead of shorter, periodic, burst-like boils over dune crests (<1 min). Here, we suggest a new analytical model to relate resuspension events to flattened dunes in estuaries.

Morphodynamics, hydrodynamics and stratigraphic architecture of intertidal compound dunes on the open-coast macrotidal flat in the south of Ganghwa Island in Gyeonggi Bay, Korea

Kyungsik Choi *School of Earth and Environmental Sciences, Seoul National University, Seoul, Korea*
– tidalchoi@snu.ac.kr

Joohee Jo *School of Earth and Environmental Sciences, Seoul National University, Seoul, Korea* –
joohe1218@snu.ac.kr

ABSTRACT: Morphodynamics and hydrodynamics of intertidal dunes on the macrotidal flat in Gyeonggi Bay, western coast of Korea were investigated to understand the external controls governing stratigraphic architecture. Simple dunes migrate faster in the channel than on the bank due to greater tidal asymmetry in the channel. The displacement of compound dunes is affected by seasonal storm waves and tidal cycle in the event of storms. Dune morphodynamics are further influenced by the proximity to tidal channel. Combined effects of tidal asymmetry, seasonal variation in the direction of wind-induced waves, precipitation-induced channel mobility, and tidal cycle make the architectures of tidal compound dunes more complicated than those of subtidal setting.

1. INTRODUCTION

Dunes are subaqueous bedforms that are ubiquitously distributed in tidal environments where tidal currents are faster than 0.5 m/s and fine to medium sands are available (Dalrymple and Rhodes, 1995). Dune morphodynamics has been regarded crucial in understanding bedload sediment transport rate and residual tidal currents over various time scales. Non-tidal effects such as wind-induced waves and channel migrations are also known to complicate dune morphodynamics in tidal environments (Choi and Jo, 2015). However, hydrodynamic observations to relate dune morphodynamics to the non-tidal effects are still rarely conducted for intertidal environment.

Tidal dune architecture has received attentions because it differs from that of tidal bars which have a flow-normal architectural component. Depending on tidal asymmetry and current speed, tidal compound dunes exhibit various internal architecture. As tidal environments are influenced by waves and channel migration as well as tidal currents, resultant architecture is presumed to be more complicated. However, impact of non-tidal processes on the stratigraphic architecture of compound dunes is scarcely explored.

The present study documents multi-year observations on the morphodynamics of intertidal dunes in the open-coast macrotidal flat in the northern Gyeonggi Bay, west coast of Korea. Various hydrodynamic conditions governing the morphodynamics of dunes and channel were analyzed based on long-term mooring data. Stratigraphic architecture of intertidal compound dunes was reconstructed based on detailed facies analysis of short cores. Discussion is made on the relative role and significance of tidal and non-tidal processes in formulating the stratigraphic architecture that varies in time and space.

2. STUDY AREA

Yeochari tidal flat is located in the south of Ganghwa Island in the northern Gyeonggi Bay, the largest macrotidal embayment. Bounded by Sukmo Channel in the west and Jangbong Channel in the south, Yeochari tidal flat measures about 6 km in width during spring low tides. Lower intertidal zone of the flat is heavily dissected by large channels that are 200-600 m wide and 1-2.5 m deep at bankfull stage. Tides are semidiurnal with mean tidal ranges ranging from 5 m during neap tides to 9 m during spring tides. Tidal current

speeds reach 1.5 m/s during spring tides. Annual precipitation ranges between 1300 and 1400 mm with two thirds occurring during summertime rainy season. Winds are generally stronger during winter and early spring when winds are northwesterly, and during summertime typhoon season when southwesterly to southerly winds prevail.

3. MATERIALS AND METHODS

High-precision profiling of dunes and tidal channel were conducted twenty times from 2011 to 2015 along four transects using RTK GPS. Current profiles and directions were measured using RDI ADCP moored at three locations for three times representing summer and winter. Wave data were obtained using pressure wave gauges at two locations for summer and AWAC at one location for winter. SSCs were measured at one location using OBS. A total of 34 undisturbed short cores were collected for the analysis of sedimentary facies and stratigraphic architecture of dunes and channel.

4. RESULTS

Dunes are present on the tributary channel and channel banks in the lower intertidal zone of Yeochari tidal flat (Figure 1). The tributary channel has an asymmetric profile with steep slope on the southern channel bank and a gentle slope on the northern channel bank (Figure 2). Simple dunes on the tributary channel migrate seaward as fast as 1-4 m/day. In contrast, those on the southern channel bank migrate either landward or seaward as fast as 0.1-1 m/day during spring to fall and 1-2 m/day during winter. Compound dunes on the southern channel bank migrate either landward or seaward at much slower rates of 2-3 m/month. Tributary channel migrates at variable rates ranging from 1 to 18 m/month with greater rates occurring during summertime rainy season. Tributary channel is ebb-dominated with pronounced tidal asymmetry, whereas tidal flats on the southern channel bank are flood-dominated with smaller tidal asymmetry. Wind-induced waves with significant wave heights over 0.4 m seem to modulate tide-induced sediment supply. Westerly to northwesterly waves during winter to spring accentuate ebbward migration of compound dunes, whereas southerly to southwesterly waves during summertime typhoon result in floodward

migration. Channel migration and displacement of compound dunes resulted in a composite architecture in which a coarsening-up compound dune succession formed on the channel bank overlies a fining-up simple dune succession formed in the point bar of the channel. Master bedding surfaces within the compound dune succession dip nearly opposite to or in the same quadrant to the accretion surfaces of the point bar.



Figure 1. Drone image showing the location of compound dunes (CD) and simple dunes (SD) in the lower intertidal zone of Yeochari tidal flat. Profiles along transect XY and YZ are given in Figure 2.

5. DISCUSSION

Compound dunes on the southern channel bank migrated either landward or seaward. Considering nearly symmetrical tides with slight flood dominance, seaward migration of the compound dunes cannot be explained by tidal currents only. Significant wave heights over 0.6 m were frequently measured during wintertime and summertime. Observed waves are sufficient to trigger the migration of the compound dunes. During wintertime, westerly to northwesterly waves with significant wave height over 0.6 m were mainly developed around high tide slack and early ebb tides. Notable seaward migration of the compound dunes indicates that sediment transport occurred during ebb tides. In summer of 2014, storm events with strong southerly to southeasterly winds occurred during the early stage of ebb tide after flood slack. Despite the prevalence of onshore winds, however, compound dunes migrated seaward. Choi and Jo (2015) documented a similar but opposite trend in which the landward

displacement of the compound dunes occurred under the presence of strong offshore winds during wintertime. This suggests that the timing of wave activity over a tidal cycle is critical in the migration of the compound dunes. This assertion is congruent with the fact that waves are responsible for the resuspension of sandy sediments and the transport of resuspended sediments is controlled by the direction of residual tidal currents and wind-induced currents. Unlike subtidal setting, the duration and fetch distance of wind-induced waves are limited by tidal cycle on the intertidal flat.

dune architecture. However, the impact of non-tidal events is not easily identifiable in the intertidal setting as the response of the compound dunes to non-tidal events can be modulated by tidal cycle, proximity to channel, and prevailing wind directions that vary in time and space. In addition, the response time of the intertidal compound dunes to the non-tidal events is much shorter than that of subtidal equivalents. As a result, the effect of non-tidal events can be frequently commingled with that of tidal currents within the architecture of compound dunes.

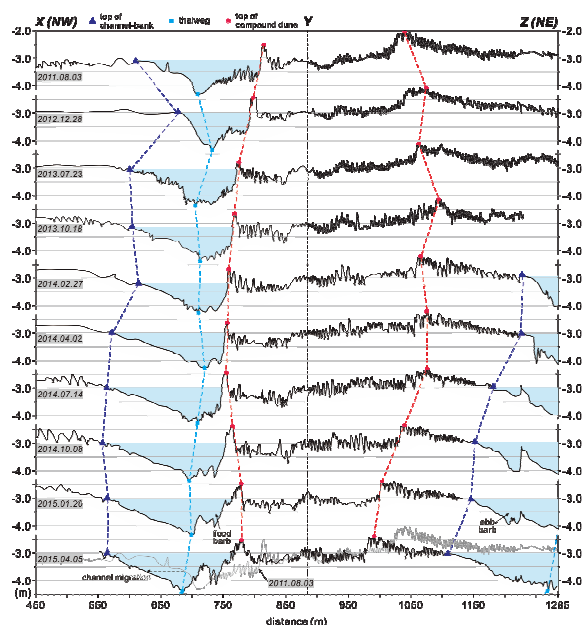


Figure 2. Repeated profiles of tributary channel and dunes along transect XYZ. Compound dunes displaced either floodward or ebbward while the tributary channel continued to migrate northwestward or northern channel bank direction along transect XY. Note the contraction of simple dune-covered area as a result of tributary channel migration along transect YZ.

Subtidal compound dunes can migrate toward subordinate current direction in the case of non-tidal events such as seasonal river discharge and wind driven currents (Le Bot and Trentesaux, 2004; Kostaschuk and Best, 2005; Ferret et al., 2010). Considering that the events are annual and semidiurnal tidal currents are unable to reverse the asymmetry of subtidal large dunes that requires longer response time, the presence of bidirectional master bedding surfaces substantiates the effects of non-tidal events in the otherwise tidal compound

6. CONCLUSIONS

Compound and simple dunes on the channel and channel bank in the lower intertidal zone of Yeochari tidal flat in the northern Gyeonggi Bay migrate actively in response to tides, waves and rain-induced discharge fluctuation. Combined influences of tidal asymmetry, seasonal variation in the direction of wind-induced waves, and the mobility tidal channel, and tidal cycle complicated the architecture of intertidal compound dunes whose master bedding surfaces may dip nearly opposite to or in the same quadrant of those of accretion surfaces of point bars of the channel.

7. ACKNOWLEDGMENT

This study was supported by the Energy Efficiency and Resources of the Korea Institute of Energy Technology Evaluation and Planning (KETEP) grant funded by the Ministry of Trade, Industry and Energy (MOTIE), Republic of Korea, and Research Institute of Oceanography (RIO) at Seoul National University.

8. REFERENCES

- Choi, K.S. & Jo, J. 2015. Morphodynamics and stratigraphic architecture of compound dunes on the open-coast macrotidal flat in the northern Gyeonggi Bay, west coast of Korea. *Marine Geology* 366: 34-48.
- Dalrymple, R.W. & Rhodes, R.N. 1995. Estuarine dunes and bars. In G.M.E. Perillo (ed), *Geomorphology and Sedimentology of Estuaries: Developments in Sedimentology*: 359-422. Amsterdam: Elsevier.
- Ferret, Y., Le Bot, S., Tessier, B., Garlan, T. & Lafite, R. 2010. Migration and internal architecture of marine dunes in the eastern English Channel over 14

- and 56 year intervals: the influence of tides and decennial storms. *Earth Surface Processes and Landforms* 35: 1480-1493.
- Kostaschuk, R. & Best, J. 2005. Response of sand dunes to variations in tidal flow: Fraser Estuary, Canada. *Journal of Geophysical Research* 110: F04S04, doi:10.1029/2004JF000176.
- Le Bot, S. & Trentesaux, A. 2004. Types of internal structure and external morphology of submarine dunes under the influence of tide- and wind-driven processes (Dover Strait, northern France). *Marine Geology* 211: 143-168.

Low-angle dunes in big rivers: morphology, occurrence and speculations on their origin

J. Cisneros *Department of Geology, University of Illinois at Urbana-Champaign, USA – jcisnrs2@illinois.edu*

J. Best *Departments of Geology, Geography and GIS, Mechanical Science and Engineering and Ven Te Chow Hydrosystems Laboratory, University of Illinois at Urbana-Champaign, Champaign, Illinois, – jimbest@illinois.edu*

ABSTRACT: Low-angle dunes (LADs), which have often been defined as those dunes possessing a leeside angle less than 30 degrees, have been reported from several large rivers and shown to possess a different fluid dynamics, and likely internal stratification, to those produced by high-angle dunes (HADs). Herein, we assemble and analyze available data to present a dataset concerning the leeside angle, morphology and classification of dunes in a range of large rivers. We find that low-angle dunes also co-exist with higher angle dunes in large alluvial channels, and suggest their presence is linked to several factors, including suspended sediment concentration, grain size and bedform superimposition. We propose that the classification of LADs should be based on the leeside angle at which permanent flow separation ceases to exist, or less than *c.* of 15°.

1. INTRODUCTION

Dunes are the most common bedform generated in sand-grade alluvial channels, and form the major building block within ancient sandy river channel sediments. Sand dune size ranges from decimetres to hundreds of metres in wavelength, and from *c.* 0.05m to maybe more than 10m in height in some of the worlds largest alluvial channels. Most interpretations of dunes have relied on analogies with dunes that have been well-documented in experimental studies and examination of smaller natural channels, in which the dunes possess a leeside angle at the angle-of-repose of the sediment. However, research over the past 20 years has shown the presence of dunes that possess a lower leeside angle, and which may have a more complex leeside morphology. Recent research has also documented the flow associated with such low-angle dunes, both in the laboratory (Best and Kostaschuk, 2002; Motamedi et al., 2012, 2014) as well as in the field (Roden, 1998; Best et al., 2007; Bradley et al., 2013). Laboratory models have demonstrated the presence of an intermittent zone of flow separation in the leeside of low-angle dunes, and suggested an angle of *c.* 15° is required to promote the onset of permanent flow separation

(Best and Kostaschuk, 2002; Motamedi et al., 2012, 2014). Such modification of the leeside flow and flow separation zone has many implications for flow resistance and the parameterization of flow separation associated with dunes (Paarlberg et al., 2007, 2009).

Recent work has also suggested that low-angle dunes may be the predominant type of dune form in large rivers (Roden, 1998; Kostaschuk and Ilersich, 1995; Kostaschuk and Villard, 1996, 1999). Several explanations have been proposed for the origin of low-angle dunes, including: i) The presence of fine material in suspension, which is reasoned to dampen turbulence and lessen the leeside influence of flow separation (Baas et al., 2015; Naqshband et al., 2014; Saunderson and Lockett, 1983); ii) increased sediment bypass of the leeside face, leading to increased deposition in the trough region and thus lessening dune height; and iii) the influence and type of leeside grain avalanche processes that have been proposed to differ on low-angle dunes in large rivers (Hendershot et al., 2015)

Here, we present results concerning the morphological characterization of dunes from a range of the world's big rivers, including the

Amazon, Mississippi, Parana, Mekong, Columbia and Jamuna Rivers. We use this data to examine the magnitude and distribution of leeside angles, and utilize this dataset to discuss the full range of factors that may lead to such low-angle leeside slopes. We also propose a classification threshold for such dunes that relies on the leeside angle at which permanent flow separation is absent, which is *c.* 15° .

2. METHODS

We have assembled, compiled and analyzed data from a wide range of sources that have reported on the form of dunes within large alluvial channels. This data ranges from longitudinal traces of dunes obtained using single beam echo sounder surveys, through to full 3D characterization of the bed using multibeam echosounding. The datasets are analyzed to quantify the leeside angle of dunes, as well as leeside shape, dune height, dune wavelength, the presence and type of bedform superimposition and the relationship of dune height to water depth.

3. RESULTS

Our results show that many large rivers contain dunes that possess a wide range of leeside angles, and that low-angle dunes are not the only type of dune present in these channels (Figure 1). However, lower leeside angles are dominant in the rivers analyzed (Figure 1). Leeside angle is found to vary considerably across the width of an individual sinuous-crested dune, and also between successive downstream dunes. This suggests that the processes that control production of these dunes are not related solely to suspended sediment concentration or water depth, and that a range of factors are influential in determining the leeside angle. Analysis of these datasets allows plotting of probability distributions (pdfs) of leeside angle for a range of large rivers. Figures 1b,d show the pdfs of two dune datasets from the Missouri River and Parana River, showing average leeside angles are 9.5 and 6.2° respectively, with between 80 and 90% of the leesides being less than 15° . These pdfs are seen to fit well with a gamma distribution. We also present examples of the longitudinal profiles of a range of morphometric types of dunes in large rivers, including those with high-angle leesides, humpback-shaped dunes with a brink point

upstream of the crest, dunes with and without secondary superimposed bedforms, and low-angle dunes with a more simple morphology (Figure 1c).

These data are used to highlight several factors that may influence the leeside angle of dunes within large rivers, including:

- 1) The grain size and grain size distribution of the sediment.
- 2) The presence of fine material in suspension that is reasoned to dampen leeside turbulence.
- 3) The influence of superimposed bedforms that serve to erode the leeside during bedform amalgamation and may lead to lower-angle leeside slopes.
- 4) The influence of superimposed bedforms that may act to provide a region of sheltered flow in the leeside region that can affect both the nature/extent of flow separation and the ability for smaller bedforms to rework with leeside slope.

Lastly, our review of the literature suggests that the classification of dunes as low-angle or high-angle should be based on a physical rationale rather than an arbitrary value, such as 30° , which may vary with grain size and grain size sorting. Rather, we propose a definition of low-angle dunes as those that do not possess a zone of permanently separated flow in the leeside. Experimental (Best and Kostaschuk, 2002; Motamedi et al., 2012, 2014) and numerical (Kotapati et al., 2014) modelling suggests that 15° may be an appropriate angle on which to base this classification.

4. CONCLUSIONS

Dunes formed in sand-grade material in large rivers show a range of leeside angles that span from several degrees and up to, and beyond, the angle of repose (*c.* 30°), but appear dominated by leeside slopes less than 10° . Low and high-angle dunes may co-exist within the same reach of an alluvial channel, and suggest that suspended sediment and water depth are thus not the sole factors responsible for their generation. Bedform superimposition, and the influence of smaller, more rapidly migrating bedforms, upon the leeside flow field and dune leeside slope, are important in producing low-angle dunes.

5. ACKNOWLEDGMENTS

We are grateful to our many colleagues who provided access to datasets concerning dune morphology from their research, and which allowed compilation of this dataset.

6. REFERENCES

- Baas, J.H., Best, J.L. and Peakall, J. 2015 Predicting bedforms and primary current stratification in cohesive mixtures of mud and sand. *Journal of the Geological Society*, doi:10.1144/jgs2015-024.
- Best, J.L. 2005 An experimental study of turbulent flow over a low-angle dune, *Journal of Geophysical Research*, 110, doi: 10.1029/2000JC000294.
- Best J.L., and R.A. Kostaschuk 2002, An experimental study of turbulent flow over a low-angle dune, *Journal of Geophysical Research*, 107, 3135 (1-18). doi:10.1029/2000JC000294.
- Best, J.L., Ashworth, P.J., Sarker, M.H. and Roden, J. 2007. The Jamuna-Brahmaputra River, Bangladesh. In: *Large Rivers: Geomorphology and Management* (Ed: Gupta, A.), 395-433, John Wiley and Sons.
- Bradley, R. W., Venditti J.G., Kostaschuk, R.A., Church, M., Hendershot, M. L. & Allison M.A. Flow and sediment suspension events over low-angle dunes: Fraser Estuary, Canada. *Journal of Geophysical Research - Earth Surface*, 118, 1693–1709, doi:10.1002/jgrf.20118. 2013.
- Hendershot, M.L., Venditti, J.G., Bradley, R., Kostaschuk, R.A., Church, M.A. & Allison, M.A. 2015 (in press) Response of low angle dunes to variable flow. *Sedimentology*
- Kostaschuk, R.A. & Illersich, S.A. 19956 Dune geometry and sediment transport: Fraser River, Canada. In: *River Geomorphology* (Ed: Hickin, E.J.), 19-36, John Wiley and Sons.
- Kostaschuk, R.A. & Villard, P.V. 1996 Flow and sediment transport over large subaqueous dunes: Fraser River, Canada. *Sedimentology*, 43, 849–863.
- Kostaschuk, R.A. & Villard, P.V. 1999 Turbulent suspension over dunes. In: *Fluvial Sedimentology VI* (Ed. Smith, N.D and Roger, J). Special Publication of the International Association of Sedimentologists, 28, 3-13.
- Kotapati, R.B., Shock, R. and Chen, H. 2014 Lattice-Boltzmann simulations of flows over backward-facing inclined steps. *International Journal of Modern Physics C*, 25, doi: 0.1142/S0129183113400214.
- Motamedi, A., Afzalimehr, H., Gallichand, J. and Abadi, E.F.N. 2012 Lee angle effects in near bed turbulence: an experimental study on low and sharp angle dunes, *Int. J. Hydraulic Engineering*, 1(6), 68-74.
- Motamedi, A., Afzalimehr, H., Singh, V.P. and Dufresne, L. 2014 Experimental study on the influence of dune dimensions on flow separation, *J. Hydrol. Eng.*, 19, 78-86.
- Naqshband, S.J., Ribberink, J.S. and Hulscher, S.J.M.H. 2014 Using both free surface and sediment transport mode parameters in defining the morphology of river dunes and their evolution tom upper stage plane beds, *Journal of Hydraulic Engineering*, 140, doi: 10.1061/(ASCE)HY.1943-7900.0000873.
- Paarlberg, A.J., Dohmen-Janssen, C.M., Hulscher, S.J.M.H. & Termes, P. 2007 A parameterization of flow separation over subaqueous dunes, *Water Resources Research*, 43, W12417, doi: 10.1029/2006WR005425.
- Paarlberg, A.J., Dohmen-Janssen, C.M., Hulscher, S.J.M.H. & Termes, P. 2009 Modeling river dune evolution using a parametrization of flow separation, *Journal of Geophysical Research – Earth Surface*, 114, doi:10.1029/2007JF00091.
- Roden J.E. 1998 The sedimentology and dynamics of mega-dunes, Jamuna River, Bangladesh, Unpublished PhD thesis, Department of Earth Sciences and School of Geography, University of Leeds, Leeds, United Kingdom, 310 pp.
- Saunderson, H.C. and Lockett, F.P. 1983 Flume experiments on bedforms and structures at the dune-plane bed transition. *Special Publication of the International Association of Sedimentologists* 6, 49-58.

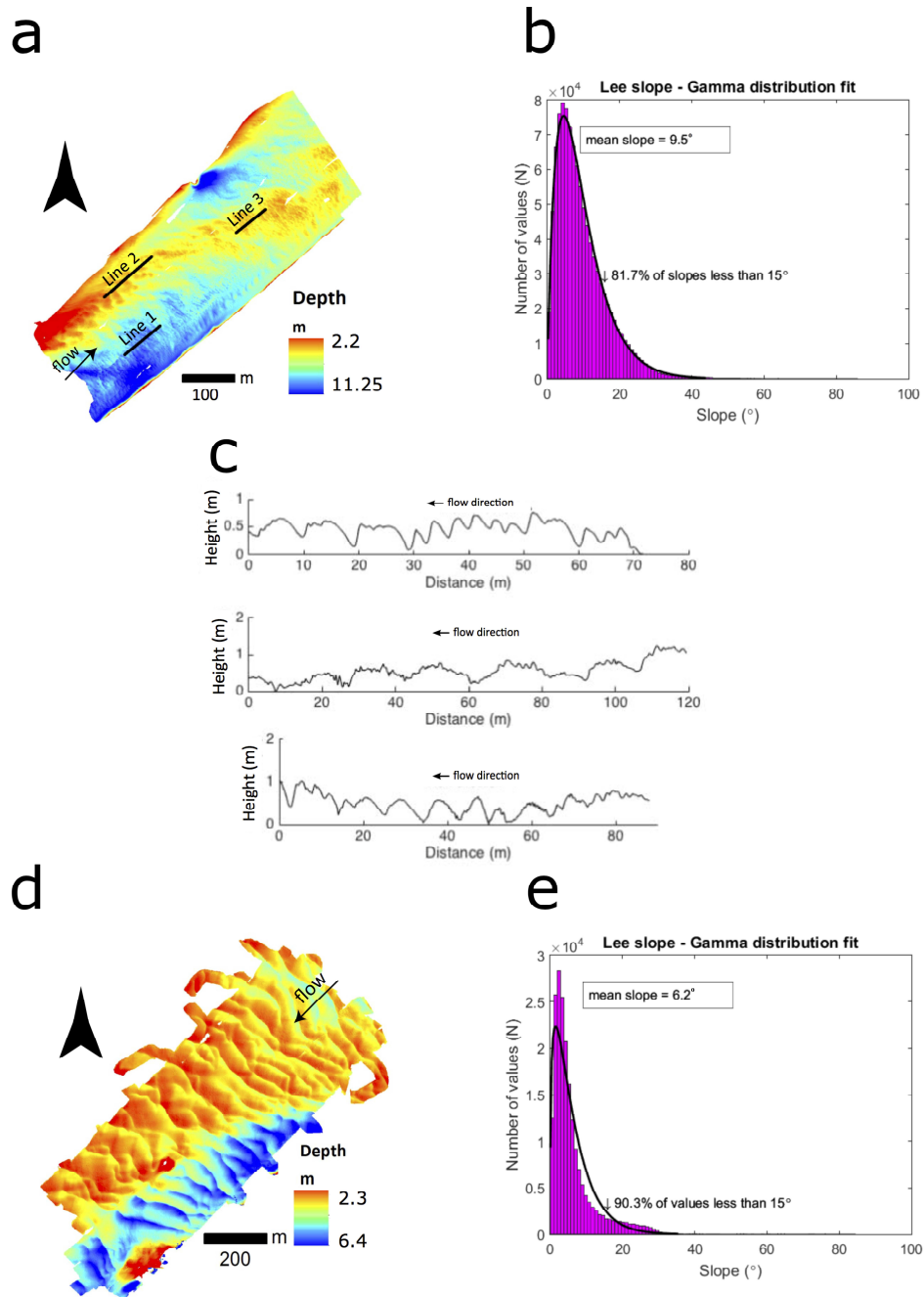


Figure 1. Example of the leeside angles of sand dunes in the a-c) Missouri River, USA, and d,e) Parana River, Argentina, using MBES survey data. a,e) Plots showing bed elevation, illustrating a range of different size sand dunes. b,e) Frequency distribution of lee slopes ($\pm 80^\circ$) from flow direction and the resulting stoss slopes; c) Bed elevation profile of bedforms from the Missouri River ($\times 10$ vertical exaggeration). From top to bottom: Line 1 dunes with a characteristic wavelength of $c. 5$ m; Line 2 dunes with a characteristic wavelength of $c. 10$ m and smaller superimposed dunes on the stoss side; Line 3 dunes with a characteristic wavelength of $c. 10$ m.

KEYNOTE: Stability of river bed forms

M. Colombini *Università di Genova, DICCA, Genova, ITALY – col@dicca.unige.it*

ABSTRACT: Linear stability analyses provide a deep insight into the mechanisms that drive bed form formation, being able to identify regions in the space of the parameters where bed forms are expected to form and to show how the onset of instability is controlled by the relevant flow and sediment parameters. Moreover, the role of some parameters in inducing a transition between different types of bed forms can be made evident, as well as the possibility for different kinds of bed forms to coexist. By examining the results obtained in the framework of linear stability analysis, a unified view of the formation of free bed forms in straight channels is obtained.

1. INTRODUCTION

A variety of sediment waves develops from an initially flat bed when a uniform flow over an erodible bed is considered. They can be classified in terms of the geometric (e.g. wavelength, amplitude, shape) or kinematic (e.g. upstream or downstream propagation) characteristics of the bed form itself, in terms of the characteristics of the flow (e.g. subcritical or supercritical, hydraulically smooth or rough regime, amplitude and phase of the free-surface wave with respect to the bed wave) or of the sediments (e.g. finer or coarser material, bed load or suspended load). In general, more than one aspect is needed to mark the distinction. For these reasons, predicting, for any given set of the relevant flow and sediment parameters, which particular bed pattern will arise among the variety of possible, and often similar, configurations, is indeed a challenging task. Although very different scales are involved and several effects can be invoked to drive the instability process, yet a simple glance at the linearized form of the Exner continuity equation reveals that a single mechanism is ultimately responsible for the appearance of those periodic patterns we usually refer to as bed forms: the lag between the sediment transport and the bed

topography, which controls both the growth and the celerity of the wave. Several effects contribute to this lag, bed evolution being ultimately due to a delicate balance between stabilizing and destabilizing effects.

2. BED FORM CLASSIFICATION

How can bed forms be told apart? How can one distinguish a dune from an antidune? Or a dune from a ripple? Or an alternate bar from an oblique dune? These questions may sound naive for the experimenter, who can often easily name a bed form just by looking at it, but are not so obvious for the theoretician, who, playing with different sets of the flow and sediment parameters, observes similar periodic patterns emerge. Moreover, though laboratory experiments are carefully designed to isolate a single type of bed form from the others, bed patterns often arise that do not easily fit in any of the above schematic categories. River bed forms are commonly classified in terms of their characteristic longitudinal wavelengths. The distinction of bed patterns into micro-, meso- and macro-forms dates back to the first geomorphological observations (Allen, 1982) and guided both experimental and theoretical researches in this field in the last century:

nowadays, it is widely accepted that ripples scale with sediment grain size, dunes and antidunes with the flow depth, bars with the channel width. However, note that the word “scale” should be used with some caution: since the constant of proportionality can go from a few units (for bars) up to one thousand (for ripples), in this context “scale” does not represent an actual order of magnitude but, more appropriately, it should be considered as the most relevant physical length scale for that particular bed form.

Thus notwithstanding, the formation of river patterns is driven by the same basic mechanism so that such a neat separation among different bed forms should not always be expected to hold when the relevant flow and sediment parameters are varied continuously.

2.1. The case of dunes and ripples.

Let us consider differences and similarities between dunes and ripples. They both appear in the subcritical regime and propagate downstream, so that it is possible to discriminate ones from the others only in terms of their characteristic wavelengths, ripples typically being about one order of magnitude shorter than dunes.

It may be useful to report here the definition of dunes given by Guy, Simons & Richardson (1966), denoted in the following as GSR, in their remarkable experimental work: “*Dunes are bed features larger than ripples that are out of phase with any water-surface gravity waves that accompany them. Dunes generally form at larger flow and sediment transport rates than do ripples; however, ripples often form on the upstream slopes of dunes at smaller rates of flow*”. About half a century later, this distinction, albeit being evident to the experimenters, is still debated. Indeed, as Raudkivi (2006) writes: “*the change from ripples to dunes is terra incognita*”. When attempting to distinguish dunes from ripples, the only strong argument available remains that of the different wavelength, so that in the literature more than often the terms “ripple” and “dune” are interchanged, as if they were synonyms. Moreover, a variety of mixed terms (mega-ripples, micro-dunes, but also giant dunes and micro-ripples) have been coined.

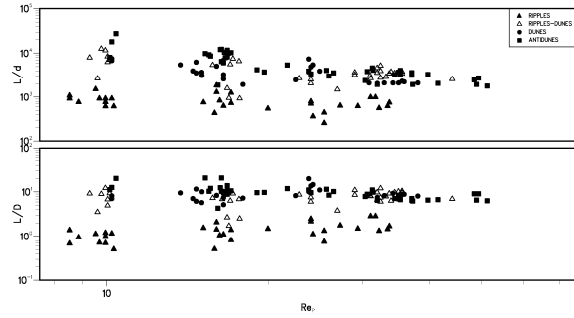


Figure 2.1: Experiments from GSR data sets: ripple and dune wavelengths as a function of Re_p ; upper panel: scaled with the sediment grain size; lower panel: scaled with the flow depth.

In Figure 2.1, experimental data on dune and ripple wavelengths from the GSR dataset are presented, scaled with the sediment diameter d^* and with the flow depth D^* in the upper and lower panels, respectively.

The particle Reynolds number Re_p is defined as

$$Re_p = \frac{\sqrt{(s-1)gd^{*3}}}{\nu} \quad (2.1)$$

where g is the gravitational acceleration, s the relative density of the sediment and ν is the kinematic viscosity of the fluid.

For the experimental range of grain sizes considered, ripple wavelengths appear to better correlate with the sediment diameter, since their ratio is found to attain an almost constant value of about 1000, as predicted by Yalin (1977), although a fairly large scatter is present. The opposite is true for dune wavelengths, which better scale with the flow depth, with a value of the ratio of about 10. It must be pointed out that, irrespective of the scaling adopted, in both panels the characteristic wavelengths for dunes and ripples are separated by about one decade.

Experimental observations reveal that dunes and ripples are morphologically similar, can coexist but are, indeed, distinct bed forms. Hence, a question remains unanswered: under which flow and sediment conditions should one expect to find ripples, or dunes or both? We will see in the following section that stability analyses can provide a hint in this regard, by relating ripple appearance to the transitional or smooth regime, whereas in the rough regime only dunes can form.

2.2. The case of alternate bars and oblique dunes.

The situation becomes even more complex when three-dimensionality is considered, since several spanwise modes can be identified, depending on the integer ratio between the channel width and the transverse half-wavelength. A typical example involves alternate and central bars, which are associated to the first and the second spanwise mode, respectively.

To investigate three-dimensional bed forms, the collection of flume experiments concerning dunes, antidunes and ripples of GSR, has been integrated with a data set, denoted as JSM, composed by the sand experimental runs extracted from Jaeggi (1984), Sukegawa (1971) and Muramoto and Fujita (1978). These runs have been selected among others since a clear distinction was made between alternate and diagonal bars, the latter being typically shorter than the former.

The distinction between diagonal and alternate bars was firstly proposed by Einstein and Shen (1964), who observed that diagonal bars are: “*a special case of the diagonal dune pattern, which occurs when the Froude number of the flow is nearly unity, at certain depth-to-width ratios. This pattern probably results from the water surface disturbance, since the diagonal bars oscillated transversely with the wave velocity of water depth and the entire bed pattern travels rapidly downstream with the flow.*”.

In Figure 2.2, wavelength data of dunes, antidunes and bars extracted from the GSR and JSM data sets are presented. Data have been normalized with the half-width of the channel in the upper panel and with the flow depth in the lower panel. A comparison between the two panels reveals that bars do not scale properly with flow depth or, at least, they are more correlated with channel width. The opposite is true for dunes and antidunes.

As for the case of dunes and ripples, irrespective of the scale chosen to normalize, alternate bars are seen to be about an order of magnitude longer than dunes and antidunes. Diagonal bars seem to not fit with any of the scalings, their wavelengths falling just in between. Experimental observations suggest that diagonal bars can be considered as intermediate bed forms associated with the

transition of dunes from two- to three-dimensional configurations.

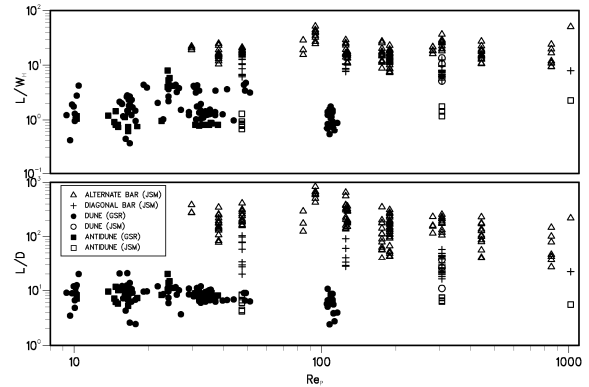


Figure 2.2: Experiments from GSR and JSM data sets: bars and dunes wavelengths as a function of the particle Reynolds number Re_p ; upper panel: scaled with the half-width of the channel; lower panel: scaled with flow depth.

Indeed, stability analysis confirms this suggestion, showing that diagonal bars represent the first transverse mode of instability of oblique dunes, which is morphologically similar to alternate bars. Alternatively, diagonal bars can be thought of as the results of the influence of the flow depth (and thus of the Froude number) on alternate bars.

3. THE PARAMETER SPACE

Bed form experimental measurements are usually collected at the end of the runs and are therefore relative to mature bed forms. To eliminate the effects of form resistance and of the sidewalls, an equivalent uniform flow is sought characterized by the same area velocity U^* and exerting the same shear stress on the bed, expressed in terms of the friction velocity u_f^* . These two quantities are related by a nondimensional Chézy coefficient C :

$$C = \frac{U}{u_f} = \sqrt{\frac{8}{f}} \quad (3.1)$$

where f is the Darcy-Weisbach friction coefficient. On simple dimensional ground, the coefficient C can be shown to depend on two nondimensional parameters, both related to the bed roughness z_R :

$$C = C(z_R, Re_R) \quad (3.2)$$

where z_R is the nondimensional roughness, which expresses the ratio between the bed roughness and the flow depth, and Re_R is the roughness Reynolds number, which expresses the ratio between the bed

roughness and the thickness of the viscous sublayer.

Moreover, it is customary to set the bed roughness equal to 2.5 times the grain diameter d^* , so that:

$$z_R = 2.5d \quad Re_R = 2.5 \frac{u_f^* d^*}{\nu} \quad (3.3)$$

where d represents the nondimensional grain size.

Several empirical relationships (ASCE, 1963; Cheng, 2008) are available for the determination of the function C of (3.2) in the different flow regimes.

Typically, river flow pertains to the turbulent rough regime ($Re_R > 70$) so that the role of Re_R can safely be neglected in the study of most bed forms. However, for relatively fine sediment and for relatively small values of the friction velocity (as is the case for ripples), flow can reach the transitional ($5 < Re_R < 70$) or the hydraulically smooth ($Re_R < 5$) regime.

Among the relevant flow and sediment parameters, we recall the Froude number Fr and the Shields parameter θ .

$$Fr = \frac{U^*}{\sqrt{gD^*}} \quad \theta = \frac{u_f^{*2}}{(s-1)gd^*} \quad (3.4)$$

It is worth noting that the parameters just presented are interrelated. Hence, we can write, for example:

$$\theta = \frac{Fr^2}{(s-1)dC^2} \quad Re_R = 2.5\sqrt{\theta}Re_p \quad (3.5)$$

Hence, if hydraulically rough regime conditions are assumed, as it is customary for most river bed forms, only two parameters are to be set to identify the state of the system: one between the nondimensional sediment grain size d and the conductance Chézy coefficient C , which are related by (3.2), and one among the Froude number Fr and the Shields stress θ , which are related by (3.5).

If ripples have to be considered, then a third parameter must enter the analysis, namely a Reynolds number: either the particle Reynolds number Re_p or the roughness Reynolds number Re_R can be chosen, the two being related by (3.5).

4. BED FORM STABILITY

What is linear stability analysis all about?

Let us consider a system under steady equilibrium conditions and imagine to alter the state of this system (the so called 'base state') by slightly modifying the values of the variables and of the parameter that characterize the state of the system itself. If the perturbations are small enough, then the equations that govern the system can be suitably linearized around the base state and an eigenvalue problem is obtained, the solution of which provides information on the stability of the system.

In the study of river bed forms, the base flow is typically a uniform flow in an infinitely wide channel with active sediment transport. Perturbations, are assigned a specific spatial structure, which is periodic in the longitudinal streamwise direction, with wavenumber k_x , (dunes, antidunes, ripples), and in the transverse spanwise direction (alternate bars, oblique dunes), with wavenumber k_y . A specific temporal structure is assigned as well, which allows the perturbations to exponentially grow (decay) in amplitude, depending on the positive (negative) sign of the growth rate, as they propagate downstream (upstream) depending on the positive (negative) sign of the celerity.

Without entering into the details, it may be worthwhile at this point to outline the procedure that leads from the formulation of the problem to the actual evaluation of the growth rate and celerity.

First of all, the problem must be formulated, which means that a suitable set of equations has to be provided, whereby the dynamics of the flow-bed system is appropriately described. We can stick on generalities here by saying that the flow and the sediment transport models should be the simplest possible for the specific process one wants to simulate.

Focussing on the flow model, if we aim at describing the formation of dunes and antidunes, then the model should account for the interactions between the free-surface and the bed, so that we can distinguish between sub- and super-critical bed forms. Hydraulically rough conditions can be safely assumed. On the other hand, if the goal is the modelling of ripples, the free-surface effect can be disregarded, but the model should cover the smooth and transitional regimes, since this appears

to be the characteristic feature of ripples. Double-periodic bed forms like alternate bars or oblique dunes would in principle require a three-dimensional flow model, even though simpler depth-averaged models can be sufficient to describe the flow if the longitudinal and transverse wavelengths are large enough with respect to the flow depth so as to satisfy the shallow-water approximation, as is the case for bars.

The minimal ingredients for the sediment transport model are the Exner equation and a suitable relationship that provides the amount of sediment moving as bedload in terms of the Shields stress.

For any given set of the flow and sediment transport parameters, the solution of the eigenvalue problem obtained after linearization provides the growth rate and celerity of the bed perturbations as a function of the wavenumber(s). Stability plots can be constructed showing the ranges of unstable (positive growth rate) and stable (negative growth rate) wavenumbers. Marginal (vanishing growth rate) curves mark the borders between stable and unstable regions. Moreover, the wavenumber of maximum growth rate identifies the wavelengths that are likely to be selected by the instability process.

The stability plot of in Figure 4.1 is relevant for the study of dunes and antidunes (Colombini, 2004). The shaded areas represent the unstable regions for dunes (lower area) and antidunes (upper area).

Let us perform an ideal laboratory experiment, whereby we want to investigate the transition from dunes to antidunes observed as the Froude number is increased. Moreover, we want to keep the flow depth constant, so as to maintain the same value of the nondimensional grain size d and thus of C . This can be accomplished by letting the discharge increase, but note that, in order to keep the depth constant, the average slope of the channel must increase as well.

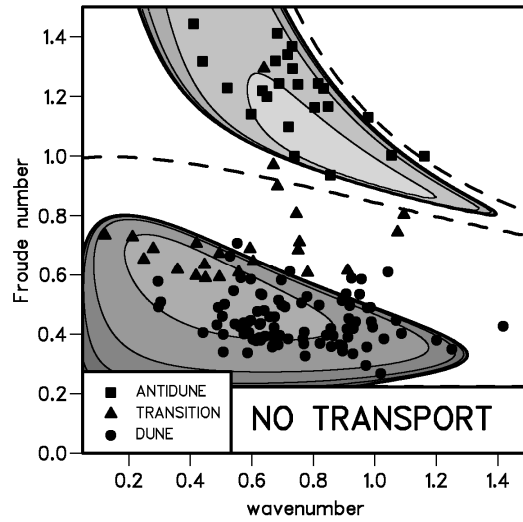


Figure 4.1: Stability plots showing the region of instability for dunes and antidunes. Markers represent experimental data from GSR.

By doing so, we move vertically along the plot of Figure 4.1, which has been obtained for a fixed value of the conductance coefficient C .

In our experiment, starting from very low values of the Froude number, we cross, in turn, the no-transport boundary (where sediments start to move), the dune region (where dunes are unstable), the upper plane bed region (where neither dunes nor antidunes form) and, finally, the antidune region (where antidunes are unstable).

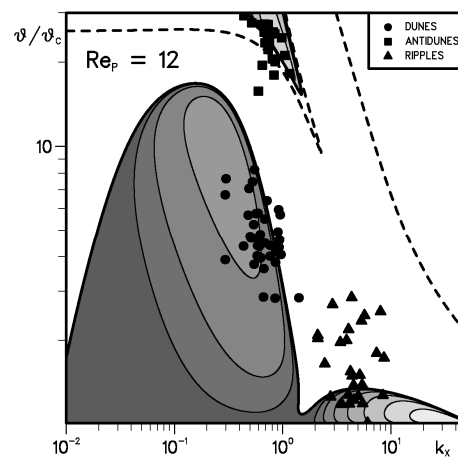


Figure 4.2: Stability plot showing the region of instability for dunes and ripples. Markers represent experimental data from GSR.

The stability plot of Figure 4.2 is relevant for the study of ripple formation (Colombini & Stocchino, 2011). The value of Re_p has been chosen small

enough for the flow to be in the hydraulically smooth regime when the Shields number is close to the threshold for sediment motion. For relatively small values of θ , two maxima of the growth rate are observed, one characterized by a wavenumber (scaled with flow depth) of $O(1)$, which represents dunes, the other of $O(10)$, which represents ripples. The presence of two maxima indicates that both ripples and dune are simultaneously unstable and compete. If a higher Re_p (i.e. a coarser material) is used, the unstable region on the right disappears and only dunes are predicted to form.

Finally, although this result cannot be illustrated by means of a single plot, a three-dimensional stability analysis is able to shed some light on the transition from two-dimensional dunes to alternate bars observed as the flow gets shallower, which includes the formation of diagonal bars as intermediate bed forms (Colombini & Stocchino, 2012).

5. CONCLUSIONS

Linear stability analysis provides a deep insight on the mechanisms that drive the formation of bed forms and on the parameter that controls the onset of the instability, together with an estimate of the most unstable wavelength, the one that will likely be selected by the instability process.

Since one of the outputs of a linear stability analysis is the regime (i.e. the region in the parameter space) where some particular bed form is expected to appear, bed form regime diagrams can be built, providing theoretical support to the analogous experimental diagrams, which guided the research on bed forms in the last decades (e.g. Vanoni, 1974). Moreover, linear stability allows to investigate the boundaries of such regions, where transition from one bed form to another takes place, a situation quite difficult to be examined experimentally.

Within the same linear framework, flow and sediment transport models can be tailored to suit the needs of the specific problem at hand. Suspended load, whereby sediment are not anymore confined in a thin layer close to the bed, can be accounted for by adding an additional equation for the sediment concentration along the vertical. Sorting, which involves bedload transport of an heterogeneous mixture of sediment of different sizes, can be included by approximating

the continuous grain size distribution with a discrete number of fractions and introducing, for each fraction, a suitable Exner-like equations.

Although all the examples cited above, as well as my personal experience, are limited to river bed forms, the same techniques can be (and have been) applied to study the formation of bed forms in tidal, estuarine, and coastal environments, by simply replacing the steady uniform flow that defines the base state in river stability analysis with a suitable combination of waves and currents. The formulation of the eigenvalue problem and the techniques adopted for its solution may look a little different, but the similarities are usually more than the differences, so that analogies can be cast between bed forms appearing in the different environments.

Aeolian bed form stability can be studied as well, but care must be taken in the modelling of sediment transport, since the sediment dynamics is strongly affected by the media.

Finally, we can certainly conclude that stability analysis has taught us a lot about the formation of bed forms. Will it be able to teach us more in the future? Or will it succumb under the weight of the increasing number of sophisticated numerical models that mimics nature so well to make the resulting simulations undistinguishable from the real thing?

A tough question, indeed.

6. REFERENCES

- Allen, J. 1982. *Sedimentary Structures: Their Character and Physical Basis* - Vol. 1. Elsevier, Amsterdam.
- ASCE, T. C. 1963. Friction factors in open channels. *J. Hydraulic Div.*, 89 (HY2):97–143.
- Cheng, N.-S. 2008. Formulas for friction factor in transitional regimes. *J. Hydraulic Engng.*, 134:1357–1362.
- Colombini, M. 2004. Revisiting the linear theory of sand dune formation. *J. Fluid Mech.*, 502:1–16.
- Colombini, M. and Stocchino, A. 2011. Ripple and dune formation in rivers. *J. Fluid Mech.*, 673:121–131.
- Colombini, M. and Stocchino, A. 2012. Three-dimensional river bed forms. *J. Fluid Mech.*, 695:73–80.

- Einstein, H. and Shen, H. 1964. A study on meandering in straight alluvial channels. *J. Geophys. Res.*, 69:5239–5247.
- Guy, H. P., Simons, D. B., and Richardson, E. V. 1966. Summary of alluvial channel data from flume experiments 1956-61. Prof. paper 462-I, U.S. Geol. Survey.
- Jaeggi, M. 1984. Formation and effects of alternate bars. *J. Hydraulic Engng.*, 110:142–156.
- Muramoto, Y. and Fujita, Y. 1978. The classification of meso-scale river bed configuration and the criterion of its formation. In *Proc. 22nd Japanese Conf. on Hydraulics*, pages 275–282, Japan.
- Raudkivi, A. 2006. Transition from ripples to dunes. *J. Hydraulic Engng.*, 132:1316–1320.
- Sukegawa, N. 1971. Study on meandering of streams in straight channels. Technical report, Bureau of Resources, Dept. Science & Technology, Japan.
- Vanoni, V. A. 1974. Factors determining bed forms of alluvial streams. *Journal of the Hydraulics Division*, 100(3):363–377.
- Yalin, M. S. 1977. On the determination of ripple length. *J. Hydraulic Div. ASCE*, 103:439–44

Spatial variations in sand waves superimposed on sand banks: an automated analysis method

J.M. Damen *Water Engineering and Management, Faculty of Engineering Technology, University of Twente, Enschede, Netherlands – j.m.damen@utwente.nl*

T.A.G.P. van Dijk *Water Engineering and Management, Faculty of Engineering Technology, University of Twente, Enschede, Netherlands – t.a.g.p.vandijk@utwente.nl, and Deltares, Department of Applied Geology and Geophysics, Utrecht, Netherlands*

S.J.M.H. Hulscher *Water Engineering and Management, Faculty of Engineering Technology, University of Twente, Enschede, Netherlands*

ABSTRACT: Sand waves superimposed on sand banks may vary in morphology due to variations in local conditions. Apart from scientific reasons to understand the processes controlling sand wave shapes, these variations are also relevant to safe navigation and offshore engineering projects. Previous research reported variations in sand wave shape and migration over sand banks based on local observations. However, quantification of shape variations for all individual sand waves in a sand wave field remains to be investigated. In this study we present a 2D approach to analyse sand wave height and asymmetry. It is applied to two study sites in the North Sea where sand waves are superimposed on sand banks. The results show that the sand wave heights only vary over sand banks at one of the locations and that asymmetry varies in magnitude and direction at these sites.

1 INTRODUCTION

Sand wave shapes are determined by various processes, such as the tidal flow (Hulscher, 1993) and storms (Le Bot, 2000). Sand banks, larger-scale topographic features, cause local variations in these processes which may lead to varying shapes of sand waves superimposed on sand banks (Houthuys, 1994; Lanckneus and De Moor, 1995; Deleu, 2004). A commonly applied method to determine sand wave shape characteristics uses an analysis of representative transects perpendicular to the sand wave crests (e.g. Van Dijk et al., 2008; Van Santen et al., 2011; Franzetti et al., 2013). This method is highly dependent on the chosen transect location and orientation. The sand wave shape characteristics of an individual transect are determined based on the positions of the crests and troughs, which has previously been done both manually (Franzetti et al., 2013) and using an automated approach (Van Dijk et al., 2008; Duffy, 2012).

Duffy (2012) presented a method that was able to analyse 2D data of sand waves by scanning all

transects of the data in the direction of the largest bed level variation.

When using the direction of largest variation, other bed features (e.g. megaripples, sand banks and dredged areas) may hinder an accurate estimate of the sand wave direction. For a large quantified account of the North Sea sand waves, the analysis methods should be applicable in areas with other bed features.

For this study we propose a Fourier-based analysis to separate sand waves from other bed forms in order to determine sand wave orientation.

We aim to describe the variation in sand wave morphology over sand banks. To this end, we improved existing methods from Van Dijk et al. (2008) and Duffy (2012) for the automated determination of sand wave shape characteristics. Our improved method is applied to two study areas with sand waves superimposed on sand banks (figure 1). The first area is located near the Brown Bank; here sand waves have typical wavelengths between 200 and 1000 m. The second study area is located at the Hinder banks and contains sand waves with wavelengths between 200 and 400 m.

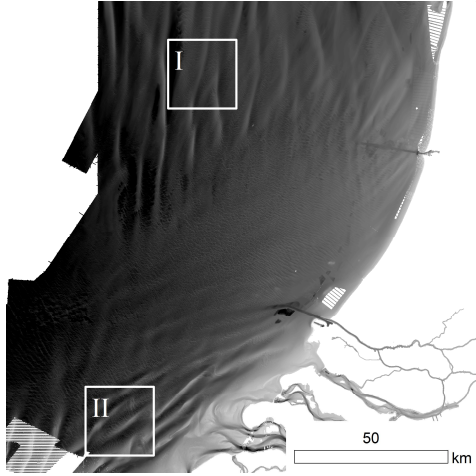


Figure 1: Study locations in the Southern Bight that contain sand waves superimposed on sand banks. Study area I is located in the northern part of the Southern Bight and study area II is located at the Hinder banks.

2 METHODS

2.1 Sand wave orientation analysis

A 2D Fourier analysis is applied to the bathymetry data to determine the orientation of the sand waves. The Fourier analysis of bed forms results in point clusters, separating the different types of bed forms depending on orientation and wavelength (Knaapen et al., 2001; Van Dijk et al., 2008). A line is fitted through the wave numbers that fall within the definition of sand waves (wavelength between 100 and 1000 m) by minimizing the residual sum of squares

$$RSS = \sum \hat{\sigma}_i^2 = \sum_{i=1}^M \sum_{j=1}^N (D_{i,j} * A_{i,j}), \quad (1)$$

where $D_{i,j}$ is the distance of a point in the Fourier space to the trend line and $A_{i,j}$ is the amplitude of an individual wave in Fourier space. The orientation of the trend line is derived as the direction perpendicular to the sand wave crests.

2.2 Sand wave shape analysis

Sand wave height h is defined as the vertical distance from the crest to the baseline that connects the two adjacent troughs (see figure 2). Sand wave asymmetry A is defined as follows:

$$A = \ln \left(\frac{L_1}{L_2} \right), \quad (2)$$

where L_1 is the distance from a trough to the next crest and L_2 the distance from that crest to the following trough. A purely symmetric sand wave is characterised by $A = 0$, whereas the sign of A reveals the direction of the asymmetry.

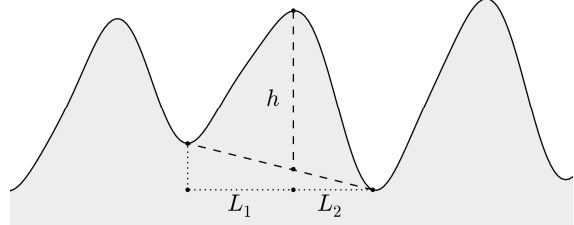


Figure 2: Definition of sand wave height h and lengths L_1 and L_2 used in the definition of the asymmetry A .

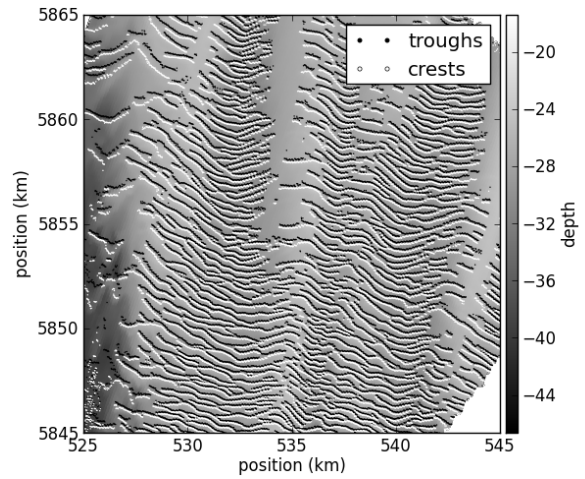


Figure 3: Sand wave bathymetry with crest and trough positions detected for a part of study area I using the method described in section 2.2.

For each transect perpendicular to the orientation of the crest lines, as derived in section 2.1, the peaks and troughs are detected (see also Duffy, 2012). To exclude bed forms smaller than sand waves, a moving average is applied to the transect data with a window size just below the minimum wavelength (100 m). Based on the slope of the smoothed bed elevation the positions of the crests and troughs are determined (see Van Dijk et al., 2008). The smoothing process leads to a reduced sand wave height (Van Dijk et al., 2008). To correct for this undesired effect, the buffering technique suggested by Duffy (2012) is applied. The sand wave crests and troughs detected for area I are shown in figure 3.

A threshold for sand wave height of 0.5 m is used to remove remaining small-scale bed patterns from the results. This was done by iteratively removing the smallest bed form below the threshold.

Sand waves will be compared in terms of their position on a sand bank, differentiating between the sand bank trough, the lee flank, the crest and the stoss flank. This classification is based on the slope of the smoothed bathymetry data.

3 RESULTS

The high-resolution analyses of all sand waves in the study areas result in spatial distributions (maps) of sand wave height and asymmetry (for example, the asymmetry at site I in figure 4) and scatter plots (figures 5 to 8). These scatter plots show that sand waves at the Hinder Banks are higher and less asymmetrical (area II) than those at the Brown Bank (figures 5 - 6 and 7 - 8, respectively) and that the shape characteristics of sand waves vary over sand banks. Preliminary results for location I reveal that sand waves are both higher (figure 5) and more asymmetrical (figure 7) at the sand bank crest. This effect is not evident at location II. However, at location II, the asymmetry direction of the sand waves varies systematically over the banks (not shown here), with the steep sides of sand waves to the NE ($A=0.5$) on the eastern flanks and to the SW ($A=-0.4$) on the bank crests and western flanks (this corresponds to earlier findings by Jones et al., 1965 and Lanckneus et al., 1995). The zonation and comparison based on sand bank position should provide more insight into these differences. The horizontal line pattern visible in the asymmetry plots (figures 7 and 8) is the effect of a discrete mapping of crests and troughs to the data cells. Some ratios are therefore more common than others. This effect becomes smaller when sand waves have longer wavelengths or when the data resolution is higher.

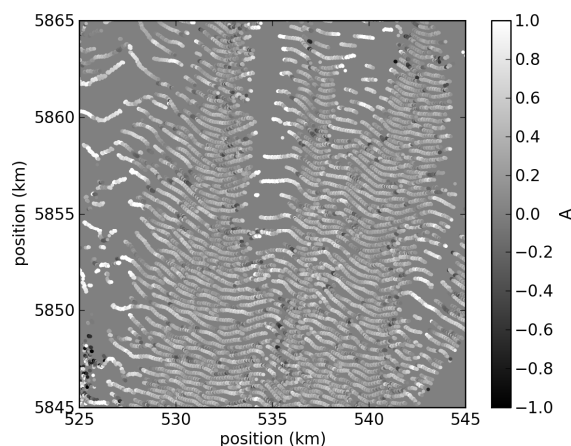


Figure 4: Sand wave asymmetry for study area I denoted at the sand wave crests.

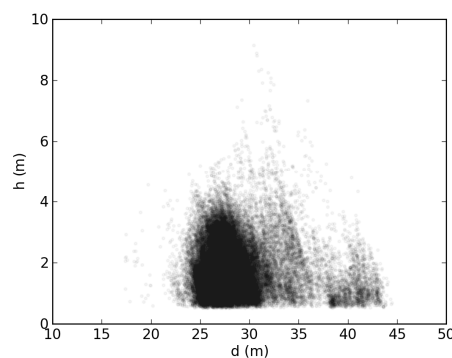


Figure 5: Scatter plot of sand wave height versus water depth above the crests. Each dot represents a single sand wave crest point detected in study area I.

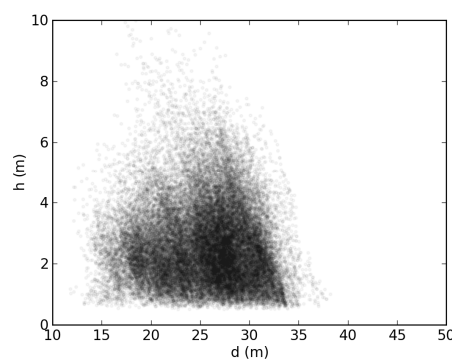


Figure 6: Scatter plot of sand wave height versus water depth above the crests. Each dot represents a single sand wave crest point detected in study area II.

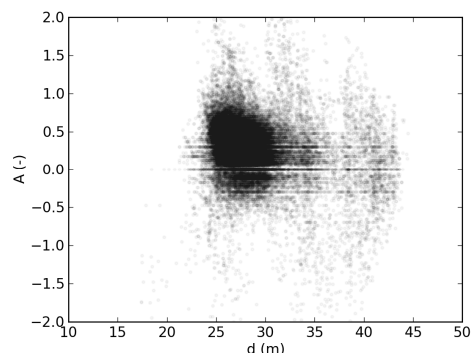


Figure 7: Scatter plot of sand wave asymmetry versus water depth. Each dot represents a single sand wave crest point detected in study area I.

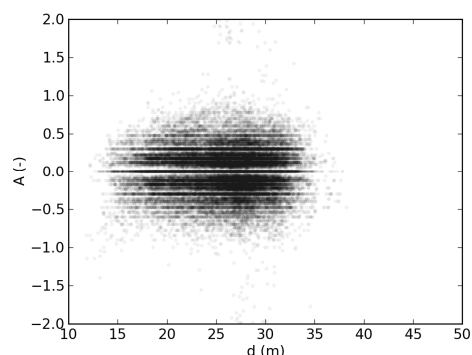


Figure 8: Scatter plot of sand wave asymmetry versus water depth. Each dot represents a single sand wave crest point detected in study area II.

4 CONCLUSION

Sand wave height and asymmetry vary depending on their position on the sand banks. For the study area near the Brown Bank both sand wave height and asymmetry are larger at the sand bank crest. At the Hinder Banks, the direction of the asymmetry varies over the bank.

Further research in the “SMARTSEA”-PhD project is aimed at unravelling the controlling processes of the variations of sand wave morphology and dynamics over sand banks.

5 ACKNOWLEDGEMENTS

This research is supported by the Dutch Technology Foundation STW, which is part of the Netherlands Organisation for Scientific Research (NWO), and which is partly funded by the Ministry of Economic Affairs.

The data used in this study were made available by the Netherlands Hydrographic Office of the Royal Netherlands Navy.

6 REFERENCES

- Deleu, S., Van Lancker, V., Van den Eynde, D. and Moerkerke, G. 2004. Morphodynamic evolution of the kink of an offshore tidal sandbank: the Westhinder Bank (Southern North Sea). *Cont. Shelf Res.*, 24: 1587-1610
- Duffy, G. 2012. Patterns of morphometric parameters in a large bedform field: development and application of a tool for automated bedform morphometry. *Irish Journal of Earth Sciences* 30: 31
- Franzetti, M., Le Roy, P., Delacourt, C., Garlan, T., Cancouët, R., Sukhovich, A. and Deschamps, A. 2013. Giant dune morphologies and dynamics in a deep continental shelf environment: Example of the banc du four (Western Brittany, France). *Mar. Geol.*, 346: 17-30
- Houthuys, R., Trentesaux, A. and De Wolf, P. 1994. Storm influences on a tidal sandbank's surface (Middelkerke Bank, southern North Sea). *Mar. Geol.*, 121: 23-41
- Hulscher, S.J.M.H., De Swart, H. E. and De Vriend, H. J. 1993. The generation of offshore tidal sand banks and sand waves. *Cont. Shelf Res.*, 13:1183-1204
- Jones, N. S., Kain, J. M. and Stride, A. H. 1965. The movement of sand waves on Warts Bank, Isle of Man. *Mar. Geol.*, 3: 329-336
- Knaapen, M. A. F., Hulscher, S. J. M. H., Vriend, H. J. and Stolk, A. 2001. A new type of sea bed waves. *Geophys. Res. Lett.*, 28: 1323-1326
- Lanckneus, J. and de Moor, G. 1995. Bedforms on the Middelkerke Bank, Southern North Sea, in B. W. Flemming and A. Bartholomä (eds), *Tidal Signatures in Modern and Ancient Sediments*, Blackwell Publishing Ltd., Oxford.
- Le Bot, S., Trentesaux, A., Garlan, T., Berne, S. and Chamley, H. 2000. Influence des tempêtes sur la mobilité des dunes tidales dans le détroit du Pas-de-Calais. *Oceanologica Acta*, 23: 129-141. In French.
- Van Dijk, T. A. G. P., Lindenbergh, R. C. and Egberts, P. J. P. 2008. Separating bathymetric data representing multiscale rhythmic bed forms: A geostatistical and spectral method compared. *J. Geophys. Res.*, 113
- Van Santen, R. B., De Swart, H. E. and Van Dijk, T. A. G. P. 2011. Sensitivity of tidal sand wavelength to environmental parameters: A combined data analysis and modelling approach. *Cont. Shelf Res.*, 31 : 966-978

Smart and sustainable design for offshore operations in a sandy seabed – the SANDBOX programme

J. H. Damveld *University of Twente, Enschede, NL – j.h.damveld@utwente.nl*

B. W. Borsje *University of Twente, Enschede, NL – b.w.borsje@utwente.nl*

P. C. Roos *University of Twente, Enschede, NL – p.c.roos@utwente.nl*

S. J.H.M. Hulscher *University of Twente, Enschede, NL – s.j.m.h.hulscher@utwente.nl*

ABSTRACT: Shallow coastal seas are subject to an increasing pressure by offshore operations, such as sand mining and the construction and operation of offshore infrastructure. The seabed topography, seabed life, sediment dynamics and hydrodynamics form a coupled system. When disturbed, this coupled system needs time to recover. Anthropogenic disturbances will affect the (local) ecosystem, which in turn will affect the sediment-water interaction and the potential of the seabed to store fine sediments. Consequently, the potential of the system for recovery may be affected. This paper poses a research outline focused on a better understanding of the functioning and stability of the coupled system during the lifetime of the offshore operation. This requires integration of knowledge from ecology, geomorphology and fine sediment dynamics, where the authors specifically focus on geomorphology.

1. INTRODUCTION

Coastal seas are highly important both from an economic and ecological perspective, as these areas support a broad variety of offshore activities (Figure 1) and form the habitat for a broad variety of organisms. Offshore activities, such as sand mining and construction and operation of offshore infrastructure, affect sediment dynamics and morphodynamics in coastal waters. Knowledge about these dynamics is also required for conservation and management of the biodiversity of sediment-dwelling (benthic) organisms in the coastal zone. Hence, there is from both an ecological and economical perspective a growing interest in the interactions between human activities, sediment dynamics and the habitat value of sediments for benthos.

The seabed of coastal seas is neither flat nor static (Figure 2). Tides, sediment, organisms and the seabed interact in nonlinear processes that are only partly understood. Previous theoretical explorations (Borsje et al., 2009) have shown that sandy offshore areas, such as found in the Southern Bight of the North Sea, can switch between different types of geomorphological behaviour (tipping points), characterized by the presence or absence of dynamic sand waves, and that small changes to the sediment characteristics

(e.g. roughness, storage of fines in the sandy matrix) caused by the activity of benthic organisms may suffice to influence tipping points between the two dynamic regimes.

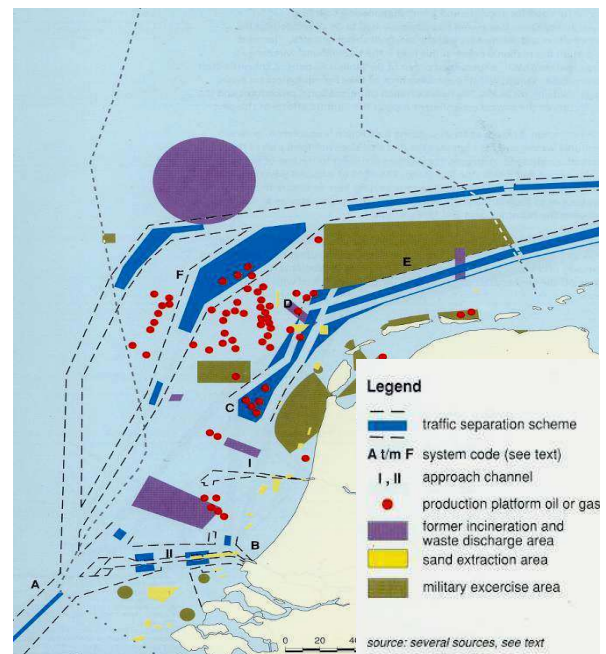


Figure 1: Map of Netherlands Continental Shelf, showing offshore activities (Data courtesy: Rijkswaterstaat).

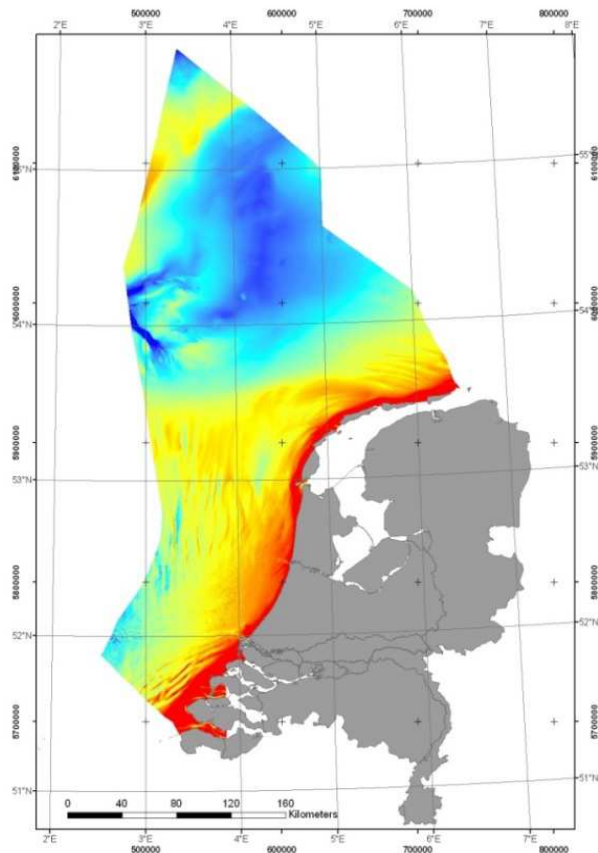


Figure 2. Bathymetric map of the Dutch part of the North Sea, showing large-scale seabed patterns (sand waves). Water depths vary between 0 m (red) up to 71 m (blue). Data courtesy: Deltares.

These explorations have large potential consequences for applications. Demands for sand and offshore constructions are increasing, but increasing environmental awareness creates the need to define modes and ranges of operation (the limits of a license to operate) where interventions in the seabed are environmentally safe. In addition, better understanding of the biogeomorphologic interactions may allow designing operations as underwater landscaping, thus combining economic exploitation with the creation of favourable habitats for benthic biodiversity and, linked to that, favourable conditions for demersal fish production.

Ecological landscaping, a well-known concept in terrestrial infrastructure works (e.g. van Bohemen, 2005), is introduced here for submarine operations. Present marine extraction policies aim at quick recovery and restoration of the original habitat, but do not consider the possibility to create

habitats designed for target organisms. Developing an ecological landscaping approach for the marine environment may stimulate social and political acceptance of future offshore activities, thus accelerating licensing procedures and project realisation. The definition of potential target communities will be based on indicators of benthic biodiversity integrity, developed in the framework of the Marine Strategy Framework Directive. Using these indicators, the work on this topic will be related to policy-relevant objectives.

The major stumbling blocks for the development of such an approach is the availability of coupled biogeomorphologic models for the dynamic regimes of offshore benthic systems. Such a coupled model must satisfy several requirements:

- The benthic biodiversity (hundreds of species are involved) is suitably summarized to model the effect of geomorphological changes on the community;
- Changes of community are translated into the parameters for the geomorphological dynamics;
- The effect of benthic communities on bed roughness (including the dynamics of fines in the sandy matrix) is properly parameterized.

In addition, application in implementation cases requires that operational models at a scale of a few wavelengths of the sand waves are developed.

2. THE SANDBOX PROGRAMME

The aim of the SANDBOX programme is to unravel the mechanisms behind the coupled seawater-seabed system, as well as the impact of offshore activities on this coupled system. This program will lead to knowledge for smart and sustainable use of the sandy seabed during the life time of the offshore operation and we will use this knowledge to arrive at a design strategy involving ecological landscaping for offshore activities. The expected outcome is an interactive design tool (SANDBOX) which is used to communicate the results of this research with utilization partners and support decision making in implementing sustainable offshore activities.

During the SANDBOX programme, implementation cases are selected in which the results of the program are implemented in the

design of new offshore operations (with a focus on ecological landscaping). These implementation cases are selected in close collaboration with Boskalis Westminster N.V. Reversely, field data gathered during these implementation cases (and provided by other consortium partners) are used as validation data for the interactive SANDBOX.

The SANDBOX programme contains three PhD projects and a Post-Doc position. PhD project 1 will focus on the short-term dynamic processes related to ripple formation, incorporation of fines in the bed and structural characteristics (roughness, erodibility) of the sediment surface. PhD project 2 will focus on the generalization of benthic biodiversity and formulation of the mutual interactions between benthic animals and bed characteristics. Effects of benthic communities on bed characteristics will be studied in close cooperation with PhD 1, while the model formulations will be developed in close collaboration with PhD 3. PhD 3 will focus on the modelling of the coupled system, in idealised as well as complex models. The Post-Doc will focus on the usability of the model products. The target application is ecological landscaping in the design of sand extraction operations and offshore constructions.

3. GEOMORPHOLOGY

Within this subproject we aim to come up with an idealised model for sandwaves coupled with benthic organisms giving insight in the dynamics of this system, as well as a more complex numerical model which can be applied in practical cases. These two approaches will be central throughout the whole subproject, where linking these combines insight in the system dynamics through fast computations with realistic results.

The first step is to determine the tipping points in the biogeomorphological system. The idealised modelling approach will be based on Hulscher (1996), where we intend to include biology using the parameterization of Crouzy et al. (2015). This allows for the investigation of the fully coupled system using stability analysis. Also, we will use Delft3D (Lesser et al., (2004)) to model sandwave dynamics (Borsje et al., 2013). Due to its structure, it allows us to incorporate the heterogeneous distribution of benthic organisms in time and space. The empirical data obtained from

subproject 2 will be used as input for both modelling approaches.

To further develop the Delft3D sandwave model, an empirical model to predict the roughness of the seabed will be included. This ripple model will be the result of the efforts of subproject 1. Since usually bed roughness is taken constant in morphodynamic models, the outcome of this step may have important implications for other model exercises.

In the next phase we intend to use the models to study the spatial-temporal evolution after anthropogenic interventions in the target areas. In the idealised model approach we can study the effect of e.g. a sand mining pit analogous to Roos and Hulscher (2003). The pit is approached mathematically as an perturbation and the linear reaction of the system can be analysed. The Delft3D model will be used to study interventions in a more realistic way, e.g. the chosen spatial extent of a human intervention within a sandwave field.

The intended overall result of the programme is to use the Delft3D sandwave-biology model to develop the concept of ecological landscaping in marine environments, which will be implemented in close collaboration with all other subprojects within the SANDBOX programme.

4. ACKNOWLEDGMENT

The authors acknowledge NWO-ALW for funding the SANDBOX programme. Also, the in-cash contribution by Boskalis is highly appreciated, as well as the in-kind contributions by Imares, RBINS OD Nature, Dienst der Hydrografie, ACRB, Deltares and Rijkswaterstaat.

5. REFERENCES

- Borsje, B.W., Hulscher, S.J.M.H., Herman, P.M.J. and De Vries, M.B., 2009. On the parameterization of biological influences on offshore sandwave dynamics. *Ocean Dynamics* 59, 659-670.
- Borsje, B.W., Roos, P.C., Kranenburg, W.M. and Hulscher, S.J.M.H., 2013. Modelling tidal sand wave formation: the role of turbulence formation, in press for continental shelf research.
- Crouzy, B., Baerenbold, F., D'Odorico P. and Perona, P., 2015. Ecomorphodynamic approaches to river anabranching patterns, in *Advances in Water Resources*.

Hulscher, S.J.M.H., 1996. Tidal induced large-scale regular bed form patterns in a three-dimensional shallow water model. *Journal of Geophysical Research* C9, 101, 20727-20744.

Lesser, G., Roelvink, J., Van Kester, J. and Stelling, G., 2004. Development and validation of a three-dimensional morphological model. *Coastal Engineering* 51, 883-915.

Roos, P.J. and Hulscher, S.J.M.H., 2003. Large-scale seabed dynamics in offshore morphology: Modelling human intervention. *Reviews of Geophysics* 41(2).

Van Bohemen, H., 2005. *Ecological Engineering: Bridging Between Ecology and Civil Engineering*. AEnas Publishers, Boxtel, Netherlands.

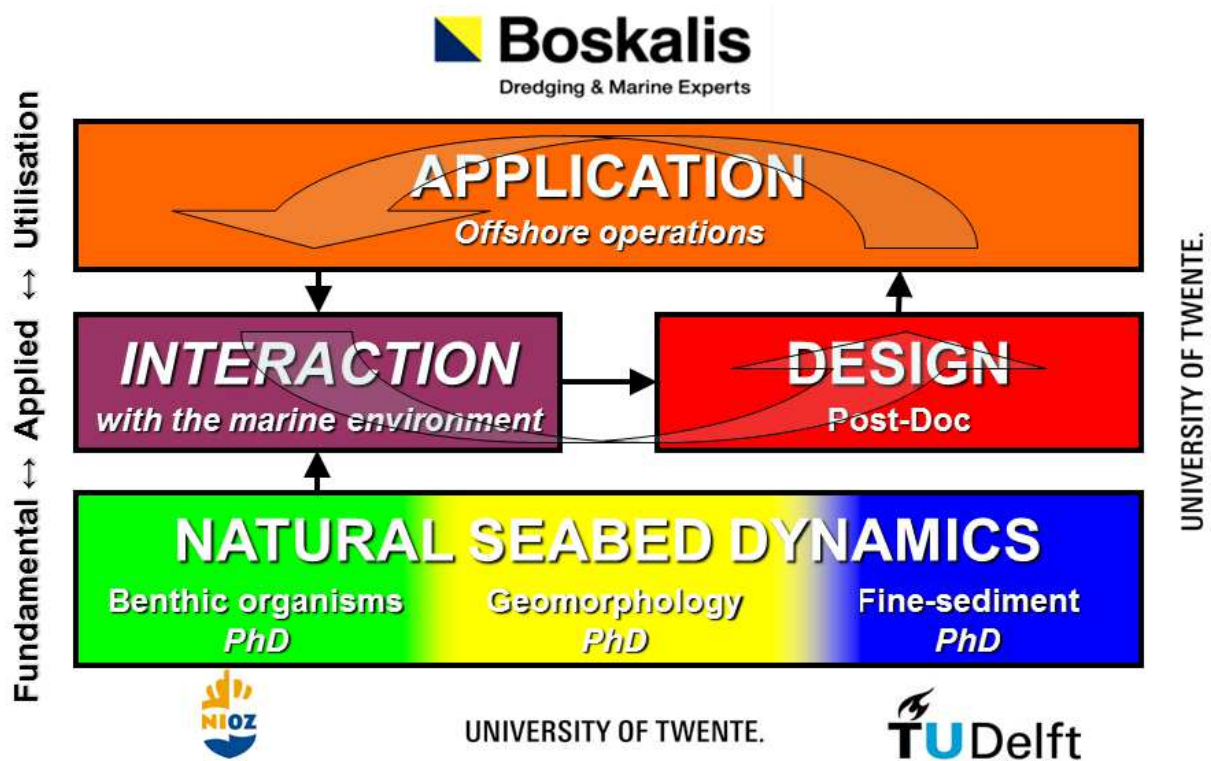


Figure 3. Outline of the consortium of the SANDBOX program and the translation from fundamental research via applied research towards utilization.

Ripple filtering and ridge enhancement applied to morpho-dynamical tracking of sand dunes.

N. Debese *ENSTA Bretagne, Brest, France – nathalie.debese@ensta-bretagne.fr*

J. J. Jacq *Mines-Telecom Institute / Telecom Bretagne, Brest, France – jj.jacq@telecom-bretagne.eu*

K. Degrendele *Federal Public Service Economy, SMEs, Self-employed and Energy – Continental Shelf Service, Brussel, Belgium – koen.degrendele@economie.fgov.be*

M. Roche *Federal Public Service Economy, SMEs, Self-employed and Energy – Continental Shelf Service, Brussel, Belgium – marc.roche@economie.fgov.be*

ABSTRACT: A 3D global semi-automatic approach based on bathymetric triangulated irregular network (TIN) is developed to extract the overall sand dunes pattern inside a given area. This method takes advantage of a new purpose-built anisotropic filter able to enhance the dominant features of the bathymetric mesh surfaces while smoothing out their ripples. The salient ridge and valley lines of the sand dunes are automatically extracted as 3D parametric curves through a saliency indicator. This new approach is tested on a fourteen years long time series of thirty MBES bathymetric datasets acquired by the Continental Shelf Service of the FPS Economy of Belgium on a monitoring area located on the northern part of the Middelkerke bank (Flemish banks, Belgian part of the North Sea). Based on the 3D vectors resulting from this approach, 3D augmented representation can right now assist geoscientists in tracking dunes morphology and dynamic but calculation methods should be specifically developed to assess the magnitude and direction of the dunes movement and evaluate the volume of sand involved in the dune dynamics.

1. INTRODUCTION

The Belgium continental shelf consists of numerous tidal sandbanks shaped by very large dunes showing various patterns. Such dynamic sedimentary structures are the result of complex interactions between the hydrodynamic and the sediment (Powell, 2000). They are of great interest for various end-users: while mobile dunes represent navigational hazards for hydrographers, due to their important volume of sand, they contribute significantly to the economic resources available for the dredging industry.

The modeling of sand dunes evolution is necessary for both scientific and practical purposes, but up to now, processes controlling their dynamics still remain far from perfect (Franzetti et al., 2013).

In parallel to theoretical and numerical approaches developed to explain the generation and the evolution of the sand dunes, morphometric approaches propose a geometrical reading of these bedforms to describe the local hydrodynamic and sediment dynamic processes within a zone of interest. Current approaches extract structural lines by mimicking manual processes or simplifying the sand dunes

shape. Such manual digitalization is usually performed individually for each dune.

In contrast to these approaches, we developed a 3D semi-automatic and global method operating on a bathymetric TIN. The extracted primitives are the salient ridges of the sand dunes and the valley lines between the sand dunes. The originality of our approach lies in the use a mesh data structure to represent the sand dunes as surfaces, their analysis through geodesic morphometry and their quantitative description using 3D parametric curves. This paper describes the application of this original approach on a real dataset acquired on a zone shaped by very large dunes located on the Middelkerke bank. The technical description of this new processing tool will be made available elsewhere.

2. DATASET DESCRIPTION

The zone of interest is the reference zone R2 located on the northern part of the Middelkerke bank. This tidal bank has been studied for many years. Its morphological and hydrodynamical setting is described in (Lanckneus et al., 1994; Lanckneus and De Moor, 1995).

As displayed in Figure 1, the North West (NW) part of R2 area is located on the summit of the bank while its South East (SE) part lies on its flank. The low water depth of R2 varies from 8 m on the north to 14 m on the south. R2 area is shaped by very large dunes which are themselves modeled with transversal superimposed medium to large dunes (according with the dune classification of Ashley (Ashley, 1990)). Very large dunes height observed on R2 are between 1 to 4 meters height with a wavelength ranging from 50 m to 100 m. The crest lines of the very large dunes are mainly North-South (NS) oriented. The very large dunes of the NW part are nearly straight to slightly sinusoidal in the SE part. The anastomotic pattern of the crest lines located in between may be explained by residual tide currents operating in opposite direction in the NW and SE parts of R2.

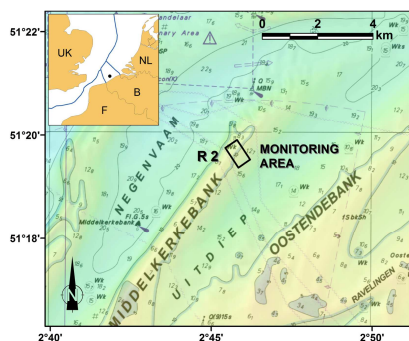


Figure 1: Location of monitoring area R2.

The local and temporal variability of the dune pattern is described by repeated bathymetric surveys. MBES data are available for a period starting from 2000 at a frequency of at least two surveys per year (Cf. Table 1). Data were acquired using a SIMRAD EM1002 and a EM3002D after 2008. Both MBES systems were installed onboard the research vessel Belgica (Degrendele et al., 2014).

3. GEODESIC MORPHOMETRY

3.1 3D global semi-automatic approach steps

A close look at the raw data displayed in Figure 2(a) points out the transversal superimposition of medium to large dunes on the very large dunes main pattern. When the extraction of salient ridges and valleys are of particular concern, the main difficulty lies in the elimination of the medium to large dunes that are found to heavily overprint any observations. To this end, the anisotropic filter, which is applied first, enhances the dominant fea-

tures while smoothing the secondary ones (see figure 2(b)). The availability of this efficient filter opens the door to the explicit extractions of both valley and crest lines of the very large dunes through a robust and automatic process. This extraction procedure basically built on high level transforms of the Mathematical Morphology makes use of a saliency indicator that is built from an ad hoc analytical recombination of the curvature coefficients. The map presented in Figure 2(c) displays sharp ridges (resp. valley) through a large positive (resp. negative) magnitude value in red (resp. blue) color – see also Table 1 for the other surveys. The last step consists of extracting the ridge and valley lines from the saliency map. The resulting global network is depicted in Figure 2(d). Lines are displayed using an ad-hoc iconographic representation enabling to assess their characteristics through their color texture and section radius.

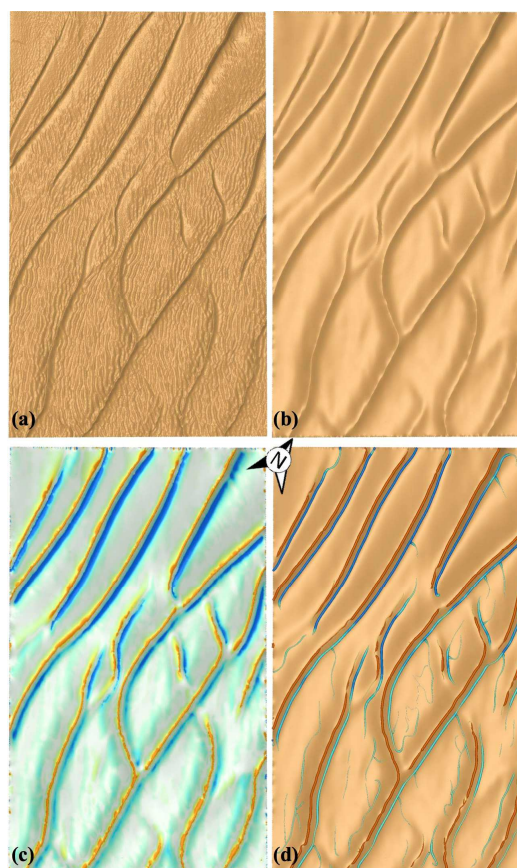


Figure 2: The four steps of the geodesy morphometry analysis applied to R2 (2014/03/14): (a) raw data ; (b) anisotropic filtering; (c) Saliency indicator mapping; (d) ridge and valley network of the filtered TIN

3.2 Morphodynamic description of R2

The time evolution of R2 is described in Table 1. The adaptive scale of the saliency indicator demonstrates the variability of very large dunes geometry during these thirty bathymetric surveys that were acquired at different tide levels.

Examples displayed in Figures 3 were chosen according to the features of their ridge and valley networks. In 2010, the very large dunes located in the NW part of R2 are symmetric regarding the distance separating adjacent valley and ridge lines, while those belonging to the SE part are asymmetric (the lee side pointing in the SW direction). Whereas a subsequent 2014 survey shows the opposite situation with the asymmetry of the very large dunes in the NW part of R2 area while very large dunes of the SE part are quite symmetrical.

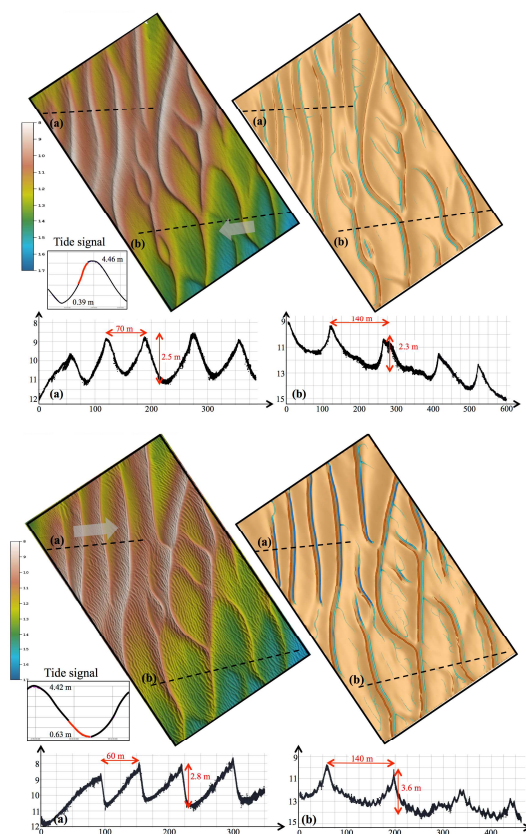


Figure 3: R2 bathymetry (top: 2010/09/06, bottom: 2014/03/14) with its ridges and valleys network and two bathymetric profiles.

The augmented database now includes a smoothed and parameterized 3D curve linked with each path. A representation of one of these structures is given in Figure 4. The latter should enable to build *ad hoc* path statistics at convenience.

4. PERSPECTIVES

A 3D global method based on bathymetric TIN is developed in order to extract and digitize semi-automatically the dune pattern in a given area. These reliable high level measurements could help marine scientists insert relevant global constraints into their complex models to calculate advanced results with tractable computational costs. Based on the 3D vectors resulting from this approach, 3D augmented representation can right now assist geoscientists in tracking dunes morphology and dynamics. However, a network tracking tool should be specifically developed to easily assess the magnitude and direction of the dunes movement. Incoming works will also track the volume of sand involved in the dune dynamics.

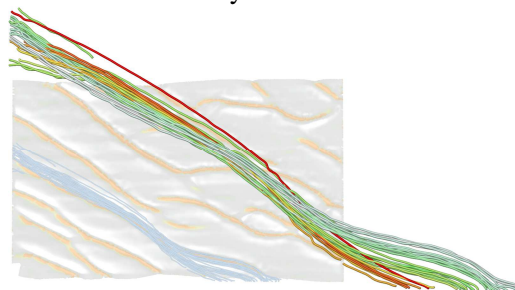


Figure 4: Merging of the noodle 3D representations of one very large dune crest over time. The colors are made to both shift and unsaturate linearly w.r.t. time.

5. REFERENCES

Ashley, G.M., 1990. Classification of large-scale subaqueous bedforms; a new look at an old problem. *J. Sediment. Res.* 60, 160–172.

Degrendele, K., Roche, M., De Mol, L., Schotte, P., Vandenreyken, H., 2014. Synthesis of the monitoring of the aggregate extraction on the Belgian Continental Shelf from 2011 till 2014. Presented at the “Which future for the sand extraction in the Belgian part of the North Sea?,” Lies De Mol and Helga Vandenreyken, Belgium Pier - Blankenberge.

Franzetti, M., Le Roy, P., Delacourt, C., Garlan, T., Cancouët, R., Sukhovich, A., Deschamps, A., 2013. Giant dune morphologies and dynamics in a deep continental shelf environment: Example of the banc du four (West. Brittany Fr). *Mar. Geol.* 346, 17–30.

Lanckneus, J., De Moor, G., 1995. Bedforms on the Middelkerke Bank, southern North Sea. *Spec Publ Int Sediment* 33–51.

Lanckneus, J., De Moor, G., Stolk, A., 1994. Environmental setting, morphology and volumetric evolution of the Middelkerke Bank (southern North Sea). *Mar. Geol.* 121, 1–21.

Powell, H.J., 2000. Wave-current interaction over bedforms: observations and model predictions, in: *Marine Sandwave Dynamics*. MARID, Lille.

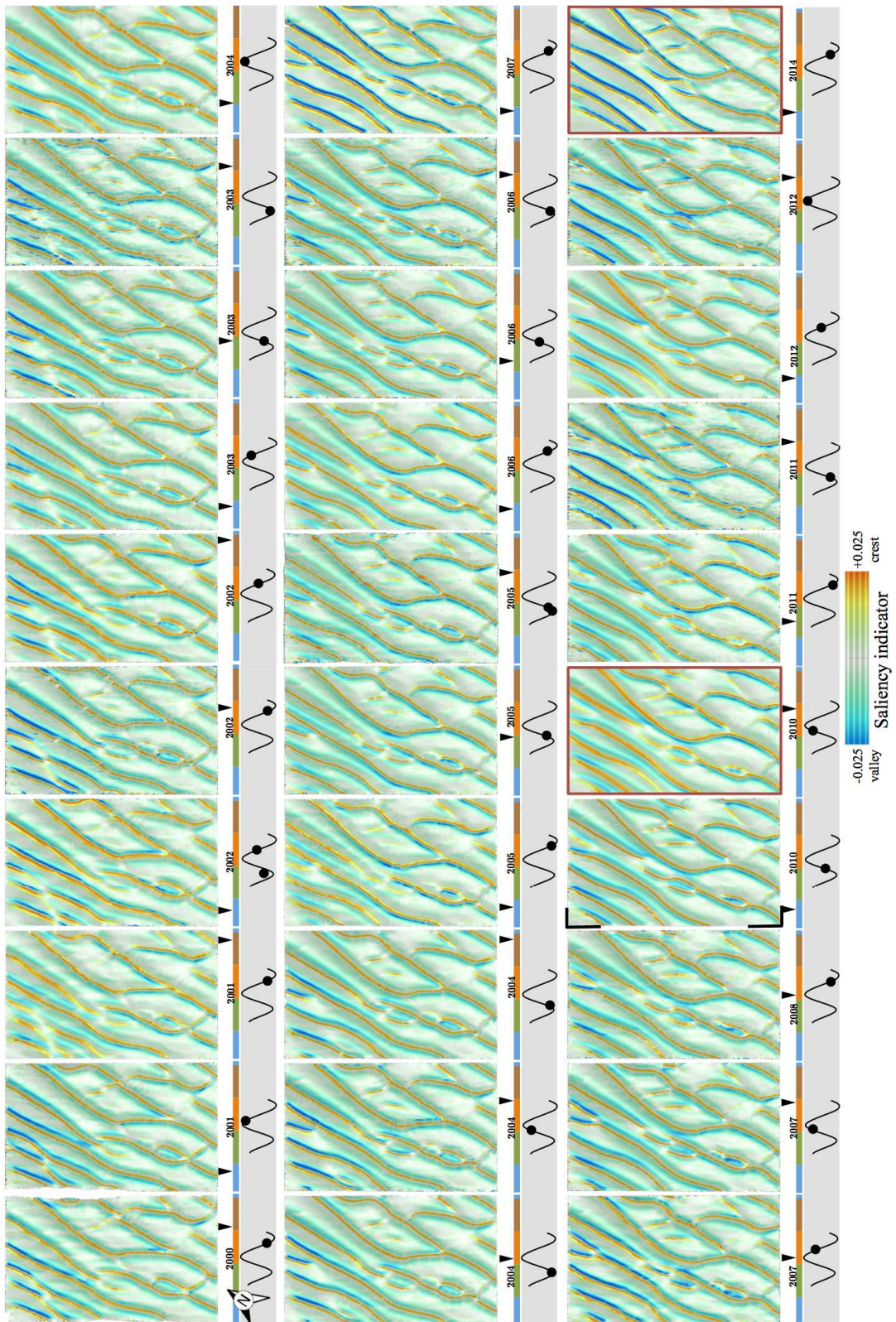


Table 1: Mapping of the saliency indicator on a sequence of thirty filtered instances of the R2 monitoring area. Dates of MBES data acquisition together with tidal level at survey time are displayed.

Holocene evolution of sand ridges in a tideless continental shelf (Western Mediterranean)

R. Durán *Instituto de Ciencias del Mar (ICM-CSIC), Spain – rduran@icm.csic.es*

J. Guillén *Instituto de Ciencias del Mar (ICM-CSIC), Spain – jorge@icm.csic.es*

J. Rivera *Instituto Español de Oceanografía, IEO, Spain – jesus.rivera@md.ieo.es*

A. Muñoz *Tragsa-SGP, Spain – amur@tragsa.es*

ABSTRACT: The evolution of sand ridges was investigated in a tideless continental shelf, the Murcia continental shelf in the Western Mediterranean, using high-resolution multibeam bathymetry and seismic data. Sand ridges are 1.5-3 m high and show a predominant E-W orientation, oblique to the shoreline. They are composed of sandy sediments and display asymmetric transverse profile, with the lee side towards the southwest. Internally, sand ridges display southwest dipping oblique reflections indicating episodic ridge migration in that direction. High-resolution seismic data show a stacked sand ridge system formed during the Holocene transgression. Smaller scale subaqueous dunes (0.3-1.3 m high) appear overimposed on the sand ridges showing a predominant NW-SE orientation, oblique to the ridge crestline, and suggesting present-day sedimentary dynamics.

1. INTRODUCTION

Large and very large subaqueous dunes (as defined by Ashley, 1990) or sand ridges (Dyer and Huntley, 1999) are pervasive bedforms on many continental shelves worldwide. In tidal-dominated settings, sand ridges show elevations up to 40 m with orientations that are primarily determined by the peak tidal direction (Dyer and Huntley, 1999; Liu et al., 2007). Sand ridges in non-tidal continental shelves, however, are smaller (up to 12 m high) and show an orientation oblique to the shoreline (Snedden et al., 2011). They show a linear, elongated shaped and a predominant asymmetric transverse profile, with steeper down-current flanks (Bassetti et al., 2006; Li and King, 2007). Internally, sand ridges display high-angle dipping reflectors that have been associated with mud beds, suggesting episodic processes related to storm events (Snedden et al., 2011; Durán et al., 2015).

Most of sand ridges located in the middle and outer shelf were formed in shallow environments as shoreface-connected sand ridges, which develop during storms and with a strong steady flow component (Calvete et al., 2001). When these

ridges detached from the shoreface during sea level rise, their growth gradually slows down and their migration rate decreases until they eventually drowned when the near-bed orbital velocity dropped below the critical velocity for sediment erosion (Nnafie et al., 2014).

Previous studies in non-tidal shelves noted that sand ridges commonly rest on a major erosional surface composed of coarse sand and gravel corresponding to the Holocene ravinement, as observed in the continental shelf off Florida (Snedden et al., 2011), New Jersey (Goff and Duncan, 2012), Valencia (Durán et al., 2015), and the Gulf of Lion (Bassetti et al., 2006). In fact, Goff (2014) argued that sand ridge migration along the basal surface provides a mechanism for formation of the shoreface ravinement in the Florida inner shelf.

In this work, we present the morphology and evolution of sand ridges identified in a tideless continental shelf, the Murcia shelf (Western Mediterranean), based on the analysis of swath bathymetry and high-resolution seismic data.

2. STUDY AREA

The Murcia continental shelf is a micro-tidal shelf with maximum tidal amplitude of 0.2 m. Wave climate follows a marked seasonal pattern with the most intense events usually occurring from September to May, and the highest waves (maximum significant height of 5.5 m) coming from NE and SW directions. The circulation on the shelf is dominated by the wind stress and the general circulation of the Northern Current, carrying old Atlantic Waters towards the southeast along the shelf break (Millot et al., 1999).

The continental shelf is 8 km wide but it narrows off Cape Cope, where it is less than 3 km wide (Fig. 1). It comprises a seaward dipping platform that is cut by shelf-indenting submarine canyons with their heads located at short distances of the coastline (Acosta et al., 2013).

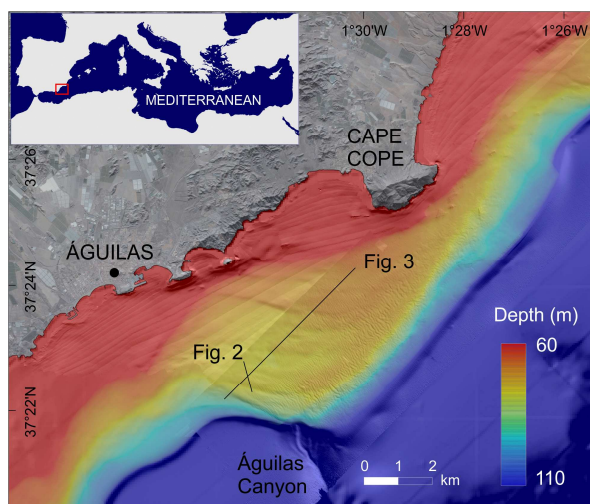


Figure 1. Location map and bathymetry of the Murcia continental shelf. Location of figures 2 and 3 is included.

3. DATA COLLECTION

High-resolution swath-bathymetry and seismic data were gathered during the COPESANDS cruise conducted on board R/V Ángeles Alvariño in February 2013. Swath bathymetry data were collected using a Kongsberg EM 710 system (70-100 kHz). Information on the shallow structure of the seabed was obtained using a Kongsberg TOPAS PS18 parametric sub-bottom profiler. In

addition, twenty sediment samples of the sand ridge field were collected using a box corer grab.

4. RESULTS

Sand ridges were observed in the outer shelf between 65 and 76 m water depth, showing a predominant E-W orientation that gradually changes to NE-SW with increasing water depth, and displaying a curved morphology (Fig. 1). The height of these bedforms ranges from 1.5 to 3 m, the spacing between 300 and 600 m and the length from 1500 to 3500 m. Sediment samples collected in the sand ridge field are consist on fine to coarse sand. Very-high resolution seismic profiles display a backstepping stacking pattern of prograding seismic units with high-angle reflectors dipping seaward and toward the southwest (Fig. 2). These units display variable thickness from 1.5 to 5 m, a limited areal distribution and an asymmetric transverse profile with the steepest slope facing southwards. They overlay a strong, continuous reflector that can be traced across the study area and displays major channel incisions, particularly near the Águilas submarine canyon (Fig. 3). The thickness of the sedimentary infill overlaying this reflector increases significantly towards the south, where it is ~12 m (considering a sound velocity in sediments of $1650 \text{ m} \cdot \text{s}^{-1}$).

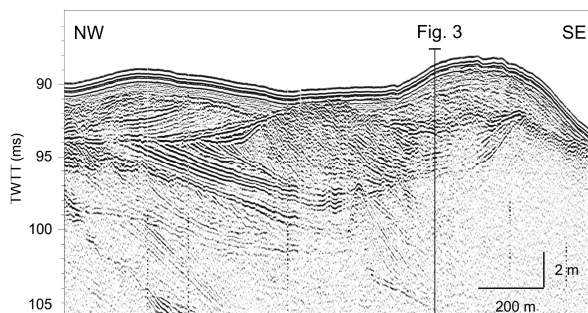


Figure 2. Very-high resolution seismic profile showing stacked sand ridges. Vertical scale in milliseconds two-way travel time (TWT). Thickness in meters is calculated considering a sound velocity in sediments of $1650 \text{ m} \cdot \text{s}^{-1}$. Profile location plotted in Figure 2 is shown. See figure 1 for location.

Smaller-scale dunes appear superimposed to the sand ridges, showing a predominant NW-SE orientation, oblique to the sand ridges. They are

0.3-1.3 m high and show an asymmetric profile with the steep slope towards the SW (Fig. 3).

5. DISCUSSION

The sand ridges identified in the Murcia outer shelf show similar morphology and internal structure to other storm-dominated sand ridges described on the NW Atlantic (e.g. Li and King, 2007, Snedden et al., 2011; Goff and Duncan, 2012) and Mediterranean shelves (Bassetti et al., 2006; Lo Iacono et al., 2010; Durán et al., 2015). They are asymmetrical and oblique to the shoreline, with the steep face towards the SW.

Sand ridges developed over a major erosional surface that shows major channel incision and can be traced along the whole shelf. This surface is related to the sea-level fall associated to the Last Glacial Maximum (LGM), based on seismic data and recent studies in the adjacent continental shelves (Lobo et al., 2015). According to this, sand ridges are interpreted as developed during the Holocene transgression, which is in agreement with previous observations that proposed sand ridge formation during the deceleration of sea-level rise around the Younger Dryas (Bassetti et al., 2006; Durán et al., 2015). The backstepping stacking pattern of sand ridges is suggestive of relative sea-level rise conditions, thus reinforcing this interpretation. As the sand ridges migrated towards the southwest, new sand ridges are continually replacing the old ones, resulting in a stacking pattern of sand ridges where some sand ridges of earlier phases might be preserved in the lower part of the stacked section. This configuration differs from previous observations in other non-tidal shelves where sand ridges commonly overlay a basal erosional surface interpreted as the ravinement (Bassetti et al., 2006; Snedden et al., 2011; Goff and Duncan, 2012; Goff, 2014; Durán et al., 2015).

Internally, sand ridges display SW dipping oblique reflections indicating episodic ridge migration in that direction, which is consistent with the configuration of the dune-field superimposed to the sand ridges. The presence of dipping reflections within the ridges was also described in other storm-dominated shelves associated with mud beds, indicating cessation of migration followed by reactivation of the sand ridge movement during major storms (Snedden et al.,

2011; Durán et al., 2015). This is supported by recent observations in the near Valencia outer shelf reported active sediment resuspension and transport episodes during storms that were able to mobilize the first centimeters of the surface sediment (mud and sand) producing a net transport transverse to the sand ridges (Simarro et al., 2015). These authors also proposed that similar events occurring during the late Holocene highstand could have contributed to the migration, maintenance or progressive degradation of these morphologies. In fact, the presence of subaqueous dunes overimposed to the sand ridges also suggests present-day sedimentary dynamics.

6. CONCLUSIONS

Sand ridges were examined in a tideless continental shelf, the Murcia shelf (Western Mediterranean). Sand ridges are 1.5-3 m high and are located between 65 and 76 m water depth, showing a predominant E-W orientation, oblique to the shoreline. Their asymmetry and internal structure indicate episodic ridge migration towards the southwest.

The continental shelf stratigraphic record reveals a backstepping stacking pattern of sand ridges formed during the last Holocene transgression. Their formation should be favoured by the deceleration of sea-level rise around the Younger Dryas, followed by a rapid sea level rise that promoted their preservation.

Smaller scale subaqueous dunes superimposed on the sand ridges suggest present-day sedimentary dynamics.

7. ACKNOWLEDGMENTS

This research was supported by the project FORMED (CGL2012-33989). We thank the Spanish Oceanographic Institute for the ship time of the COPESANDS cruise. We appreciate the R/V *Ángeles Alvariño* crew for their kind assistance. R. Durán is supported by a CSIC JAE-Doc contract co-funded by the FSE.

8. REFERENCES

Acosta, J., Fontán, A., Muñoz, A., Muñoz-Martín, A., Rivera, J., Uchupi, E., 2013. The morpho-tectonic setting of the Southeast margin of Iberia and the

- adjacent oceanic Algero-Balearic Basin. *Mar. Pet. Geol.* 45: 17–41.
- Ashley, G.M., 1990. Classification of large-scale subaqueous bedforms: a new look at an old problem. SEMP Bedforms and Bedding Structures Research Symposium. *J. Sediment. Petr.*, 60: 160-172.
- Bassetti, M.A., Jouet, G., Dufois, F., Bern, S., Rabineau, M., Taviani, M. (2006). Sand bodies at the shelf edge in the Gulf of Lions (western Mediterranean): deglacial history and modern processes. *Mar. Geol.*, 234. 93-109.
- Calvete, D., Falqués, A., de Swart, H.E., Walgreen, M. (2001). Modelling the formation of shoreface-connected sand ridges on storm-dominated inner shelves. *Journal of Fluid Mechanics*, 441. 169-193.
- Duran, R., Guillén, J., Simarro, G., Ribo, M., Puig, P., Muñoz, A., Palanques, A., 2015. Sand ridges in the mid-outer shelf as potential sand borrows areas (NE Mediterranean). *Proceed. Coastal Sediments 2015*. 1-13.
- Dyer, K.R., Huntley, D.A., 1999. The origin, classification and modelling of sand banks and ridges. *Cont. Shelf Res.*, 19 (10). 1285-1330.
- Goff, J.A., Duncan, L.S. 2012. Re-examination of sand ridges on the middle and outer New Jersey shelf based on combined analysis of multibeam bathymetry and backscatter, seafloor grab and chirp seismic data. *Int. As. Sed.*, 44, 121-142.
- Goff, J. A., 2014. Seismic and core investigation off Panama city, Florida, reveals sand ridge influence on formation of the shoreface ravinement. *Cont. Shelf Res.* 88, 34–46.
- Li, Z., King, E.L. (2007). Multibeam bathymetric investigations of the morphology of sand ridges and associated bedforms and their relation to storm processes, Sable Island Bank, Scotian Shelf. *Mar. Geol.*, 243: 200-228.
- Lo Iacono, C., Guillén, J., Puig, P., Ribó, M., Ballesteros, M., Palanques, A., Farrán, M., Acosta, J. 2010. Large-scale bedforms along a tideless outer shelf setting in the western Mediterranean. *Cont. Shelf Res.*, 30: 1802-1813.
- Lobo, F.J., Durán, R., Roque, C., Ribó, M., Carrara, G., Mendes, I., Ferrín, A., 2015. Shelves around the Iberian Peninsula (II): Evolutionary sedimentary patterns. *Boletín Geológico y Minero*, 126, 377-408.
- Millot, C., 1999. Circulation in the Western Mediterranean sea. *J. Marine Syst.*, 20: 423-442.
- Nnafie, A., de Swart, H.E., Calvete, D., Garnier, R. (2014). Effects of sea level rise on the formation and drowning of shoreface-connected sand ridges, a model study. *Cont. Shelf Res.*, 80: 32-48.
- Simarro, G., Guillén, J., Puig, P., Ribó, M., Lo Iacono, C., Palanques, A., Muñoz, A., Durán, R., Acosta, J. (2015). Sediment dynamics over sand ridges on a tideless mid-outer continental shelf. *Mar. Geol.*, 361: 25-40.
- Snedden, J.W., Tillman, R. W., Culver, S.J. (2011). Genesis and evolution of a mid-shelf, storm-built sand ridge, New Jersey continental shelf, U.S.A. *J. Sediment. Res.*, 81: 534-552.

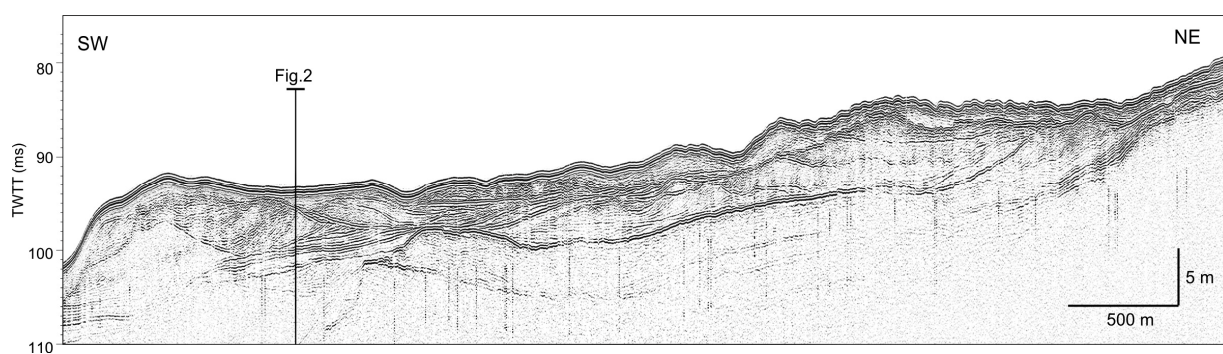


Figure 3. Very-high resolution seismic profile across the sand ridge field. Vertical scale in milliseconds two-way travel time (TWTT). Thickness in meters is calculated considering a sound velocity in sediments of $1650 \text{ m} \cdot \text{s}^{-1}$. Profile location plotted in Figure 2 is shown. See figure 1 for location.

High-speed phase-separated PIV over laboratory sand ripples

D. Frank *National Research Council Postdoctoral Fellow – donya.frank.ctr.jm@nrlssc.navy.mil*

A. Penko *Naval Res. Laboratory, Stennis Space Center, MS, USA – allison.penko@nrlssc.navy.mil*

J. Calantoni *Naval Res. Laboratory, Stennis Space Center, MS, USA – joe.calantoni@nrlssc.navy.mil*

ABSTRACT: Coastal hydrodynamics are intricately coupled with bedform generation and migration, which are important mechanisms for sediment transport and wave energy dissipation. We investigated the transport of sand as bed load and suspended load over ripples in a small-oscillatory flow tunnel and measured the resulting morphological evolution of the bedforms. High-resolution fluid and sediment velocity measurements were made with high-speed phase-separated Particle Image Velocimetry. Coherent structures were identified and determined to play a significant role in the transport of suspended sediments. Bedload transport during ripple migration was quantified within an oscillatory flow cycle using a surface tracking system. The relationship between turbulent kinetic energy dissipation and ripple migration was assessed.

1. INTRODUCTION

Ripples and other bedforms are ubiquitous in shallow water along sandy coastlines. The dynamics of sand ripples are vital to understanding numerous coastal processes such as sediment transport, wave attenuation, boundary layer development, and seafloor acoustic properties. The hydrodynamics above sand ripples are dominated by the coherent vortices formed on the ripple slopes and ejected into the water column at flow reversal. Sediment is entrained from the surface of the ripple and suspended into the water column where it is then advected with the flow (Thorne et al., 2003, van der Werf et al., 2006) and deposited onto the neighboring ripple.

New technology has recently allowed for the measurement of small-scale sediment dynamics in the laboratory. Here, phase-separated Particle Image Velocimetry (PIV) and a laser bed tracking system coupled with a water level sensor and a profiling Acoustic Doppler Velocimeter in a Small-Oscillatory Flow Tunnel (S-OFT) are used to measure fluid and sediment dynamics in the bottom boundary layer. We assess the relationship between sand ripple characteristics, migration rates and turbulent kinetic energy dissipation.

2. LABORATORY EQUIPMENT

The S-OFT is located at the Naval Research Laboratory at Stennis Space Center, Mississippi, USA. The S-OFT has a 2-m long test section and a flow cross-section of 25 cm x 25 cm (Figure 1). Oscillatory flow is generated with a piston flywheel to drive sediment transport and ripple formation. The instruments used to measure the fluid and sediment dynamics are described below.

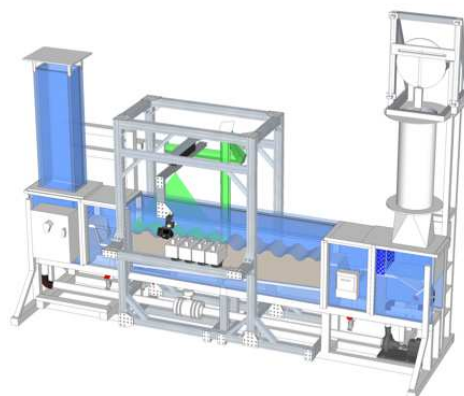


Figure 1: Small-Oscillatory Flow Tunnel.

PIV was used to measure three-dimensional velocities in the bottom boundary layer. However, standard PIV techniques severely limit direct observations of the fluid-sediment interface.

Intense reflections at the bed inhibit our ability to separate phase velocities during sediment entrainment. We have implemented phase-separated PIV by adding fluorescent tracer particles to the fluid in order to observe fluid flow and sediment transport simultaneously under oscillatory flows using multiple cameras with varying optical filters. The sediment particles scatter the 532 nm wavelength light. The fluorescent particles absorb the light and re-emit at a higher wavelength. Optical long pass filters were installed on two cameras to capture only the light re-emitted by the fluorescent tracer particles used to determine fluid velocities (Figure 2). A third high-speed camera was used to capture the light scattered by the sand grains allowing for sediment particle tracking. Together, these overlapping, simultaneously recorded images provided sediment particle and fluid velocities at high temporal (100 Hz) and spatial (< 1 mm) resolution.

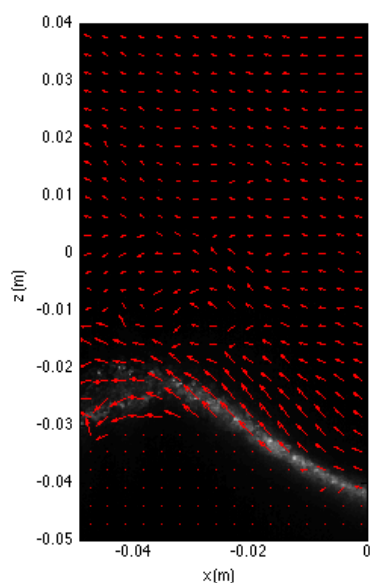


Figure 2: Near-bed fluid velocities over a sand ripple.

A Nortek Vectrino Profiler provided a longer time-series of the three-components of fluid velocity in a one-dimensional vertical profile. The instrument was positioned to measure the velocities within 3 cm of the bed in vertical bins of 1 mm approximately 5 cm upstream of the PIV field of view.

A Bed LASer Surface Tracking (BLAST) system measured the sediment bed elevation. The BLAST

system consists of two 520 nm, continuous wave (CW), fan beam lasers that project a ~1-m laser line on the sediment bed in the along-flow direction. Two Canon DSLR cameras capture images and video of each of the laser lines projected on the bed. One CW laser was stepped across the width of the S-OFT with a high precision stepping motor in 0.5-mm increments, while the DSLR camera with a 10-mm fisheye lens captured images of the laser line at every step. Each image size is 5184 x 3456 pixels, resulting in an average of 5-6 pixels/mm resolution. The bed surface elevation was scanned before and after each experiment. The second DSLR camera captured high-definition (HD) video (1080p) at 30 frames per second of sediment bed elevation profiles in the along-flow direction at the center of the test section over several oscillatory flow cycles (Figure 3). The measurements were used to determine the flow phase at which the sand grains were mobilized and estimate sediment transport rates.

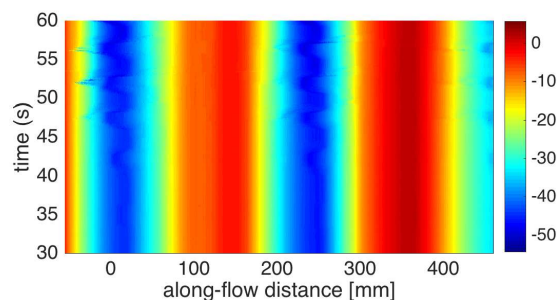


Figure 3. Initial sediment bed elevation after ripple generation in mm.

3. CONCLUSIONS

Measurements were made over a range of periods, orbital excursion amplitudes, symmetric and asymmetric oscillatory flows. Ripple crests were observed to move back and forth at a distance proportional to the orbital excursion amplitude with a migration rate consistent with the estimated bedload transport rate. Additionally, sediment grains were picked up from the flank of one ripple and transported as suspended sediment before being deposited on the flank of the adjacent ripple. Asymmetric oscillatory flows produced a net migration of the ripples proportional to the velocity asymmetry. Pressure gradients were deemed to be an important mechanism for mobilizing the sediment grains. Coherent

structures were identified and determined to be a significant mechanism for transporting suspended sediments.

4. ACKNOWLEDGMENT

Donya Frank was supported by the National Research Council Research Associateship Program at the Naval Research Laboratory Stennis Space Center. Allison Penko and Joseph Calantoni were supported under base funding to the Naval Research Laboratory from the Office of Naval Research. The authors would like to acknowledge NRL staff members Edward Braithwaite and

Abigail Hode for their assistance with experimental setup and data collection.

5. REFERENCES

- Thorne, P.D., Davies, A.G., & Williams, J.J. 2003. Measurements of near-bed intra-wave sand entrainment above vortex ripples. *Geophys. Res. Letters* 30(20): 2028.
- Van der Werf, J.J., Ribberink, J.S., O'Donoghue, T., & Doucette, J.S. 2006. Modelling and measurement of sand transport processes over full-scale ripples in oscillatory flows. *Coastal Engineering* 53: 657–673.

A Self-Organization Model for Multi-Scale Bedforms in Tidal Inlets and Bedform-Induced Roughness

E. Gallagher *Franklin and Marshall College, Lancaster, PA, USA – edith.gallagher@fandm.edu*

ABSTRACT: Bedforms are predicted with a self-organization model. The model predicts realistic features and their dynamics. Predicted features are compared with bedforms from field experiments and from the literature. One goal of this work is to estimate roughness based on predicted bedforms.

1. INTRODUCTION

Bedforms are ubiquitous in unconsolidated sediments. They range in size from small orbital ripples (□□ ~5-50 cm) to megaripples (□□~1-5 m) to large dunes (□□~10s-100s m). Bedforms are important because they affect sediment transport, flow energy dissipation, and larger-scale hydro- and morpho-dynamics. Bedforms in different environments (eg, deserts, rivers and oceans) are thought to be dynamically similar, therefore modeling approaches from one environment can be used to predicted features in another (Gallagher 2011). Here, a self-organization model is used to simulate the formation and development of bedforms in the combined flows of the surf zone, tidal inlets and river mouths. Sediment flux is determined from combined wave and current flows using different formulations, but, interestingly, the transport formulation has little effect on model results. Random bed irregularities, either imposed or resulting from small variations in the flow representing turbulence, are seeds for bedform development. Feedback between the bed and the flow in the form of a shadow zone downstream of a bedform and increasing flow velocity with elevation over bedform crests alter the transport

such that organized bedforms emerge. The model has been used to predict surf zone megaripples and bedforms in tidal inlets and river mouths.

Many observations report multiple scales of bedforms existing simultaneously in tidal inlets and in rivers (Barnard et al. 2006, Baujisman and Ridderinkof 2008, Parsons et al. 2005, Ernstsens et al. 2005, Lefebvre et al. 2011). Large-scale features take longer to adapt to changing flows, simply because there is more sand to move, thus they will maintain their orientation or equilibrium (like under flow direction changes in a tidal inlet). Whereas superimposed smaller-scale features can change shape more quickly and change direction. A recent study by Lefebvre et al. (2013) found that the boundary layer thickness and resulting bedform-induced roughness was different for single and multiple bedform fields. During one phase of the tide large features induced flow separation and generated increased flow roughness. When the tide turned these large features no longer induced separation and only smaller-scale features, which changed their orientation, generated flow roughness.

2. PRELIMINARY RESULTS

The present model predicts multiple bedform scales and is being used to examine the development and the temporal evolution of primary and secondary bedforms as a function of flow characteristics and water depth (the two factors that Sterlini et al. 2009 said were most important). The present model does not accurately represent the vertical flow profile above the bedforms. However, using the modeled bedforms shape, inferences about the time-history of the drag over changeable bedforms can be made. Following the observations of Lefebvre et al. (2013), if a bedform is asymmetric in the downstream direction, with a steep lee slipface, then it will cause flow separation and it will generate more drag on the flow, thus the bedform-induced roughness will increase dramatically (an order of magnitude). If a bedform is not oriented with the flow and/or its slopes are gentler (less than 10-15 degrees, Paarlberg et al. 2009), then they do not induce separation and they appear smoother to the flow.

Observations from the New River Inlet (Fig 1) come from Peter Traykovski, (pers. comm., <https://vimeo.com/44806773>) and show dramatic bed changes over a tidal cycle. There are bedforms of 1-3 m lengths that exist most of the time. But they change orientation with the tide, they sometimes have superimposed, smaller-scale bedforms, and they are sometimes smoothed or even wiped out. In contrast to Lefebvre et al. (2013), these observations are from shallow water and there are no permanent bedforms with fixed orientation. However, these features will generate their own roughness time series, including increased roughness owing to secondary bedforms and reduced roughness when features are reorienting and there is no lee slip face and separation. Figure 2 shows modeled results that are similar to those in Fig 1. The four sets of panels illustrate changes in bedforms from one slack period to the next. Near slack tide ($t=19200s$, top panels in Fig 2) the model predicts a bed where large bedforms (oriented to the left) have been smoothed by the waning water velocities just before slack. This is similar to the third panel in Fig 1, which is just before slack tide. As the tidal flow begins to pick up strength in the opposing direction, the existing bedforms begin to reverse direction and secondary features start to build

($t=19320s$, second panel, Fig 2, similar to left panel in Fig 1). In the third panel ($t=19450s$ in Fig 2), the larger bedforms are still visible, but the strong flows have helped to build the secondary features (similar to second panel in Fig 1). (Note that the model makes bedforms too tall and peaky when flows are strong. This is owing to anomalously large transport gradients at the bedform crests, because there is no sediment suspension and bypassing in the present simplistic model.) As the tidal flows wane again the large features are smoothed and the underlying bedforms again are visible. This series of images is similar to what is observed in the natural tidal inlet (Fig 1).

Results like this are encouraging and it is expected with a few model improvements, the correspondence with the observations will be better and our understanding of bedform growth, development, adaptation, sediment transport and roughness will all be informed and improved. Using model results, roughness time series will be constructed and compared with measurements of roughness from velocity profiles. From this understanding, fluid flow models can be improved with predictions of time varying roughness.

3. CONCLUSIONS

Bedforms in a natural tidal inlet are highly dynamic, changing shape and orientation and migrating over the course of a tidal cycle. The roughness induced by these bedforms can also change depending on their characteristics (Lefebvre et al. 2013). A self-organization model is being used to predict bedform characteristics and from that changing roughness regimes. The goal of this work is to inform larger-scale hydro- and morpho-dynamic models.

4. ACKNOWLEDGMENT

The author is grateful to the U.S. Office of Naval Research, Coastal Geosciences Program. The author would also like to thank Peter Traykovski for generously sharing data and experience.

5. REFERENCES

- Barnard, P.L., D.M. Hanes, D.M. Rubin and R.G. Kvitek, 2006. Giant sand waves at the mouth of San Francisco Bay. *EOS*, 87(29) 18 July, 2006, 285-289.
- Buijsman, M.C. and H. Ridderinkhof, 2008, Long-term evolution of sand waves in the Marsdiep inlet. II: Relation to hydrodynamics. 28, 1202-1215. doi:10.1016/j.csr.2008.02.014
- Ernstsen, V.B., R. Noormets, C. Winter, D. Hebbin, A. Bartholoma, B.W. Fleming, and J. Bartholdy, 2005. Development of subaqueous barchanoid-shaped dunes due to lateral grain size variability in a tidal inlet channel of the Danish Wadden Sea: *Journal of Geophysical Research*, 110, F04S08, doi:10.1029/2004JF000180, 2005.
- Gallagher, Edith L., 2011. Computer Simulations of Self-Organized Megaripples in the Nearshore, *Journal of Geophysical Research-Earth Surface*, 116, F01004, doi:10.1029/2009JF001473.
- Jerolmack, D.J. and D. Mohrig, 2005. A unified model for subaqueous bed form dynamics: *Water Resources Research*, 41, W12421, doi:10.1029/2005WR004329.
- Lefebvre, A., V.B. Ernstsen, C. Winter, 2011. Influence of compound bedforms on hydraulic roughness in a tidal environment. *Ocean Dynamics*, 61, 2201-2210. DOI 10.1007/s10236-011-0476-6
- Lefebvre, A., V.B. Ernstsen, C. Winter, 2013. Estimation of roughness lengths and flow separation over compound bedforms in a natural tidal inlet. *Continental Shelf Research* 61-62, 98-11.
- Paarlberg, A.J., C.M. Dohmen-Janssen, S.J.M.H. Hulscher, P. Termes, 2005. Modeling river dune evolution using a parameterization of flow separation. *Journal of Geophysical Research-Earth Surface*, F01014. http://dx.doi.org/10.1029/2007JF000910.
- Parsons, D.R., J.L. Best, O. Orfeo, R.J. Hardy, R. Kostaschuk, and S.N. Lane, 2005. Morphology and flow fields of three-dimensional dunes, Rio Parana, Argentina: Results from simultaneous multibeam echo sounding and acoustic Doppler current profiling. *Journal of Geophysical Research*, 110, F04S03, doi:10.1029/2004JF000231.
- Sterlini, F., S.J.M.H Hulscher and D.M. Hanes, 2009. Simulating and understanding sandwave variation: A case study of the Golden Gate sand waves. *Journal of Geophysical Research*, 114, F02007, doi:10.1029/2008JF000999.

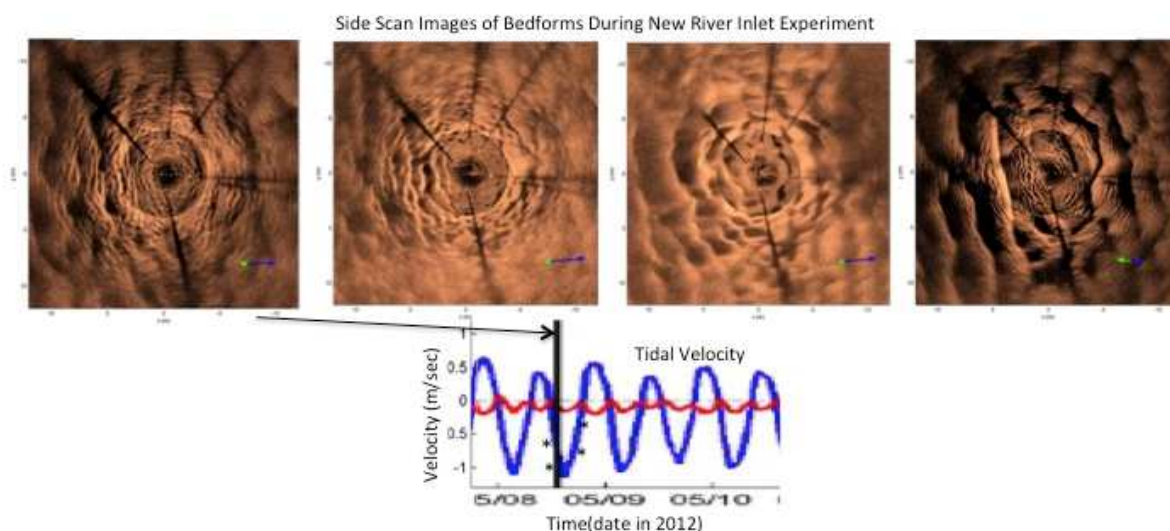


Figure 1. Examples of bedforms from side scan sonar images from the New River Inlet experiment (Traykovski, per.s comm., <https://vimeo.com/44806773>). The four panels are from a single ebb tide and the time of each image (from left to right) is indicated by an asterisk in the lower velocity panel. This time series of bedforms over an ebb tidal cycle suggests a change in orientation, an increase and then a decrease in bedform roughness. Dark brown color indicates acoustic shadows and lighter colors indicate surfaces sloped toward the sonar. Outward rays are shadows of the sensor platform.

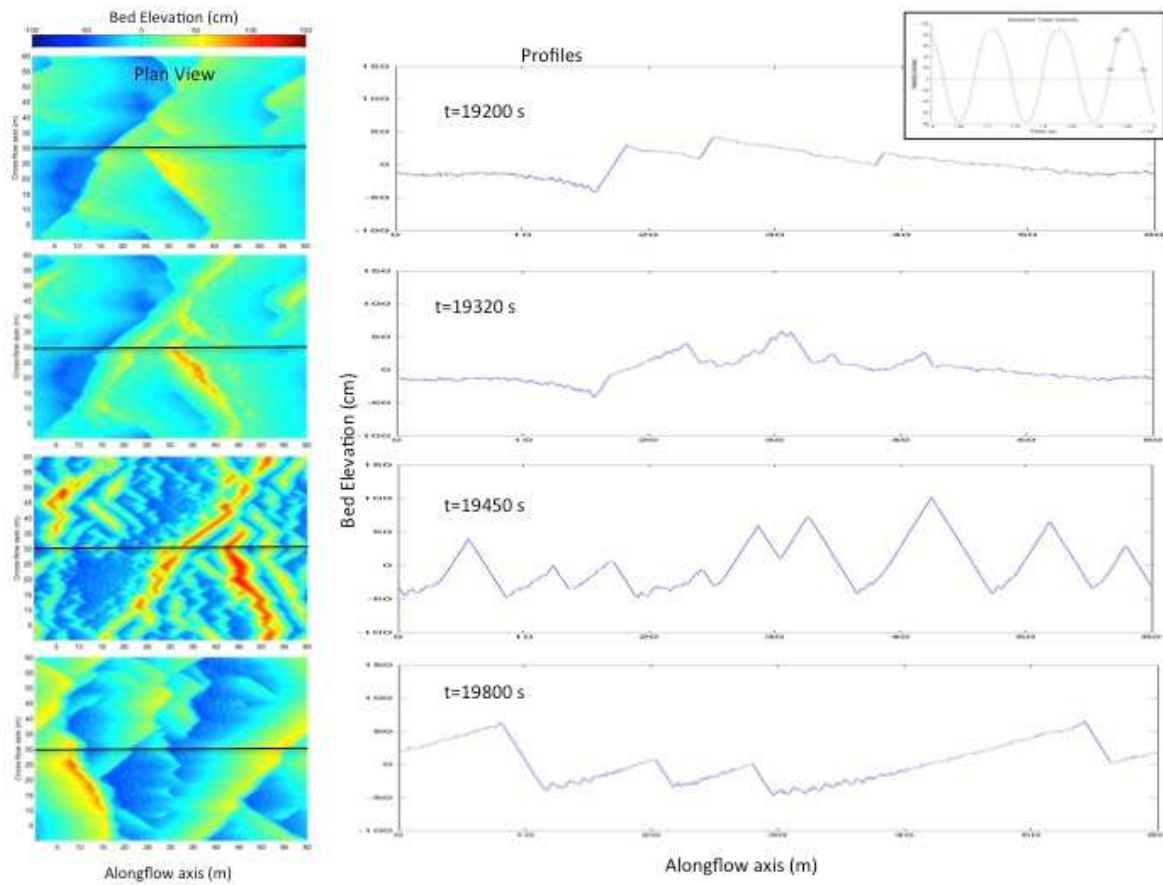


Figure 2. Modeled bedform time series over a single ebb tidal cycle (asterisks in small top panel indicate time in the cycle). Left panels show plan views of beds, right panels show profiles along black line in left panels. Large bedforms with wavelengths of about 15 to 20 m have formed, but are broken down and reformed with each tidal cycle (similar to observations Fig 1). The time series of roughness can be estimated from bedform predictions like these. (Note, peaky bedforms in panel 3 are anomalously high, see text.) Conditions are steady flow, $S = 15$ cm/sec, oscillatory flow amplitude, $A=95$ cm/sec, tidal period, $P=1200$ sec. Positive velocity is from left to right. This model run was for 20000 secs.

From regional variability of the morphology of dunes to a new method of their classification

T. Garlan *SHOM, HOM /Sedimentology, France* - thierry.garlan@shom.fr

E. Brenon *SHOM, HOM /Sedimentology, France* – emeric.brenon@shom.fr

E. Marchès *SHOM, HOM /Sedimentology, France* – elodie.marches@shom.fr

O. Blanpain *SHOM, HOM /Sedimentology, France* – olivier.blanpain@shom.fr

ABSTRACT: Dunes exist in all the sand environments. Most of dune classifications come from observations in desert which have been adapted to the marine environment, with profiles and side scan sonar images. During the last years, Multibeam Echo Sounders (MES) have showed a great diversity of morphologies, for example, trochoidal dunes present 3D features which are not completely described by the height and wavelength. This leads us to return to in situ environments to study the various forms of dunes and their characteristics in terms of physical properties. This paper presents some examples of dunes which seem to be specific of the marine environment and proposes a reflection on a more complete classification of marine dunes.

1. INTRODUCTION

Dunes exist in many environments: deserts, rivers, oceans, on other planets, and at every depth in sandy marine environments. For example, small dunes, fully comparable to those observed in shallow water, had been photographed at depths greater than 3000 metres (Lenôtre, 1977). As terrestrial field is more accessible, dune classification has been defined on the basis of desert observations and has been used for marine dunes. But the dune heights are different in aeolian and hydrological environments, star dunes are exclusively founded in deserts and seif dunes are very rare in seas.

The symposium 'Classification of large flow transverse bedforms' led to the general adoption of the classification proposed by Ashley (1990). This empirical classification concerns sand structures generated by unidirectional currents, alternating currents, and combinations of both. Flemming (2000) established a compilation of descriptive parameters for 1500 dunes from various marine environments throughout the world (with nearly one-third of the data acquired near the coasts of South Africa) and thereby proposed a continuous statistical model for sand structures ranging from ridges to giant dunes with the following

characteristics: dune height comprised between 0.001 and 20 meters, wavelength ranging from 0.01 to 1000 meters, mean dune height with respect to spacing λ : $H_{\text{mean}} = 0.0677 \lambda^{0.8098}$, maximum dune height: $H_{\text{max}} = 0.16 \lambda^{0.84}$. According to Ashley, the dunes are classified by wavelength, and Flemming's diagram can then be used to obtain their corresponding heights. To enhance this classification it is possible to use four parameters derived from measured profiles: wavelength (L), amplitude (H), stoss slope angle (α) and lee slope angle (β) to calculate four shape parameters : flattening index = λ/H , symmetrical index = $\lambda_{\text{am}}/\lambda_{\text{sv}}$ (equal to one for symmetrical ridges), linearity index = ld/d , bifurcation index = LB/λ . These results were obtained before the appearance of multibeam echo sounders, and all these parameters came from profiles spaced of 100 meters or more and the studies on dunes had always focused on their crests and their slopes.

2. MORPHOLOGY OF DUNES

The dunes are oriented almost perpendicularly to the principal direction of the currents with angular variations of up to 20° (Le Bot, 2001). They are situated in environments where bottom currents are between 50 cm/s and 1m/s (Belderson et al., 1982).

Granularity of sediments, current transport capacity and availability of sands are the three main parameters defining the shape and the volume of the dunes. The shape of dunes can be used to qualify sedimentary processes. As currents increase, an evolution is observed from linear dunes (rectilinear or anastomosed) to sigmoid or barchanoid dunes. The barchans dunes are for some authors symptomatic of slopes, of a sediment deficit or of a high velocity of currents. Knaapen (2004) observe a correlation between the migration speed and the symmetrical index. According to several authors, dunes with linear crests have the lowest migration velocity, and barchanoid dunes have the highest. Superposed, juxtaposed and interference dunes have been also described since half a century in desert and since less than twenty years in shallow water. As noted by Bartholdy (2004), the mere existence of superposed dunes contradicts the relationship between dune height and depth proposed by preceding authors. The presence of these superimposed structures is important and could be the main agent of sand migration (Idier et al, 2002) and by consequence of marine dune dynamics. As Flemming noted, H / λ models depend on the hydrodynamic conditions, so in theory the morphology of dunes could be used to estimate the intensity of dune dynamics. The variability of dunes comes from the granularity, heterogeneity, composition and availability of sediment, and in addition to hydrodynamic forcings. The dynamics of the dunes integrates the impact of tidal currents and swell at different time scales applied on a complex mixture of particles. The morphology of dunes can be seen as a synthesis of all these processes.

3. A CLASSIFICATION TO MAP THE VARIABILITY OF DUNES

All these elements show a relationship between the morphology of the dunes and their dynamics. The observation of hundreds of marine dunes in 2D, thanks to high-resolution (MES), shows that dune fields are not always constituted by regular transversal dunes. And it seems necessary to construct a classification which must at least include a two input table with shape and height (or wavelength) of dunes. In fact in the marine environment, we observe dunes with different shapes: barchans, rhomboidal, trochoidal and

transverse. Foremost, a dune classification must distinguish the environment; *i.e.* must differentiate isolated dune, fields of dunes and superimposed dunes (Figure 1). Then it must differentiate the morphology because transverse, trochoidal dune or barchan, do not reflect the same granular and hydrodynamic characteristics and peculiarities (Figure 2). For transverse dunes specification could be associated to specify the dune morphology, the availability of sediment could be associated with this classification (Figure 3).

Type	Organisation		
	Isolated	Field of dunes	On a bank
Transverse s.s.			
Rhomboidal			
Trochoidal			
Agglomerated			
Composite			
Split			
Barchanoid			
Barchan s.s.			

Figure 3. Morphological classification of marine dunes

Then, dune parameters such as height, wavelength, granularity, depth, the flattening, symmetry, linearity and bifurcation index must be characterized. Sediments must be translated by several elements (Mean Grain Size, Sorting, Skewness, or even percentage of each granular classes) to carefully consider the heterogeneity. To be complete, these 2D morphologies must be added to the four shape parameters and to the height (the more important for hydrography) or the wavelength (the easiest to measure). Finally the direction of dune movement and the annual average speed can complement the description of the dune or at least of the dune field if that information per unit is missing. The last element concerns superimposed dunes or megaripples. These structures are highly mobile and can move at speeds about one meter per hour, are fleeting, and can appear or disappear at the whim of storms. This information is thus highly dependent on the resolution of the acquisition system as well as hydrodynamic conditions preceding the survey. Nevertheless, it appears that these features should be retained because it carries information related to the splitting of the dunes, and can be associated with non-unique ridges, or complex dunes, which complicate the automatic calculation of dunes settings.

4. CONCLUSIONS

Synthesis on the different physical processes affecting the dynamics of the dunes (Naqshband and 2014, Doré 2015 ...) show how numerous are the phenomena and the importance of their links; but they also show how much progresses have been huge in the last 20 years. However, as in the study of the morphodynamics of beaches, progresses seem much less perceivable in the consideration of sediment. The work seems to be now on the angle of measurement of sediments which must provide descriptions of the dunes variation at the resolution of physical models. What about the variability of the average sediment grain size or of the sediment heterogeneity when models used grids of some meters on the profile of a dune. From measures in a water tank, Dréano (2009) proposes that barchans are due to fine sand, when resource in sediment is limited and for strong currents. In contrast when the sand is coarser and the resource important dunes are transverse and linear. But frequently dunes of different shapes appear in the same environment. It is the case of barchan and transverse dunes of Portsall, of trochoidals dunes often neighbouring transverse dunes, and more frequently cited, of megaripples superimposed on the dunes. The improvement seems to come back to field measurements to be at resolutions and scales of the processes described precisely by physics.

The mapping of dunes with a classification based on morphology and shape parameters could be a product adapted to estimate the areas where dunes are more or less active. This kind of map could be useful for hydrographic survey strategy, in particular in areas where only one MES survey has been done. It could be a tool to studying the impact of wind or tidal turbines and for all models and applications concern by dune dynamics.

5. ACKNOWLEDGMENT

We are grateful to SHOM/GHOA which realized these surveys and to the crews of Hydrographic ships : Borda, Lapérouse, Beautemps-Beaupré and Pourquoi-Pas?

6. REFERENCES

- Ashley, G.M. 1990. Classification of large-scale subaqueous bedforms: a new look at an old problem. *Journal of Sedimentary Petrology*, 60, 1: 160-172.
- Bartholdy, J. Flemming, B.W. Bartholomä, A. & Ernstsen, V.B. 2004. On the dimensions of depth-independent, simple subaqueous dunes. *Proceedings MARID II*, Twente, The Netherlands. Hulscher S., Garlan T., Idier D. Ed: 352 p.
- Belderson, R.H. Kenyon, N.H. Stride, A.H. 1982. Holocene sediments on the continental shelf west of the British Isles. Delany F.M. Ed, Institut of geological Sciences Report, 70/14: 157-170.
- Doré, A. 2015. Modélisation de l'évolution morphodynamique des dunes sous-marines. PhD Bordeaux University: 260p.
- Dréano, J. 2009. Dynamique et morphologie des dépôts sédimentaires en chenal expérimental. PhD Rennes University: 150p.
- Flemming, B. 2000. The role of grain size, water depth and flow velocity as scaling factors controlling the size of subaqueous dunes. *Proceedings MARID I*, Lille, France, A. Trentesaux & T. Garlan Ed., 61-67.
- Garlan, T. 2007. Study on marine sandwave dynamics. *International Hydrographic Review*, 8 (1), 26-37.
- Idier, D. Ehrhold, A. & Garlan, T. 2002. Morphodynamique d'une dune sous-marine du détroit du pas de Calais. *C.R. Geoscience* 334: 1079–1085.
- Knaapen, M.A.F. 2004. Measuring sand wave migration in the field. Comparison of different data sources and an error analysis. *Proceedings MARID II*, Twente, The Netherlands. Hulscher S., Garlan T., Idier D. Ed: 352 p.
- Le Bot, S. 2001. Morphodynamique de dunes sous-marines sous influence des marées et des tempêtes. *Processus hydrosédimentaires et enregistrement*. PhD Lille University: 273p.
- Lenôtre, N. 1977. Etude des marques de courant par photographie sous-marine. PhD Bordeaux Univ.: 100p.
- Naqshband, S. Ribberink, J.S. Hurther, D. & Hulscher, S.J.M.H. Bed load and suspended load contributions to migrating sand dunes in equilibrium, *J. Geophys. Res.*, 119: 1043-1063.
- Van Landeghem, K.J.J. Uehara, K. Wheeler, A.J. Mitchell, N.C. & Scourse, J.D. 2009. Post-glacial sediment dynamics in the Irish Sea and sediment wave morphology: Data-model comparisons. *Continental Shelf Research* 29: 1723–1736.

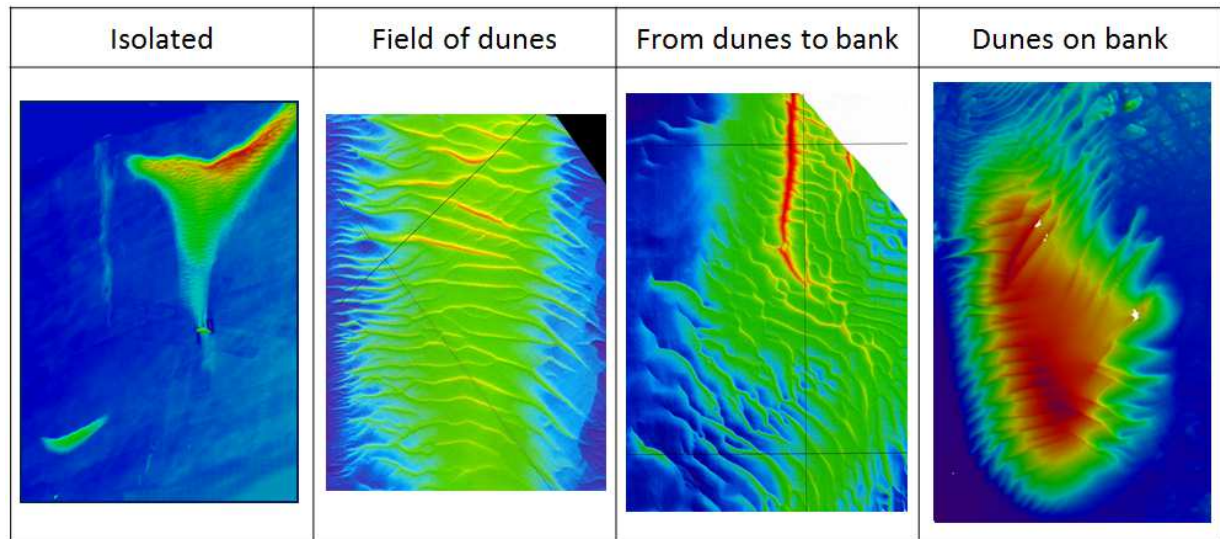


Figure 1. Intermediate steps between dunes and sandbank

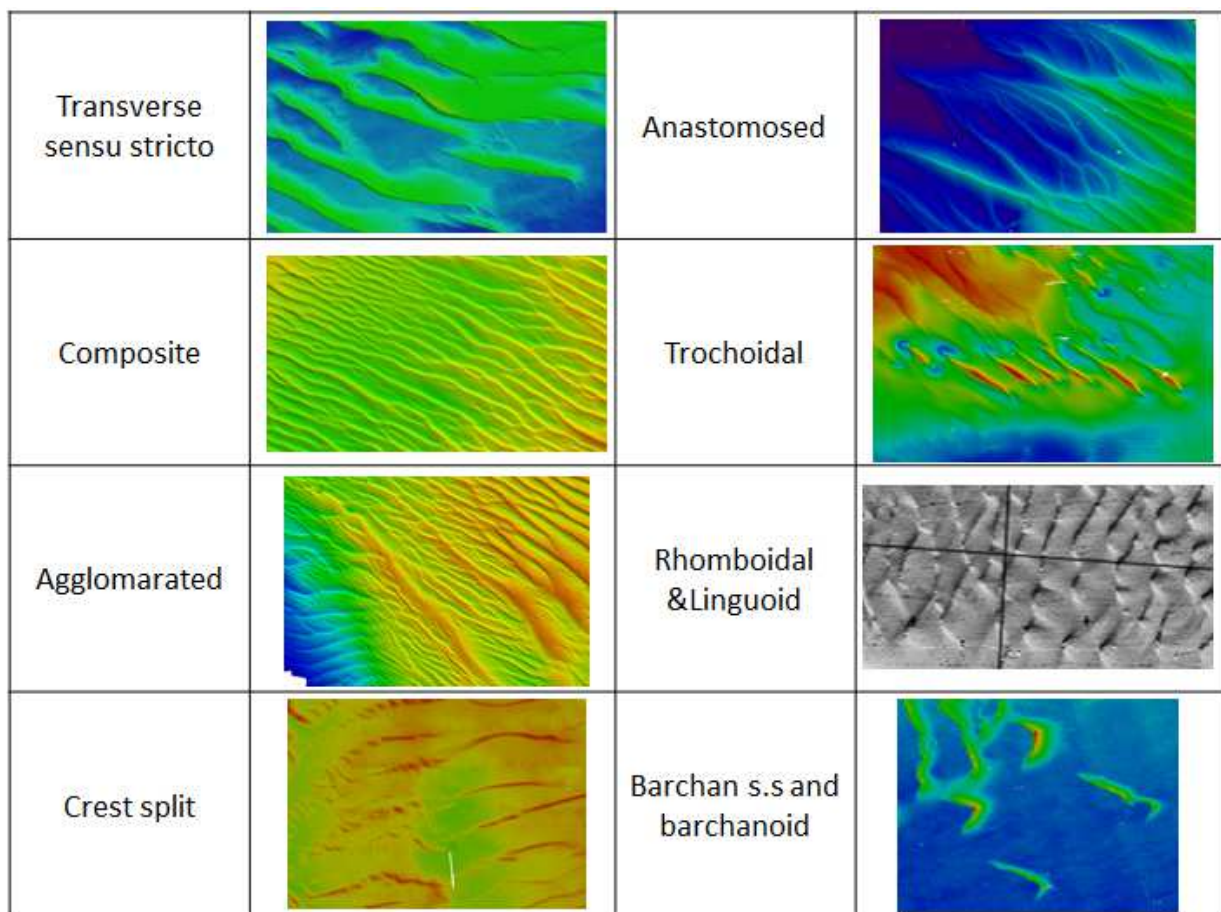


Figure 2. Examples of different dunes from a series of thousands of dunes of the English Channel and Celtic sea (SHOM, MES EM1002 & EM1002S).

Contemporary subaqueous dune-field development off an abandoned river mouth in the Ebro Delta (NW Mediterranean)

Q. Guerrero *Institut de Ciències del Mar (ICM-CSIC), Barcelona, Spain – queralt@icm.csic.es*

J. Guillén *Institut de Ciències del Mar (ICM-CSIC), Barcelona, Spain – jorge@icm.csic.es*

R. Durán *Institut de Ciències del Mar (ICM-CSIC), Barcelona, Spain – rduran@icm.csic.es*

R. Urgelés *Institut de Ciències del Mar (ICM-CSIC), Barcelona, Spain – urdeles@icm.csic.es*

ABSTRACT: High-resolution multibeam bathymetry, bottom sediment samples and time series of turbidity and currents were collected over a dune-field on the Ebro Delta coastal area in the north-western Mediterranean. The acquired bathymetry images a 3.6 km² dune-field with dunes of 1 m of mean height and 240 m of mean wavelength. Comparison between historical charts and contemporary aerial photographs show that the dune-field lied over the same location where a river mouth sand bar emerged in 1880. Onset of the dune-field is suggested to happen when the former river mouth was abandoned and the shoreline underwent fast retreatment since the forties. Nowadays, strong currents induced by north-westerly winds produce a dynamic seabed over dunes, including ripple development suggesting that the dune-field would be currently active during the high-energetic events.

1. INTRODUCTION

Numerous examples of dynamic dune-fields on continental shelves are related to strong currents (i.e. Kubicki, 2008). On the Western Mediterranean tideless shelves, several dune-fields have been described, most of them interpreted to be formed in coastal areas during periods of lower sea level (Durán et al., 2013; Simarro et al., 2015). However, current examples of dunes development in shallow areas are scarce, probably because sea waves tend to wash out these features.

This study deals with a dune-field located on the shoreface of the Ebro Delta. Present-day sediment dynamics on the dune-field and the morphological evolution of the delta plain during the last century are analysed to unravel the formation mechanisms and present-day dynamics.

2. STUDY AREA

The Ebro Delta is ~325 km² and it is one of the most important wet coastal ecosystems in the Western Mediterranean (Fig. 1a). It is located in a micro-tidal wave-dominated coast (maximum tidal range of 0.25 m). Seasonal wave regime predominates with relatively high-energetic events

between October and March when the most intense storms occur. These storms have an annual return period and a significant wave height (H_s) of 3.5 m (Bolaños et al., 2009). The area is subject to three main storm directions (E, NW, and S), with the most intense swell-dominated storms coming from the east. The wind regime is characterized by NW winds, which are extremely intense and persistent due to the orography, providing sea-dominated storms (García et al., 1993).

The deltaic plain evolution is essentially summarized in a progradational period of the Cape Tortosa mouth between 1880 and 1937; and an erosional period of this mouth from 1937 to present (Guillén and Palanques, 1997). The contemporary morphological changes of the present day deltaic lobe are primarily attributed to changes in the Ebro River mouth position and orientation. The opening of the current river mouth occurred in 1937, although it played a secondary role until the mid-twentieth century when it became the main river channel. (Fig. 1b).

3. DATA COLLECTION

High-resolution swath-bathymetry data of the Ebro Delta coast was acquired in summer 2004 with a

Simrad EM3002d multibeam echosounder by the *Arraix* survey boat in the frame of the Spanish PRODELTA RTD project and during October of 2013 with an ELAC NautikSeaBeam 1050D by the B/O *García del Cid* in the frame of the FORMED project.

An instrumented benthic tripod was also deployed off Cape Tortosa over the dune-field at approximately 13 m depth from the 13th of October of 2012 to the 10th of January of 2013. The tripod was equipped with an Aanderaa current meter (RCM9) located at 1 mab, which recorded time series data of current intensities and directions and suspended particles concentrations every 30 minutes. The tripod was also equipped with a GOPRO camera that recorded sequences of 10 seconds every 4 hours. A sediment sample was recovered by a HAPS core at the tripod location.

Wave field measurements and statistics from the buoy offshore Tarragona were provided by the Spanish Ports Authority (Puertos del Estado) with hourly sampling. The wave data was propagated from the buoy, located at 688 m depth, to the tripod position considering only the shoaling effect.

Finally, an historical chart of 1880 from the Spanish Hydrographic Survey and aerial photographs obtained by the Cartographic and Geologic Institute of Catalonia (ICGC) were used to determine changes in the configuration of the river mouth.

4. RESULTS AND DISCUSSION

4.1. Dune-field characteristics

The dune-field extends over ~3.6 km² of the swath-mapped deltaic lobe in between the isobaths of 8 and 15 m, off the abandoned Cape Tortosa mouth (Fig. 1b). The bedforms are better-developed and slightly more symmetric in the north-western area than in the south-eastern one. The crests of these features are rather rectilinear and their orientation changes as they are arranged perpendicular to the bathymetric contours of the deltaic lobe. The dunes are composed of fine sand. Their height ranges from 0.5 to 2.2 m with a mean value of 1 m, while their wavelength ranges from 140 to 600 m with a mean value of 240 m. Small-

scale bedforms (ripples) were observed during the deployment superimposed on the dunes (Fig. 2a).

4.2. Sediment dynamics

The time series measurements indicate that strong currents and waves are able to mobilize the bottom sediment (Fig. 2). The maximum near-bottom current intensities were approximately 0.6 m/s flowing towards the SSE (Fig. 2b). These strong currents were mainly driven by NW winds (Mistral) and displayed 30-40 degrees angle with respect to the crestline of the dunes, at the tripod location. On the one hand, current intensities and wave-height increases were associated with increments in the water turbidity (Fig. 2). On the other hand, ripple formation, migration or decay were observed during these higher-energetic periods. Ripples morphologies varied depending on the hydrodynamic conditions from wave-dominated to wave- and current-dominated conditions (Fig. 2). Formation and evolution of the dunes, particularly considering the dunes crestline orientation, can therefore be reasonably related to the strong wind-induced SSE-directed currents. The observations suggest that interaction between dunes and the subordinated bedforms (ripples) is probably key to the evolution of the dunes; however it has to be further studied.

4.3. Dune-field development

The Ebro River mouth prograded from 1880 to 1937 when a new mouth opened to the north. This northern mouth progressively became the main Ebro River channel. Thereafter, the former Cape Tortosa river mouth was progressively abandoned leading to a severe shoreline retreatment of ca. 2,300 m from 1947 to 2014 (Fig. 1b). The sediment eroded from the Cape Tortosa mouth was transported by waves and currents and redistributed along the delta plain. The location of the current dune-field coincides with that of a partially emerged mouth sand bar in 1880 and it is very close to the shoreline of Cape Tortosa during the forties (Fig. 1a and b, respectively). Therefore, the dune-field onset presumably began in the forties favoured by the availability of large amounts of sand on the shoreface supplied from the eroded delta plain. Strong near-bottom currents induced by NW winds generated the dune-field in this erosional shoreface.

5. CONCLUSIONS

High-resolution seafloor mapping allowed identifying a dune-field located over the former Cape Tortosa river mouth in the Ebro Delta. The dune-field is ~3.6 km² of the swath-mapped area. Dunes display a maximum wave height and wavelength of 2.2 and 600 m, respectively. The dunes are composed of fine sand and are better-developed in the north-western area. They are mostly symmetric with crestlines oriented perpendicular to the bathymetric contours.

The dune-field presumably developed because of the abandonment of the former Cape Tortosa river mouth since the forties. The measured currents, wave-field and turbidity time series data suggest that the studied dune-field can currently be active. Moreover, observations showing continuous formation, migration and decay of ripples during storm periods evidence a dynamic area of sediment remobilization.

Analysis of the contemporary development of this dune-field in an erosional coastal deltaic system can provide new insights for better understanding bedforms genesis during transgressive episodes at geological time-scales. Despite most Mediterranean continental shelves are occupied by relict, waning or low-dynamic bedforms, examples of present-day formation are very scarce. Finally, the time-scale over which the dune-field has evolved (several decades) may provide a useful example to predict the morphodynamic shoreface evolution in a future sea level rise scenario.

6. ACKNOWLEDGMENT

Q. Guerrero was supported by the Spanish Government by FPI grant (Ref. BES-2013-066261). This research was supported by the project FORMED (CGL2012-33989). We appreciate the captain and the crew of the R/V *García del Cid* and the *Arraix* for their kind assistance. R. Durán is supported by a CSIC JAE-Doc contract co-funded by the FSE.

7. REFERENCES

- Bolaños, R., Jorda, G., Cateura, J., Lopez, J., Puigdefabregas, J., Gomez, J., Espino, M., 2009. The XIOM: 20 years of a regional coastal observatory in the Spanish Catalan coast. *J. Mar. Syst.* 77, 237–260.
- Durán, R., Canals, M., Lastras, G., Micallef, A., Amblas, D., Pedrosa-Pàmies, R., Sanz, J.L., 2013. Sediment dynamics and post-glacial evolution of the continental shelf around the Blanes submarine canyon head (NW Mediterranean). *Prog. Oceanogr.* 118, 28–46.
- García, M. A., Sánchez-Arcilla, A., Sierra, J.P., Sospedra, J., Gómez, J., 1993. Wind waves off the Ebro Delta, NW Mediterranean. *J. Mar. Syst.* 4, 235–262.
- Guillén, J., Palanques, A., 1997. A historical perspective of the morphological evolution in the lower Ebro river. *Environ. Geol.* 30, 174–180.
- Kubicki, A., 2008. Large and very large subaqueous dunes on the continental shelf off southern Vietnam, South China Sea. *Geo-Marine Lett.* 28, 229–238.
- Simarro, G., Guillén, J., Puig, P., Ribó, M., Lo Iacono, C., Palanques, A., Muñoz, A., Durán, R., Acosta, J., 2015. Sediment dynamics over sand ridges on a tideless mid-outer continental shelf. *Mar. Geol.* 361, 25–40.

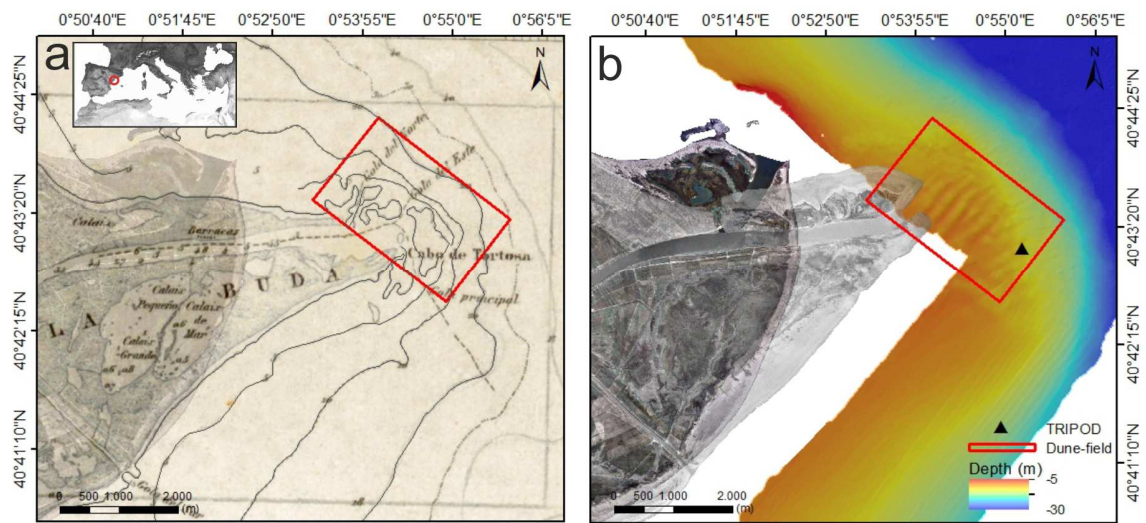


Figure 1. (a) Location of the study area on the 1880 hydrographic chart superposed on the 2014 aerial photograph. (b) 1947 and 2014 aerial photographs; bathymetric map; and location of the dune-field and the tripod (red square and black triangle, respectively).

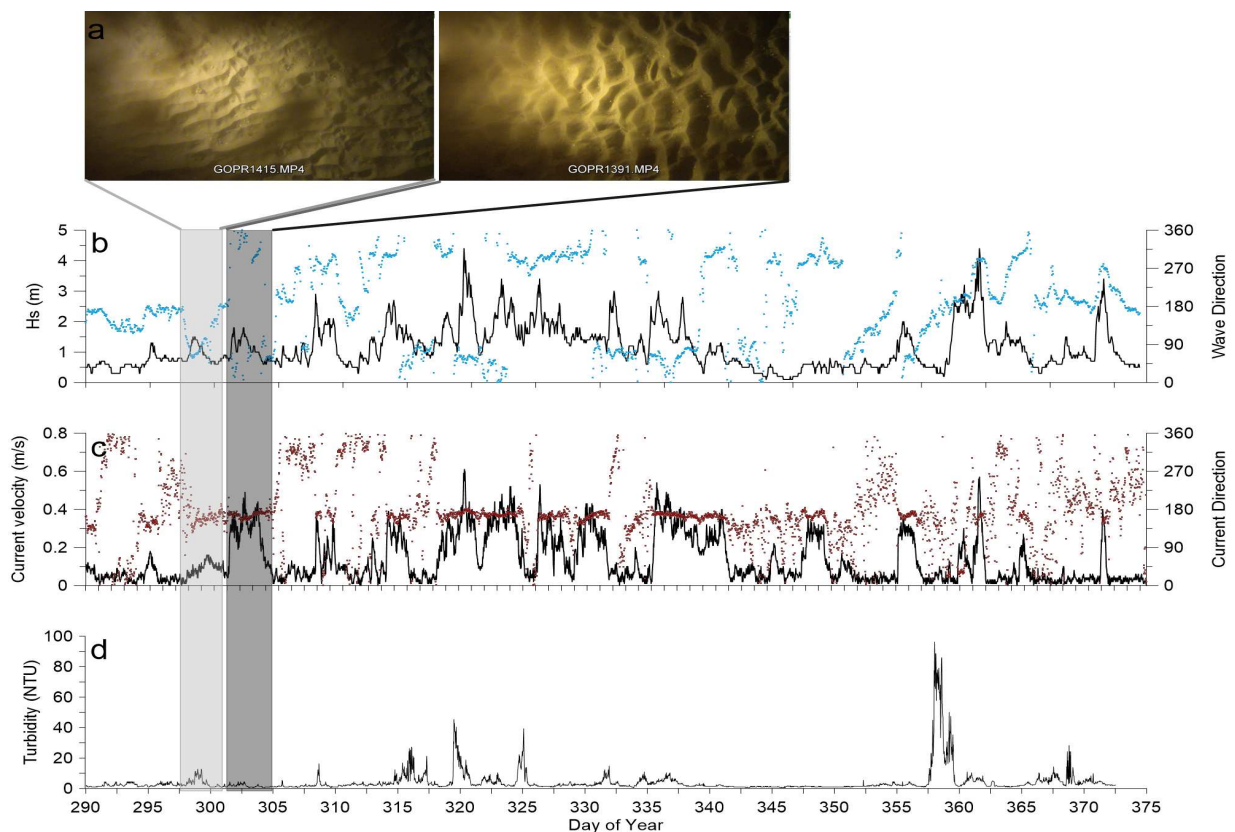


Figure 2. (a) Examples of the two rippled morphologies observed as a result of wave-dominated (to the left marked with lighter polygon) or wave and current-dominated hydrodynamic conditions (to the right marked with dark polygon). Time series data from 18th October of 2013 (day 291) to 10th of January of 2014 (day 375) of: (b) Significant wave height (black line) and wave direction (blue dots); (c) Current velocities (black line) and current directions (red dots); (d) Turbidity time series data.

Suspended sediment dynamics above submerged compound sand waves observed during a tidal cycle

I. Hennings *GEOMAR Helmholtz-Zentrum für Ozeanforschung Kiel, Kiel, Germany – ihennings@geomar.de*

D. Herbers *GEOMAR Helmholtz-Zentrum für Ozeanforschung Kiel, Kiel, Germany – ihennings@geomar.de*

ABSTRACT: Detailed Acoustic Doppler Current Profiler (ADCP) data of the three-dimensional current-field, echo intensity, modulation of suspended sediment concentration (SSC), and related water level and wind velocity have been analyzed as a function of water depth over asymmetric submerged compound sand waves during a tidal cycle in the Lister Tief of the German Bight in the North Sea. Signatures of vertical current component, echo intensity and calculated SSC modulation in the water column depend strongly on wind and horizontal current speed as well as on wind and horizontal current direction, respectively. Bursts of vertical current component and echo intensity are triggered by the sand waves itself and also by superimposed megaripples due to current/wave interaction.

1. INTRODUCTION

Ocean color and its transparency are related to turbidity caused by substances in water like organic and inorganic material. One of the essential climate variables (ECV) is ocean color. However, this implies that measurements of water quality parameters are needed to understand and analyze climate change. Measurement of the wavelength variation of the beam attenuation coefficient c provides information on the major constituents of the water which influenced its color. Ocean color is also important for technical applications and operations, because the usage of new remote sensing technologies for hydrographic purposes such as airborne light detection and ranging (LIDAR) bathymetry (ALB) systems for shallow coastal surveys depends strongly on turbidity of the water column.

Substantial phenomena of suspended matter concentration during two tidal cycles at two anchor stations in the southern North Sea were described by Joseph (1954). It was shown by Hennings & Herbers (2014) that strong currents flowing over steep bottom topography are able to stir up the sediments to form both a general continuum of suspended sediment concentration (SSC) and localized pulses of higher SSC in the vicinity of

the causative bed feature itself. These observations were in agreement with the basics on dynamics of the circular vortex with applications to oceanic vortex and wave motions (Bjerknes, 1921; Defant, 1961). A decrease in water clarity of the southern and central North Sea was reported by Capuzzo et al. (2015). The authors concluded that changes in water clarity were more likely driven by an increase in SSC.

Our study area was the Lister Tief, a tidal inlet of the German Bight in the North Sea bounded by the islands of Sylt to the South and Rømø to the North, respectively, as shown in Figure 1. The tidal gauge station List is located 4.8 km southerly of transects AB shown in Fig. 1. Present seabed morphology created in the Lister Tief is a complex configuration of different bed forms. The submerged compound sand waves (Van Dijk & Kleinans, 2005) investigated in this study are four-dimensional in space and time. Small-scale as well as megaripples are superimposed on sand waves as presented and discussed in Hennings & Herbers (2006). The analyzed flood dominated sand waves have gentle slopes of the order of 1° and steep slopes up to 31° .

Our primary intention is to investigate how wind speed and direction and speed over ground of the measuring platform will affect signatures of

vertical current component w , echo intensity E_3 , and SSC modulation $\log((\delta c/c_0)_3)$ over submerged compound sand waves during a tidal cycle. Another central question is whether localized pulses of higher SSC in the vicinity of the causative sea bed features depending on wind velocity and spatial resolution rise high enough in the water column and become resolvable to the extent that they create distinct signatures in space-borne optical imagery.

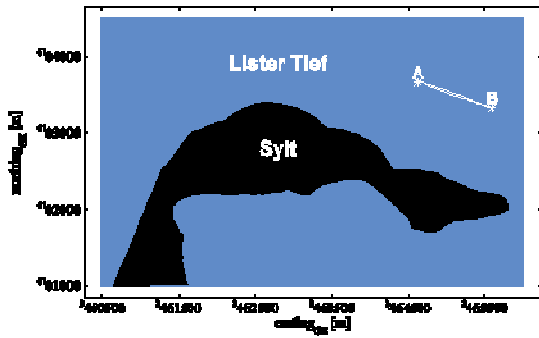


Figure 1. Study area of the tidal inlet of the Lister Tief located northerly of the island of Syt in the German Bight of the North Sea. Transects of the analyzed ADCP measurements are indicated by capital letters AB.

2. MEASUREMENTS

The water level measured at the tidal gauge station List, the wind and current velocity w , E_3 of beam No. 3 (fore beam) measured by the Acoustic Doppler Current Meter (ADCP) and the SSC modulation expressed as $\log((\delta c/c_0)_3)$ of beam No. 3 as a function of water depth over asymmetric submerged compound sand waves on the sea bottom of transect AB (for location see Fig. 1) are shown in Figures 2a-e for ebb tidal current phase. The duration of the measurement time during the tidal phase is indicated by a vertical black beam in Fig. 2a. Each transect has been rotated by an angle of 19° that the current component u is directed perpendicular to the sand wave crest. By using this procedure the v -component of the current field is minimized and can be neglected as a first approximation. The rotation point is marked at the highest sand wave crest (reference crest) shown in Fig. 2c-e. The current velocities shown in Figs. 2b are water depth averaged current velocity values. The time resolution of the wind and current velocity arrows shown in Figs. 2b is 30 s.

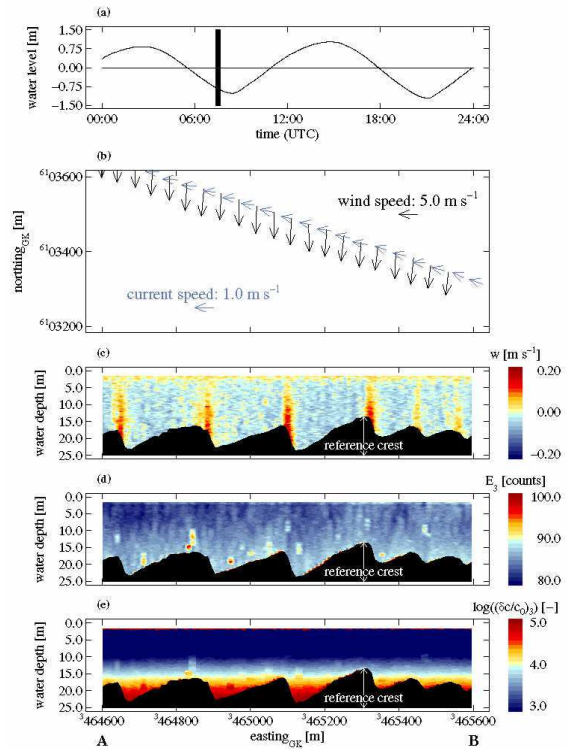


Figure 2. Analyzed data of ADCP beam No. 3 as a function of position and water depth over asymmetric sand waves of transect AB indicated in Fig. 1 in the study area of the Lister Tief during ebb tidal phase at 0721-0740 UTC on 10 August 2002; a) water level measured at the tidal gauge station List, b) wind and current velocity (the two horizontal arrow-scales indicate a wind speed of 5.0 m s^{-1} and a current speed of 1.0 m s^{-1} , respectively), c) vertical current component w of the three-dimensional current field, d) echo intensity E_3 , and e) calculated SSC modulation of $\log((\delta c/c_0)_3)$. The duration of the measurement time is marked by a vertical black beam in a). The position of the reference crest is indicated at the highest sand wave crest in c)-e) of transect AB..

The acquisition time of the measurements shown in Figs. 2a-e was during ebb tidal phase at 0721-0740 UTC on 10 August 2002, after previous high water at station List at 0226 UTC on 10 August 2002. A measured wind speed between 6.7 m s^{-1} and 7.5 m s^{-1} from northerly direction has been observed (Fig. 2b). The mean current speed u_0 was 0.7 m s^{-1} with a mean current direction of 281° . It is shown in Fig. 2b that the angle between the current and wind direction is 90° . The up- and downward components w of the current velocity (Fig. 2c) are regularly distributed above the stoss

and lee slopes of sand waves. Echo intensity counts E_3 are reduced in the water column and near the sea bottom of sand waves because the observation time of transect finished 45 minutes before low tide at station List. The modulations in $\log((\delta c/c_0)_3)$ (Fig. 2e) show enhanced values only near the sea bottom of sand waves.

2.1. Time dependent measurements

The water level measured at the tidal gauge station List with the acquisition times of analyzed transects while the research vessel is sailing against the current direction during ebb tidal current phase, the wind velocities, the current component u (east direction), the echo intensity E_3 of beam No. 3 (fore beam) measured by the ADCP, the vertical current component w , the calculated suspended sediment concentration SSC modulation expressed as $\log((\delta c/c_0)_3)$ of beam No. 3 as a function of time over asymmetric submerged sand waves on the sea bottom of transects AB (for location see Fig. 1) are shown in Figures 3a-h. The parameters u , E_3 , w , and $\log((\delta c/c_0)_3)$ are a function of time and space observed before low water at 0829 UTC on 10 August 2002 at tidal gauge station List. All parameters are vertically water depth averaged values of five single transects during ebb tidal current phase between 0516 UTC and 0740 UTC on 10 August 2002 while the research vessel is sailing against the current direction (acquisition times see Fig. 3a). Measured wind speeds between 5.8 m s^{-1} and 7.5 m s^{-1} from northerly directions have been observed (Fig. 3b). Negative, enhanced and positive values of u , E_3 , and w , respectively, show definite phase relationships with the sand wave crests of the sea bed. In contrast, enhanced $\log((\delta c/c_0)_3)$ shows a phase relationship with the sand wave troughs of the sea bed. All signatures of u , E_3 , w , and $\log((\delta c/c_0)_3)$, respectively, show spatially dependent variations. During the pronounced ebb tidal current phase the intensities of u , w , and $\log((\delta c/c_0)_3)$ are not time dependent. Only E_3 shows a time dependent behavior (see Fig. 3d).

3. CONCLUSIONS

It can be summarized here that our investigations are a further step forward to understand the complex links between wave current interaction,

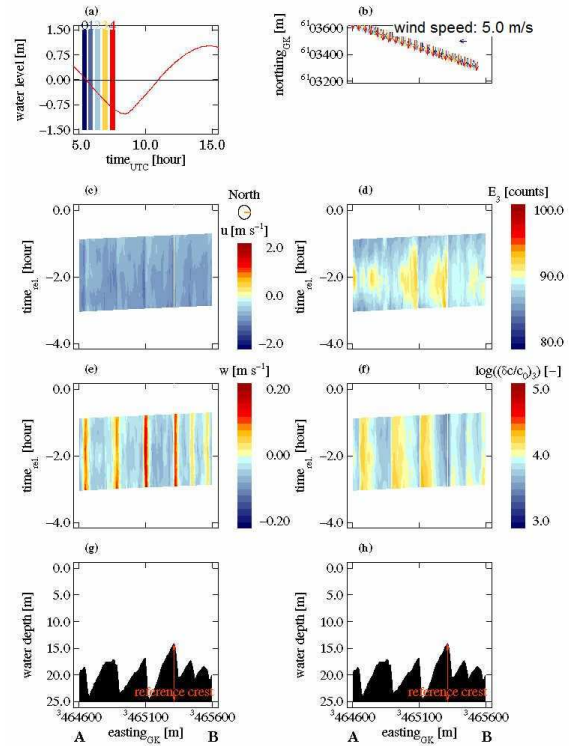


Figure 3. a) Water level measured at the tidal gauge station List with the acquisition times (marked by Nos. 1-5) of analyzed 5 single transects during ebb tidal current phase (current direction from B to A) while the research vessel is sailing against the current direction on 10 August 2002, b) wind velocities (the horizontal arrow-scale indicates a wind speed of 5.0 m s^{-1}), c) current component u (east direction), d) echo intensity E_3 of beam No. 3 (fore beam) measured by the ADCP, e) vertical current component w , f) calculated suspended sediment concentration SSC modulation expressed as $\log((\delta c/c_0)_3)$ of beam No. 3, and g-h) water depth profiles of asymmetric submerged sand waves on the sea bed of transects AB (for location see Fig. 1).

turbulence, bed morphology and sediment transport above compound sand waves in a tidal inlet.

We would like to add here that our phase shift measurements of u , E_3 , w , and $\log((\delta c/c_0)_3)$ are consistent with the experimental data published by Joseph (1954) of time dependent measurements over almost four tidal cycles at an anchor station in the North Sea where turbidity maxima had been first observed near the sea bed before tidal current speeds maximized.

Based on in situ measurements of several oceanographic and meteorological parameters

regarding the hydrodynamics above submerged compound sand waves the following conclusions are drawn:

1. The magnitudes of echo intensity E_3 and calculated suspended sediment concentration SSC modulation expressed as $\log((\delta c/c_0)_3)$ depend on wind and current speed as well as on wind and current direction.

2. Sand suspensions are strongly dependent on the impact of wave activity to maintain high concentrations in the water column. Wave orbital motion at the sea bed is sufficient at measured wind speeds between 11.7 m s^{-1} and 13.3 m s^{-1} from southeasterly direction to stir up sand particles.

3. Bursts of w and E_3 may be also triggered at the disturbances due to megaripples superimposed on sand waves by current/wave interaction at high current and wind speeds observed of opposite directions and measured at high spatial resolution.

4. All averaged signatures of u , E_3 , w , and $\log((\delta c/c_0)_3)$ show spatially variations during ebb and flood tidal current phases.

5. Negative, enhanced and positive values of u , E_3 , and w , respectively, show a definite phase relation with the sand wave crest and upper gentle slope regions of the sand waves during ebb tidal current phase while the research vessel is sailing with or against the current direction. In contrast, enhanced $\log((\delta c/c_0)_3)$ shows a phase relationship with the trough regions of sand waves during ebb tidal current phase. Moderate wind speeds between 5.8 m s^{-1} and 7.5 m s^{-1} from northerly directions were observed.

6. Positive, enhanced and positive values of u , E_3 , and w , respectively, show a phase relationship with the sand wave crest and upper gentle slope regions of sand waves during flood tidal current phase while the research vessel is sailing with and against the current direction. In contrast, enhanced $\log((\delta c/c_0)_3)$ shows a phase relationship with the trough regions of sand waves during flood tidal current phase. All averaged signatures of u , E_3 , w , and $\log((\delta c/c_0)_3)$ show spatially variations due to enhanced wind speeds. High wind speeds between 9.2 m s^{-1} and 13.3 m s^{-1} from southeasterly directions were observed.

7. During pronounced ebb and flood tidal current phases the intensities of u , w , and $\log((\delta c/c_0)_3)$ are not time dependent, whereas the local magnitudes

of these parameters are variable in space above the sand waves.

8. Intense ejections caused by tidal current velocity can transport higher SSC near the bottom boundary at the causative sea bed features towards the free water surface. Such hydrodynamic mechanism creates distinct SSC signatures visible in air- and space-borne optical imagery.

4. ACKNOWLEDGMENT

For the management of the OROMA project we thank F. Ziemer as the responsible coordinator. The captain and crew of the R/V *Ludwig Prandtl* are gratefully acknowledged for their excellent cooperation and assistance during the OROMA experiments. The measurement campaigns have been partially funded by the EU FP5 project OROMA, EVK-CT-2001-00053.

5. REFERENCES

- Bjerknes, V. 1921. On the dynamics of the circular vortex with applications to the atmosphere and atmospheric vortex and wave motions. *Geofysiske Publikationer* 2 (4): 1-90.
- Capuzzo, E., Stephens, D., Silva, T., Barry, J. & Forster, R. M. 2015. Decrease in water clarity of the southern and central North Sea during the 20th century. *Global Change Biology* 21: 2206-2214.
- Defant, A. 1961. *Physical Oceanography Vol. II*. New York: Pergamon Press.
- Hennings, I. & Herbers, D. 2006. Radar imaging mechanism of marine sand waves of very low grazing angle illumination caused by unique hydrodynamic interactions. *Journal of Geophysical Research* 111: C1008 1-15.
- Hennings, I. & Herbers, D. 2014. Suspended sediment signatures induced by shallow water undulating bottom topography. *Remote Sensing of Environment* 140: 294-305.
- Joseph, J. 1954. Die Sinkstoffführung von Gezeitenströmen als Austauschproblem. *Archiv für Meteorologie, Geophysik und Bioklimatologie. Serie A*, 7: 482-501.
- Van Dijk, T. A. G. P. & Kleinans, M. G. 2005. Processes controlling the dynamics of compound sand waves in the North Sea, Netherlands. *Journal of Geophysical Research* 110: F04S10 1-15.

Unit bars formed by dune stacking in a recirculating flume

C. M. Herbert *University of East Anglia, Norwich, Norfolk, UK – Christopher.Herbert@uea.ac.uk*
J. Alexander *University of East Anglia, Norwich, Norfolk, UK – J.Alexander@uea.ac.uk*

ABSTRACT: The flume experiment described in this presentation was designed to study the initiation and development of unit bars. The flume runs started with an initially flat bed within a 10 m long observation channel. Initial unit bar formation resulted from dune amalgamation. Subsequent growth was from bedforms superimposed on the incipient bar amalgamating with it. Bars accreted vertically, upstream and downstream and the lee face prograded downstream. Unit bar internal structure was initially dominated by trough cross-stratification.

1. INTRODUCTION

Smith (1974) defined unit bars as relatively unmodified bars with morphologies determined mainly by depositional processes. Unit bars form in most river types over most climatic regimes. Previous flume research on unit bars (e.g. Jopling, 1965; Reesink & Bridge, 2007, 2009) focused on angle-of-repose lee face development and the resulting high angle cross-stratification, which Cant and Walker (1978) suggested to be the dominant feature of unit-bar deposits. However, Sambrook Smith *et al.* (2006), Lunt *et al.* (2013) and Parker *et al.* (2013), examining ground penetrating radar data from American perennial rivers, suggest that dune cross-sets can make up a significant, or dominant, proportion of preserved unit bar deposits. Lunt and Bridge (2004) and Parker *et al.* (2013) suggest that this may result from scour in the lee of dunes migrating over the bar, cutting deeply into the bar top, replacing the original bar forests with dune cross-strata. Conversely, Sambrook Smith *et al.* (2006) suggest it may result from dune stacking.

Bar formation has been linked to local hydraulic changes such as a downstream change in flow or sediment conditions (Smith, 1974; Cant & Walker,

1978). In published flume research the bar initiation point has been the entry to the experimental channel, a sediment input point (at or upstream of the entry to the channel; e.g. Reesink & Bridge, 2007, 2009), or a constructed bed step mimicking an angle of repose lee-face (e.g. Jopling, 1965). Consequently these publications concentrate on unit bar migration but not bar formation, either because they started with a pre-formed bar-shape bed feature, or because the bars formed at the upstream end of the flume where they could not be fully observed. The flume runs described here were designed so that bars formed spontaneously within the glass-wall section of a flume channel allowing bar initiation to be observed.

2. METHODS

Three flume runs, each of 7200 s duration, are described here. These used a 10 × 1 × 1 m glass-sided channel with 1.95° bed slope, with water and sediment circulated continuously in a closed loop, via pipes and pumps with no holding or settling tanks. Pumping started 1200 s before each run to establish steady conditions. In all 3 runs, the mean flow velocity decreased and water depth increased down the length of channel. Velocity was

measured at fixed points using two acoustic Doppler velocimeters and an ultrasonic Doppler velocity profiler array. Observations were made throughout each run via the glass side walls and the bed was cored and sampled after each run.

Run 1 started with a clean steel floor and involved steady addition of 1000 kg of well sorted sand ($D_{50} = 725 \mu\text{m}$, standard deviation = 1.3). Before Run 2 the bed was mixed and flattened. During Run 2, 2000 kg of sand was added steadily. Before Run 3 the bed was again mixed and flattened. During Run 3, 1000 kg of sand was added steadily. The flow conditions in all runs were as similar as possible, however as the bed aggraded the water surface rose and in Run 3 the water level had to be controlled to avoid water overtopping the channel. In this case, the discharge (controlled by the pumping rate) was reduced to keep the mean velocity at the upstream end of the channel similar to the previous runs.

3. RESULTS

Unit bars formed in all three runs. In Runs 1 and 3 unit bars initiated c. 1 m down the flume (Figure 1). The higher sediment input rate in Run 2 led to unit bar formation nearer the upstream end of the channel where the initiation processes could not be fully observed.

In Runs 1 and 3, flow conditions at the upstream end of the flume caused rapid dune migration. Dune migration slowed downstream and amalgamation was induced by the changes in flow conditions along the channel, creating an incipient unit bar. Following the amalgamation of dunes, the incipient bar accreted vertically, downstream and upstream (Figure 1B). This was achieved by superimposed bedforms stacking on the stoss side of the bar. With small superimposed bedforms, their lee face amalgamated with the bar lee face, but larger superimposed bedforms resulted in major modification of the bar lee face (cf. Reesink & Bridge, 2009).

As dune amalgamation and stacking was key to the formation of unit bars in Runs 1 and 3, and because of the repeated modification of the bar lee face in the lee of larger superimposed bedforms, unit bar internal structure was dominated by small

scale cross-stratification formed by the superimposed bedforms (Figure 1A). In both Runs 1 and 3 an avalanche face began to form by the end of the run.

In Run 2 the rapid growth of the bar was such that the superimposed bedforms were relatively small and resulted in less modification of the lee face of the bar (cf. Reesink & Bridge, 2009). The bar had a steep lee-side avalanche face over most of the run. Consequently the deposit was dominated by bar-lee cross-stratification.

Bar development tended towards a near-horizontal bar stoss surface (Figure 1A). This leads to more uniform, higher velocity flow above the bar, which has the capacity to transport all the sediment entering the upstream end of the channel. Once this threshold of total sediment transport is reached, unit bar growth is dominated by progradation down the channel, unless the flow or sediment conditions change.

4. DISCUSSION

In Runs 1 and 3 unit bar development was controlled by the amalgamation of dunes, consistent with Sambrook Smith *et al.* (2006) proposal that dune stacking could be a mechanism of unit bar formation. This formation mechanism may account for some of the dune cross-stratification observed within unit bar deposits in some North American rivers.

Where bedform amalgamation and stacking leads to bar initiation and growth, and the growth pattern is mostly vertical accretion, the deposits will tend to be dominated by small cross-stratified sets. In contrast, where progradation dominates bar growth, the deposit may be dominated by a larger scale high-angle cross-stratified set.

The formation of an avalanche face is influenced by the relative size of superimposed bedforms. Early in Runs 1 and 3 the superimposed dunes were often a similar height to the unit bar avalanche face (e.g. Figure 1B, 2280 s). As the unit bar grew the relative height of superimposed bedforms reduced, limiting modification of the bar avalanche face by scour in the lee of the superimposed bedforms, and so favoring the

formation of a continuous high angle cross-stratified set.

5. CONCLUSIONS

The flume experiments demonstrate that unit bar growth can be initiated by dune amalgamation encouraged by downstream changes in flow and sediment transport. Initial incipient unit bar growth consisted of vertical, upstream and downstream accretion.

The internal structure of the unit bars was dominated by trough cross-stratification, with high angle planar cross-stratification occurring where progradation was the dominant unit bar growth mechanism.

6. ACKNOWLEDGMENT

This work was supported by the Natural Environment Research Council [grant number NE/L50158X/1]. Thanks to Maria Martínez de Álvaro, Osgur Mcdermott Long, Tom Read, Ruth Kirk, Richard Jones, Emily Peckover, Jenny Stevenson, Simon Ellis and Andy Macdonald for assisting during the flume runs.

7. REFERENCES

Cant, D.J. & Walker, R.G. 1978. Fluvial processes and facies sequences in the sandy braided South Saskatchewan River, Canada. *Sedimentology*: 25, 625-648.

Jopling, A.V. 1965. Laboratory study of the distribution of grain sizes in cross bedded deposits. In G.V. Middleton (ed.), *Primary sedimentary structures and their hydrodynamic interpretation*; SEPM special publication 12: 53-65.

Lunt I.A. & Bridge J.S. 2004. Evolution and deposits of a gravelly braid bar, Sagavanirktok River, Alaska. *Sedimentology* 51: 415-432.

Lunt, I.A., Sambrook Smith, G.H., Best, J.L., Ashworth, P.J., Lane, S.N. & Simpson, C.J. 2013. Deposits of the sandy braided South Saskatchewan River: implications for the use of modern analogs in reconstruction channel dimensions in reservoir characterization. *AAPG Bulletin* 97: 553-576.

Parker, N.O., Sambrook Smith, G.H., Ashworth, P.J., Best, J.L., Lane, S.N., Lunt, I.A., Simpson, C.J. & Thomas, R.E. 2013. Quantification of the relation between surface morphodynamics and subsurface sedimentological product in sandy braided rivers. *Sedimentology* 60: 820-839.

Reesink, A.R.J. & Bridge, J.S. 2007. Influence of superimposed bedforms and flow unsteadiness on formation of cross strata in dunes and unit bars. *Sedimentary Geology* 202: 281-296.

Reesink, A.R.J, & Bridge, J.S. 2009. Influence of bedform superimposition and flow unsteadiness of the formation of cross strata in dunes and unit bars – Part 2, further experiments. *Sedimentary Geology* 222: 274-300.

Sambrook Smith, G.H., Ashworth, P.J., Best, J.L., Woodward, J., & Simpson, C.J. 2006. The sedimentology and alluvial architecture of the sandy braided South Saskatchewan River, Canada. *Sedimentology* 53: 413-434.

Smith, N.D. 1974. Sedimentology and bar formation in the upper Kicking Horse River: a braided outwash stream. *Journal of Geology* 82: 205-223.

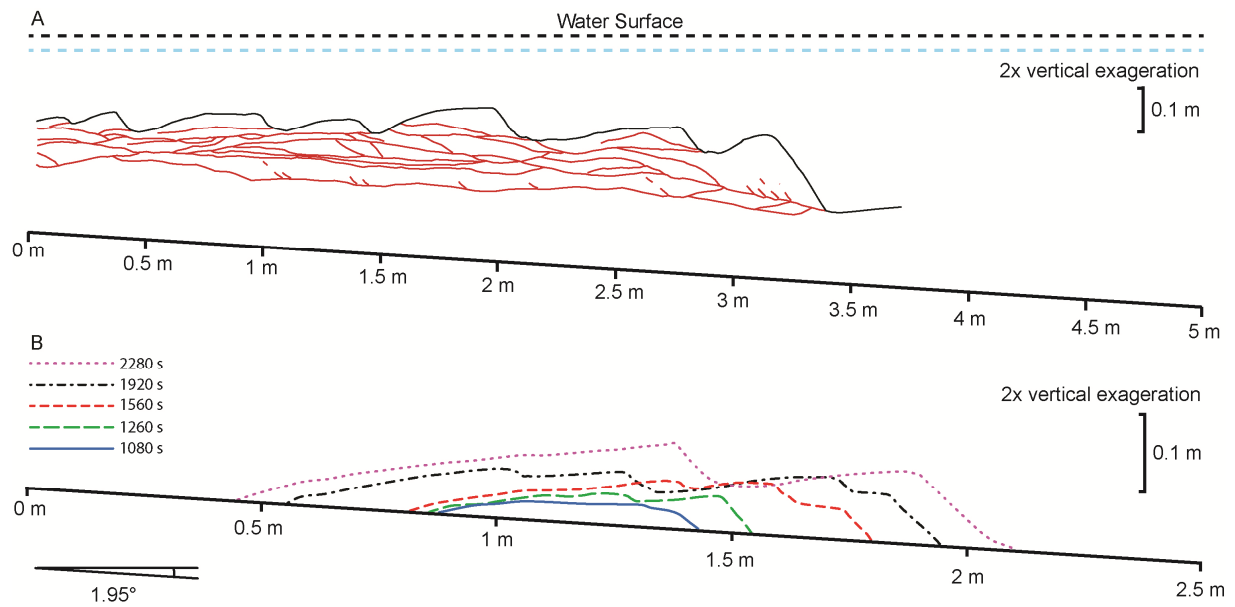


Figure 1. Schematic diagram of; A) the unit bar formed by the end of Run 3, with details of the internal erosion surfaces observed through the right side wall. The water level at the start (lower line) and end (upper line) of Run 3 are denoted with dashed lines; B) unit bar development over 20 minutes of Run 1, recorded from the right side wall.

Larger morphological sea-floor features and bedforms associated to the Mediterranean Outflow Water in the Gulf of Cadiz

F.J. Hernández-Molina, *RHUL, Egham, UK* – Javier.Hernandez-Molina@rhul.ac.uk

G. Ercilla, *ICM, CSIC, Barcelona, Spain* – gemma@icm.csic.es

D. Casas, *IGME, Madrid, Spain* – d.casas@igme.es

C. Roque, *IDL, Univ. Lisbon, Portugal* – cristina.roque@ipma.pt

V. Stow, *D.A. Heriot-Watt University, Edinburg, UK* – dorrik.stow@pet.hw.ac.uk

& *MOWER Cruise team*

ABSTRACT: Larger morphological sea-floor elements and longitudinal and transverse bedforms associated to the overflow of the Mediterranean Outflow Water (MOW) are identified in the Gulf of Cadiz after the Strait of Gibraltar. They are located between 400 and 1000 m water depth, being the larger morphological elements indicative of the MOW deceleration, the along-slope circulation of its upper and lower cores, in addition to a secondary circulation oblique to the main flow due to the Ekman effects. In more detail, the identified bedforms are fundamental for understanding the local boundary layer and the progressive bottom friction of the proximal part of the overflow. This is the case of the large sandy 2D / 3D dunes, which are found within the main erosional channels and furrows in high-velocity bottom current settings, which constitute a very good example of dunes in deep-marine sedimentary environments.

1. INTRODUCTION

The role that bottom currents and associated processes plays in deep marine setting remains poorly understood. Overflows associated to deep Gateway constituted one of these permanent processes (Rebesco et al., 2009), and represents a dense gravity current, carrying a particular water mass, descending the regional slope to a greater depth until it reaches density equilibrium. Entrainment of surrounding water, bottom friction and inertial accelerations modify the bottom current along the slope and frictional transport is confined to a thin layer near the bottom, the *boundary layer* (Legg et al., 2009).

This is the case of the Mediterranean Outflow Water (MOW) after the exit of the Strait of Gibraltar (SG). This strait conditions the Mediterranean–Atlantic water-mass exchange, and is one of the most important oceanic gateways worldwide, enabling the addition of highly saline MOW into the Atlantic Ocean. Upon exiting, the MOW cascades downslope representing an overflow of 0.67 ± 0.28 Sv of warm saline water (Legg et al., 2009). It flows northwestwards after exiting the Strait, settling as an intermediate contour current along the middle slope, at water

depths between 400 and 1400 m (mwd), with two differentiated cores: the Upper Core (MU) and the Lower Core (ML). An extensive Contourite Depositional System (CDS) was generated by the interaction of the MOW and the middle slope. The present work is focused on the proximal sector of the Gulf of Cadiz after the exit of the SG (Fig. 1), characterized regionally by an abrasion surface oriented along-slope between 500 and 800 mwd, ~100 km long and 30 km wide, and by sandy-sheeted drifts, scours, ripple marks, sand ribbons and sediment waves (Hernández-Molina et al., 2014).

Here, we described larger morphological sea-floor features and bedforms generated by the overflow of the MOW in the Gulf of Cadiz, after it is funneled through the SG (Fig. 1). Regional sedimentary processes are considered and their implications discussed. For the characterization of large morphological features, we used oceanographic data, swath bathymetry, seismic, and sedimentological characterization. However, local bedforms information derived from an ARGUS ROV (Fig. 2) used at 19 sites during the MOWER Cruise, September 2014 (Casas et al., 2015; Ercilla et al., 2015).

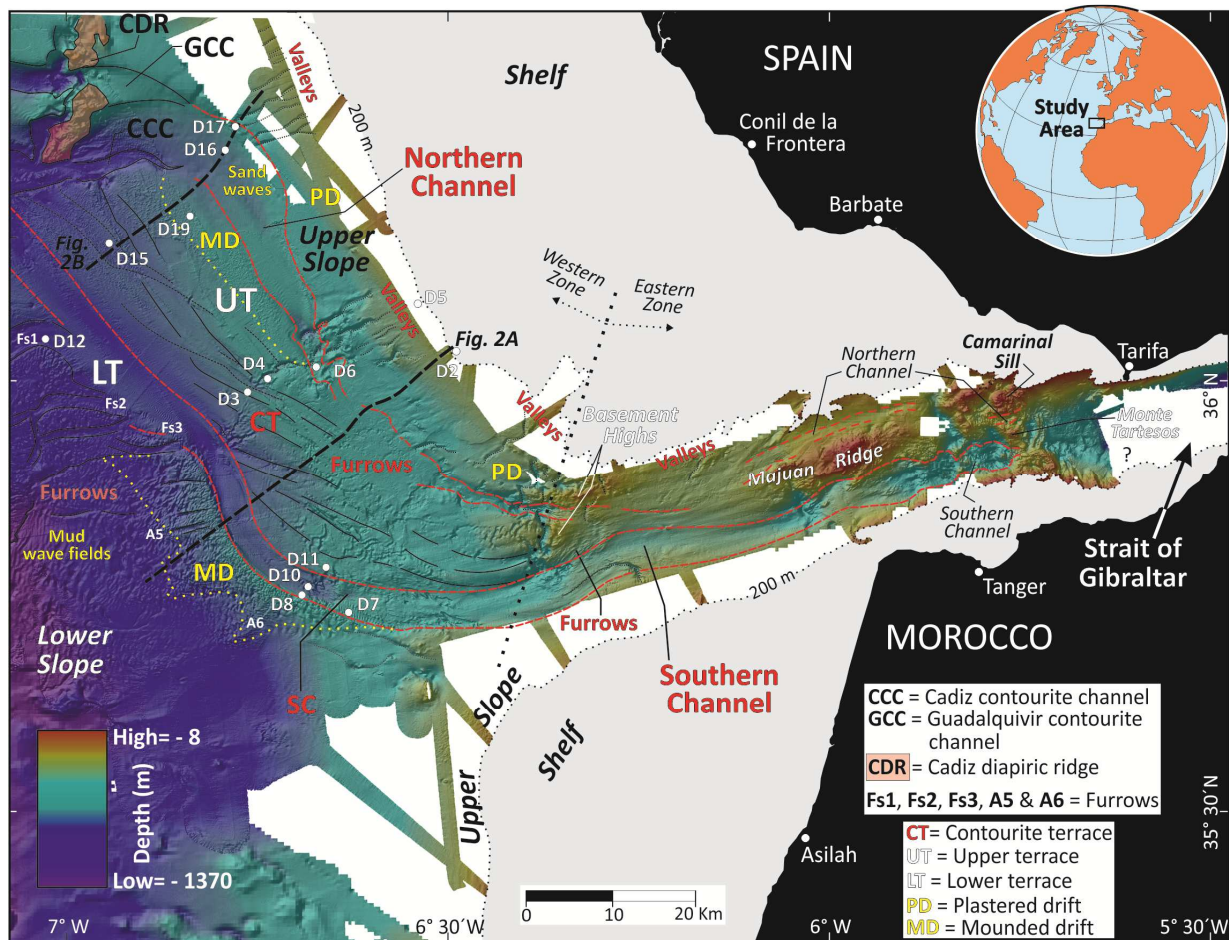


Figure 1. Study area location with swath bathymetry indicating the morphological features (Hernández-Molina et al., 2014) and the dive ROVs' position (D2 to D 19, but positions of dives 13, 14 and 18 are out of this figure).

2. RESULTS

Two terraces (upper & lower) have been identified along the middle slope. They comprise several associated morphologic depositional and erosional elements, including furrows and two large erosive channels (southern and northern, Fig. 1 and 3). When these erosional features were visualized with the ROV, exposed bedrock surfaces are commonly composed by (blue?) marls, and rarely by other rocks types (as calcarenites).

Dive ROVs' results allow to identify smaller scale erosional and depositional features within the aforementioned major morphological elements. Longitudinal and transverse bedforms are abundant (Fig. 4), with a variable sediment composition of bioclastic, terrigenous and mixed. Sandy and bioclastic gravel deposits are dominant, including locally rip-up clasts from the marly substrate. *Linear longitudinal bedforms* are:

scours, grooves and ridges, (bioclastic/gravel) ribbons, crag and tails, ribbon marks, and lineations. Comet scours are common around obstacles. *Transverse bedforms* are sandy ripples, small dunes, large 2D / 3D dunes and giant mudwaves. Gravel dunes are also occasionally reported. Ripples have few cm in height (H) and ~10 to 20 cm in wavelength (λ). They present straight, sinuous, catenary, linguoid, cusped, or lunate shapes. Small 2D dunes have ~0.5-1 m in H and several m in λ , being straight and sinuous the usual shapes. Large 2D and 3D dunes have several m in H and a λ of ~10 to 20 m. Superposition of longitudinal and transverse bedforms is frequent as well as the progressive lateral change of the ripples types. For example, ripples changes from straight to linguoid over the *stoss* of dunes, being straight on their *lee* side. Interference of ripples and small dunes is typical.

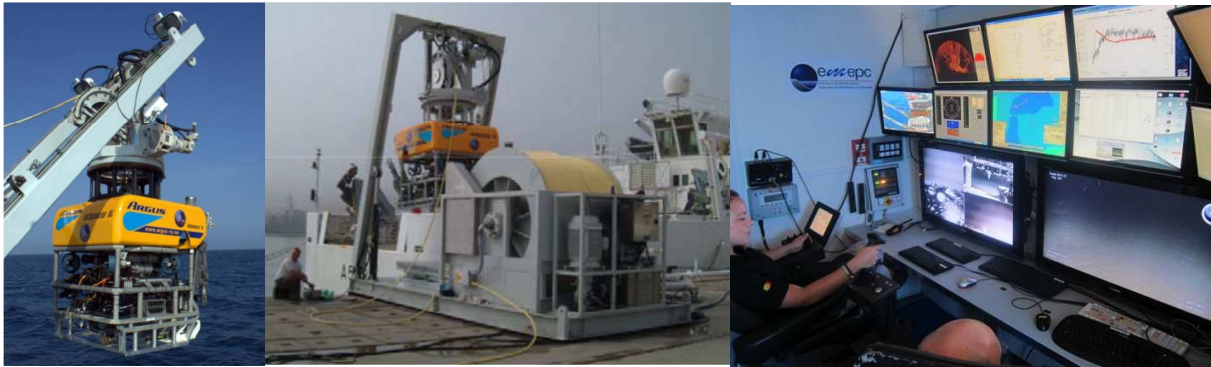


Figure 2. Image of the ARGUS ROV system (left), ROV with its umbilical cable (middle), and control cabin (right).

3. DISCUSSION

Large identified morphological elements indicated on the Fig. 1 result from the MOW undergoing a marked reduction in density, increase in volume, and deceleration within the first ~100 km after its exit from the SG. They evidence for along-slope circulation of the MOW's upper and lower cores (Fig. 3), in addition to a secondary circulation oblique to the main flow due to the bottom Ekman effects (Hernández-Molina et al., 2014).

Limited data existed in the study area from scattered bottom photographs (e.g.; Melières et al., 1970; Stow et al., 2013). Therefore, images of the ARGUS ROV system have been essential for determining the nature of the seafloor and bedforms distribution due to the interaction between the MOW and the seafloor within each

major morphological element. However, even more significantly, they are fundamental for the understanding of the boundary layer and the progressive bottom friction of the proximal and laminar part of the overflow. Longitudinal and transverse bedforms are indicative of the behavior of processes in that boundary layer and how it is affected by both sea-floor irregularities and regional MOW dynamic. That is the case of the sandy large 2D / 3D dunes, which are located within the main channels and furrows. Therefore, their formation corresponds to the particularities of the bottom flow in these deep-marine settings. Based on Stow et al (2009) bottom current higher than 0.5-1 m/s are required for developing those dunes, but > 1 for generating the gravel dunes, gravel ribbons and scours.

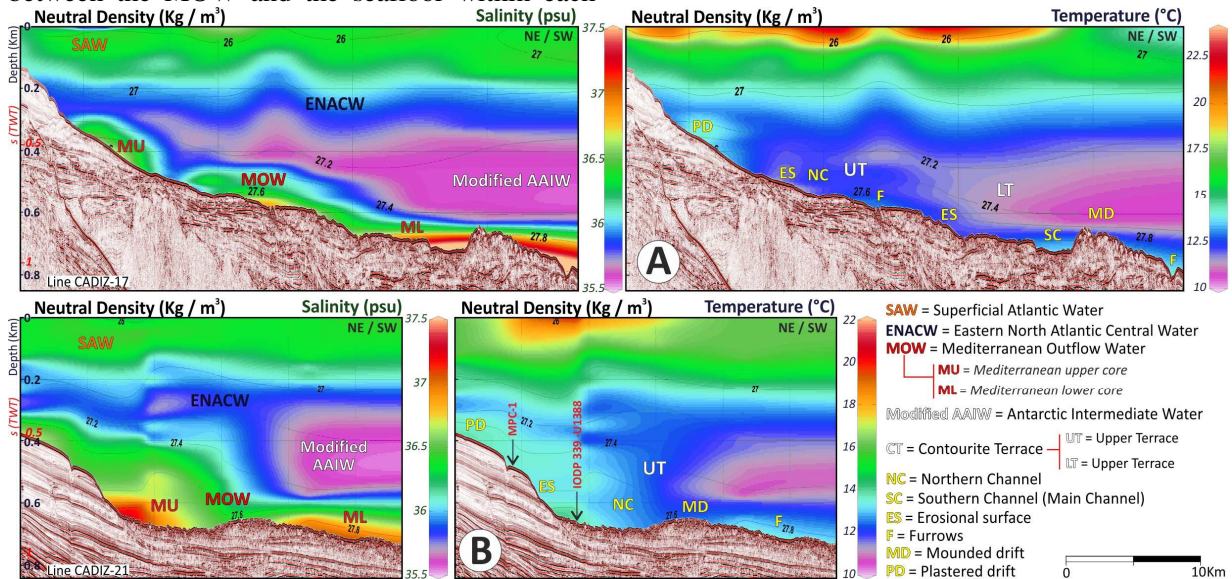


Figure 3. Seismic and hydrographic vertical sections from the exit of the Strait (from Hernández-Molina et al., 2014). The water column colors indicate salinity (left) and temperature (right). Water-mass interpretations are shown on the left sections and major contourite features, on the right sections. Profile locations in Fig 1.

4. CONCLUSIONS

Larger morphological sea-floor elements and bedforms are identified associated to the overflow of the Mediterranean Outflow Water (MOW) and the local behavior of its boundary layer. In this setting, excellent example of large sandy 2D / 3D dunes in deep-marine sedimentary environments are located within main erosional channels and furrows in high-velocity bottom current settings.

5. ACKNOWLEDGMENT

This research was supported through the PTDC/GEO-GEO/4430/2012, CTM 2008-06399-C04/MAR and CTM 2012-39599-C03 projects. Research was conducted in the framework of the Continental Margins Research Group of the Royal Holloway Univ. of London.

6. REFERENCES

Casas, D., Ercilla, G., Hernández-Molina and MOWER cruise team, 2015. Bottom current-generated bedforms: the action of the MOW (Mediterranean outflow). 31st IAS Meeting of Sedimentology, 22-25 June, 2015, Krakow, Poland. Abstract Book p. 111.
 Ercilla, G., Casas, D., Hernández-Molina, F. J., Roque, C. and MOWER cruise team, 2015. Bottom current-generated bedforms: the action of the MOW (Mediterranean outflow) at the exit of the Strait of

Gibraltar. In: J. Acosta, S. Berné, F. Chiocci, A. Palanques, J. Guillen (eds) *Atlas of Bedforms in the Western Mediterranean* ELSEVIER, In press.
 Hernández-Molina, F.J., Llave, E., Preu, B., et al, 2014a. Contourite processes associated to the Mediterranean Outflow Water after its exit from the Gibraltar Strait: global and conceptual implications. *Geology*, 42: 227-230.
 Legg, S., Briegleb, B., Chang, Y., Chassignet, E.P., et al., 2009. Improving Oceanic overflow representation in climate models. The Gravity Current Entrainment Climate Process Team. *Bulletin of the American Meteorological Society*, 657-670.
 Melières, F., Nesteroff, W.D., Lancelot, Y., 1970. Etude photographique des fonds du Golfe de Cádiz. *Cah. Océanogr.* 22, 63-72.
 Rebesco, M.; Hernández-Molina, F.J.; Van Rooij, D., Wåhlin, A., 2014. Contourites and associated sediments controlled by deep-water circulation processes: state of the art and future considerations, *Marine Geology*, 352: 111-154.
 Stow, D.A.V., Hernández-Molina, F.J., Llave, E., Bruno, M., García, M., Díaz del Río, V., Somoza, L. and Brackenridge, R.E. 2013. The Cadiz Contourite Channel: Sandy contourites, bedforms and dynamic current interaction. *Marine Geology*, 343, 99-114.
 Stow, D.A.V., Hernández-Molina, F.J., Llave, E., Sayago-Gil, M., Díaz-del Río, V., Branson, A. 2009. Bedform-velocity matrix: The estimation of bottom current velocity from bedform observations. *Geology* 37, 327-330.

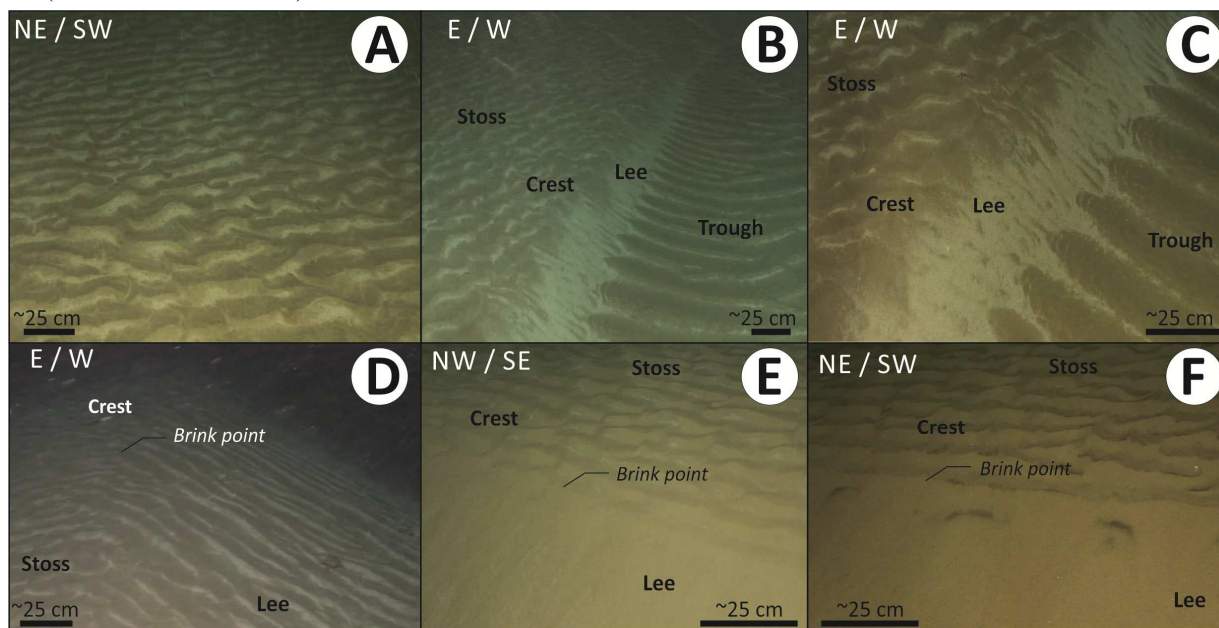


Figure 4. Examples of transverse bedforms related to the MOW. A) Ripples (D13); B and C) Small dunes (D12); D, E and F) Large Dunes (D07 for D and D15 for E and F). See position of ROV sites in Fig. 1.

The response of bedforms and bed elevation to sudden hydrodynamics changes

H. Hu *University of Hull, Hull, UK – H.Hu@2014.hull.ac.uk*

D.R. Parsons *University of Hull, Hull, UK*

A. Ockelford *University of Hull, Hull, UK*

R.J. Hardy *Durham University, Durham, UK*

P.J. Ashworth *University of Brighton, Brighton, UK*

J. Best *University of Illinois Urbana- Champaign, USA*

ABSTRACT: Investigations of bedform generation and development has mostly been conducted under steady flow conditions. However, all fluvial and estuarine environments exhibit temporal variations in flow discharge, creating unsteadiness in flow-sediment transport interactions. The research presented here investigates how bedforms develop under changes in hydrodynamics, and discusses the impact which induces the unexpected development. The results confirm the effect of water depth and velocity on equilibrium bedform height under steady flow, and also highlights the importance of bed elevation adaptations in reaching equilibrium after hydraulic condition variation. The rate of bed elevation variation plays a significant role on bedform generation and development: the higher the flow velocity is, the greater inhibiting effect the bedforms suffers. These Findings provide a specific findings and enrich our comprehension of bedform generation and development under sudden hydraulic condition jumps.

1. INTRODUCTION

The majority of our systematic research on bedforms is based on steady uniform flows in controlled flume experiments. However, all fluvial and estuarine environments exhibit temporal variations in flow discharge, which creates unsteady changes in the flow field. Previous research on dunes under unsteady flow conditions [Raudkivi, 1966; Raudkivi and Witte, 1990; Dalrymple and Rhodes, 1995; Julien and Klaassen, 1995; Yen and Lee, 1995; Carling et al., 2000a; Carling et al., 2000b; Hendershot, 2014] focused primarily on field observations, and fundamental questions about the interactions between morphology, hydrodynamics and sediment transport remain unresolved and there is no universal explanation for the development and response of bedforms to unsteady flows [Best, 2005; Venditti, 2013].

Rapid changes in hydraulic conditions is an extreme condition in the field, and has rarely been investigated [Wijbenga and Klaassent, 2009]. This research aims to investigate how bedforms develop and sediment transport processes respond to

sudden changes in water depth or flow velocity in a set of laboratory experiments.

2. METHODS

Two series of mobile sand bed experiments were undertaken in the TES Flume Facility at the University of Hull. The TES is a large recirculating flume which was configured as a 1.6 m wide and 10 m long channel. The bed material sediment used herein was medium sand with $D_{50} = 400 \mu\text{m}$.

Table1. List of experimental conditions of the six basic states (Series 1)

Velocity (m/s)	Depth (m)	
	0.2 m	0.4 m
0.6 m/s	State 1	State 4
0.75 m/s	State 2	State 5
0.9 m/s	State 3	State 6

In series 1 (Table 1), six basic states were set to run over 6 hours to meet equilibrium conditions, which would provide preliminary views of these six different hydraulic conditions. Additionally,

based on the bedform phase diagram of *Southard and Boguchwal* [1990], the six states all locate at the area where dunes should be generated (Figure 1).

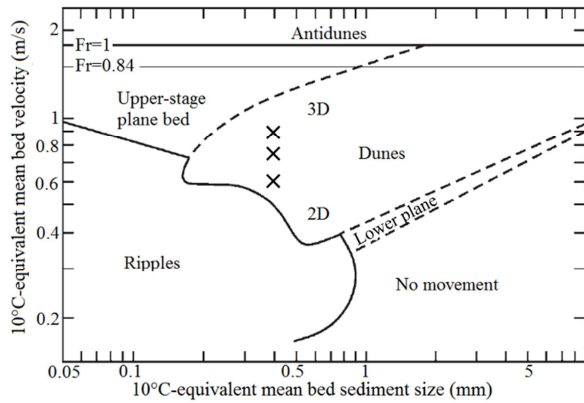


Figure 1. Hydraulic conditions in the bedform phase diagram (after Southard and Boguchwal, 1990).

In series 2, five different hydraulic condition changes were run. For Run 7, 8 and 9, water depth (h) changes from 0.2 to 0.4 m, with velocity keeping constant, while for Run 10 and 11, velocity (U) increase from 0.6 to 0.9 m/s, but water depth remained unchanged. All of the first stage (the first 6 hours) of the five experiments in Series 2 can be treated as basic state runs (Figure 3), as they start from a flat bed, followed by a continuous six hours running to reach equilibrium before the hydraulic conditions were altered again.

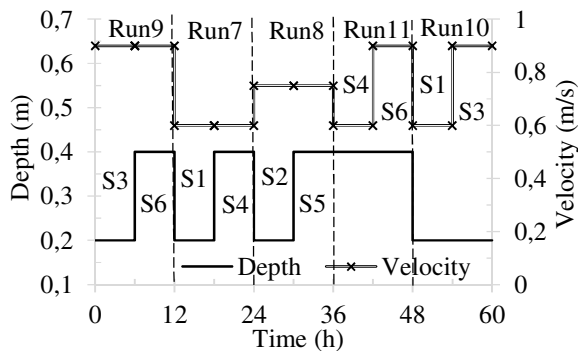


Figure 2. Summary of Series 2. The time here indicates the order of these experiments carried out.

A series of 12 ultrasonic sensors (URS) perpendicular to the main flow were set and used to continuously measure a 4.5m long and 0.6m wide swathe in the middle of the channel. Meanwhile, a set of four Acoustic Doppler Velocimeters (ADV) and one Vectrino ADV

profiler were used to quantify the three-dimensional flow velocities. An Acoustic Backscatter Sensor (ABS) system, which was used to quantify suspended sediment dynamics, was set up downstream of the end of URS measurement area.

3. RESULTS

3.1. Six steady states

3.1.1. Variation between experiments with same water depth

From the first stages of Figure 3a-c ($h = 0.2\text{ m}$), it is clear that with the increase of flow velocity from 0.6 to 0.9 m/s, the equilibrium bedform height (H_e) increased from nearly 4 cm to 5.8 cm. Similarly, the red dashed lines of Figure 3a-c, which present Run 4 to 6 ($h = 0.4\text{ m}$), respectively, show how H_e rises from 4 to nearly 8 cm.

Both of the hydraulic conditions of the first stage of Run 7 (Figure 3a) and Run 10 (Figure 3d) are the same (0.6 m/s flow velocity and 0.2 m water depth), but the processes of the bedform generation and development are different. For the former experiment, the bedform height (H) rises from 2.5 to 4.5 cm within 30 minutes, and reaches equilibrium immediately, while for the latter, H grows from 2.5 to 7 cm within 30 minutes, followed by a decrease to reach equilibrium ($H = 4\text{ cm}$) in 150 minutes. Additionally, both the first stage of Run 8 and Run 9 displays an increase-decrease-equilibrium trend, but the time for reaching equilibrium, which is 100 and 70 minutes respectively, shows a negative relationship with flow velocity. Nevertheless, for the three experiments with a 0.4m water depth (red lines in Figure 3a-c), the increase-decrease-equilibrium trend for H is not evident, and all of the bedform heights in these three experiments attain equilibrium at the very beginning of each experiment.

For experiments with different flow velocities (Figure 3a-c), the processes of bed elevation display somewhat different results. For $h = 0.2\text{ m}$, the processes of the bed elevation of Run 7 and 10 (i.e. state 1) decrease from nearly 3 to -2 cm during the whole six hours, while those of Run 8 and 9 drop to -2 cm at 180 and 100 minutes respectively, and then keep approximately constant. However, the variations of bed elevation for $h = 0.4\text{ m}$

present different trends that both that of Run 7 and Run 8 displays a slight fluctuation along 3 cm during the whole 6 hours, while that of Run 9 increases dramatically from 1 to 6 cm within 30 minutes, followed by a large fluctuation along 6 cm.

Additionally, from Figure 3, it is evident that, the higher velocity the experiments has, larger and more vigorous fluctuations in TKE.

3.1.2. Variation between experiments with the same flow velocity

For experiments with the same velocity but different water depth, H_e is higher in larger water depths, except those with lowest velocity ($U = 0.6$ m/s) whose H_e remains unchanged (Figure 3).

3.2. Sudden hydraulic condition changes

Figure 3d and e show the results of sudden velocity change from 0.6 to 0.9 m/s with water depth 0.2 and 0.4m respectively. In terms of Run 10 (Figure 3d), the initial bed condition of its latter half part (i.e. stage 2) is generated by state 1 which has already developed bedforms, while for Run 3, it starts from flat bed. The sudden change of velocity (Run10) does not affect H_e and it reaches equilibrium rapidly like Run 3, as well. Moreover, both of their bed elevations are about -1.5 cm at equilibrium. The initial bed elevation for the second stage of Run 10 is nearly -2 cm, while that of Run 3 is nearly 4 cm, and it takes 110 minutes to reach equilibrium. However, the variation of TKE does not display a clear trend corresponding to that of bedform height and bed elevation, except that the TKE of Run 3 is generally smaller in magnitude.

Interestingly, for Run 11, the sudden enhancement of velocity does not rise bedform height, instead vanishing to a very low level. Besides, unlike run 6, the bed elevation of stage 2 of Run 11 remains constant, and the fluctuations of TKE are also more intense.

4. DISCUSSIONS

Bedform height prediction is one of the main scientific questions which has been thoroughly investigated during the past 50 years, but remains unsolved [Fredsoe, 1982; Van Rijn, 1984; Yalin, 2013]. As it is well known, equilibrium bedform

height under steady flow is related to water depth, particle size and flow velocity [Van Rijn, 1993] and more recently, clay content [Schindler *et al.*, 2015]. However, our experiments confirm the effect of water depth and velocity, and reflect the importance of bed elevation adaption to equilibrium bedform height for sudden hydraulic condition changes, as well. For our experiments, the sediment is water worked and circularly recirculated. Therefore, the whole system can be regarded as sediment supply limited.

For the lowest velocity run (Run 7), the rate of bed elevation increase is slight, and H_e is not affected. In contrast, for higher velocities (Run 8 and 9), the quicker adaptation of bed elevation apparently influences the generation and development of bedforms. This may be because, the sudden change of water depth (and discharge) alters the mechanisms of sediment transport, such as the ratio of suspended to bedload transport rate and the influence of sediment supplement. This assumption will be verified by data of ABS in further research.

5. CONCLUSIONS

Our experiments confirm the effect of water depth and velocity to equilibrium bedform height under steady flow, and indicates the importance of bed elevation adaption to reach equilibrium, as well. The results show that:

1. For hydraulic condition with lower velocities, the sudden water depth change induces bed elevation's automatic adaption, but the slight rate of increase has little or no effect on bedform development.
2. For hydraulic condition with higher velocities (i.e. discharge), the sudden increase of water depth leads to faster growth of bed elevation, which forbids the development of larger bedforms. After the bed elevation reaches equilibrium, the velocity plays a significant role on the development of bedforms. It may attribute to different mechanisms of sediment transport, which will be further investigated by the data of ABS.

These results give a specific point of view on bedform generation and development under unsteady flow, and can be used to improve numerical models.

6. ACKNOWLEDGMENT

The author is grateful to Ross Jennings who gave some advice on writing, and to Brendan Murphy for assistance of laboratory experiments. This research was partly supported by grant NE/I014101/1 from the UK Natural Environment Research Council (NERC).

7. REFERENCES

- Best, J. (2005), The fluid dynamics of river dunes: A review and some future research directions, *Journal of Geophysical Research: Earth Surface* (2003–2012), 110(F4).
- Carling, P., E. Golz, H. Orr, and A. Radecki-Pawlik (2000a), The morphodynamics of fluvial sand dunes in the River Rhine, near Mainz, Germany. I. Sedimentology and morphology, *Sedimentology*, 47(1), 227-252.
- Carling, P., J. Williams, E. Golz, and A. Kelsey (2000b), The morphodynamics of fluvial sand dunes in the River Rhine, near Mainz, Germany. II. Hydrodynamics and sediment transport, *Sedimentology*, 47(1), 253.
- Dalrymple, R. W., and R. N. Rhodes (1995), Estuarine dunes and bars, *Geomorphology and sedimentology of estuaries*, 53, 359-422.
- Fredsoe, J. (1982), Shape and dimensions of stationary dunes in rivers, *Journal of the Hydraulics Division*, 108(8), 932-947.
- Hendershot, M. (2014), Low angle dune response to variable flow, dune translation, and crestline dynamics in Fraser Estuary, British Columbia, Canada, *Environment: Department of Geography*.
- Julien, P., and G. J. Klaassen (1995), Sand-dune geometry of large rivers during floods, *Journal of Hydraulic Engineering*, 121(9), 657-663.
- Raudkivi, A. (1966), Bed forms in alluvial channels, *Journal of Fluid Mechanics*, 26(03), 507-514.
- Raudkivi, A., and H. Witte (1990), Development of bed features, *Journal of Hydraulic Engineering*, 116(9), 1063-1079.
- Schindler, R. J., D. R. Parsons, L. Ye, J. A. Hope, J. H. Baas, J. Peakall, A. J. Manning, R. J. Aspden, J. Malarkey, and S. Simmons (2015), Sticky stuff: Redefining bedform prediction in modern and ancient environments, *Geology*, 43(5), 399-402.
- Southard, J. B., and L. A. Boguchwal (1990), Bed configurations in steady unidirectional water flows. Part 2. Synthesis of flume data, *Journal of Sedimentary Research*, 60(5).
- Van Rijn, L. C. (1984), Sediment transport, part III: bed forms and alluvial roughness, *Journal of hydraulic engineering*, 110(12), 1733-1754.
- Van Rijn, L. C. (1993), *Principles of sediment transport in rivers, estuaries and coastal seas*, Aqua publications Amsterdam.
- Venditti, J. G. (2013), Bedforms in sand-bedded rivers, *Treatise on Geomorphology*, 137-162.
- Wijbenga, J., and G. Klaassent (2009), Changes in bedform dimensions under unsteady flow conditions in a straight flume, *Modern and Ancient Fluvial Systems (Special Publication 6 of the IAS)*, 35.
- Yalin, M. S. (2013), *River mechanics*, Elsevier.
- Yen, C., and K. T. Lee (1995), Bed topography and sediment sorting in channel bend with unsteady flow, *Journal of Hydraulic Engineering*, 121(8), 591-599.

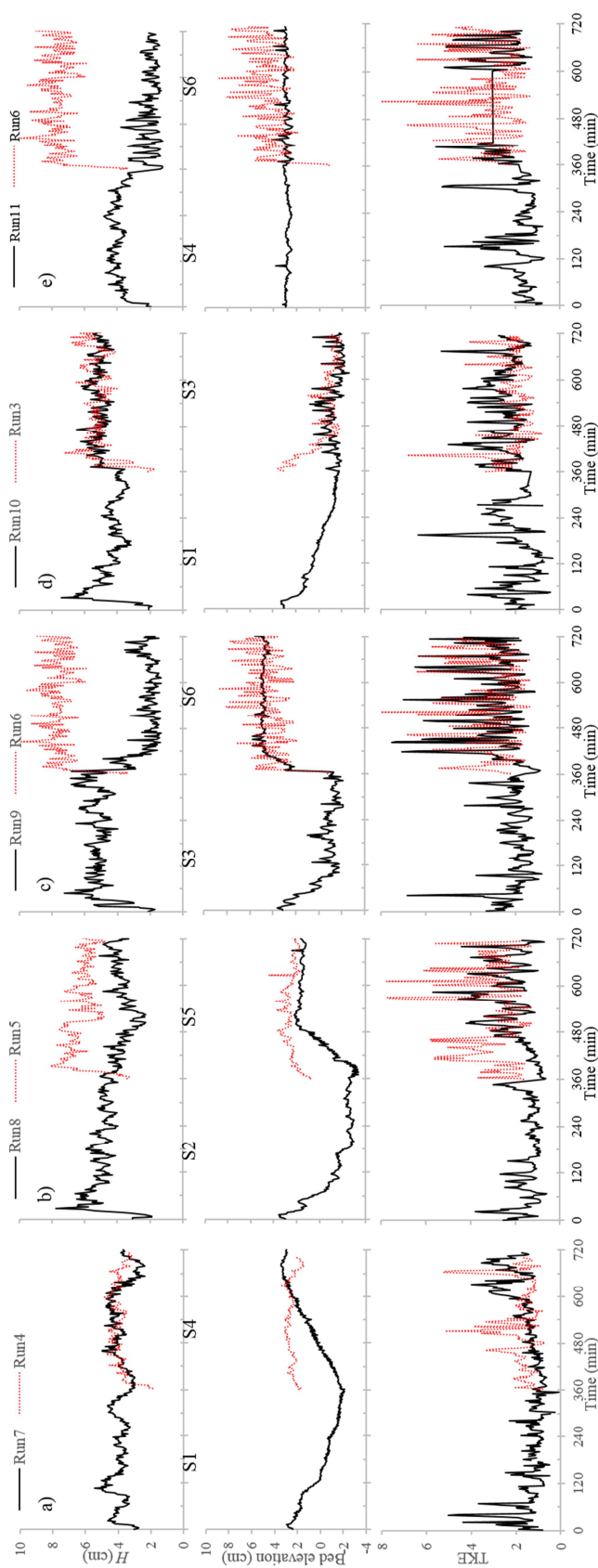


Figure 3. Changes in dune height, derived from the bed profiles using Van der Mark et al. (2008), bed elevation (set at the same datum) and Turbulence Kinetic Energy (TKE, calculated from the lowest ADV, 5 cm above the initial bed): a) Run 7 compared with Run 4; b) Run 8 compared with Run 5; c) Run 9 (i.e. Exp9) compared with Run 6; d) Run 10 compared with Run 3; e) Run 11 compared with Run 6. Notably, the data of ADV was lost between 420 and 600 min, and has been replaced with a straight line; S1-6 denote State 1 to 6.

Application of artificial dunes to shoal protection in waterway regulation practice

Z. Fu *Changjiang Waterway Planning Design and Research Institute, Wuhan, Hubei, China*

W. Huang *Changjiang Waterway Planning Design and Research Institute, Wuhan, Hubei, China, huangvy@whu.edu.cn (corresponding author)*

F. Chen *Changjiang Waterway Planning Design and Research Institute, Wuhan, Hubei, China*

Z. Yue *Changjiang Waterway Planning Design and Research Institute, Wuhan, Hubei, China*

J. Yan *Changjiang Waterway Planning Design and Research Institute, Wuhan, Hubei, China*

J. Geng *Changjiang Waterway Planning Design and Research Institute, Wuhan, Hubei, China*

F. Yang *Changjiang Waterway Planning Design and Research Institute, Wuhan, Hubei, China*

ABSTRACT: To preserve or improve the waterway conditions, shoal protection measures are common taken into. One of common ways is to pave concrete blocks on the shoal to keep sands from erosion. The top surface of the traditional concrete block is plane and relatively smooth, which destroys the natural uneven shape and thus reduces the river bed roughness. In order to keep the natural uneven shape and to be more environmental friendly to the river environment and the aquatic organism, a kind of dune-like concrete block is proposed. The present paper experimentally investigated the flow resistance features, flow structures and sand sedimentation dynamics of the proposed shoal protection measures. In addition, two patterns of pavement were proposed to represent the two - and three - dimensional dunes in the field. Compared to two dimensional dunes, the three dimensional dunes were more stable and were with better effect in prompting sediment deposition.

1. INTRODUCTION

Dunes are ubiquitous in river and marine environments. There are lots of works focusing on flow structures (Maddux et al. 2003a, b; Best 2005; Schindler and Robert 2005; Xie et al. 2013), mechanisms of sediment transport over dunes (Qian and Wan 1983; Van Rijn 1984; Best 2005; Wren et al. 2007; Claude et al. 2012), dune initiation (Venditti et al. 2005) and migration celerity (Giri and Shimizu 2006; Paarlberg et al. 2009; Martin and Venditti 2013). Although great progress in knowledge of understanding dunes has been witnessed, there is few works about how to unitize dunes or to mitigate adverse impact of dunes in the riverine and marine environments. In the present work, artificial dune-like concrete blocks are proposed to replace the traditional plain ones as the ballasts in waterway engineering. The top surface of the traditional concrete block is plane and relatively smooth, which destroys natural uneven shape and thus reduces river bed

roughness. The dune-like blocks can keep natural uneven shape and are more environmental friendly to the river environment and aquatic organisms. The vertical velocity distribution, turbulent intensity and sediment transport are investigated over the dune-like concrete blocks. Influence of different plain layouts of the dune-like concrete blocks on the dune formation and sediment transport are also studied.

2. EXPERIMENT SETUP

The experiments were carried out in a rectangular glass flume which is 36m long, 3.2m wide and 1.0 m high. The Polymethacrylates particles were adopted as sands with a diameter of 1.2mm, dry density of about 450kg/m³ and threshold velocity of about 0.16m/s. The experiments were dedicated to investigate the flow resistance, bedload transport and the deposit characteristics over the dune-like concrete blocks.

The flume is divided into three regions, including the sand paved region (SPR), the test region (TR)

paved by concrete blocks and the rest region. The SPR is 6m long and is just upstream of the TR (Figure 1). The TR is set to be 12 m to minimize the influence of flow and sediment transport in the transition range between different ranges on the results. Three kinds of concrete blocks with different top surface features or different arc heights are used in the experiments, i.e., Plain, Dune-1, Dune-2 (Table 1). The averaged height of Dune-1 is 10 cm which is the same as that of the Plain.

For the velocity and turbulence distribution, there is no sand paved on the bed upstream of the concrete block domain, while the sand is paved for the sediment transport and deposition experiment.

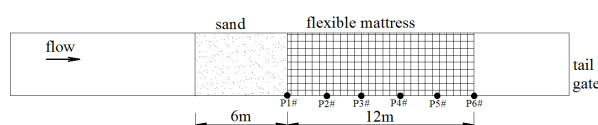


Figure 1. Plane view of the flume and experiment setup.

Table 1. Summary of concrete block sizes (in cm)

Type	Plain	Dune-1	Dune-2
Size	40×40×10	40×40×(8+4)	40×40×(8+7)

3. RESULTS

3.1 Flow resistance

Flow resistance is calculated by gradient of water level. The gradients are 0.025%, 0.074% and 0.104% for Plain, Dune-1 and Dune-2 respectively. It is shown that the flow resistance is larger with a larger height. It is implied that the dune-like concrete blocks can increase the roughness of the bed compared with the traditional plain one. Moreover, it will induce more deposition.

3.2 Vertical velocity and turbulence

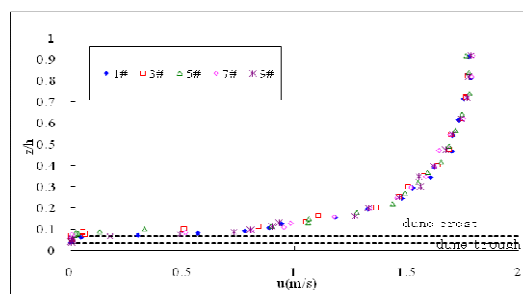
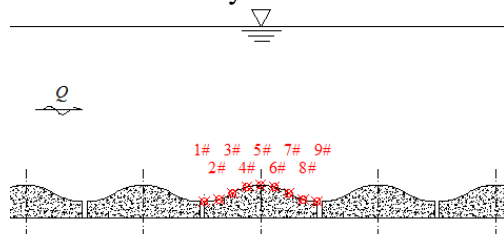


Figure 2. Vertical velocity distribution over Dune-2.

The vertical velocity distribution of Dune-2 is shown in Figure 2. Vertical velocities at nine sites are measured. It is shown that the vertical velocity is generally in line with logarithmic distribution. The difference of velocity among different sites confined to $z/h < 0.16$. For the near bed velocity, the velocity in the dune crest is larger than that in the other sites and that in the trough is with smallest velocity.

The turbulence intensity distribution has illustrated that the maximum value occurs in the near-bed boundary for the Plain and it decreases with the z/h increased (Figure 3). In contrast, the maximum turbulence intensity occurs at the crest of the dune block and it declines in the trough.

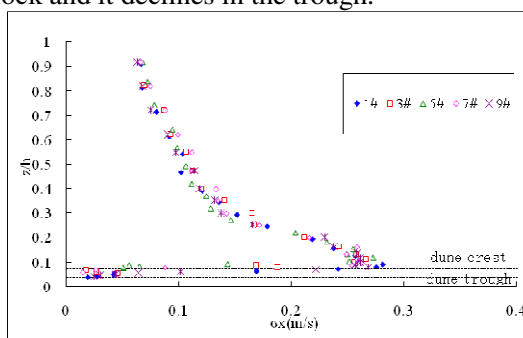


Figure 3. Turbulence intensity distribution over Dune-2.

3.3 Sediment transport and deposition

To investigate the sediment transport and deposition characteristic of different kinds of concrete blocks, experiments over mobile bed are carried out. In a 6m range domain of the flume sands are paved on to provide sands in the concrete block domain. Two types of dune plain layout are proposed representing two- and three- dimensional dune distributions in the field. i.e., symmetric and staggered distribution respectively(Figure 4).

The influence of dune height and plain layout of dune are also studied.

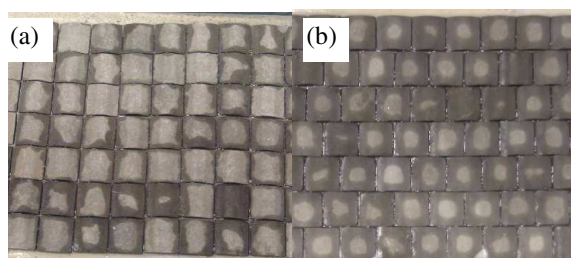


Figure 4. Symmetric (a) and staggered distribution dunes (b), the water flows from left to right.

The results demonstrate that sands in the SPR are moved and transported downstream to the TR (Figure 5). The dunes are formed downstream in the TR. Over all, the characteristics of the dune are different for different bed surface. If there is no concrete blocks paved on the bed in the TR, the length of dune in the equilibrium state is about 5~7cm, the height is about 2~3 cm, the slope for the stoss side and lee side are 1:3~4 and 1:1~2 respectively.



Figure 5. Dunes over glass bed in the test region.

If the Plain blocks are paved in the TR, characteristics of dune is similar to those over glass bed, with dune length of about 10cm, height of 2~3cm stoss and lee side slopes of 1:3~4 and 1:1~2 respectively (Figure 6).



Figure 6. Dunes over Plain blocks in the test region.

If the Dune-2 is paved on in the TR, the dunes are different from those on glass bed and Plain blocks. Due to the uneven shape of the dune-like blocks,

there is circulation current in the trough region. The dunes will form until the trough is filled by sands. It should be note that the sands deposited in the trough remains unmoved as the dunes move downstream. Moreover, the dunes are not moved in continuous form (Figure 7). Sands covering the crest of dune block may be moved away, which lead the crest to be exposed. The crest can also be covered by the sands from upstream. The height of dunes over the crest is up to 5~6cm for Dune-1, which is much higher than those over glass bed and over Plain blocks. What's more, the height of dunes over Dune-2 is larger than that of Dune-1. It means higher dune blocks will lead to higher dunes.



Figure 7. Dunes over Dune-1 in symmetric layout.

Both the symmetric and staggered layout of dune blocks can induce sand deposition in the trough region. However, the deposition form is different. The dunes are in parallel and the space between dunes are similar for the symmetric layout. The dunes are likely the point bar and forms a continuous sediment transport passage at the interface of two group of dunes (Figure 8).

It is also shown that the height of two dimensional dunes are smaller than that of the three dimensional dunes.



Figure 8. Dunes over Dune-1 in staggered layout.

4. CONCLUSIONS

The paper presents flow and sediment transport over dune-like blocks. Vertical velocity distribution implies the influence of the dunes geometry confined in a small region. The results

show that the dunes over dune-like blocks are much higher than those over glass bed and plain blocks. The height of formed dunes will increase with a larger height of dune blocks. Different layouts of dune-blocks also result in different dune forms and dune heights, two dimensional dune-block induces higher dunes than those of three dimensional dune-blocks.

5. ACKNOWLEDGMENT

The author is grateful to National Natural Science Funds of China (Grant No. 11502032).

6. REFERENCES

- Best, J. 2005. The fluid dynamics of river dunes: A review and some future research directions. *Journal of Geophysical Research* 110: 1-21.
- Claude, N., Rodrigues, S., Bustillo, V., Br  h  ret, J.-G., Macaire, J.-J., Jug  , P. 2012. Estimating bedload transport in a large sand–gravel bed river from direct sampling, dune tracking and empirical formulas. *Geomorphology* 179: 40-57.
- Giri, S., Shimizu, Y. 2006. Numerical computation of sand dune migration with free surface flow. *Water Resources Research* 42 (W10422): 1-19.
- Maddux, T.B., Nelson, J.M., McLean, S.R. 2003a. Turbulent flow over three-dimensional dunes: 1. Free surface and flow response. *Journal of Geophysical Research: Earth Surface* 108(F1): 1-20.
- Maddux, T.B., McLean, S.R., Nelson, J.M. 2003b. Turbulent flow over three-dimensional dunes: 2. Fluid and bed stresses. *Journal of Geophysical Research: Earth Surface* 108(F1): 1-17.
- Martin, C.Y. and Venditti, J.G. (2013) An empirical model of subcritical bedform migration. *Sedimentology* 60(7): 1786-1799.
- Paarlberg, A.J., Dohmen-Janssen, C.M., Hulscher, S.J., Termes, P. 2009. Modeling river dune evolution using a parameterization of flow separation. *Journal of Geophysical Research: Earth Surface* 114: 1-17.
- Qian, N. and Wan, Z. H. 1983. *Mechanics of sediment transport*. Science Press, Beijing. (in Chinese)
- Schindler, R.J., Robert, A. 2004. Suspended sediment concentration and the ripple–dune transition. *Hydrological Processes* 18: 3215-3227.
- Van Rijn, L.C. 1984. Sediment transport III: bed forms and alluvial roughness. *Journal of Hydraulic Engineering*, 110(12): 1733-1754.
- Venditti, J.G., Church, M.A. and Bennett, S.J. 2005. Bed form initiation from a flat sand bed. *Journal of Geophysical Research: Earth Surface* 110(F1): 1-19.
- Wren, D.G., Kuhnle, R.A., Wilson, C.G. .2007. Measurements of the relationship between turbulence and sediment in suspension over mobile sand dunes in a laboratory flume. *Journal of Geophysical Research: Earth Surface* 112: 1-14.
- Xie, Z., Lin, B., Falconer, R.A., Maddux, T.B. 2013. Large-eddy simulation of turbulent open-channel flow over three-dimensional dunes. *Journal of Hydraulic Research* 51: 494-505.

Dune migration around a bar within a tidal system

C.E. Keevil *University of Hull, Hull, UK – c.keevil@hull.ac.uk*

D.R. Parsons *University of Hull, Hull, UK – d.parsons@hull.ac.uk*

P.J. Ashworth *University of Brighton, Brighton, UK – p.ashworth@brighton.ac.uk*

J.L. Best *University of Illinois, Urbana-Champaign, Illinois, USA – jimbest@illinois.edu*

A.P. Nicholas *University of Exeter, Exeter, UK – a.p.nicholas@exeter.ac.uk*

E.W. Prokocki *University of Illinois, Urbana-Champaign, Illinois, USA – prokock1@illinois.edu*

S.D. Sandbach *University of Exeter, Exeter, UK*

G.H. Sambrook Smith *University of Birmingham, Birmingham, UK – g.smith.4@bham.ac.uk*

C.J. Simpson *Fulcrum Graphic Communications, Alberta, Canada – cjsimpson@fulcrumgraphics.com*

ABSTRACT: Sediment transport processes within river-estuary systems are governed by the complex interplay between tidal and fluvial hydrodynamics, resulting in a poorly defined transition zone between fully tidal and fully fluvial bedforms. This paper investigates the morphodynamics of large scale bedforms around a large bar within a braided tidal-fluvial transition zone. The migration and adjustment of the bedforms to local flow patterns are investigated using multibeam echosounder (MBES) bathymetric surveys and acoustic Doppler current profiler (ADCP) flow measurements. Bedforms are observed on multiple scales, with the largest found to be fluvially-dominated, and steered around the barhead. Smaller superimposed bedforms exhibit a tidally-derived morphology, notably in seaward regions of the bar. Results also show that migration of the larger bedforms, whilst appearing fluvial in terms of their morphology, are actually dynamically linked to the tidal flows with some upstream migration. This has implications for our understanding of the process mechanics of bedforms in this complex region.

1. INTRODUCTION

The combined tidal and fluvial inputs to river-estuary systems result in a complex landward transition from tidally-dominated zones through to tidally-influenced river systems. This transition is highly mobile, depending on local tides and fluvial flows, moving on daily, monthly and seasonal cycles. The maximum upstream incursion of the tide, known as the tidal maximum, occurs within the fluvially-dominated region of the river-estuarine system, at which point the fluvial currents are only slowed and modulated by high tides. Closer to the ocean, tidal influence increases and fluvial flow will stop or can be reversed (Dalrymple and Choi, 2007). At a given time, the position of the tidal limit will vary dependent on local river levels, tidal range and estuary geometry (Dalrymple et al., 1992).

The resultant flows and sediment transport processes, whilst sharing characteristics, will reflect the environment in which they formed (e.g., Best et al., 2003; Bridge, 1993; Fustic et al., 2012;

Martinius and Gowland, 2010). Sediment transport will vary through this region as the fluvial flow is modulated or reversed (Dalrymple and Choi, 2007; Dalrymple et al., 2012). Whilst distinct patterns of bedforms may be observed from fully-tidal to fully-fluvial, the resultant bedforms may be modified or have a variable morphology due to the movement of the tidal-fluvial transition.

This paper investigates the bedforms found in a fluvially-dominated estuary system and their accommodation to local flow conditions and topographic forcing. The effects of the tidal-fluvial interaction on the resultant bedforms and their migration will be investigated.

2. FIELDSITE

The Columbia River is the largest river on the Pacific coast of North America, with a drainage basin of 660,480 km², entering the Pacific Ocean near to Astoria, Oregon, US (Gelfenbaum, 1983; Simenstad et al., 2011). A meso-tidal system, the turbidity maximum is highly mobile in response to

variations in river flow and tides, moving by up to 20 km (Gelfenbaum, 1983). The estuary is predominantly sand-bedded, with the rate of bedload transport varying with river flow (Jay et al., 1990). The area studied is near Astoria, OR about 40 km upstream from the mouth of the estuary (Jay et al., 2011). This region is fluvially-dominated and contains significant bar complexes with two primary channels, a regularly dredged navigation channel which is the main shipping route and a second deep channel to the south (Figure 1). The present work investigates the bathymetry and flow around a single bar in the landward region of the Columbia River Estuary, located within the secondary channel (Figure 1).

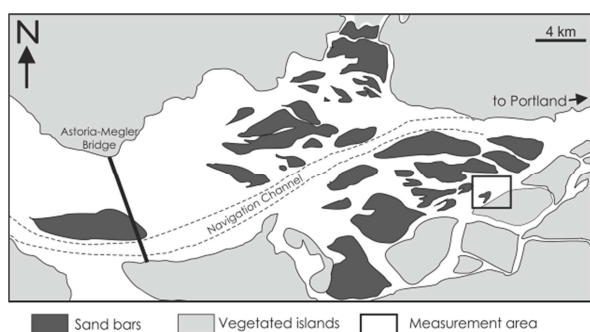


Figure 1. The Columbia River Estuary, WA, USA. Well-developed bar complexes can be seen throughout the estuary, some of which are vegetated. The bar investigated herein is located within the landward region of the bar complex, adjacent to the secondary deeper channel.

3. METHODOLOGY

Bathymetric measurements were made using a Multibeam Echosounder (MBES) of a region 1.9 km by 1 km surrounding a large bar which became fully submerged at high tides. This bar is situated within the braided region of Cathlamet Bay at the landward end of the estuary and is 950 m in length and 400 m wide (Figure 2). The measured section mainly consists of a shallowing sand bar with surrounding bifurcated channels. Flow measurements were also made using an acoustic Doppler current profiler (ADCP) along several transects around the bar at different tidal-fluvial conditions to investigate the local fluid flow structure through the evolving tidal conditions.

4. RESULTS

Bathymetry measurements were made as close to the bar top as the equipment allowed. The shallowest regions measured, on the bar top, are 1.1 m deep relative to local mean sea level, with small scale dunes, which increase to a 2 m wavelength in slightly deeper regions. The edge of the bar is marked by deeper channels containing larger scale bedforms. The southeastern edge of the measured section contains channel 9.5 m deep relative to local mean sea level, with sinuous dunes up to 4m in wavelength, oriented in a seaward direction. The northwestern margin contains a wider channel 7 m deep, with large dunes 40 m in wavelength and relative crest heights of 0.9 m. The region landward of the barhead contains several northeast – southwest oriented longitudinal dune crests with crest separations of up to 200 m and crest heights of approximately 1.5 m. Cross cutting these dunes are large sinuous dunes with a northwest – southeast orientation, with crest lines continuing across the longitudinal dune margins. These dunes are approximately 40 m in wavelength with relative crest heights of 0.9 m; again, superimposed on the dunes crests are smaller dunes.

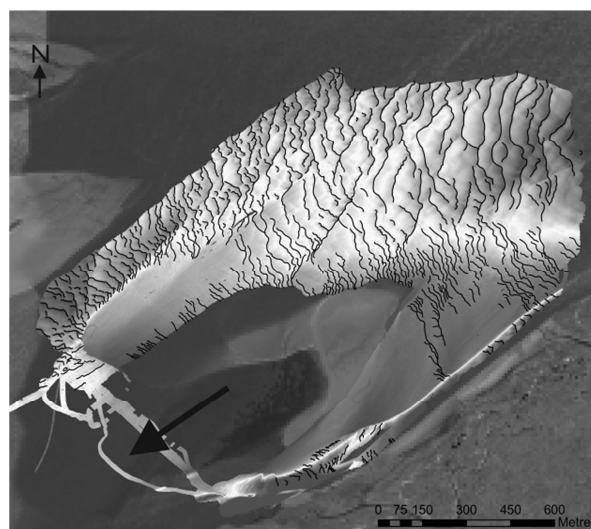


Figure 2. Multibeam echosounder bathymetry of the bar investigated herein (location shown in Figure 1). The variation in crest orientation (marked in figure) can be clearly seen the largest of which form longitudinal crests oriented north-east southwest, oblique to the dominant flow direction (shown as an arrow). Smaller bedforms are oriented with the dominant flow.

The longitudinal dune features have formed with crests oblique to the local flow patterns and matches the orientation of dunes further landward within the same channel. The cross-cutting smaller dune crests are oriented with the local flow, showing the adaptation of sediment transport to the local topographic conditions. Modification of sediment re-routing structures by the incoming flood tide is observed close to dune crests.

Smaller bedforms (< 2 m in wavelength) are superimposed on the larger dune crests across the entire domain, with crest orientations matching the larger bedforms. Whilst those observed in the shallower bar adjacent regions have a more symmetrical, tidally-influenced geometry, the superimposed bedforms are more fluvially-dominated.

Migration of bedforms at all scales can be observed in repeated measurements made across several days. Some landward migration is observed, although the morphology of the bedforms remains strongly fluvial in nature.

5. CONCLUSIONS

Within a tidal system, detailed bathymetric and flow measurements around a large bar reveal fluvially-dominated bedforms. These bedforms occur at a number of scales and show rapid migration and adjustment to flow around the local topography. Although the bedforms appear to be fluvial in character, their migration is also influenced by the incoming tides. This cryptic nature may result in the misinterpretation of similar bedforms as fully fluvial, missing the tidal nature of the system.

6. ACKNOWLEDGMENT

The work in this project was carried out as part of NERC grant NE/H007954/1. Thanks to CMOP (Portland), Clatsop College and MERTS in Astoria, OR (Michael Wilkin in particular), Pat and Sandee Killion, and Mike Stecher.

7. REFERENCES

- Best, J.L., Ashworth, P.J., Bristow, C.S. & Roden, J., 2003. Three-dimensional sedimentary architecture of a large, mid-channel sand braid bar, Jamuna River, Bangladesh. *Journal of Sedimentary Research* 73: 516-530.
- Bridge, J.S. 1993. Description and interpretation of fluvial deposits: A critical perspective. *Sedimentology* 40: 801-810.
- Dalrymple, R.W. & Choi, K. 2007. Morphologic and facies trends through the fluvial-marine transition in tide-dominated depositional systems: A schematic framework for environmental and sequence-stratigraphic interpretation. *Earth-Science Reviews* 81: 135-174.
- Dalrymple, R.W., Mackay, D.A., Ichaso, A.A. & Choi, K.S. 2012. Processes, morphodynamics, and facies of tide-dominated estuaries. In: Davis Jr, R.A. and Dalrymple, R.W. (Eds.), *Principles of Tidal Sedimentology*, Springer, 79-107.
- Dalrymple, R.W., Zaitlin, B.A. & Boyd, R. 1992. Estuarine facies models: Conceptual basis and stratigraphic implications. *Journal of Sedimentary Petrology* 62: 1130-1146.
- Fustic, M., Hubbard, S.M., Spencer, R., Smith, D.G., Leckie, D.A., Bennett, B. & Larter, S., 2012. Recognition of down-valley translation in tidally influenced meandering fluvial deposits, Athabasca Oil Sands (Cretaceous), Alberta, Canada. *Marine and Petroleum Geology* 29: 219-232.
- Gelfenbaum, G. 1983. Suspended-sediment response to semidiurnal and fortnightly tidal variations in a mesotidal estuary: Columbia River, USA. *Marine Geology* 52: 39-57.
- Jay, D.A., Giese, B.S. & Sherwood, C.R. 1990. Energetics and sedimentary processes in the Columbia River Estuary. *Progress in Oceanography* 25: 157-174.
- Jay, D.A., Leffler, K. & Degens, S. 2011. Long-term evolution of Columbia River tides. *Journal of Waterway, Port, Coastal, and Ocean Engineering* 137: 182-191.
- Martinius, A.W. & Gowland, S. 2011. Tide-influenced fluvial bedforms and tidal bore deposits (Late Jurassic Lourinã Formation, Lusitanian Basin, Western Portugal). *Sedimentology* 58: 285-324.
- Simenstad, C.A., Burke, J.L., O'Connor, J.E., Cannon, C., Heatwole, D.W., Ramirez, M.F., Waite, I.R., Counihan, T.D. & Jones, K.L. 2011. Columbia River Estuary Ecosystem Classification—Concept and Application: U.S. Geological Survey Open-File Report 2011-1228, 54 pp.

Field measurements of small scale bedform dynamics in tidal environments in the German Bight

K. Krämer *MARUM, University of Bremen, Bremen, Germany – kkraemer@marum.de*

C. Winter *MARUM, University of Bremen, Bremen, Germany – cwinter@marum.de*

ABSTRACT: In a series of field campaigns an autonomous sea floor observatory has been deployed at a number of representative locations in the German Bight. For periods covering semidiurnal tidal cycles of ca. 25 h, these measurements yield information on the hydrodynamic forcing due to tidal currents and waves and their effect on the properties and dynamics of small scale bedforms. Data from several campaigns allow the assessment of seafloor dynamics for different sedimentary environments under different forcing conditions.

1. INTRODUCTION

The dynamics of bedforms like ripples and dunes in sandy sediments are well studied in laboratory flume experiments (Yalin, 1985; Baas, 1994) and in field measurements in rivers (Vanoni, 1974; van Rijn, 1984). Field observations in shallow shelf sea tidal environments with alternating or rotating tidal flow directions and varying wave conditions are rare (Bolaños et al., 2012) and so far do not systematically cover different sedimentary environments. We make use of autonomous sea floor observatories to measure hydrodynamic forcing and the response of the sea bed in terms of existence of small scale bedforms, their dimensions and migration rates. Within the project *NOAH (North Sea Observation and Assessment of Habitats)* this information is integrated together with biological data on microbiology and benthic fauna to characterize sea floor habitats and their dynamics.

Nine sites of different sedimentary characteristics in the North Sea have been investigated repeatedly. Water depths range from 28 to 41 meters. Bed sediments range from well-sorted fine sand to coarse sand with shell fragments. 10-minute averages of near bed peak tidal flow velocities range from 0.1 to 0.4 m/s. Small scale bedforms

(ripples) of a few centimeters in height and 10-20 cm in length are abundant at most of the stations. Observed conditions span moderate tidal driven periods and moderate wave conditions up to storm events with significant wave heights exceeding 2 m.

2. METHODS

2.1. Observation platform and devices

The autonomous seafloor observatory *SedObs* is a quad pod steel frame which provides installation space for instruments at the four legs and on a platform located ca. 1.8 m above the sea bed. The observatory has been deployed at a number of representative sites for periods of at least 25 hours to cover the semidiurnal daily inequality in the tidal cycle. A photo of the recovery of the *SedObs* observatory is shown in **Figure 1**.

The lander instrumentation comprises hydroacoustic and optical sensors for the measurement of hydrodynamic forcing and morphodynamic response of the sea floor. The bathymetry below the platform in a range of around 3 m is recorded by a 3D profiling pencil beam sonar similar to the one described by Bell and Thorne (2007). Upward and downward

looking ADCPs contribute information on wave parameters and current velocity. Pointwise measurements of flow velocity and turbulence characteristics are recorded at two heights above the sea floor by Vector velocimeters. A LISST device is used to obtain the grain size distribution of suspended sediments while a CTD records pressure and environmental parameters. The sensors are operated continuously with sampling frequencies of 1 Hz (ADCPs, CTD and LISST) or in successive 8 minute bursts with a sampling frequency of 32 Hz (ADVs). The sonar takes 12 minutes for a complete 360° bathymetry scan.

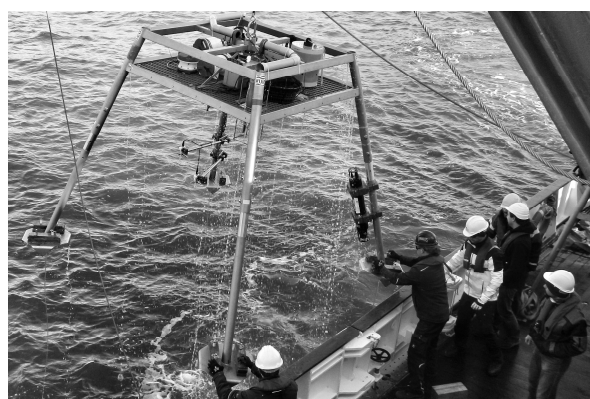


Figure 1. Recovery of seafloor observatory SedObs. Instruments visible are the upward looking ADCP on the instrumentation platform as well as two Vector-ADVs and the LISST device on the legs.

Sedimentological data such as grain size distribution statistics are calculated from Coulter laser diffractometer analysis of bed grab samples taken at the deployment sites.

2.2. Data processing

The raw data recorded by the different sensors is processed to gain a set of parameters for further analysis. Seabed characteristics are extracted from the water column echo of the profiling sonar by picking the maximum echo amplitude. The resulting scattered points are gridded with a resolution of 25 mm to obtain digital elevation models (DEMs) of the bathymetry. The central area of 2×2 m is cropped for further analysis (Figure 2).

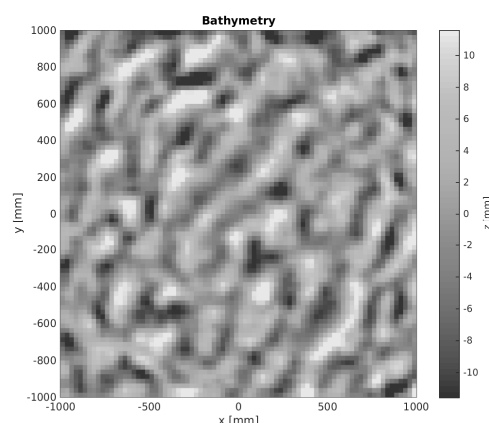


Figure 2. Exemplary dataset of small scale bedforms visible in detrended bathymetry DEM from 3D profiling sonar.

After detrending, the individual scans are subjected to image processing techniques to identify individual bedforms as objects defined by connected pixels exceeding a given threshold height. The orientation of the bedforms is used to rotate the scan which can then be analyzed in transects perpendicular to the average bedform crest orientation. Bedform dimensions height η and length λ are identified in the individual transects by detection of local extremes. Different methods for the assessment of bedform migration are applied: Bedform migration rates are derived from successive scans using either 1D cross correlation of individual transects and successive averaging of the displacement or by 2D spatial cross correlation methods related to particle image velocimetry (PIV).

To relate observed bedform migration to the tidal forcing, bottom shear stresses $\tau_{0,c}$ exerted by the tidal currents are computed by fitting a logarithmic profile to the measured velocity profile in the lower water column (Soulsby, 1997). Wave induced shear stresses $\tau_{0,w}$ are derived from wave properties (T_p , H_s) by computing wave orbital velocities using linear wave theory and a wave friction factor (Soulsby, 1997).

3. RESULTS AND DISCUSSION

Preliminary results include the observation of bedform dimensions, critical thresholds for bedform migration, and bedform celerity for consecutive tidal cycles. These are related to

common predictors like the grain size dependent critical shear stress of particle motion τ_{crit} . Time series for shear stress from currents and the ripple migration rates indicate critical thresholds and their dependency. It can be shown that the results for ripple migration are similar for different analysis methodology, thus the results are considered reliable.

Interestingly, bedform migration may commence already at the threshold of bed motion, thus much longer in the tidal cycle than expected. On the other hand tidal currents may be asymmetric, resulting in bedform migration into one direction only (Figure 3).

The comparison of different sedimentological environments and hydrodynamic regimes will evaluate the validity of common bedform descriptors.

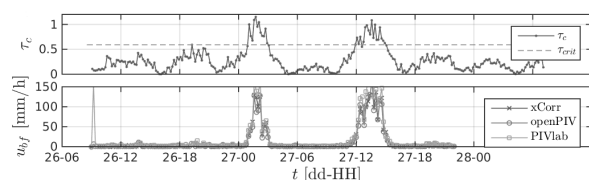


Figure 3. Current shear stress and bedform migration rates. In the upper panel, the dashed line indicates the critical shear stress computed for the median grain size. The lower panel shows the bedform migration rates computed by three different methods.

4. CONCLUSIONS

Field data on bedform characteristics in tidal environments helps to understand the dynamics of seabed ripples under varying hydrodynamic forcing conditions. Different analysis methodology has been evaluated. As the same field sites were investigated repeatedly in different situations, thresholds for bedform migration due to tidal currents and waves can be described and compared to models in literature. Furthermore, the methods outlined above allow for the computation of a robust set of parameters describing hydrodynamic forcing and morphodynamic response of the sandy

sea bed. Commonly used thresholds for the initiation of motion are evaluated.

Information on bedform dimensions and migration rates can be further transferred into sediment reworking rates. These are important boundary conditions for the distribution of nutrients and oxygen for benthic organisms and bacteria in the upper part of the sea floor (Ahmerkamp et al., 2015).

5. ACKNOWLEDGMENT

The observation platform *SedObs* was developed during the *COSYNA* initiative. The research presented is funded through the *NOAH* project by the *German Ministry of Education and Research*.

6. REFERENCES

- Ahmerkamp, S., Winter, C., Janssen, F., Kuypers, M. M.M. and Holtappels, M. 2015. The impact of bedform migration on benthic oxygen fluxes. *Journal of Geophysical Research: Biogeosciences*, 2015JG003106
- Baas, J. H. 1994. A flume study on the development and equilibrium morphology of current ripples in very fine sand. *Sedimentology*, 41(2)
- Bell, P.S. and Thorne, P.D. 2007. Field measurements of wave induced sand ripples in three dimensions. 2nd International Conference on Underwater Acoustic Measurements: Technologies & Results. Greece
- Bolaños, R., Thorne, P.D. and Wolf, J. 2012. Comparison of measurements and models of bed stress, bedforms and suspended sediments under combined currents and waves. *Coastal Engineering*, 62.
- Soulsby, R.L. 1997. *Dynamics of Marine Sands*. Thomas Telford Publications, London.
- Yalin, M. S. (1985). On the Determination of Ripple Geometry. *Journal of Hydraulic Engineering*, 111(8).
- Vanoni, V. A. (1974). Factors Determining Bed Forms of Alluvial Streams. *Journal of the Hydraulics Division*, 100(3).
- van Rijn, L.C. (1984). *Sediment Transport, Part III: Bed forms and Alluvial Roughness*. *Journal of Hydraulic Engineering*, 110(12).

Giant Subaqueous Dunes on a Tideless Sea Bottom, Rozewie Bank, Southern Baltic

M. Kubacka *Maritime Institute in Gdańsk, Gdańsk, Poland –*

S. Rudowski *Maritime Institute in Gdańsk, Gdańsk, Poland – starud@im.gda.pl*

R. Wróblewski *University of Gdańsk, Gdańsk, Poland & Maritime Institute in Gdańsk, Gdańsk, Poland – dokrw@ug.edu.pl*

K. Szeffler *Maritime Institute in Gdańsk, Gdańsk, Poland – kaszef@im.gda.pl*

Ł. Gajewski *Maritime Institute in Gdańsk, Gdańsk, Poland – lukgaj@im.gda.pl*

ABSTRACT: A series of giant sand waves, upwards of 1000 m in wavelength and 10 m in height, have been observed on a 30–40 m deep bottom located approx. 20 km north of Cape Rozewie. Waves of this size have not been previously noted in the Baltic Sea. Their morphology and structure indicate that they were formed under a constant deposition from a flow with a speed of up to 1.0 m/s and with a rich supply of sandy bed load. Such conditions may be related to bottom currents caused by undulations during very strong storms. A multibeam echosounder, side-scan sonar, and bottom profiler were used, and scoop and core samples were also collected. The aim of the study was to indicate that sand waves can also appear on tideless sea bottoms, and to underline the scientific and practical importance for research on the structure and morpholithodynamics of the bottom and of water body hydrodynamics.

1. GENERAL INFORMATION

The morphology and structure of well-developed giant sand waves were analysed based on data collected between 2006 and 2012 from a 5x10 km research site. The site (Figure 1) is located in the sandy Rozewie Bank, which constitutes the eastern part of a vast erosion – aggradation platform stretching from the Słupsk Bank to the Gdańsk Basin.

The obtained results, together with general knowledge of the studied area (e.g. Mojski 1995, Uścińowicz 2012), allowed for initial conclusions regarding the origin and the dating of these forms (Questions included: Were they extant or contemporary forms? And were they the result of marine, fluvoglacial, or river processes?).

The study used integrated systems for non-invasive registering, primarily with a multi-beam echosounder (Reson Seabed 8101), a side-scan sonar (EdgeTech 4200), and a seismic bottom profiler (SIG Energy boomer). Also used were the results of granulation analyses of the sediments

from samples obtained using a scoop and a vibration probe. A DGPS integrated with a specialised system for underwater navigation enabled precise positioning.

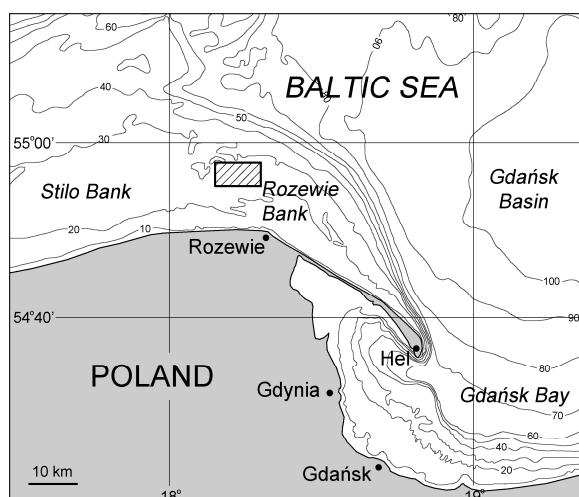


Figure 1. Location of the study area.

2. RESULTS

The studied forms showed a surprisingly recent morphology (Figure 2). Their crests were asymmetric in the cross-section: with longer, mild western slopes; and shorter, steep eastern slopes. The crest lines were slightly curved in a wave-like manner. Similarly shaped but smaller forms with a wavelength of up to 100 m and a height of up to 2 m were also present on the proximal slopes. The structure of the waves showed a two-part series of diagonally stratified, unimodal, sorted, and mostly undifferentiated medium sands. The series was divided by a surface of unconformity, with coarse sands and pebbles. A similar layer of pavement was also present in the bedrock of the sandy series, on the erosion surface that sheared the marginal wetland sediments (loams and silts) and/or tills. Similar subaqueous dunes from the bottom of the North Sea are known to be formed by strong tidal currents (vide Ashley 1994, Berne et al. 1994, Brew 1996). However, the Baltic is a tideless sea, and thus the sand waves present in the area must occur due to other causes. The morphology and structure of these waves indicate that they were formed (after Einsele 2000) under a constant redeposition, related to a relatively constant flow at

between 0.5 to 1.0 m/s, with a rich supply of sandy bed load and a generally weak erosion of the bottom. Model-based research indicates the possibility that bottom currents with a speed of 0.5–1 m/s, related to storm waves over 40 m in length, may be occurring in the area. The recentness of the morphology and the generally unimodal (except for the erosion pavements) granulation constitute primary evidence against the hypothesis that the studied forms may be relics (e.g. the extant fragments of a former riverbed, an outwash plain, or berms).

3. CONCLUSIONS

Giant sand waves may occur on the bottom of tideless seas. They may be formed not only by tide currents, but also by currents related to undulation. Determining the state of the sand waves has a scientific and a practical importance for research on the structure and morpholithodynamics of the bottom and for the hydrodynamics of a water body, as well as for the assessment of environmental conditions (e.g. during the exploitation of resources or the installation and use of hydrotechnical equipment, cables, pipelines, etc.).

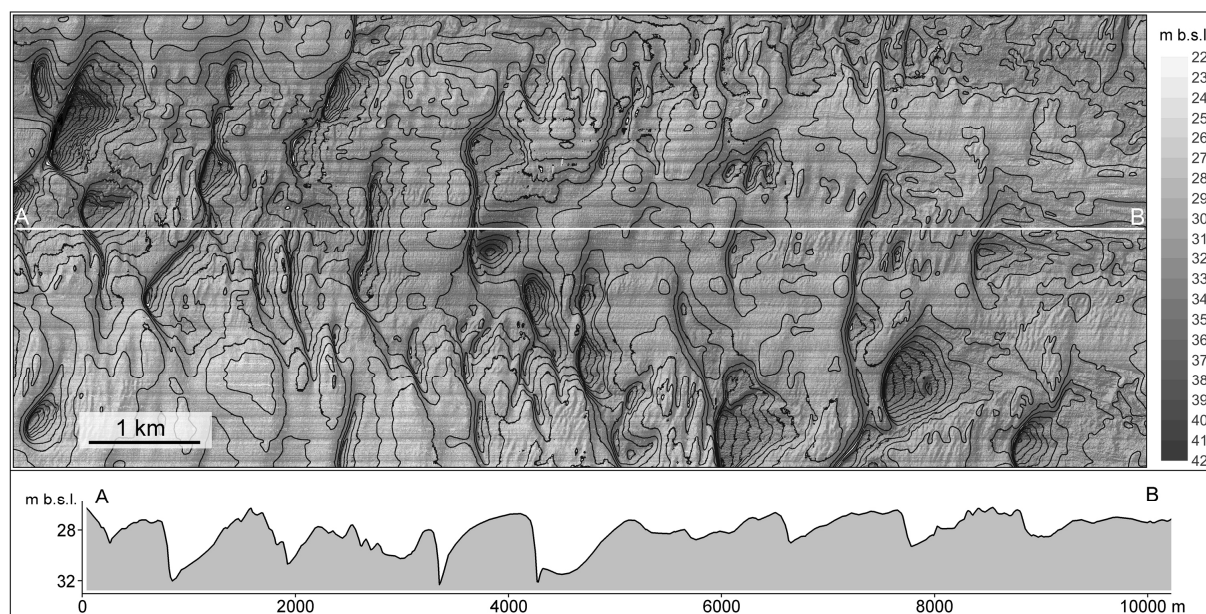


Figure 2. Bathymetric map of the research area and its bathymetric profile.

4. REFERENCES

- Ashley, G.M. 1989. Classification of large-scale subaqueous bedforms a new look at an old problem. *J. Sed. Petrol.* 69: 160–172.
- Berne, S., Trentesaux A., Missiaen T., de Batist M. 1994. Architecture and long term evolution of a tidal sandbank: the Middelkerke Bank (Southern North Sea). *Marine Geology*, 121: 57-72.
- Brew, D.S. 1996. Late Weiselian to early Holocene subaqueous dune formation and burial off the North Sea Northumberland coast. *Marine Geology* 134: 203-211.
- Einsele, G. 2000. *Sedimentary Basins*. Springer, Berlin, 792 pp.
- Mojski, J.E. 1995. *Geological Atlas of the Southern Baltic*. Polish Geological Institute, Warszawa.
- Uścińowicz, S. 2012. Continental Shelf of Baltic Sea. (in) Chiocci F. & Chivas A. (eds) *Continental Shelves*.

Influence of complex bedform morphology on flow and shear stress

A. Lefebvre *MARUM – Center for Marine Environmental Sciences, Germany – alefebvre@marum.de*

A. J. Paarlberg *HKV CONSULTANTS, Lelystad, the Netherlands – a.paarlberg@hkv.nl*

C. Winter *MARUM – Center for Marine Environmental Sciences, Germany – cwintere@marum.de*

ABSTRACT: This study investigates how complex morphology of natural bedforms affects the flow compared to the well-studied triangular bedforms. Four bed profiles from two rivers are analysed to determine a typical bedform morphology. The most commonly occurring morphological elements are a stoss side made one segment and a lee side made of a gently sloping upper lee side and a relatively steep (6-21°) slip face. The Delft3D modelling system is used to simulate flow over fixed bedforms with various morphology inspired by the analysis of the naturally occurring bedforms. For slip face angles smaller than 18°, no reversed flow is observed. For slip face angles steeper than 18°, the size of the flow separation zone increases with increasing slip face angle. Both shear stress and turbulence increase with increasing slip face angle and are only marginally affected by the dimensions and positions of the upper and lower lee side.

1. INTRODUCTION

The majority of laboratory or numerical modelling studies on the hydrodynamics above bedforms have investigated angle-of-repose bedforms of idealised shape; that is, bedforms with a lee side angle of 30° having a triangular or sine-shaped stoss side and straight lee side shape. However it is now recognised that many large rivers are characterised by bedforms with lee side slopes lower than the angle-of-repose, the so-called low angle bedforms (Best, 2005); field measurements also show that natural bedforms mostly display a morphology that differs from the triangular or sine-straight profiles (e.g. Best and Kostaschuk, 2002, Kostaschuk and Villard, 1996, Parsons et al., 2005) with stoss and lee sides having one or more brink points, i.e. breaks in the bed slope (Figure 1). Over bedforms with a straight angle-of-repose lee side, the flow separates at the crest, a reverse flow forms above the lee side, and a turbulent wake is produced at the flow separation point, extending and expanding downstream (Best, 2005). Energy transformation in the flow separation zone and

associated turbulent wake are largely responsible for form roughness, which constitutes an important part of the shear stress in environments where bedforms are present (Kostaschuk and Villard, 1996, Lefebvre et al., 2014a, Smith and McLean, 1977). The angle of the lee side is often thought to be a crucial component of bedform morphology because of its influence on the flow: a permanent flow separation zone is present only over steep lee sides and is temporary or absent over bedforms with a gentle lee side (Best and Kostaschuk, 2002, Kostaschuk and Villard, 1996). Turbulence production, hence form roughness, is therefore reduced over low angle bedforms compared to angle-of-repose bedforms. Commonly, the average slope between the crest and trough (i.e. the average angle of the lee side) has been used to assess whether a flow separation zone is present. However, bedforms with an average lee side angle too gentle for the flow to separate may still have a steep slip face over which flow separation occurs (cf. Figure 1). Therefore, taking into account only the crest and trough positions and assuming a triangular bedform shape may lead to a wrong

estimation of whether there is flow separation and the intensity of turbulence and shear stress. Thus this study aims to compare the influence that bedforms with a typical natural morphology have on the flow compared to triangular bedforms.

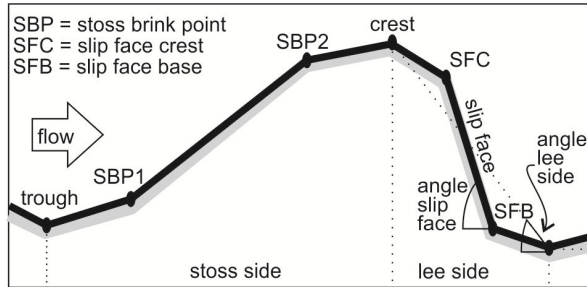


Figure 1. Bedform profile including brink points.

2. BEDFORM MORPHOLOGY

2.1. Methods

Field data of four 1 km-long longitudinal profiles, extracted from two river bed datasets, were used to characterise bedform morphology. The profiles were extracted from three-dimensional bathymetry of the Rio Paraná, Argentina (Parsons et al., 2005) where each profile contains around 20 bedforms (ca. 1.5 m high and 50 m long, average depth of 7 m) and the Lower Rhine, the Netherlands (Frings, 2007) where each profile contains around 70 to 90 bedforms (height 0.6 m, length 15 m and water depth 9 m).

The positions of crests and troughs of individual bedforms were determined using a bedform-tracking-tool (Van der Mark and Blom, 2007). Thereafter, typical bedform features in the form of brink points (Figure 1) were sought based on bed slopes. In particular, the slip face has been defined as the part of the bedform lee side which has angles steeper than 5° . The horizontal length, height and angle of each segment were calculated.

2.2. Results

Most of the stoss sides of the investigated bedforms are made of one segment (58% of all considered bedforms). Another common type features one brink point (26%). The lee side most often is best represented by two segments, the upper stoss side and the slip face (50% of all

considered bedforms). One third of the bedforms feature two brink points (33%).

Interestingly, the slip face angles never reach the angle-of-repose, being on average 14° (Table 1), and less than 21° for 95% of the bedforms; the steepest slip face determined from our dataset has an angle of 24.4° .

Table 1: Summary of bedform morphology results.

Element	Average value
Bedform length (L_b)	25.2 m
Bedform height (H_b)	0.9 m
Stoss side length	17.5 m (18.5 H_b)
Upper lee side length	5.5 m (6 H_b)
Upper lee side angle	1.9°
Slip face length	3.0 m (3.6 H_b)
Slip face angle	13.8°
Lower lee side length	1.6 m (1.9 H_b)
Lower lee side angle	2.5°

3. MODELLING EXPERIMENTS

3.1. Methods

The non-hydrostatic Delft3D modelling system has been used to setup a two-dimensional vertical (2DV) numerical model to simulate horizontal and vertical velocities, turbulent kinetic energy (TKE) and water levels above fixed bedforms. The model has been shown to reproduce flow separation, turbulence and shear stress over idealised, angle-of-repose bedforms under unidirectional flow conditions (Lefebvre et al., 2014b) and velocities, TKE and water levels in a tidal environment over natural bedforms (Lefebvre et al., 2014a).

Simulations were performed on a 2DV plane Cartesian model grid over a fixed bed composed of 20 similar bedforms with a logarithmic velocity profile at the upstream boundary, and a water surface elevation of 0 m at the downstream boundary.

Five series of simulations were carried out; for all simulations, the bedform height and length, the length of the stoss side and the water depth were taken from the average dimensions calculated from the analysed bedform (Table 1) and the dimensions of the upper and lower lee side and the slip face were kept within the range determined from the analysis of the natural bedform shape.

The first series of simulations (Figure 2a) examines the influence of slip face angle, which is

hypothesised to be the morphological parameter having the strongest effect on how bedforms impact the flow. The second experiment investigates the influence of the dimensions of the upper lee side by varying the position of the slip face crest (Figure 2b). Thirdly, a series of simulations tests the influence of the lower lee side by changing the position of the slip face base (Figure 2c). In a fourth series of simulations, the length and height of the upper and lower lee sides are simultaneously varied to change the position of the slip face (Figure 2d). Another set of simulations is carried out to test the influence of the angle of the upper lee side. (Figure 2e).

From the simulation results, the horizontal and vertical velocities and the TKE above the 16th bedform (of total 20 bedforms) are analysed. The position and size of the flow separation zone, when present, is calculated following the method detailed in Lefebvre et al. (2014b). The average slope of the water level, which has adjusted to the flow conditions over the bedform field, is used to calculate the total shear stress.

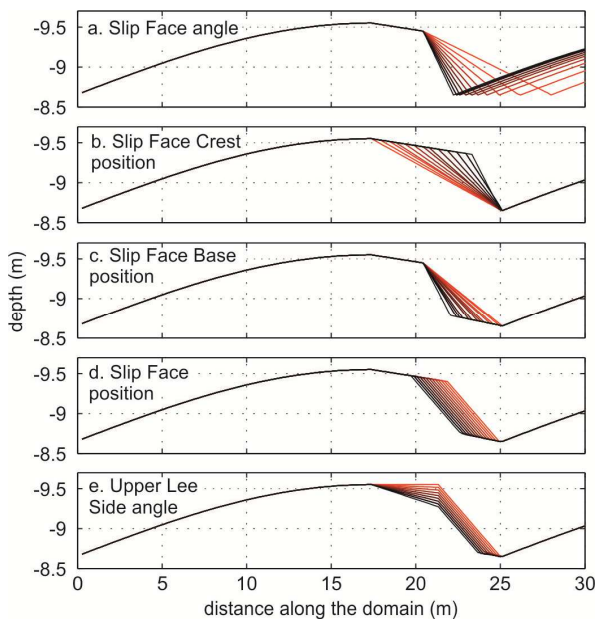


Figure 2. Simulated bedforms.

3.2. Results

Simulated horizontal velocities show the general pattern of flow over bedforms with flow acceleration over the bedform stoss side and deceleration over the bedform lee side. For slip

face angles smaller than 18° the flow decelerates considerably but no reverse flow develops. For slip face angles steeper than 18°, the flow separation zone is first restricted to the trough and is getting larger as the slip face angle increases. For a slip face angle of 24° (the steepest slip face tested), the flow separation zone starts just under the slip face crest and extends to a distance of 4.8 height of the slip face. This pattern is recognised over all bedforms of all simulations, with the presence of the flow separation zone being related only to the angle of the slip face and not to the presence or the size of the upper or lower lee sides.

When there is no flow separation zone, the TKE along the bedform is low, with a small region of higher turbulence recognisable over the trough. As the flow separation zone appears, TKE increases and a noticeable wake forms. For a full size flow separation zone, TKE is high with a well-defined wake extending from the crest along the flow separation line and above the following stoss side. Shear stress increases with increasing slip face angle, being lowest for the smallest slip face angle tested and highest for the steepest face angle (Figure 3a).

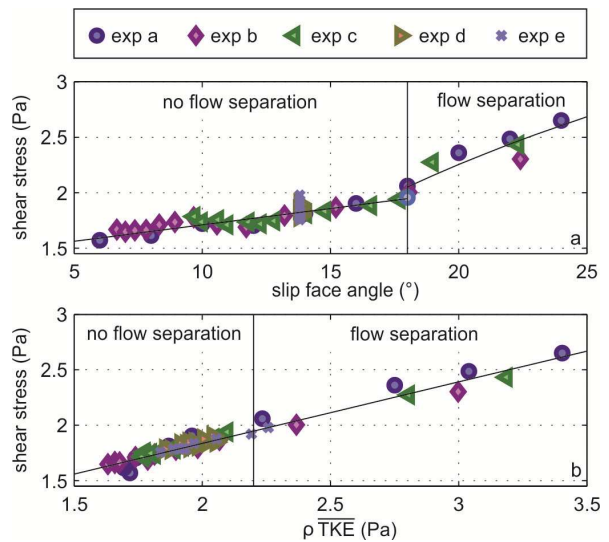


Figure 3. Shear stress as a function of (a) slip face angle and (b) mean TKE along the bedform; refer to Figure 2 for detail of the experiments.

The morphology of the lee side has little influence on the shear stress; shear stress of experiments having varying slip face angles and upper and lower lee side dimensions varies in the same range as shear stress from experiments where only the

slip face angle is varied. Shear stress increases linearly with the mean TKE along the bedform (Figure 3b).

4. CONCLUSIONS

The analysis of bed profiles from two alluvial environments shows that common morphological elements of bedforms detected along these profiles are a stoss side that is best described by a single segment and a lee side composed of two segments, a gently sloping upper lee side and a relatively steep slip face. The slip face angles never reach the angle-of-repose and are in the range of 6 to 21°. Numerical simulations with a non-hydrostatic model show how different bedform shapes influence the flow and shear stress over bedforms. The occurrence and length of a flow separation zone is mainly determined by the slip face angle: no flow separation is detected for slip face angles smaller than 18°; for slip face angle steeper than 18°, the size of the flow separation zone and the strength of the turbulent wake are increasing with increasing slip face angle. The shear stress is principally influenced by the slip face angle through turbulence intensity and little affected by the dimensions or positions of the upper and lower lee sides.

This work contributes to the characterisation of typical river bedform morphology. It is important to note that the average slip face angle determined from the bed profiles is 14°, over which no flow separation is predicted, and shear stress and turbulence are much lower than over angle-of-repose bedforms. Thus it is likely to be inaccurate to assume enhanced shear stress simply due to the presence of bedforms. Instead, the slip face angle (and not only the average lee side angle) should be determined in order to correctly parameterise the influence of bedforms on the flow.

5. ACKNOWLEDGMENT

This study was funded through the DFG Research Center/Cluster of Excellence “The Ocean in the Earth System”. The authors wish to thank R. M. Frings and D. R. Parsons for providing the multibeam echosounder data used in the analysis.

6. REFERENCES

- Best, J. 2005. The fluid dynamics of river dunes: A review and some future research directions. *Journal of Geophysical Research* 110 (F04S02): 21.
- Best, J. and Kostaschuk, R. 2002. An experimental study of turbulent flow over a low-angle dune. *Journal of Geophysical Research* 107 (C9): 3135.
- Frings, R.M. 2007. From gravel to sand. Downstream fining of bed sediments in the lower river Rhine. Utrecht University, the Netherlands. Also published as *Netherlands Geographical Studies* 368, Royal Dutch Geographical Society, Utrecht.
- Kostaschuk, R. and Villard, P. 1996. Flow and sediment transport over large subaqueous dunes: Fraser River, Canada. *Sedimentology* 43 (5): 849-863.
- Lefebvre, A., Paarlberg, A.J., Ernstsen, V.B. and Winter, C. 2014a. Flow separation and roughness lengths over large bedforms in a tidal environment: A numerical investigation. *Continental Shelf Research* 91 (0): 57-69.
- Lefebvre, A., Paarlberg, A.J. and Winter, C. 2014b. Flow separation and shear stress over angle of repose bedforms: a numerical investigation. *Water Resources Research* 50 (2): 986-1005.
- Parsons, D.R., Best, J.L., Orfeo, O., Hardy, R.J., Kostaschuk, R. and Lane, S.N. 2005. Morphology and flow fields of three-dimensional dunes, Rio Paraná, Argentina: Results from simultaneous multibeam echo sounding and acoustic Doppler current profiling. *Journal of Geophysical Research* 110 (F4): F04S03.
- Smith, J.D. and McLean, S.R. 1977. Spatially averaged flow over a wavy surface. *Journal of Geophysical Research* 84 (12): 1735-1746.
- Van der Mark, C.F. and Blom, A. 2007. A new and widely applicable tool for determining the geometric properties of bedforms. University of Twente, Enschede, Netherlands.

Bedform migration in an intertidal environment influenced by cohesion

I. D. Lichtman *Bangor University, Wales, UK & National Oceanography Centre, Liverpool, UK – doulich@noc.ac.uk*

P. D. Thorne *National Oceanography Centre, Liverpool, UK – pdt@noc.ac.uk*

J. H. Baas *Bangor University, Wales, UK – j.baas@bangor.ac.uk*

L. O. Amoudry *National Oceanography Centre, Liverpool, UK – laou@noc.ac.uk*
& the *COHBED* team

ABSTRACT: The migration rate of small-scale bedforms is important in determining bed material transport for the management of coastal morphology. Although many coastal and estuarine environments are dominated by mixtures of non-cohesive sand and cohesive, biologically active mud, there is a lack of field data on the effects of cohesion in mixed sediment. To address this gap in knowledge, measurements were taken of migrating bedforms in sand-mud mixtures on intertidal flats. When clay and EPS contents were below 2% and 0.04% respectively, the derived field bedform migration rates were found to not be significantly different from laboratory results for non-cohesive sand bedforms. Above these limits, cohesive forces hindered bedform migration. These results are important for sand-only bedform migration transport formulae in mixed sand-mud environments, as they can only be applied below these low limits of clay and EPS content when the sediment can be considered free of physical and biological cohesion.

1. INTRODUCTION

Sediment transport models are essential for managing coastal and estuarine morphological change. Many of these environments are dominated by mixtures of sand and mud. While reasonably accurate sediment transport predictors are available for pure sands, a knowledge gap exists for the behavior of mixed sediments composed of cohesive mud and non-cohesive sand. In addition to the physical cohesion caused by clay minerals in the mud, mixed sediments are also affected by biological cohesion, resulting from extracellular polymeric substances (EPS) produced by benthic organisms.

Knowing the rate of migration of sedimentary bedforms, such as ripples and dunes, is important in determining the bed material transport rate in sediment transport models (e.g., van Rijn, 2006; van den Berg, 1987). Such models may be inaccurate, if the bedform migration rates in sand-mud mixtures and non-cohesive mud-free sands are different.

Recent laboratory experiments using mixed cohesive and non-cohesive sediments have shown that bedforms dimensions and development rate are reduced by physical and biological cohesion

(Baas *et al.*, 2013; Malarkey *et al.*, 2015). This implies that cohesive forces within the bed may control the bed material transport rate, as a few percent of clay and more than 0.063% of EPS can be sufficient to significantly slow bedform growth (Baas *et al.*, 2013; Malarkey *et al.*, 2015). However, Baas *et al.* (2013) and Malarkey *et al.* (2015) also showed that the clay and EPS were selectively taken into suspension while bedforms formed and migrated on the bed, causing them to migrate as if they were composed of clean sand.

Here experimental laboratory data of bedform migration for pure-sand in unidirectional current (Baas *et al.*, 2000) are compared with similar bedforms in sand-mud mixtures on intertidal flats in the Dee Estuary, United Kingdom.

2. FIELDWORK

Fieldwork was carried out on intertidal flats in the Dee estuary, United Kingdom, near West Kirby. The Dee is tidally dominated, with a 7-8 m mean spring tidal range at the mouth. The intertidal flats studied are at the mouth of the Dee, separated from the main estuary by an Island. Waves affecting the intertidal flats are mainly generated locally within Liverpool Bay.

Three sites were selected over a spring-neap cycle in May and June 2013, in order to cover different mixtures of substrate sand and mud. Instrumentation was deployed at each site consecutively to measure the currents, waves, and bedform morphology, when the tidal flats were inundated. The bed sediment was sampled when the flats were exposed during low tide. This study presents the hydrodynamic data, collected using an Acoustic Doppler Velocimeter, and the seabed topography data, provided by a 3D Acoustic Ripple Profiler.

3. DATA ANALYSIS

The bedform migration rate was calculated from the spatial difference between successive half-hourly 0.5 by 0.5 m bed scans, determined by 2D cross-correlation (van den Berg, 1987). The minimum ripple migration rate detectable was $2.8 \times 10^{-6} \text{ m s}^{-1}$, and values at and below this limit were excluded from the regression analysis.

The wave-related, current-related, and combined maximum bed shear stress were calculated from the wave and current parameters (Malarkey and Davies, 2012) and used to calculate the Shields mobility parameter. Using the combined maximum bed shear stress accounted for the influence of waves, allowing comparison with the current-only laboratory data.

Baas *et al.* (2000) proposed a simple power law relationship between experimental data of the bedform migration rate, u_b , for current ripples and Shields parameter, θ' (Figure 1):

$$u_b = \alpha \theta'^{\beta} \quad (1)$$

where α and β are coefficients that vary with the bed sediment size. The bed material transport rate per unit width, Q_b , can then be calculated from the migration rate and the size of the bedforms (van den Berg, 1987):

$$Q_b = \rho_s (1 - p) f u_b \eta \quad (2)$$

where η is the bedform height, f is the bedform shape factor and p is the porosity of the bed (van Rijn, 2006; van den Berg, 1987). Equation (2) was used to calculate bed material transport rate by mass at each site, with the heights of the bedforms computed using the zero-crossing method. The

zero-crossing method detects where the bed profile crosses the mean level, between these points lie the crests and troughs, and the difference between successive crest and trough gives the bedform height. The shape factor, f , the porosity, p , and the sediment density, ρ_s , were kept constant at 0.6, 0.4, and 2650 kg m^{-3} , respectively (van den Berg, 1987; van Rijn, 2006).

4. RESULTS

4.1. Flow forcing and bedforms

During the study period the tide changed from neaps to springs and back to neaps (Figure 1a,b). North-westerly winds dominated at Site 1, from moderate breezes up to gale force (5.8 - 17.6 m s⁻¹), generating wind-driven flows that increased the bed shear stress of the flood tide, compared to the fair-weather conditions at the other sites (Figure 1b). The combined maximum bed shear stress shows that bed stress is dominated by the currents, except for part of Site 1 that was influenced by waves (Figure 1b,c,d).

The time-series of mean bedform height is compared with the predicted equilibrium heights for current ripples, calculated from the grain size using empirically derived formulae (Baas, 1999; Soulsby *et al.*, 2012) (Figure 1e). During periods of strong forcing the bedforms became larger than expected for current ripples, transitioning towards dunes, scaling with the water depth and the bed shear stress. The time-series of maximum bedform migration rate for each tidal cycle is shown in Figure 1f. The migration rates at Site 1 appear to have been enhanced by wind-driven flow and waves. The bedforms at Site 2, which was dominated by relatively fast-flowing tidal currents, had higher migration rates than the bedforms at Site 3, where bed shear stresses were only able to move the bedforms for the first four tidal cycles.

4.2. Bed composition

The bed samples collected during the exposure period at low tide were analyzed for mud content. X-ray diffraction data, based on samples taken during the fieldwork, show that the mud fraction at the field sites contained on average 36% cohesive clay minerals and this fraction was used to calculate the clay content of the mud.

Separate bed samples were collected and analyzed for carbohydrate content (EPS) and clay fraction. From these samples it was found that low EPS fractions less than 0.04% corresponded to clay fractions below 2% at Sites 1 and 2, and high EPS and clay fractions were found at Site 3.

4.3. Flow and migration comparison

Figure 2 shows the relationship between bedform migration rate and skin friction Shields parameter for the field data, and the data of Baas *et al.* (2000) for comparison. The field data reveal a strong positive relationship between u_b and θ'_{\max} for cohesive clay fractions below 2%. These low bed mud and clay fractions coincided with low EPS values of below 0.04%.

The migration rate of the bedforms in the field, for $D_{50} = 227 \mu\text{m}$, appear lower than the migration rate of the bedforms in the laboratory obtained with similar pure sand, $D_{50} = 238 \mu\text{m}$ (Figure 2). When the bed material transport rate is calculated, using Equation 2, the inclusion of bedform height corrects for the difference in bedform dimensions between the laboratory and field data. This results in the bed material transport rates of mixed mud-sand from the field being not significantly different from non-cohesive sand in the laboratory at 95% confidence, for bed clay fractions below 2% and EPS fractions below 0.04%.

The clay content of the bed remained below 2% until 31 May. When the cohesive clay fraction increased above 2% (blue line, Figure 1f), the migration rate reduces below the limit of detection. This occurs despite the bed shear stress being above the threshold of motion (Figure 1d). These cohesive clay fractions above 2% cluster along the line of ‘no migration’ in Figure 2 (purple line).

5. CONCLUSIONS

The field bed material transport rates for sand-mud mixtures were not significantly different from laboratory results of sand-only bedforms, after the effect of waves is accounted for, when the clay content was below 2% and the EPS below 0.04%. Above these limits, which correspond approximately to where clay and EPS begin to significantly affect the migration rate and bedform dimensions in the mixed clay-sand laboratory experiments of Baas *et al.* (2013) and the mixed

sand-EPS laboratory experiments of Malarkey *et al.* (2015), the cohesive forces hindered bedform migration for the presented field data.

These results are important for the application of sand-only bedform migration transport formulae in natural mixed sand-mud environments; particularly as 2% clay is within the common definition of ‘clean sand’ (Shepard, 1954). Existing formulae for the transport rate associated with bedform migration can only be applied below these low limits of clay and EPS content, when the sand can be considered free of physical and biological cohesion. Further research is needed to establish whether these threshold values are universal or unique to the sediment type on the tidal flats off West Kirby in the Dee Estuary.

6. ACKNOWLEDGMENTS

This work was supported by the UK Natural Environment Research Council (NERC) under grant NE/I027223/1 (COHBED). We are grateful to the NOCL Ocean Technology and Engineering group, for instrument set up and deployment, and to the Liverpool Bay Coastal Observatory for weather data.

7. REFERENCES

- Baas, J. H. (1999), An empirical model for the development and equilibrium morphology of current ripples in fine sand, *Sedimentology*, 46, 123–138.
- Baas, J. H., R. L. van Dam, and J. E. A. Storms (2000), Duration of deposition from decelerating high-density turbidity currents, *Sedimentary Geology*, 136, 71–88.
- Baas, J. H., A. G. Davies, and J. Malarkey (2013), Bedform development in mixed sand-mud: The contrasting role of cohesive forces in flow and bed, *Geomorphology*, 182, 19–39.
- Malarkey, J. and A. G. Davies (2012), A simple procedure for calculating the mean and maximum bed stress under wave and current conditions for rough turbulent flow based on method, *Computers & Geosciences*, 43, 101–107.
- Malarkey, J., J. H. Baas, J. A. Hope, R. J. Aspden, D. R. Parsons, J. Peakall, D. M. Paterson, R. J. Schindler, L. Ye, I. D. Lichtman, S. J. Bass, A. G. Davies, A. J. Manning, and P. D. Thorne (2015), The pervasive role of biological cohesion in bedform development, *Nature Communications*, 6:6257 doi: 10.1038/ncomms7257.

Shepard, F. P. (1954), Nomenclature based on sand-silt-clay ratios, *Journal of Sedimentary Petrology*, 24, 151-158.

Soulsby, R. L., R. J. S. Whitehouse, and K. V. Marten (2012), Prediction of time-evolving sand ripples in shelf seas. *Continental Shelf Research*, 38, 47-62.

van den Berg, J. H. (1987), Bedform migration and bed-load transport in some rivers and tidal environments. *Sedimentology*, 34, 681-698.

van Rijn, L. C. (2006), Bed form tracking, *Manual Sediment Transport Measurements in Rivers Estuaries and Coastal Seas*, Sub-section 5.5.2., Delft Hydraulics Laboratory, Delft, The Netherlands.

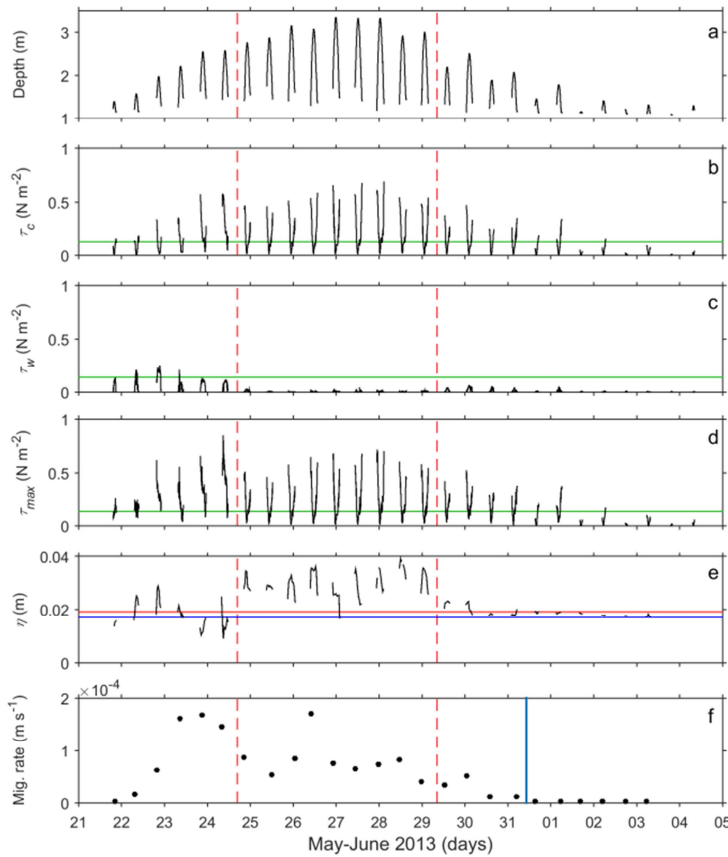


Figure 1: (a) water depth; (b,c,d) current, wave and combined maximum bed shear stress, τ_c , τ_w , τ_{max} ; (e) bedform height, η , (the blue and red lines are the ripple equilibrium heights of Baas (1999), 0.017 m, and Soulsby *et al.* (2012), 0.020 m, respectively) and (f) maximum bedform migration rate for each tidal cycle (the vertical blue line marks the point where the bed clay content increases above 2%). The vertical red dashed lines separate the three sites. The horizontal green lines denote the critical stress limit of bedform migration, based on the best-fit equation for the migration data (Figure 2).

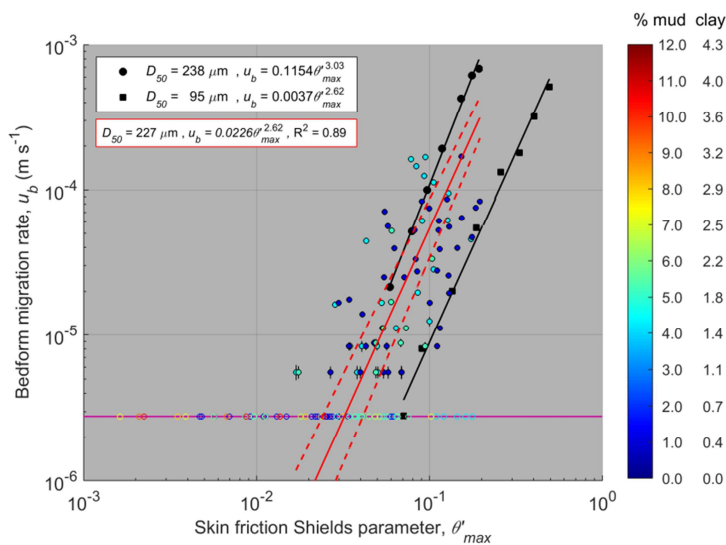


Figure 2: Bedform migration rate against Shields parameter for combined currents and waves. The color filled circles denote the field data; the black dots and squares denote the experimental data of Baas *et al.* (2000). Marker colors represent % bed mud and % bed clay fraction for the field data points. The colored open circles are bedform migration rates that were too low to be determined with sufficient confidence and lie on the purple line denoting the minimum migration rate measurable. The black lines denote the regression lines for the laboratory data of Baas *et al.* (2000). The red line is the regression line for the field data, with the red dashed lines denoting the 95% confidence limits of the regression line. The data points represented by the open circles were not included in the regression analysis. The error bars for u_b represent the 3D-ARP resolution.

Newborough Sand Dune Rejuvenation Project

E. Litt *Natural Resources Wales, North Wales, UK.* – emmer.litt@cyfoethnaturiolcymru.gov.uk

ABSTRACT: Sand dunes are typically dynamic systems, undergoing periods of erosion and accretion. However, the majority of Welsh sand dunes are in a static state, despite a plethora of statutory protections. Many species adapted to living in harsh dune environments are thus declining at an alarming rate. Morfa Dyffryn is Wales' bench-mark dune site for pioneer habitat conditions and there is a precedent to emulate the bare mobile sands seen there at other sand dune sites across Wales, with a target conservatively set at 10-15%. A large-scale mechanical intervention was undertaken to tackle the stabilisation problem at Newborough via three intervention phases since the winter of 2012-13 and, to date, 14 hectares of new bare sand has been created. This brings the total areal coverage of mobile bare sands at this site up by 1%, to a total of 4%, although it is still far from the 1940s levels of 51%.

1. INTRODUCTION

Newborough is located on the southern tip of Anglesey (Figure 1). The area is a key part of the Anglesey Area of Outstanding Natural Beauty (AONB), it is also a Special Area of Conservation (SAC), Site of Special Scientific Interest (SSSI) and a Geological Conservation Review (GCR) site.

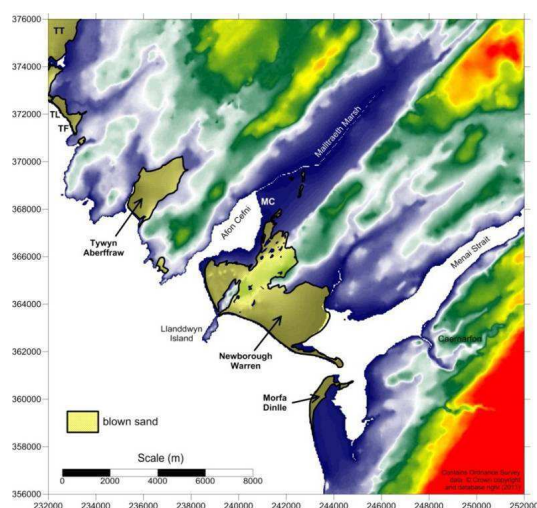


Figure 1. Regional setting of Newborough Warren and neighbouring dune systems at Tywyn Aberffraw, Morfa Dinlle, Tywyn Fferam (TF), Tywyn Llyn (TL)

and Tywyn Trewan (TT). MC = Malltraeth Cob embankment. Elevations taken from Ordnance Survey Land-Form data (50 m grid), and the extent of blown sand based on British Geological Survey 1:50,000 scale and Soil Survey of England and Wales 1:250,000 scale maps. Taken from; Pye and Blott (2012).

Newborough's designated features include areas of rocky shore, shingle ridges, estuary and dune habitats – such as mudflats, saltmarsh and sandy foreshore, strandline, fore-dunes, mobile and more stable dunes, areas of bare sand, wet dune slacks and dune heath. There are also fresh-water lakes and ponds. These habitats vary in their proportion and location in response to naturally changing geomorphological and hydrological processes.

The two estuaries (Figure 1); the Afon Menai (mouth of the Menai Strait) and Afon Cefni form a dynamic coastal system characterised by distinctive coastal landforms. Natural processes powered by wind, waves and tides continuously modify beaches, dunes, slacks, estuarine flats and shingle ridges (Figure 2).



Figure 2. Schematic of broad scale coastal processes Taken from; WoW SMP2, 2011.

The Newborough dune system consists of three main elements (Figure 3):

1. dunes which have developed and moved inland behind Traeth Penrhos on the north side of Ynys Llanddwyn (Llanddwyn Island) (i.e. in Malltraeth Bay)
2. dunes which have developed and moved inland behind Traeth Llanddwyn on the south side of Ynys Llanddwyn (i.e. in Llanddwyn Bay)
3. dunes which have developed on the sand and shingle barrier spit which extends in a southeasterly direction from Newborough Warren towards Abermenai Point (Trwyn Abermenai).



Figure 3 Main locations mentioned in the text (base 2009 aerial photograph). Taken from; Pye and Blott (2012).

2. SAND DUNE REJUVENATION

Sand dunes are inherently dynamic, undergoing periods of erosion and accretion and constantly changing in response to weather, climate, succession and management (Howe *et al.*, 2012). However, all of the Welsh sand dune systems have become increasingly stable (Pye *et al.*, 2014), resulting in major losses of pioneer and early successional habitat such as bare sand, sparsely-vegetated dunes and open dune slacks to fixed dune grassland and mature slacks. Mobile dunes currently occupy just 6% of the entire Welsh dune resource, compared to over 70% in the 1950s.

The three most important factors which control the scale, form and dynamism of sand dune systems are wind energy, sand availability and the nature of vegetation cover (Pye and Blott, 2012). The degree of overall mobility within a dune field at any moment in time is determined by the balance between a number of drivers (Table 1). This balance typically changes over time, and is reflected by episodes of mobility and stabilisation, which are naturally characteristic of dune systems.

Table 1. Drivers of dune dynamics (after Pye & Blott, 2012).

Dune Mobility	Dune Stability
High wind speeds	Low wind speeds
Low rainfall	High rainfall
High temperatures/High rates of evaporation	Low temperatures/Low rates of evaporation
Nutrient deficiency limiting plant growth	Nutrient excess promoting plant growth
High rates of littoral sand supply	Low rates of littoral sand supply
Coastal erosion	Coastal progradation
High visitor pressure	Low visitor pressure
Low-level management measures	High-level management measures e.g. marram planting

The immediate sources of sand for dune formation are adjacent sand flats. The foreshore, the area of sand between the mean low water and high tide levels, provides 10-20% of the sand. The proportion depends on areas of the foreshore drying out at least temporarily, and thus being blown by the wind followed by accumulation above the normal limits of the tide. Predominantly the sand in the backshore (mean high tide to

dunes) provides the majority of the dune-building sand (80%) as this area is only submerged during storms or high tides (Ranwell and Boar, 1986).

2.1. Newborough

At Newborough Warren, 51% of the blown sand area comprised bare sand in the 1940s compared to 3% in 2009. Pioneer dune slack habitat is all but absent at Newborough, with remaining areas being small, fragmented and of poor quality (Bratton, 2012). In contrast Boyce (2015), found 5,784m² of pioneer dune slack habitat at Morfa Dyffryn and confirmed the observation that Morfa Dyffryn is probably the most dynamic dune system remaining in Wales.

Focused geomorphological assessment was carried out at 12 sand dune sites across Wales including Newborough Warren (Pye and Blott, 2012). Pye and Blott (2012) listed a number of options for increasing dune mobility at Newborough ranging from small to large scale interventions, including;

- Vegetation density / height reduction
- Sand supply and sand mobility enhancement
- Wind speed and sand transport enhancement

Due to the scale of the stabilisation problem at Newborough, large scale mechanical intervention was undertaken, consisting of; excavation of breaches in frontal dunes, new deflation basins and troughs; stripping of rank vegetation and localised placement of excavated sand.

Work began at Newborough in the winter of 2012-13. Initially a 4 ha area of bare sand was created in the inner dunes as a trial, termed Phase 1. Further opportunity was presented the following winter and Phase 2 was undertaken in the forest area directed by Welsh Government, with approximately 3.9 ha created at Zone 1 West and 3.5 ha at Zone 1 East. Phase 3 was completed in the winter of 2014-15 with 6.6 ha of bare sand created in the foredunes of the Warren (Figure 4 and Table 3).

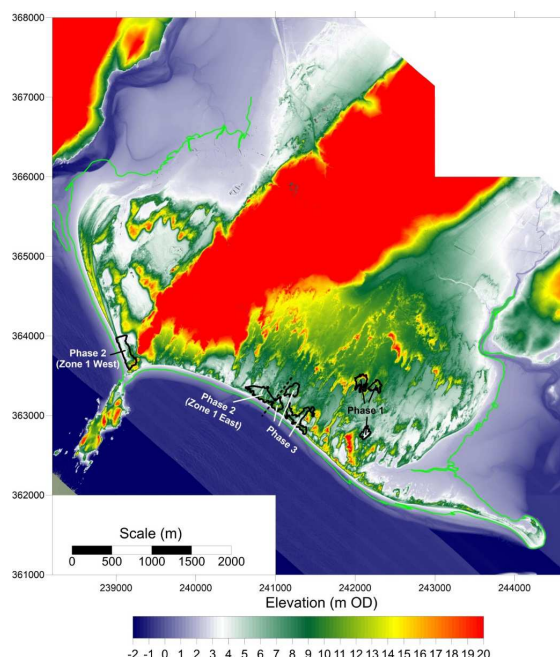


Figure 4. Locations of Phases 1, 2 and 3 dune restoration works at Newborough, overlaid on LiDAR DEM flown on 9 April 2014. Taken from; Pye and Blott (2015a).

Table 3. Bare sand created at each of the rejuvenation sites. See KPAL; 2013, 2014 and 2015a-d monitoring reports.

Newborough	Bare sand created (ha)
Phase 1 Winter 2012-2013	3.96
Phase 2 Winter 2013-2014	Zone 1 West 3.85 Zone 1 East 3.54
Phase 3 Winter 2014-2015	6.63
Total	14.44

3. CONCLUSIONS

The Newborough site in 2009 consisted of 1222 ha of intact dune of which 40 ha was calculated as bare sand, equating to 3% of the site. Morfa Dyffryn, on the Meirionnydd coast, is Wales' bench-mark dune site for dynamic processes, see Pye and Blott (2012). There is a need to be emulating the dynamic processes to achieve figures in the order of 30 to 40% pioneer habitats, including 10 to 15% bare sand, on senescent dune systems such as Newborough. The management work to date, as of 2015 monitoring, has provided an extra 14.4 ha of bare sand which raises the percentage by an extra 1% of bare sand at

Newborough to a total of 4%, although it is still a long way from the 1940s levels of 51%.

Unfortunately, the 2016 monitoring results were not available in time for this paper. However, the initial 4 ha area of bare sand created in the inner dunes as phase 1, at the latest survey March 2015, showed the bare sand area had increased by 0.5 ha. This depicted that even in the inner dunes where wind speeds and fresh sand supply are relatively low, the bare sand area is currently increasing, although modestly.

As a result of the management interventions, the aim is that within the near future, Welsh dunes will be more dynamic and self-sustaining, supporting extensive areas of pioneer and early successional habitats and be able to maintain that dynamism without the need for regular intervention (Howe *et al.*, 2012).

4. ACKNOWLEDGMENT

The author is grateful to everyone involved in the project; Michael Howe, Graham Williams, Julie Creer, Nicola Rimington, Ceri Seaton (all NRW), Ken Pye and Simon Blott of Ken Pye Associates, Guy Walker-Springett, Tim D'Urban Jackson and Michael Roberts from SEACAMS and Alan Roberts of DTM Technologies.

5. REFERENCES

- Boyce, D. C. 2015. Condition assessment of the invertebrate fauna of pioneer dune slacks at Morfa Dyffryn SSSI in 2011 and 2012. CCW Contract Science Report No. 1049. Countryside Council for Wales, Bangor.
- Bratton, J H. 2012 *Condition assessment of the invertebrate fauna of pioneer dune slacks at Newborough Warren - Ynys Llanddwyn SSSI in 2011*. CCW Contract Science 1001. Countryside Council for Wales.
- Howe, M. A., Litt, E. & Pye, K. 2012. Rejuvenating Welsh Dunes. *British Wildlife*. 24. pp 85-94.
- KPAL. 2013. Newborough Phase 1 Dune Rejuvenation Works Topographic Survey, May 2013. NRW Evidence Report No. 93. Kenneth Pye Associates Ltd., Solihull.
- KPAL. 2014. Newborough Phase 1 Dune Rejuvenation Works Topographic Survey, March 2014. NRW Evidence Report No. 95. Kenneth Pye Associates Ltd., Solihull.
- KPAL. 2015a. Newborough Phase 1 Dune Rejuvenation Works Topographic Survey March 2015. NRW Evidence Report No. 101. Kenneth Pye Associates Ltd., Solihull.
- KPAL. 2015b. Newborough Dune Rejuvenation Works Topographic Survey March 2015 Phase 2 Site: Zone 1 East. NRW Evidence Report No. 102. Kenneth Pye Associates Ltd., Solihull.
- KPAL. 2015c. Newborough Dune Rejuvenation Works Topographic Survey March 2015 Phase 2 Site: Zone 1 West. NRW Evidence Report No. 103. Kenneth Pye Associates Ltd., Solihull.
- KPAL. 2015d. Newborough Phase 3 Dune Rejuvenation Works Topographic Survey March 2015. NRW Evidence Report No. 104. Kenneth Pye Associates Ltd., Solihull.
- Pye, K & Blott, S J .2012. *A geomorphological survey of Welsh dune systems to determine best methods of dune rejuvenation*. CCW Contract Science 1002. Countryside Council for Wales.
- Pye, K., Blott, S J. & Howe M A. 2014. Coastal dune stabilization in Wales and requirements for rejuvenation. *Journal of coastal conservation*. 18:27-54
- Ranwell, D.S. & Boar, R. 1986. *Coast Dune Management Guide*. London, Institute of Terrestrial Ecology, HMSO.
- WoW SMP2. 2011. Policy Development Coastal Area F, PDZ 16. MENAI STRAIT: Trwyn Maen Dylan to Garizim and Pen y Parc to Trwyn Penmon. 50-153.

Geometry and internal structures of dunes in the bedload convergence regions in Beibu Gulf, northwest South China Sea

X. Ma *Key Laboratory of marine geology and environment, Institute of Oceanology, Chinese Academy of Sciences, Qingdao, China – mxch@qdio.ac.cn*

J. Yan *Key Laboratory of marine geology and environment, Institute of Oceanology, Chinese Academy of Sciences, Qingdao, China – jyan@qdio.ac.cn*

ABSTRACT: Geometry and internal structures of sand dunes were surveyed with multibeam sonar and seismic profiler in the bedload convergence regions near several ridges in the Beibu Gulf, northwest South China Sea. The data reveal that the sand dunes are much steeper and higher than that in other areas. The heights of some dunes are even larger than a quarter of the depth. A good height-length correlation is built: $H=0.1192 L^{0.901}$ ($R^2=0.8766$), which strikingly deviates from the Flemming's global mean relation. The seismic profiles illustrate the superposition, collision and mixing of the bidirectional inclining formations inside the sand dunes in the transitional areas. Bidirectional sediment supply in different periods encourage the vertical construction of the dunes. Erosions in the dune trough also enhance the height. Mutli-temporal evolution of the dunes and the affecting factors in the bedload convergence regions need to be further studied.

1. GENERAL INSTRUCTIONS

Through recent surveys, some relatively symmetrical dunes have been found in Beibu Gulf. In the two sides of these dunes, sand dunes usually have opposite asymmetry. No detail description on the geometry has been given. Their origins are still in the debate and ascribed to various triggers like reverse currents, surface waves in the limited literatures (Xia et al., 2001; Cao et al., 2006). Moreover, rare information is provided on internal structures of the dunes in Beibu Gulf.

We used a mutlibeam sonar and a seismic profiler (3.5KHz) to investigate the morphology and architecture of these dunes. The lengths and heights of sand dunes were measured and counted. Surface samples were obtained using a grab sampler and then processed and analyzed in the lab. The bathymetrical image was made using WGS 1984 UTM projection (49N zone). Bathymetrical data obtained in 2007, 2009, 2010, and 2014 were used to define the migrations of the dunes.

1.1. The bedload convergence regions

The study area is in the southeast of Beibu Gulf, which is a semi-enclosed gulf in the northwest

South China Sea. Now there are several ridges developing in the study area which may largely affect the local hydrodynamics. Sand dunes are commonly found and have complex morphologies (Cao et al., 2006). The five regions (A,B,C1,C2,D) that we focused are mainly located in the head and the trough of the ridges, at depths of 8-45 m (Fig. 1). Sand dunes have opposite inclinations in the two sides (north and south, west and east) of these regions. Hydrodynamics data are not available here. However, bathymetric profile comparisons between different years are made and show that the dunes migrated oppositely. We inferred these regions as bedload convergence regions because the opposite dune migrations were coincident with the asymmetries and could indicate face-to-face bedload transport in the same period (Fig. 2). The bathymetric profile (P5) in region R display that the dunes have the same asymmetry, and the profile comparison also show one-side dune migrations accordant with the asymmetry (Fig. 3). This could mean that region R is not a convergence region. Here region R is used to make a comparison with other regions when discussing dune morphology.

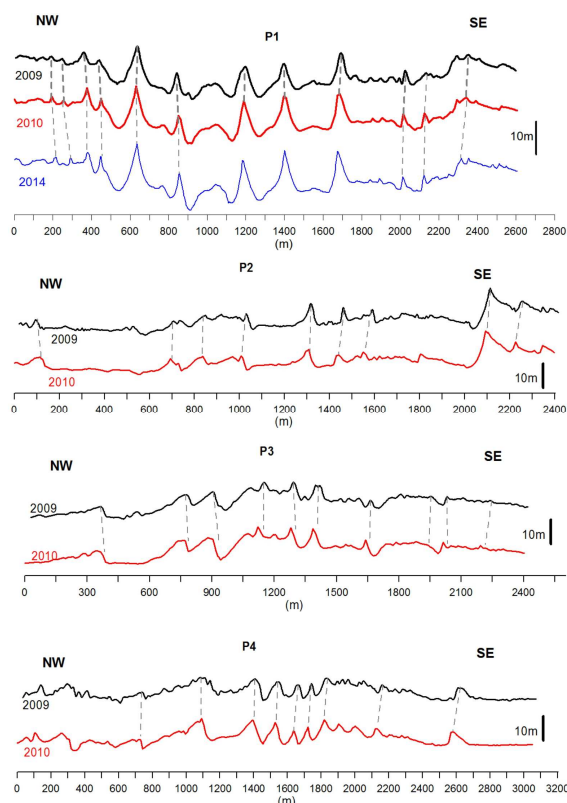


Figure 2. Bathymetric profile comparisons (P1-P4) show opposite migrations in the two sides of the focused regions. Seeing profile locations in Figure 1.

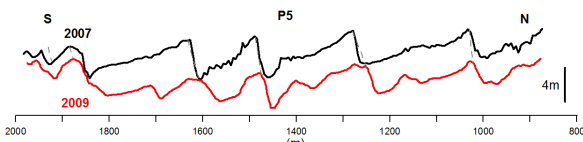


Figure 3. Bathymetric profile comparison (P5) in region R. The profile location can be seen in Figure 1.

1.2. Geometry of sand dunes

Sand dunes are developing in these convergence regions. These sand dunes have lengths of 20~180m and some heights up to 15 m (Figs. 4 and 5). The dunes are oppositely inclined in the two sides of "transitional lines" (Fig. 1). The heights and lengths of dunes near the transitional lines are counted and analyzed. The lengths and heights of sand dunes in all regions except region R have a good correlation: $H=0.0676 L^{1.0838}$ ($R^2=0.834$). This relation largely deviates from the Flemming's global mean relation, which is close to the upper limit of Flemming's relation (Fig. 4). Most dunes are very steep that have very large heights and relatively small lengths.

However, the heights and lengths of dunes on the ridge (region R) fit very well to the global mean relation of Flemming and other previous regression lines (Fig. 4).

The heights of the dunes in the study area seem to be independent of the depths. According to Francken et al. (2004), heights of sand waves are smaller than a quarter of water depths in river environment. In sea water, the heights are even smaller at the same depth (Yalin, 1977; Van Landeghem et al., 2009). Here, most dunes in region A and region C have much larger heights than that in other areas, while the others in the focused areas seem to be normal in heights (Fig. 5).

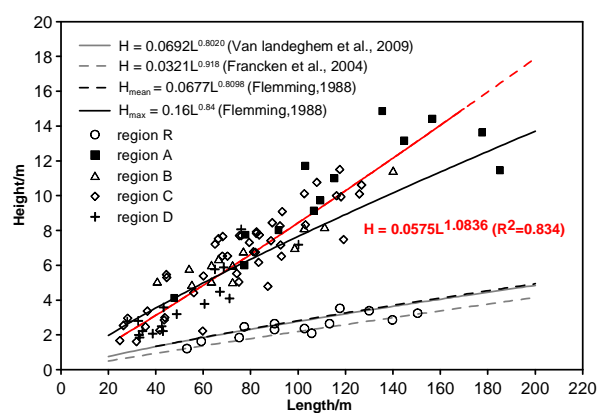


Figure 4. Height-Length relation of the dunes. (region C including C1 and C2)

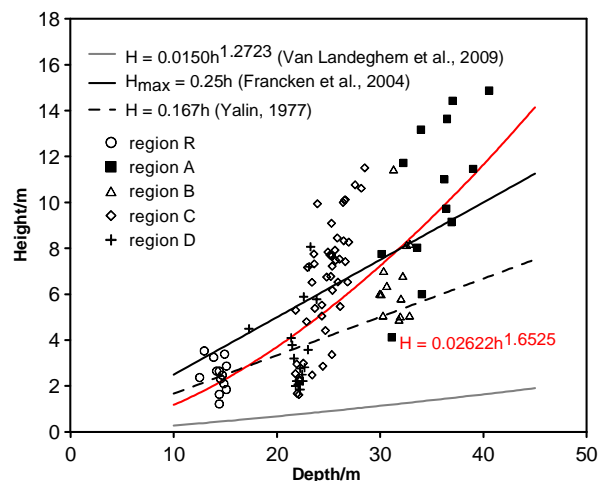


Figure 5. Height-Depth relation of the dunes

1.3. Internal structures of sand dunes

The profile of a typical sand dunes in region A show that the overlying beddings are oppositely asymmetrical, where the north-dipping layers overlie the south-dipping layers. Reflectors are

truncated in the trough of the sand dunes (Fig. 6), reflecting the erosion in the trough.

Bi-directional layers also exist in the sand dunes in regions C1 and C2 (Figs. 7 and 8). Just like that in region A, the layers inside the sand dunes also change from south-dipping to north-dipping. The troughs are also partly eroded. Some reverse beddings just begin to but do not completely change the asymmetry of the dunes (Fig. 7).

Figure 9 illustrate that the opposite inclining beddings seem to collide inside the relatively symmetrical dune in region D, which may indicate the nearly same active bedload flux from the two sides.

Data show that the sediment near the transitional line becomes finer comparing with that in the north side and the south side in region D (Fig. 10). In contrast, sediment changes to be coarser from the outside to the inside of the region A (Fig. 11). This different trends may reveal that sediment are still moving together in region D while this process is largely decreased or even stopped in region A.

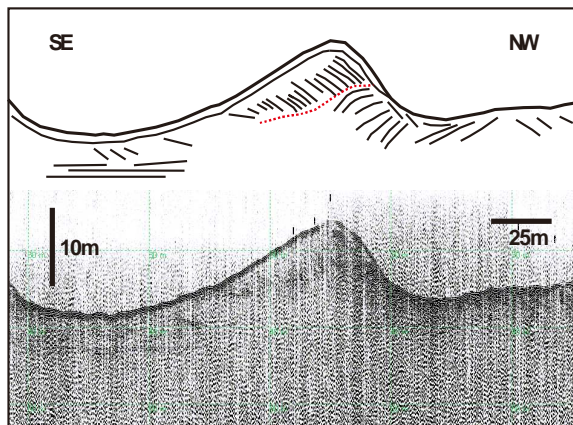


Figure 6. Detail interpretation of the internal structures of a large dune in region A. (Location seeing Figure 2)

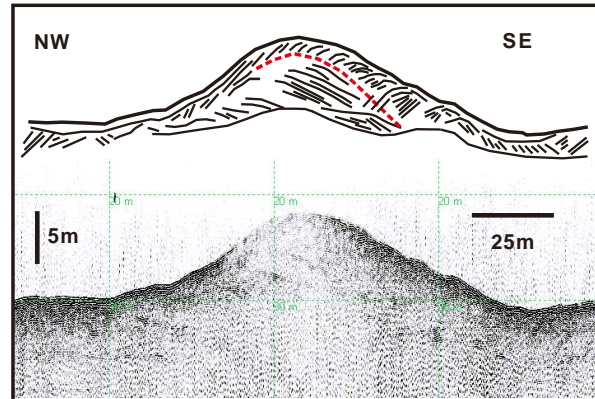


Figure 7. Detail interpretation of the internal structures of a typical dune in region C1.

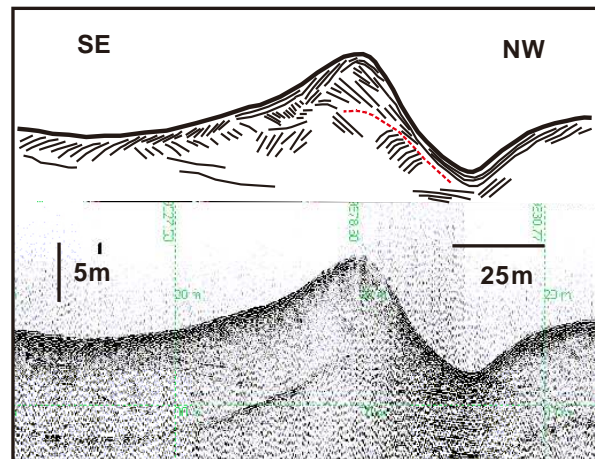


Figure 8. Detail interpretation of the internal structures of a typical dune in region C2.

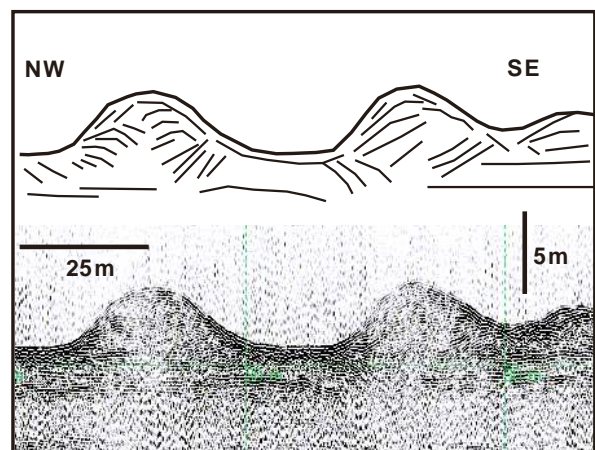


Figure 9. Detail interpretation of the internal structures of a typical dune in region D.

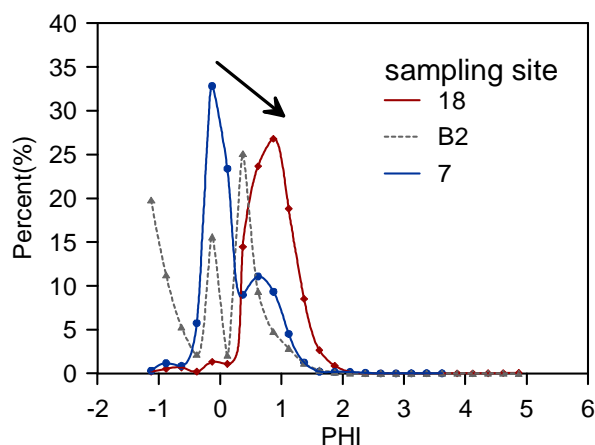


Figure 10. The characters of sediment in the two sides of region D.

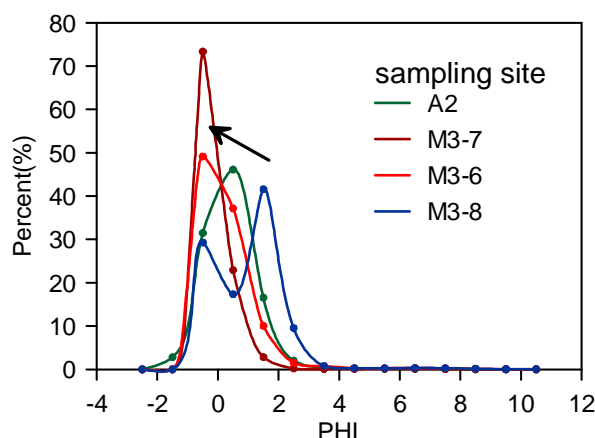


Figure 11. The characters of sediment around the region A.

2. CONCLUSIONS

The areas with opposite asymmetrical dunes in their two sides are suggested to be bedload convergent regions in Beibu Gulf. These dunes are also migrating oppositely under modern flows. The convergent regions other than dune individuals are focused in the present data.

In several bedload convergence regions in Beibu Gulf, steep sand dunes develop near the transitional lines (regions A-D) which display very different geometrical characters from that of dunes

under one-side net sediment input (region R). The very large heights of dunes in region A, C1, and C2 can be attributed to the overlap of reverse formation and the erosions in the trough of the dunes. Sand dunes near the transitional line are mainly supplied by erosions as the supply from outside are blocked by the huge dune heights. Sediment from the north and south sides of region D are accumulating on the dunes near the transitional line. Superposed reversed beddings inside these dunes indicate the large changes of bedload transport or the hydrodynamics in the past. The evolution of the convergence regions and the inside sand dunes and the affecting factors should be further studied.

3. ACKNOWLEDGMENT

The authors are grateful to the crew on the R/V KEXUE III. This study is funding by National Natural Science Foundation of China (41406041).

4. REFERENCES

- Cao, L.H., et al., 2006. High-resolution morphological characteristics of sand waves off the west Hainan Island. *Mar. Geol. Quat. Geol.* 26, 15–22 (in Chinese).
- Flemming, B.W., 1988. Zur Klassifikation Subaquatischer, Strömungstransversaler Transport körper. *Boch. Geol. Geotech. Arb.* 29, 44-47.
- Francken, F., Wartel, S., Parker, R., Taverniers, E., 2004. Factors influencing subaqueous dunes in the Scheldt Estuary. *Geo-Mar. Lett.* 24 (1), 14-21.
- Xia, D.X., et al., 2001. Research on the activity of submarine sand waves off Dongfang, Hainan Island. *J. Oceanogr. Huanghai Bohai Seas* 19, 17–24 (in Chinese).
- Yalin, M.S., 1977. *Mechanics of Sediment Transport*. Pergamon Press, Toronto. 298 pp.
- Van Landeghem, K.J.J., Wheeler, A.J., Mitchell, N.C., Sutton, G., 2009. Variations in sediment wave dimensions across the tidally dominated Irish Sea, NW Europe. *Marine Geology*, 263: 108-119.

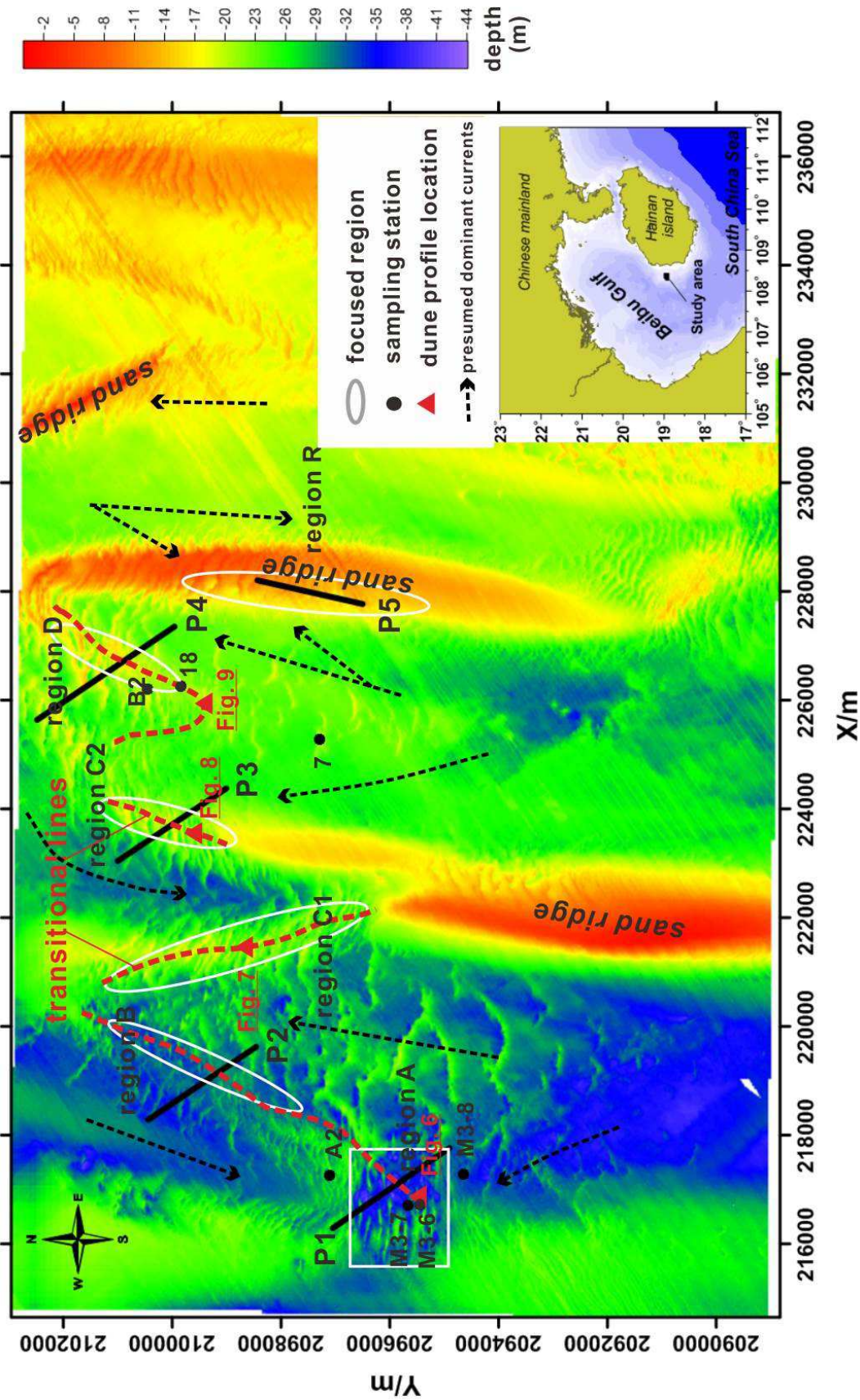


Figure 1. The focused regions (white circle) in the study area and the details of seabed topography. The dominant current paths are induced by the asymmetries of dunes.

High resolution coastal DEM of the Dover Strait: managing dynamic bedforms

A. Maspataud, SHOM, Brest, France – aurelie.maspataud@shom.fr

T. Schmitt, SHOM, Brest, France – thierry.schmitt@shom.fr

L. Biscara, SHOM, Brest, France – laurie.biscara@shom.fr

R. Créach, SHOM, Brest, France – ronan.creach@shom.fr

ABSTRACT: The Dover Strait has a high diversity of dynamic seabed sedimentary features. In this paper we present recent work undertaken to compile a high resolution 20 m grid spacing bathymetric digital elevation model extending along British and French coastlines. At this resolution, it is important to take particular precautions on the precision of the datasets (both vertically and horizontally). More importantly, in a highly dynamic environment, we had to take care of the temporal aspect of the dataset and their potential overlap to ensure the best continuity of the bedforms. In order to get the best coverage, a variety of dataset from different data providers, from different surveying systems, referenced at different vertical and horizontal datum, had to be harmonized prior to be interpolated. This DEM is intended to be used by hydrodynamic modeler in the context of the assessment of tsunami wave propagation.

1. INTRODUCTION

Bathymetric DEMs are essential input elements for numerous applications in geosciences, research and civil engineering, hydrodynamic modeling, planning and resource exploitation, mapping and positioning, data validation, military operational works... Specifically, building accurate and up-to-date coastal DEMs is a prerequisite for accurate modeling and forecasting of hydrodynamic processes at local scale in the context of marine flooding, originating from tsunamis, storm surges or waves (Eakins and Taylor, 2010). They are computed from a synthesis of bathymetric information sampled in an appropriate manner that conveniently represents underwater bedforms. However, because of practical considerations, this synthesis can only be composed of various datasets collected through times by various sounders, with various precision and density. A detailed work is needed to select the appropriate sources in order to sample the seafloor accurately, with respect to its temporal component. This is especially true in complex sedimentary environments, where seabed experienced migration and geometry changes. This study presents the main challenges encountered during the production of the high

resolution DEM of the Dover Strait, where surveys of subaqueous dunes and sandbanks were collected by the French hydrographic office (SHOM) for the last decades.

2. WORK CONTEXT

The present work is undertaken within the framework of the TANDEM project (2014-2017), dedicated to the appraisal of coastal effects of tsunami waves on civil nuclear facilities along the French coastlines (Owen and Maslin, 2014). A special focus is brought on the Atlantic and The English Channel coasts where French civil nuclear facilities have been operating since about 30 years (Hébert *et al.*, 2014). For this project, seamless integrated topographic and bathymetric high resolution (20 m) coastal DEMs (Maspataud *et al.*, 2015) are generated for specific coast configuration (embayment, gulf, estuary, harbor, island...). These sites are used to simulate expected wave height at regional and local scale on the French coasts, for a set of defined Tsunami generation scenario, such as earthquake (Roger and Gunnell, 2012 ; Garcia-Moreno *et al.*, 2015) or landslide triggering.

3. PRESENT KNOWLEDGE ON STUDY AREA

The Dover Strait area, located between the North Sea and the English Channel, is submitted to semi-diurnal macrotidal regime, with tidal currents with strong alternative character enhanced by the strait configuration. Soft sands along with the tidal regime are responsible for the local complexity of the study composed of superimposed bedforms.

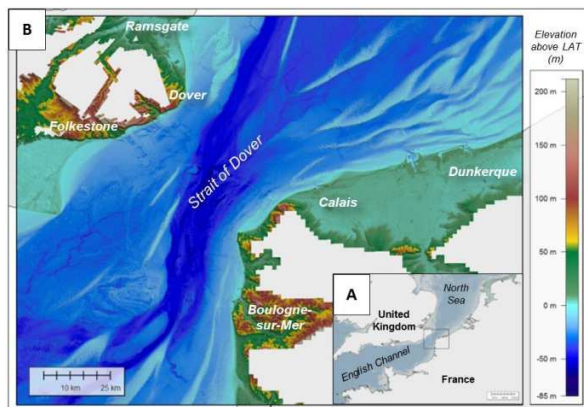


Figure 1. Location of (A) the studied area and (B) the coastal topo-bathymetric DEM prototype on the Dover Strait.

Active sand dunes as part of giant dune fields, or as associative bedforms usually well developed on the flanks of sandbanks, are particularly well organised and dynamic. In the French side, SHOM performs regular surveys to detect the exact position of dune crests, especially in the Dover Strait (Garlan *et al.*, 2007, 2008). Previous studies that were based on an optimum recurrence of re-surveying (annual, bi-annual or decadal) identified: 1) the highly sensitive sectors, 2) the direction in which the dunes preferentially move (either NE or SW in this area), and 3) the mean rates of displacement, or those of particular structures (Le Bot *et al.*, 2000 ; Garlan *et al.*, 2008).

In this area there is a general tendency of dune migration imitating the tidal scheme: SE isolated dunes commonly undergo the direct influence of the dominant ebb with SW migrations at the rate of 1 to 12 m/yr, while NW dunes migrate slowly in the opposite direction (to the NE) at an average rate of 3 m/yr (Le Bot *et al.*, 2000).

4. KEY POINTS IN COASTAL DEM DEVELOPMENT

4.1. Strategy and DEM development process

Challenges in coastal DEMs development deal with good practices throughout model development that can help minimizing uncertainties (Eakins and Grothe, 2014). In details, the main tasks to face were (1) making sure of the best detailed data coverage throughout a detailed inventory of available data for the area, (2) ensuring the vertical and horizontal precision of the data by getting access to corresponding metadata or reports and processing (punctual editing, tide correction,...) them if needed, (3) minimizing overlap between redundant dataset collected at different periods in time, (4) horizontal and vertical datum conversions, on the basis (national and/or local) datum conversion grids based on known measurements (Maspataud *et al.*, 2015) and (5) interpolating the entire dataset in order to fill gaps and get a continuous and regular surface. Locally, gaps between marine and terrestrial data have also required the introduction of new methods and tools to solve interpolation. Through these activities the goal was to improve the production line and to enhance tools and procedures used for the improvement of processing, validation and qualification algorithms of bathymetric data and merging of bathymetric data with a special focus on dataset collected in dynamic areas.

4.2. Data assessment

Data collection work required a substantial and precise effort to build a consistent dataset prior to DEM interpolation. This is particularly true as scattered elevation data with variable density, from multiple sources and from many different types (paper fieldsheets to be digitized, single beam echo sounder, multibeam sonar, airborne laser data...) were gathered (Figure 2).

In addition to available surveys from the French bathymetric database in this area (from SHOM and French harbour authorities), external data were also gathered: from the United Kingdom Hydrographic Office (UKHO) in the British waters and the Belgium hydrographic office (*Vlaamse Hydrografie*) in French waters. SHOM digitized

Belgian paper fieldsheets (single beam surveys) available in French waters. Topographic data for the French, British and Belgium coastal parts of the DEM were made available by national topographic offices or international databases.

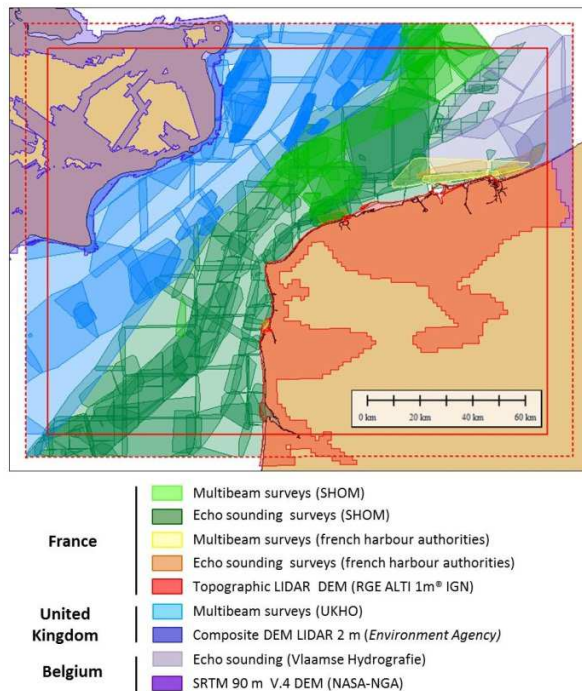


Figure 2. Source, type and coverage of selected datasets, available for each country, on the extend of DEM. Red dash and solid lines respectively represent the extracted data area and the final DEM coverage.

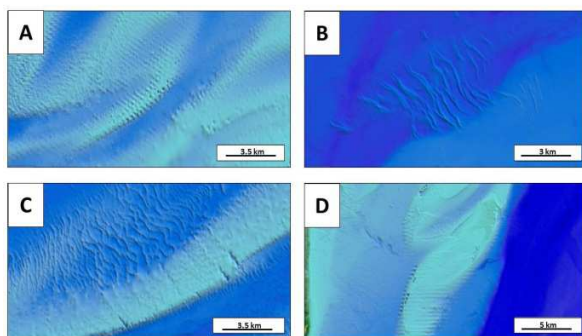


Figure 3. Examples of morphological artefacts of sedimentary bedforms encountered during bathymetric data assessment in the Dover Strait area.

Consequently, datasets were first assessed internally for both quality and accuracy and then externally with other to ensure consistency and

gradual topographic/bathymetric transitioning along limits of the datasets. On the overall of the gathered datasets, 67.4% were selected among the approximately 651 available surveys, i.e. 439 selected surveys including 38% carried out from multibeam sensors.

4.3. Managing with complex morphology and bedforms mobility

Sediment dynamics can locally induce artifacts on the resulting DEM or poor temporal accuracy of the representation of these bedforms. In some cases, it leads to unproper shifting of the crests on dune fields (Figure 3 B ; Figure 4 A) or of the overall shape of sandbanks (Figure 3 A, C, D).

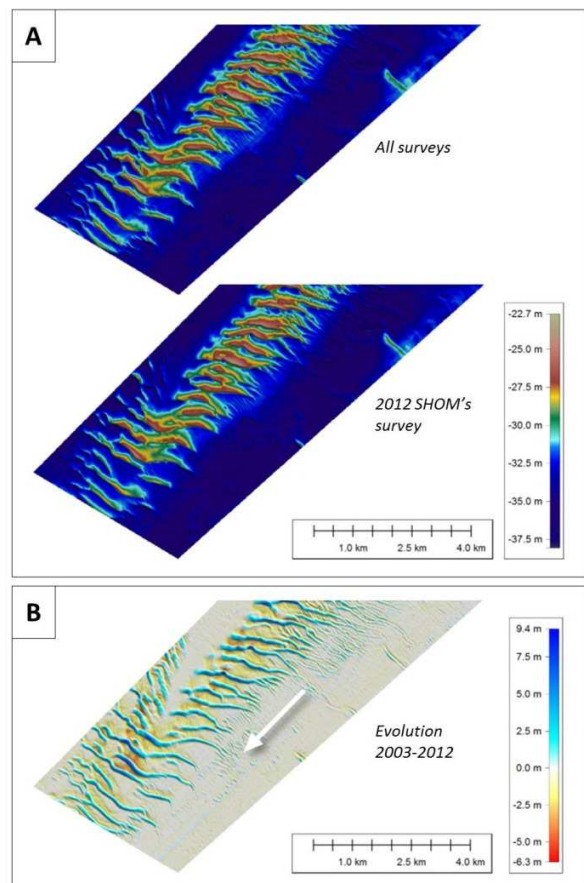


Figure 4. (A) DEM interpolation without and with specific selection between available bathymetric surveys, and (B) difference between 2003 and 2012 SHOM's bathymetric surveys in the North Sea.

This complex sedimentary environment led us to carefully consider the moving rates of sand dunes

in this area and estimate whether these values are significant with respect to the expected resolution of the final DTM. Locally, differences with previous bathymetric surveys, on sandbanks and dune fields, are sometimes larger than the grid spacing. In the case of the Dover Strait, considerations on the local sedimentology have been taken into account from:

- decadal survey of specific dunes reveals that they can move from about 50 to 100 m to the SW (or NE elsewhere ; Garlan *et al.*, 2008) as experienced in Figure 4B ;
- dunes movements could reach several meters to several dozen meters per year, up to 17 to 23 m per year, according to their exposure to main currents ;
- isolated dunes in southern North Sea could move 1.5 times faster than dune grouped in dune fields (Garlan *et al.*, 2008).

5. CONCLUSIONS

The navigation channel of the North Sea is unique in hydrographic surveys conducted by SHOM because it is the only environment where surveys are repeatedly carried out, excepted in harbor jurisdiction areas for the French coasts. The data therein acquired are rich in information on the dynamics of sedimentary bedforms but required, in our high resolution DTM production line, a large and attentive work in deconflicting numbers of surveys (varied extent, age and type) for a coherent and realistic modeling of sedimentary seabed.

In particular, the heterogeneous ages of the input data stress the importance of taking into account the temporal variability of bathymetric features, and their migration rates, especially in the most active areas.

6. ACKNOWLEDGMENT

This work is supported by a French ANR program in the frame of "Investissements d'Avenir", under the grant ANR-11-RSNR-00023-01. The authors thank H. Hébert (CEA), coordinator of the TANDEM Project team.

The authors are grateful to I. Laeremans (Vlaamse Hydrografie), J. Thomas (UKHO), F. Guyot (IGN), the Archive data team (Environment Agency), the BELGICA team, and french harbor

authorities (Boulogne-sur-Mer, Calais and Dunkerque) for providing complementary bathymetric and topographic data. The efficient technical help provided by S. Thépaut and J. Genevier (SHOM) for data cleaning and digitization work was greatly appreciated.

7. REFERENCES

- Eakins, B.W. & Grothe, P.R.. 2014. Challenges in building coastal digital elevation models. *Journal of Coastal Research*, 30, 5, 942-953.
- Garcia-Moreno, D., Verbeeck, K., Camelbeeck, T., De Batist, M., Oggioni, F., Zurita Hurtado O., Versteeg, W., Jomard, H., Collier, J.S., Gupta, S., Trentesaux, A., Vanneste, K. 2015. Fault activity in the epicentral area of the Dover Strait (Pas-de-Calais) earthquake (northwestern Europe). *Geophysical Journal International*, 201, 528-542.
- Garlan, T. 2007. Study on marine sandwave dynamics. *International Hydrographic Review*, 8 (1): 26-37.
- Garlan, T., Le Faou, Y., Guyomard, P., Gabelotaud, I. 2008. French marine sand dune project. *Marine and River Dune Dynamics*, 1-3 April 2008, Leeds, United Kingdom, 133-138.
- Hebert, H. & the TANDEM project team. 2014. Project TANDEM (Tsunamis in the Atlantic and the English Channel: Definition of the Effects through numerical Modeling) (2014-2018): a French initiative to draw lessons from the Tohoku-oki tsunami on French coastal nuclear facilities, *EGU 2014*, Vienna, 28 April-2 May 2014, Vol. 16, Poster.
- Le Bot, S., Idier, D., Garlan, T., Trentesaux, A., Astruc, D. 2000. Dune dynamics: from field measurements to numerical modelling. Application to bathymetric survey frequency in the Calais-Dover Strait. *In Marine Sandwave Dynamics, International Workshop*, Université de Lille 1, 23-24 mars 2000, 101-108.
- Maspataud, A., Biscara, L., Hébert, H., Schmitt, T., Créach, R.. 2015. Coastal Digital Elevation Models (DEMs) for tsunami hazard assessment on the French coasts. *EGU 2015*, 13-17 avril 2015, Vienna, Autriche. Poster.
- Owen, M.J. & Maslin, M.A.. 2014. Underappreciated Atlantic tsunami risk. *Nature Geoscience*, Vol. 7, August 2014, p. 550.
- Roger, J. & Gunnell, Y. 2012. Vulnerability of the Dover Strait to coseismic tsunami hazards: insights from numerical modeling. *Geophysical Journal International*, 188, 2, 680-686.

Sediment transport and bedform morphodynamics in sand-gravel mixtures.

C. McCarron *Bangor University, North Wales, UK – c.j.mccarron@bangor.ac.uk*

N. Howard *Bangor University, North Wales, UK*

K. Van Landeghem *Bangor University, North Wales, UK – k.v.landeghem@bangor.ac.uk*

J. Baas *Bangor University, North Wales, UK – j.baas@bangor.ac.uk*

L. O. Amoudry *National Oceanographic Centre, Liverpool, UK – laou@noc.ac.uk*

ABSTRACT: Bedform morphodynamics and sediment transport have been widely investigated in alluvial environments where grain size distributions and current flows are assumed to be uniform. This is not reflective of shelf sea environments characterized by oscillatory currents and sediment mixtures. The presence of sand-gravel mixtures causes a reduction of sediment mobility and additionally incorporates an effect known as the ‘hiding-exposure’ effect resulting in complex morphodynamics. In this research, the complexity of this problem is highlighted through recent flume tank experiments, inspired by offshore analyses, in which an attempt was made to quantify ‘hiding-exposure’ effects and the effect of sediment mixtures on the development and migration of ripples. Initial results indicate the presence of the ‘hiding-exposure’ effect and the dependence of bedform dynamics on the composition of sediment mixtures with smaller more uniform ripples formed in the presence of gravel and sediment transport rates decreased by more than 66% in mixtures containing 15% gravel compared to that in pure sand.

1. INTRODUCTION

Bedform morphodynamics are controlled primarily by sediment transport processes that have been widely investigated resulting in a vast number of predictive bedload transport formulae. The most commonly reported of which are those of Meyer-Peter and Müller (1948), Einstein (1950), Yalin (1963), Bagnold (1956; 1966), Engelund and Hansen (1967), Ashida and Michiue (1971), van Rijn (1984) and Nielsen (1992), and the widely used formula of Engelund and Fredsøe (1976). These formulae were originally developed for application in open channel flows with quasi-steady current velocities; however, they are not entirely reflective of shelf sea environments due to inherent assumptions such as unidirectional current flows and uniform grain size distributions.

Shelf seas are typically characterized by bi-directional currents and/or waves, and the presence of sediment mixtures as a result of paleo-glacial or -fluvial processes during the quaternary period between the last glacial maximum. In a sand-gravel mixture, less sediments will typically be available to form bedforms, which influences the dynamics of the bed. The presence of these

mixtures also incorporates an effect known as the ‘hiding-exposure’ effect where small grains are ‘hidden’ by larger, more ‘exposed’ grains changing the efficiency of the flow to mobilize different grain size fractions. As the flow further entrains and redistributes sediments, the mixture will change, as will the ‘hiding-exposure’ effect, depending on the strength and asymmetry of the flow. This could potentially lead to varying depths of the active layer, from armoured gravels to mobile sands, and is thought may significantly affect bedload transport processes and seabed morphodynamics.

The presence of sediment mixtures and their interaction has been accounted for through the development of fractional transport formulae in recent years. This has been accomplished through adaptation of formulae such as that of Meyer-Peter and Müller (1948), van Rijn (1984), van Rijn *et al.* (2007) and Ribberink (1998) for the transport of both uniform and non-uniform sediments. Similarly, the formulae of Parker *et al.* (1982), Wu *et al.* (2000) and Wilcock and Crowe (2003) have been developed directly for the fractional transport of mixed-sized sediments. The ‘hiding-exposure’

effect has also been quantified for steady flows and incorporated into bedload transport formulae through the application of corrective formulae such as that developed by Ashida and Michiue (1972), Egiazaroff (1965), Parker et al. (1982) and Wilcock and Crowe (2003). This has led to advances in the prediction of mixed sediment transport; however, the focus so far has been on alluvial environments.

This ongoing research aims to investigate the ‘hiding-exposure’ effect under conditions similar to that observed in offshore environments (i.e. with oscillatory currents and non-uniform sediment mixtures). Both offshore data analyses and flume experiments are discussed to highlight the complexity of this problem.

2. METHODOLOGY

2.1. Offshore Data Analysis

Llanelli Sand Dredging Ltd (LSDL) provided acoustic data (MBES, backscatter & side-scan sonar) and sediment sample data, both inside and outside a dredged area of seabed, for the purposes of this research. These results and other studies across the Irish Sea (e.g. Van Landeghem et al., 2009, 2015) indicated that where sand and gravel were present in a mixture, the ratio of gravel to sand on average was approximately 15:85. This informed trial flume tank experiments to extend the offshore analysis into environments with different forcing factors (i.e. current strengths, sediment distributions, etc.).

2.2. Flume Tank Experiments

An attempt was made to quantify the threshold of motion for pure sand, gravel and sediment mixtures. Fractional transport rates, quantified through collection and PSA of transported sediment from each run, were used to calculate the threshold of motion of each mixture at a dimensionless reference transport rate of 0.002 using the method of Parker *et al.* (1982). Comparison of the threshold of motion for each mixture allowed the identification of ‘hiding-exposure’ effects where observable.

The effect of different sediment mixtures on the development and migration of ripples was investigated using a 10 m long by 0.3 m wide recirculating flume. Bedform development during

reversing current flows, as well as changes to the bed at the end of each experiment was monitored using an array of 16 *SeaTek* 5MHz transducers.

3. PRELIMINARY RESULTS

3.1. Offshore Data Analysis

A series of asymmetric, flow-transverse, progressive sand waves were identified with a complex pattern of migration direction and speed. Surficial sediments grade across the area from gravelly (or gravelly-muddy) sand in the southeast corner of the study area to sand in the north-west (Figure 1). The link between the properties of the sediment mixture and the sediment wave dynamics is subject to further analyses.

3.2. Flume Tank Experiments

During shear flume experiments, the mobility of gravel fractions increased in a mixture with sand, whose mobility decreased. A relationship was derived between the grain size (D_i) and the calculated dimensionless critical shear stress of each grain size fraction ($\tau_{cr,i}^*$) (Figure 2). As the sediment becomes less uniform, from pure sand to a mixture of 15% gravel to 85% sand, the critical shear stress at incipient motion increases for the smallest fractions ($D_i = 0.15 \text{ mm}$) by up to 33% and decreases for the largest fractions ($D_i = 6.82 \text{ mm}$) by up to 20%. The quantification was complicated by the shape of the gravel grains, as irregularly shaped grains would be more mobile, yet caught by other grains more easily. ‘Hiding-exposure’ corrections ideally allow for variable grain shape (e.g. Bridge and Bennett, 1992), as indeed the shape of grains influenced sediment transport in a marine setting considerably (Le Roux, 2005; Durafour et al. 2014).

The sedimentary bedform dynamics in the larger, horizontal flume tank were noticeably dependent on the properties of the sediment mixture, as with increased gravel percentage more uniform and smaller ripples formed, taking longer to form a stable set of bedforms and migrating slower. A sediment mixture containing 15% gravel displayed a decrease in transport rate by more than 66% compared to pure sands. The ‘hiding-exposure’ effect was difficult to quantify in this experimental setting, as sediment mobility was the dominant factor, and temporary armouring effects behind

sporadically mobile gravel grains rendered the dynamics more complex.

4. TENTATIVE CONCLUSIONS

Sediment mixtures influence sedimentary bedforms in various ways:

- The critical shear stress at incipient motion increases for the smallest fractions ($D_i = 0.15\text{ mm}$) by up to 33% and decreases for the largest fractions ($D_i = 6.82\text{ mm}$) by up to 20% in a mixture of 15% gravel, 85% sand compared to that in 100% sand.
- Bedform dynamics are dependent on the properties of sediment mixtures: an increased presence of the gravel fraction caused the formation of smaller, more uniform ripples with slower migration rates.
- Although gravel in a mixture with sand exhibited increased mobility, this was not reflected in bedform migration rates.
- Bedforms formed in sediment mixtures containing 15% gravel were found to have decreased transport rates by more than 66% compared with those formed in pure sands.

5. FUTURE WORK

Data from different environments across the Irish Sea will be analysed to investigate the link between sediment mixtures and sediment wave dynamics. Results will then be used to further constrain flume tank experiments in which the effect of different sediment mixtures on sediment transport processes and bedform morphodynamics will be explored.

6. ACKNOWLEDGEMENTS

The author is grateful to Ian Taylor of Boskalis Westminster Ltd and Llanelli Sand Dredging Ltd for providing the datasets used in this research; SEACAMS for providing the facilities and guidance to collect additional datasets; and the Natural Environment Research Council (NERC) for funding this project through their Doctoral Training Partnership (DTP).

7. REFERENCES

- Ashida, K. & Michiue, M. 1971. An investigation of river bed degradation downstream of a dam. In Proc. of 14th IAHR Congress. Wallingford, U.K: 1–9.
- Ashida, K. & Michiue, M. 1972. Study on hydraulic resistance and bed-load transport rate in alluvial streams. Proceedings of the Japan Society of Civil Engineers (206): 59–69.
- Bagnold, R.A. 1966. An Approach to the Sediment Transport Problem. General Physics, Geological Survey Professional Paper 422(I): 43.
- Bagnold, R.A. 1956. The Flow of Cohesionless Grains in Fluids. Philosophical Transactions of the Royal Society A: Mathematical, Physical and Engineering Sciences 249(964): 235–297.
- Bridge, J.S. & Bennett, S.J. 1992. A model for the entrainment and transport of sediment grains of mixed sizes, shapes, and densities. Water Resources Research 28(2): 337–363.
- Durafour, M., Jarno, A., Le Bot, S., Lafite, R. & Marin, F. 2014. Bedload transport for heterogeneous sediments. Environmental Fluid Mechanics 15(4): 731–751.
- Egiazaroff, I. 1965. Calculation of nonuniform sediment concentrations. Journal of the Hydraulics Division, ASCE 91: 225–248.
- Einstein, H.A. 1950. The bed-load function for sediment transport in open channel flows. Transactions of the American Society of Civil Engineers 107(1): 561–577.
- Engelund, F. & Fredsøe, J. 1976. A Sediment Transport Model for Straight Alluvial Channels. Nordic Hydrology 7(5): 293–306.
- Engelund, F. & Hansen, E. 1967. A monograph on sediment transport in alluvial streams, Copenhagen.
- Le Roux, J.P. 2005. Grains in motion: A review. Sedimentary Geology 178(3-4): 285–313.
- Meyer-Peter, E. & Müller, R. 1948. Formulas for bed-load transport. International Association for Hydraulic Structures Research 6: 39–65.
- Nielsen, P. 1992. Coastal Bottom Boundary Layers and Sediment Transport. Advanced series on ocean engineering 4: 324.
- Parker, G. Klingeman, P.C. & McLean, D. 1982. Bedload and Size Distribution in Paved Gravel-Bed Streams. Journal of the Hydraulics Division, ASCE 108(4): 544–571.
- Ribberink, J.S. 1998. Bed-load transport for steady flows and unsteady oscillatory flows. Coastal Engineering 34(1-2): 59–82.
- van Rijn, L.C. 1984. Sediment Transport, Part I: Bed Load Transport. Journal of Hydraulic Engineering 110(10): 1431–1456.

van Rijn, L.C. 2007. Unified View of Sediment Transport by Currents and Waves. III: Graded Beds. *Journal of Hydraulic Engineering* 133(7): 761–775.

Wilcock, P.R. & Crowe, J.C. 2003. Surface-based Transport Model for Mixed-Size Sediment. *Journal of Hydraulic Engineering* 129(2): 120–128.

Wu, W. Wang, S.S.Y. & Jia, Y. 2000. Nonuniform sediment transport in alluvial rivers. *Journal of Hydraulic Research* 38(6): 427–434.

Yalin, M.S. 1963. An expression for bed-load transportation. *J. of the Hydr. Div.* 89(HY3): 221–250.

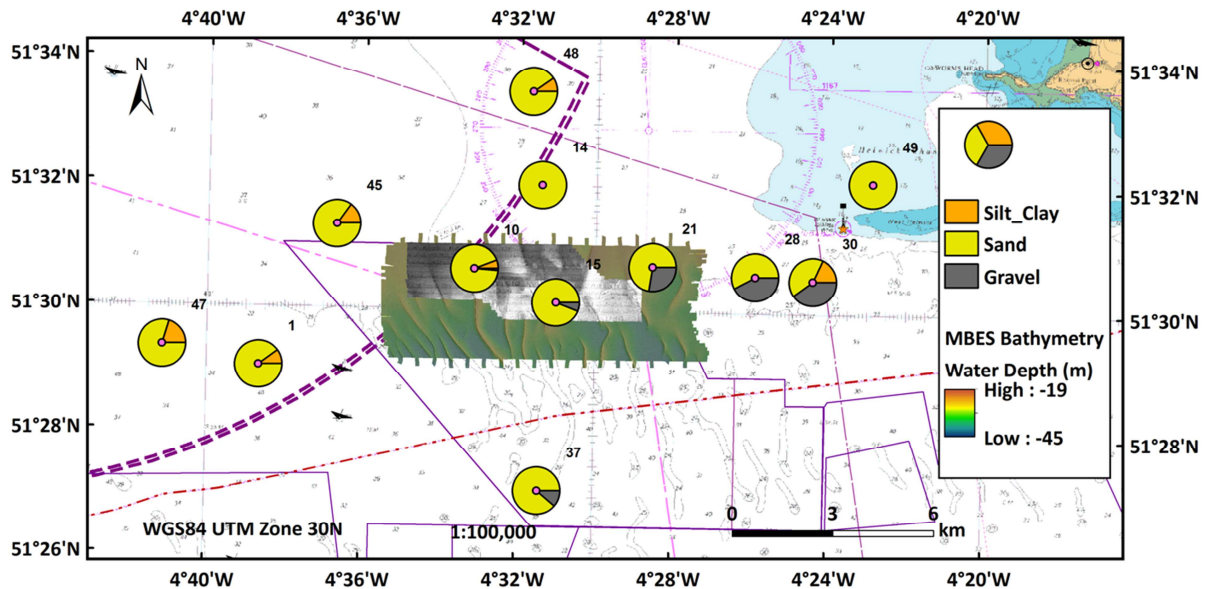


Figure 1. Distribution and average percentage composition of surficial sediments fractions (silt/clay, sand and gravel) across the study area

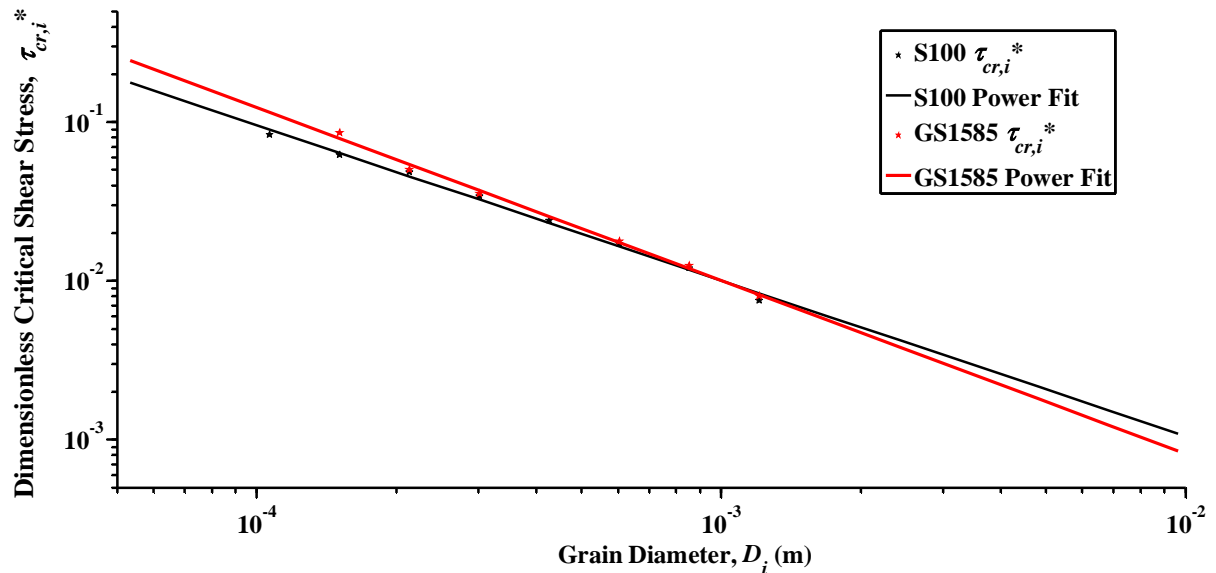


Figure 2. Dimensionless critical shear stress ($\tau_{cr,i}^*$) vs. mean grain diameter (D_i) of the i^{th} grain size for 100% sand (S100) and a mixture of 15% gravel, 85% sand (GS1585).

Towards the automation of sand dune detection in the bathymetry.

J. Ogor *ENSTA-Bretagne, Lab-STICC UMR CNRS6285, France* – julien.ogor@ensta-bretagne.fr

B. Zerr *ENSTA-Bretagne, Lab-STICC UMR CNRS6285, France* – benoit.zerr@ensta-bretagne.fr

ABSTRACT: Underwater sand dunes are complex features of the seafloor. They are the consequences of coupled phenomena: bedload transport, sediment properties, seabed morphology and hydrodynamics. The advances in the echo sounder (MultiBeam EchoSounder) and positioning (GPS) technologies of the past two decades revealed how diverse these structures are in terms of shape, spatial organization, dimensions, sedimentary properties, locations, etc. In order to cope with the large volume of bathymetric data available, the development of new tools allowing to quantitatively describe their morphology and dynamics seems necessary. The automation of the process will mainly enable to objectively characterize the sand dunes and banks. With this goal of dune characterization, the first step consists in detecting the dunes in the bathymetry. As a preliminary approach, we propose a detection technique inspired from geomorphometry.

1. INTRODUCTION

Underwater dunes and banks have been discovered on continental shelves as well as in rivers all around the world. They have the particularity of being dynamic features capable of distorting or migrating.

These dunes have become an actively researched subject for several reasons. First, their dynamic nature makes them worth of attention especially when it comes to human activities at sea. For instance, they constitute a risk to navigation safety; can cause damage to offshore structures (pipelines, communication cables, wind farms, etc.). In addition, it is the source of environmental concerns (aggregate extraction, biodiversity or coastal protection).

Dunes are the visible part of a complex system linking seabed morphology to sediment dynamics and hydrodynamics. Two main complementary research axes exist on dunes. The first focuses on the understanding and modelling of these not well-understood physical mechanisms (Németh et al., 2002; Besio et al., 2004). The other axis aims at describing qualitatively and quantitatively the underwater dunes and banks. From these studies, few dune classifications have emerged as well as methods providing descriptive parameters

(wavelength, height or length) on dune fields (Lisimenka, 2013; Dorst, 2004).

In this context, the purpose of our work is to design an automatic algorithm to delineate dunes in the bathymetry. Parameters could, then, be derived from the extracted dunes to analyze their morphology and dynamics. The algorithm should make as few assumptions as possible and take into account the dune specificities.

In this paper, a new method, inspired from geomorphometry, is presented. The preliminary results are encouraging, even though, the current algorithm is, yet, too heuristical.

2. DATA

To realize this study, data are key point. Indeed, when comes the validation phase, the used datasets should be representative of diversity of dunes shape and dynamics. Such data were made available to us by SHOM (the French Hydrographic office) and the FPS Economy (Belgium Economy ministry) continental shelf service. Although both offices collect data on dunes, they have clearly distinctive objectives. In this regard, they are complementary.

The aim of the Belgian is to monitor the impact of aggregate extraction on the sediment stocks. Consequently, a limited number of areas have been surveyed regularly (few times per year) and for about fifteen years. These data are shallow water (few tens of meters deep). Added to the use of cutting-edge acquisition equipment, the collected data are ideal to study the dune dynamics. However, the complex spatial organization of dunes makes their extraction very challenging. In fact, dunes are often on banks and depict rhythmic or fingerprint-like patterns. Furthermore, megaripples can superimpose on top of the dunes.

The French available datasets were acquired on the continental shelf off the coast of Brittany, France. Lines were run across the continental shelf during campaigns spaced by at least one year. Different vessels and equipment were used for these campaigns. Ultimately, the aim is to survey the entire continental shelf. The French data can sparsely contain dunes. Furthermore, the dunes are very likely to be partially described as survey lines are not overlapping. The depth ranges from a couple of meters to about two hundred meters deep. Thus, the data accuracy is not consistent through the entire dataset.

Yet, the covered area being very wide, very miscellaneous dunes were discovered. The most interesting regions were fully surveyed but only a couple of times. Hence, these data are very useful to understand how diverse dunes can be.

For both databases, acquisition equipment was changed from one survey to another having an impact of the data quality. This must be considered as it necessarily influences the quality of the dune extraction and, consequently, the descriptive parameters estimation.

3. GEOMORPHOMETRY

Techniques have been designed to semi-automatically or even automatically characterize dune morphology. Generally, they rely on the fact that dunes are quasi periodic structures.

They either adjust a model with a periodic component to the bathymetry or frequently analyze the bathymetry with 2D Fourier Transform or Wavelet Transform. From these analyses,

parameters (e.g. dune height or wavelength) can reliably be teased out.

We made the choice to design a method inspired from geomorphometry in order to avoid making assumptions such as the dune periodicity. Indeed, are sometimes isolated or having very unique shapes (e.g. barchan dunes) and our algorithm should be able to identify dunes indifferently.

Geomorphometry has been used to delineate landforms of the landscape. It is based on the estimation of attributes quantitatively describing the land surface. In our case, these attributes are derived from the depth. Classically used attributes are the slope, the aspect, and the curvatures.

The methods exploiting these attributes to detect land elements can be divided in several categories:

- (1) Object-based algorithms
- (2) Algorithms based on disparity lines
- (3) Drainage basin –based algorithms
- (4) Region growing algorithms

Such methods have been developed to detect features such as mountains, drumlins, volcanoes (Graff, 1992; Grosse et al., 2012; d’Oleire-Oltmanns et al., 2013). Most of the time, they use a DTM (Digital Terrain Model) as representation of the land surface.

The first category demands to identify a list of attributes that are homogeneous within each structure to be extracted. It does not seem suited to our case as no attribute is homogeneous on an entire dune.

The algorithms based on disparity lines have the opposite approach to the feature detection. In fact, it focuses on the identification of the feature boundaries. Boundaries are seen as loci of disparity.

For strongly asymmetric dunes, the foot of the Stoss side tends to be smooth. Hence, the transition continuity between the seafloor and the dune is continuous. This type of algorithms is suited to the extraction of features whose presence briskly modifies the land surface. The algorithm capacity to detect disparity lines also depends on the data resolution/ level of smoothness.

For dune detection, the drainage divides obtaining from a third category algorithm potential includes

the dune crests. Nevertheless, the algorithm results highly depend on the noise/smoothness of the input DTM. The risk is the under or over segmentation of the land surface. In the first case, dune crests could be omitted and, in the second, a selection among the drainage divides would need to be made. Furthermore, drainage divides would have to be merged to form the dune crests. Then, the transition from a crest to a dune is not trivial. All this demands to tune numerous parameters in order to avoid the under or over segmentation and construct crests.

Considering the disparities in the quality and resolution of the available data and the diversity of dune shape, such an approach appeared inappropriate to our objectives.

A region growing technique is composed of two steps. First, one searches for notable loci in the data. They are called the seed regions. Then, the seed regions are extended to the connected cells in accordance with a chosen criterion. This is the type of approaches we chose to develop.

4. THE ALGORITHM

The choice of a region growing was made since, intuitively, the crests are remarkable structural lines of the seafloor. They are lines characterized by the high sharpness of the seafloor. In addition, they can be differentiated from the other sharp structures of the seafloor such as rock heads by their length. Henceforth, crests are used as seed regions.

Among the available geomorphometric attributes, curvature is the one capable of highlighting the sharpness of the surface at dune crests.

At each point of a surface, there is infinity of curvatures. The intersection of the surface with a plane defines a curve. The curvature enables to quantify the speed of change of the curve direction.

For an analytical surface, the curvatures can be calculated from the first and second derivatives.

Consequently, at each cell of the input DTM, a bivariate quadratic function was fitted in the least squares sense over a $N \times N$ centered neighborhood (N being an arbitrary selected odd number).

The curvatures calculated in a plane containing the normal to the surface are named normal curvatures. Two of them are called the principal curvatures and correspond to the minimum and maximum of the normal curvatures at the calculation point. Their main advantage is that their calculation is independent from the first degree coefficients of the quadratic function. Hence, the curvatures allow making the distinction between being flat and having a zero slope. Crest lines correspond to high maximum curvature values, though the slope, there, is commonly close to zero.

The seed regions are created by gathering connected DTM cells where the maximum curvature is higher than a user-defined threshold in regions. More than crest lines, the seed regions are more influence regions of the true crests.

The regions that are too small to be dune crests are deleted.

Then, the seed regions are iteratively extended to connected cells where the slope is higher than a chosen threshold. The idea is that the Lee and Stoss sides of a dune are relatively steep regions near a crest.

5. RESULTS AND PERSPECTIVES

The algorithm was tested on dune fields in order to analyze in which conditions it succeeds or fails to extract dunes and why. It was able to extract correctly most of the dunes. Dunes were detected either the French or Belgian data, though that have different characteristics. The higher the dune is and the sharper the crest is, the more satisfactorily the dune is extracted.

In addition, isolated dunes are simpler to detect splitting and merging dunes belonging to dense dune fields or banks. The results show that a region growing algorithm has the potential to tackle the dune extraction problem. Furthermore, it enables understanding where the difficulties in the dune extraction can raise from.

For correct results to be obtained, it demands to adjust by a trial-error process the curvature and slope thresholds as well as the neighborhood size. In fact, they are not intuitive heuristics. The curvature threshold has a large impact on the detected crest regions. There is no optimal value

since an increase of its value can prevent the detection of features not sharp enough for being crests but, also, can cause the split of crests in few crest regions. On the contrary, close dune crests are merged in one seed region when the threshold is too low. In the same manner, the slope threshold influences the under or over growth of the crest regions leading to abnormally large or small dunes. Dunes are so different that the use of common threshold values to all of them is not realistic. For instance, the slope threshold cannot be the same on the Lee and Stoss sides of an asymmetric dune. By consequent, the detection of the crest lines and the growth step need to be thought differently.

The neighborhood size impacts the smoothness of the estimated curvature and slope maps. If too large, the attributes map ranges tend to decrease and the detection gets more difficult. And, if too small, the input data noise can induce false detection. This leads to another issue: the data uncertainty. Ultimately, it would be interesting to be able to quantify the uncertainty on the detection dune and to compare it with the dunes dimensions.

To conclude, the algorithm parameters (e.g. thresholds) definition must be more data-driven and less user-defined and their number should be kept low. The user-defined thresholds have to be intuitive (nothing like a curvature threshold). The problem of automatic dune extraction is very challenging as each dune/dunefield is unique and lay in a different environment (seafloor, rocks, wrecks, etc.). In addition, these structures are represented by noisy measurements.

The ongoing work aims at studying deeper data-driven algorithms for crest detection. A promising approach based on these mathematically well-defined algorithms is currently under development.

6. ACKNOWLEDGMENT

The author would like to thank the FPS Economy Continental Shelf Service as well as SHOM for sharing their data. Many thanks are due to Marc Roche and Thierry Garlan for the discussions about dunes and the data. Also, the author is grateful to the DGA for its financial support.

7. REFERENCES

- Besio, G., Blondeaux P., Brocchini M. & Vittori G. 2004. On the modeling of sand wave migration. In *Journal of Geophysical Research: Oceans*, 109 (C4).
- Dorst, L.L. 2004. Geodetic deformation analysis: new method for the estimation of seabed dynamics; *Proc. MARID Workshop, Enschede, 1-2 April 2004*.
- Graff, L. H. 1992. Automated classification of basic-level terrain features in digital elevation models. DTIC Document.
- Grosse, P. & al. 2012. Systematic morphometric characterization of volcanic edifices using digital elevation models. In *Geomorphology*, 136 (1): 114–131.
- Lisimenka A. & Rudowski S. 2013. Bedform characterization in river channel through 2D spectral analysis. *Proc. MARID Workshop, Bruges, 15-16 April 2013*.
- Németh, A.A., Hulscher S.J. M.H. & de Vriend H.J. 2002. Modelling sand wave migration in shallow shelf seas. In *Continental Shelf Research*, v. 22, (18–19): 2795–2806.
- d’Oleire-Oltmanns S., EisankC., Dragut L. & Blaschke T. 2013. An Object-Based Workflow to Extract Landforms at Multiple Scales From Two Distinct Data Types. In *IEEE Geoscience and Remote Sensing Letters*, 10(4): 947-95.

Bedform morphology across the fluvio-tidal-marine hydraulic transitions: Lower Columbia River, USA

E. W. Prockocki *University of Illinois (UIUC), Champaign, Illinois, USA – prockock1@illinois.edu*

J. L. Best *University of Illinois (UIUC), Champaign, Illinois, USA – jimbest@illinois.edu*

P. J. Ashworth *University of Brighton, Brighton, UK – p.ashworth@brighton.ac.uk*

D. R. Parsons *University of Hull, Hull, UK – d.parsons@hull.ac.uk*

G. H. Sambrook Smith *University of Birmingham, Birmingham, UK – g.smith.4@bham.ac.uk*

A. Nicholas *University of Exeter, Exeter, UK – a.p.nicholas@exeter.ac.uk*

S. Sandbach *University of Exeter, Exeter, UK – s.sandbach@exeter.ac.uk*

C. J. Simpson *Fulcrum Graphic Communications, Airdrie, Alberta, CANADA – chris_simpson@outlook.com*

C. Keevil *University of Hull, Hull, UK – c.keevil@hull.ac.uk*

M. M. Perillo *ExxonMobil Upstream Research Company, Spring, Texas, USA mauricio.m.perillo@exxonmobil.com*

S. Constantine *University of Illinois (UIUC), Champaign, Illinois, USA – sjconst2@illinois.edu*

M. Marti *University of Illinois (UIUC), Champaign, Illinois, USA – marti2@illinois.edu*

ABSTRACT: Multibeam Echo Sounder (MBES) data collected within the main channel of the lower Columbia River (LCR), USA, from river kilometer (rkm) 0 to 90, provides insight into the spatial changes in bedform morphology across the marine-tidal-fluvial hydraulic transitions. Preliminary results suggest both bedform height and wavelength increase in magnitude from the (downstream) tidally-dominated, hydraulic regime to the (upstream) fluvially-dominated, tidally-influenced, hydraulic regime, even although maximum flow depths remain constant at ≥ 15 m. Furthermore, the greatest variance in bedform height and wavelength occur within the mixed tidal-fluvial, hydraulic regime, where combined-flows dominate, whilst maximum bedform heights (~ 2 m) occur within the tidally-dominated, tidally-influenced, hydraulic regime. However, the maximum bedform heights of ~ 2 m are lower than predicted given maximum flow depths of ≥ 15 m. This suggests that the complex structure of unsteady flows may potentially mitigate the growth of bedform height.

1. INTRODUCTION

There currently exists a paucity of understanding regarding the spatio-temporal changes in bedform morphology in combined flow environments such as estuaries, delta distributary channels, and tidal bays. However, a multibeam echo sounder (MBES) data set acquired between 2007-2009 by the National Oceanic and Atmospheric Administration (NOAA), across the lower Columbia River (LCR), USA, fluvio-tidal-marine hydraulic regime transitions, provides rare insight into the along-channel spatial changes in bedform characteristics as a function of differing hydraulic regimes (e.g., fluvially-dominated, tidally-influenced regime, mixed tidal-fluvial regime, and tidally-dominated, wave-influenced regime). Herein, we utilize this data set to compare/contrast

LCR bedform metrics such as height and wavelength, in order to identify distinct bedform morphological changes dictated by the along channel transitions in dominant flows.

2. BACKGROUND

The LCR possesses a mean annual discharge of $\sim 7300 \text{ m}^3 \text{ s}^{-1}$ (Naik & Jay, 2011), with maximum peak flows of $15000\text{-}17000 \text{ m}^3 \text{ s}^{-1}$ occurring between April and June (i.e. spring freshets) (Gelfenbaum, 1983; Naik & Jay, 2011; Simenstad et al., 2011). The LCR also experiences mixed diurnal and semidiurnal tides where the mean range of tide (MN) and highest astronomical tide (HAT) are 1.7 and 3.6 m at river kilometer (rkm) 0 (mouth of LCR). In contrast to its location along the active Cascadia Subduction Zone (CSZ)

margin, the LCR maintains a gentle mean channel slope equal to $c. 1.15e^{-5}$ (Jay, 1984). During low river flow, the relatively low channel slope promotes: (a) tidal modulations of water surface heights as far upstream as rkm 233 (Kukulka & Jay, 2003), (b) flood-tide induced current reversals to \sim rkm 109 (Clark & Snyder, 1969), and (c) saltwater intrusion to \sim rkm 37 (Fox et al., 1984). Post dam closures, the LCR total sediment discharge (Q_{tot} , where $Q_{tot} = Q_{bl} + Q_{wl}$ (where Q_{bl} and Q_{wl} represent the bedload and suspended/wash-load components of Q_{tot})) is estimated to be $\sim 10 \text{ Mtyr}^{-1}$ (Milliman & Syvitski, 1992). The majority of Q_{tot} is conveyed as Q_{wl} in the form of very-fine sand, silt and clay, whereas approximately 10% of Q_{tot} is delivered as Q_{bl} in the form of fine to medium sand (Sherwood & Creager, 1990). Thus, the longitudinal LCR channel reach investigated herein ranges from its mouth (rkm 0) to immediately upstream of the Beaver Army Terminal gauge station (\sim rkm 90) (Figure 1). This channel reach covers three basic hydraulic zones defined by Jay et al. (1990) (Figure 1): (a) the tidally-dominated lower river (rkm 0 to 21), (b) the region of minimum “energy flux divergence” (EFD), or mixed tidal-fluvial, hydraulic regime (rkm 21 to 56), and (c) the fluvially-dominated, tidally-influenced regime upstream of rkm 56.

3. METHODOLOGY

3.1 Bedform Measurement Techniques

Bedform heights and wavelengths were measured at thirteen zones along the LCR study reach (Figure 1). Two different measurement techniques were utilized: (i) manual measurements conducted at five out of thirteen zones (Z-1, Z-6, Z-7, Z-8, and Z-13) using cross-sections oriented perpendicular to bedform crestlines produced from MBES XYZ surface maps viewed within Global Mapper geographic information system (GIS) software, and (ii) automated measurements performed at all thirteen zones using exported XYZ values (sampled at 0.01m spacing) taken from cross-sections generated from MBES XYZ surface maps, where bedform heights and wavelengths were computed within Matlab software using the procedures outlined in Perillo et al. (2014).

4. RESULTS

4.1 Manual vs Automated Metrics

Manual versus automated bedform height and wavelength computations were compared and contrasted at Z-1, Z-6, Z-7, Z-8, and Z-13 along the LCR study reach (Figure 2). From this analysis, the automated computed bedform metrics from identical cross-sections, show that results from the automated procedure: (i) is consistent with manually-derived values (see Figure 2), (ii) circumvents human introduced measurement errors, and (iii) significantly reduce the total time necessary for bedform metric calculations, thus permitting a more robust investigation of the wider LCR study reach.

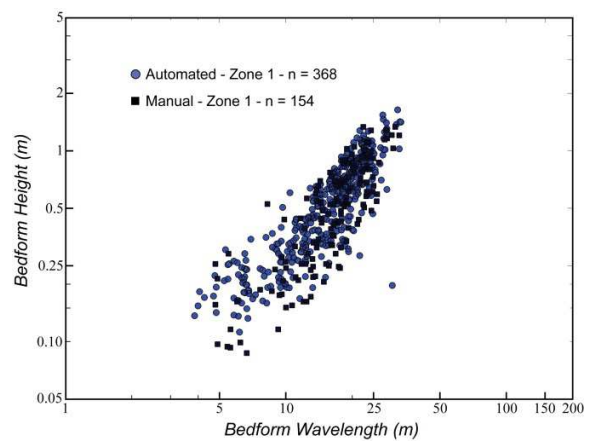


Figure 2. Comparison of manual versus automated bedform height and wavelength measurements at Z-1 located within the marine to tidally-dominated, hydraulic regime (see Figure 1 for location).

4.2 Bedform Metrics : LCR Study Reach

The values of computed bedform heights and wavelengths across all thirteen zones investigated are shown in Figure 3. These results suggest that within the main channel of the LCR, bedform heights and wavelengths increase from the tidally-dominated, hydraulic regime to the fluvially-dominated, tidally-influenced hydraulic regime. The greatest variance between measured bedform heights and wavelengths exists within the mixed tidal-fluvial, hydraulic regime. This variance is hypothesized to be a function of the presence of multiple groups of bedforms produced by differing ratios of combined-flow energy sources operating within the thalweg of the main LCR channel, and within immediately adjacent shallower channel depths. Furthermore, the largest bedform heights ($\sim 2\text{m}$ high) are found in the fluvially-dominated,

tidally-influenced, hydraulic regime, but are significantly lower than would be hypothesized given maximum flow depths of > 15m. This finding stimulates the question of whether unsteady flows driven by tidal forces may limit maximum bedform heights preserved within the fluvially-dominated, tidally-influenced, hydraulic regime. However, a much greater number of bedform height measurements are required, accompanied by rigorous statistical analysis, to officially test this hypothesis.

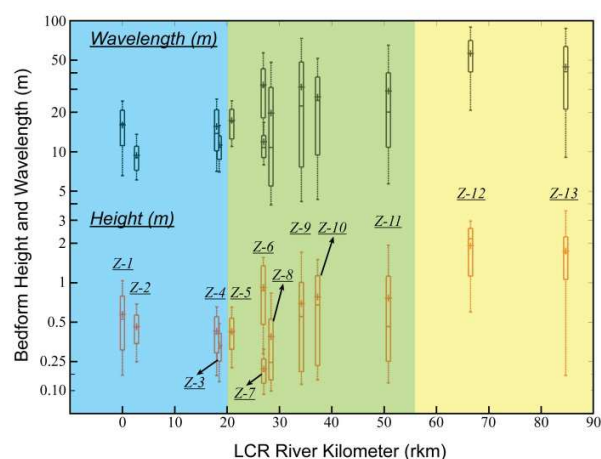


Figure 3. Bedform heights and wavelengths across the LCR study reach (Z-1 to Z-13; see Figure 1) as a function of differing hydraulic regimes. Rkm 0 to 21 (blue) represents the marine to tidally-dominated, hydraulic regime, rkm 21 to 56 (green) denotes the mixed tidal-fluvial hydraulic regime, and rkm 56 to 90 represents the fluvially-dominated, tidally-influenced, hydraulic regime.

5. CONCLUSIONS

- Measured dune heights and wavelengths systematically increase from the (downstream) tidally-dominated, hydraulic regime to the (upstream) fluvially-dominated, tidally-influenced, hydraulic regime.
- Given flow depths of ≥ 15 m, maximum dune heights are lower than would be hypothesized across all hydraulic regimes.
- The greatest variance in bedform height and wavelength is found within the mixed tidal-fluvial, hydraulic regime, where combined flows are most prominent.

6. ACKNOWLEDGMENT

This research was funded by UK Natural Environment Research Council (NERC) grant award NE/H007954/1, NE/H006524/1, NE/H007261/1 and NE/H00582X/1. We thank the Clatsop Community College Marine and Environmental Research and Training Station; we thank António Baptista, Michael Wilkin and Katie Rathmell for all their help and services. Lastly, we offer a special thanks to Pat Killion whose local knowledge of the lower Columbia River made all research possible.

7. REFERENCES

- Clark, S.M. & Snyder, G.R. 1969. Timing and extent of flow reversal in the lower Columbia River. *Limnology and Oceanography*, v.14, 960-965.
- Fox, D.S., Nehlsen, W., Bell, S., Damron, J., 1984. The Columbia River estuary-Atlas of physical and biological characteristics. Columbia River Estuary Data Development Program (CREDDP), Astoria, Oregon, 1-89.
- Gelfenbaum, G., 1983. Suspended-sediment response to semidiurnal and fortnightly tidal variations in a mesotidal estuary: Columbia River, USA. *Marine Geology* 52, 39-57.
- Jay, D.A., 1984. Circulatory processes in the Columbia River estuary. CREST, Astoria, Oregon, 1-169.
- Jay, D.A., Giese, B.S., Sherwood, C.R. 1990. Energetics and sedimentary processes in the Columbia River estuary. *Prog. Oceanog.* 25, 81-112.
- Kukulka, T. & Jay, D.A. 2003. Impacts of Columbia River discharge on salmonoid habitat: 1. A nonstationary fluvial tide model. *Journal of Geophysical Research* 108(C9), 3293.
- Milliman, J.D. & Syvitski, J.P.M. 1992. Geomorphic/Tectonic control of sediment discharge to the ocean: the importance of small mountainous rivers. *Journal of Geology* 100(5), 525-544.
- Naik, P.K. & Jay, D.A. 2011. Distinguishing human and climate influences on the Columbia River: Changes in mean flow and sediment transport. *Journal of Hydrology* 404, 259-277.
- Perillo, M.M., Best, J.L., Yokokawa, M., Sekiguchi, T., Takagawa, T., Garcia, M.H., 2014. A unified model for bedform development and equilibrium under unidirectional, oscillatory, and combined-flows. *Sedimentology* 61, 2063-2085.
- Sherwood, C.R. & Creager, J.S. 1990. Sedimentary geology of the Columbia River estuary. *Prog. Oceanog.* 25, 15-79.

Simenstad, C.A., Burke, J.L., O'Connor, J.E., Cannon, C., Heatwold, D.W., Ramirez, M.F., Waite, I.R., Counihan, T.D., Jones, K.L. 2011. Columbia River estuary ecosystem classification – concept and application. U.S. Geological Survey Open-File Report 2011-1228, Reston, 1-54.

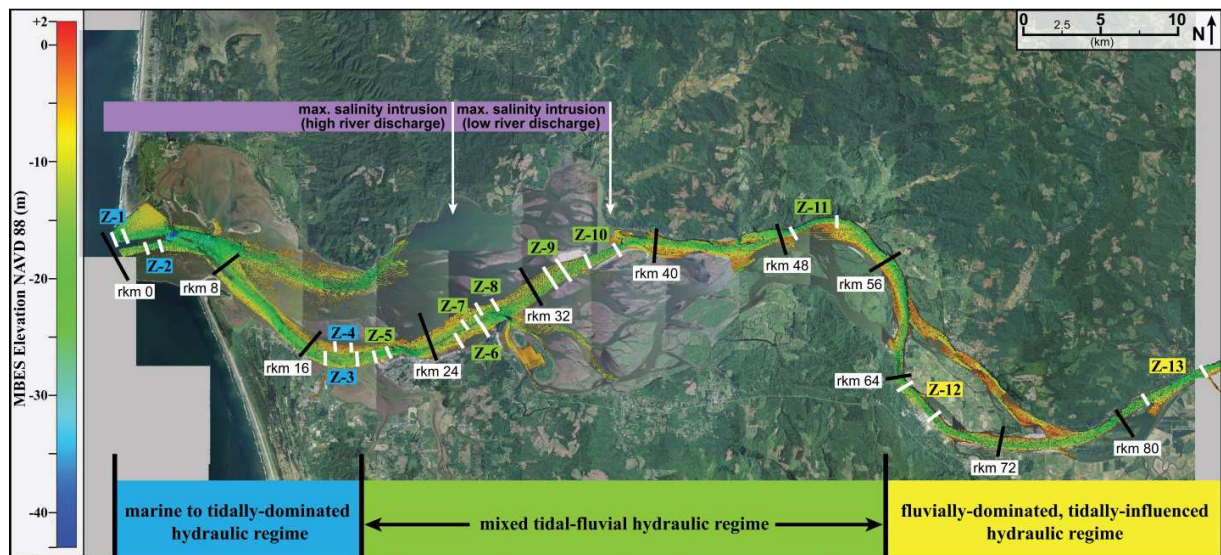


Figure1. Aerial image (2009) of the lower Columbia River (LCR) study reach displaying: (a) NOAA MBES channel surveying coverage (2007-2009), (b) the thirteen zones where bedform metrics were measured (Z-1 to Z-13), and (c) the longitudinal channel extent of the three major LCR hydraulic regimes as defined by Jay et al. (1990). Aerial image from US National Agriculture Imagery Program (NAIP) at <https://gdg.sc.egov.usda.gov/>.

Visualizing bed deformation and sediment dispersal across dune fields

A.J.H. Reesink *Geography and Environment, University of Southampton, UK* – a.j.reesink@soton.ac.uk

D.R. Parsons *Geography, Environment and Earth Sciences, University of Hull, UK*

P.J. Ashworth *School of Environment and Technology, University of Brighton, UK*

J.L. Best *Mechanical Science and Engineering and Ven Te Chow Hydrosystems Laboratory, University of Illinois at Urbana-Champaign, USA*

S.E. Darby *Geography and Environment, University of Southampton, UK*

R. J. Hardy *Department of Geography, Durham University, UK*

ABSTRACT: Dunes deform as they migrate downstream over time, and this deformation is enhanced when the dunes are not in equilibrium with the flow. However, we still have an incomplete knowledge of *how* dunes deform. This study presents a cross-correlation method (cf. McElroy and Mohrig, 2009) for the visualization of dune deformation. In this analysis, dune profile length determines the spatial context of the observed deformation, and temporal resolution determines the timescale of the processes that are being visualised. Different deformation patterns indicate different sediment dispersal processes, and highlight that significantly more sediment dispersal processes exist in nature than are included in current explanations and predictions of dune dynamics. The analysis highlights that dunes act as local sources and sinks of sediment within the dune field, thus always involving multiple dunes. This paper provides both a methodology and a theoretical background for the interpretation of dune deformation, variability in sediment transport across dune fields, and enhanced deformation during bedform growth and decay under unsteady flow conditions.

1. INTRODUCTION

Dunes are known to deform continuously in rivers even in cases where the mean geometric parameters have converged to a stable value (McElroy and Mohrig, 2009). Resolving the relative importance of such natural variability, the inheritance of morphology from past events (Allen and Collinson, 1974), and spatial changes in channel morphology (e.g. Jackson 1975; Nittrouer et al., 2008) requires fundamental understanding of the sediment transport processes that cause the dunes to deform. Without understanding these processes, we can neither adequately explain dune development, nor the variability in sediment transport across dune fields. While quantifications of flow over disequilibrium dunes (e.g. Unsworth et al., 2013) and more general approaches to dune deformation are being developed (McElroy and Mohrig, 2009), our understanding of the sediment

transport processes and the associated geometrical signatures of dune deformation remain underdeveloped. This paper therefore presents: 1) a method for the quantification and visualization of the geometric changes of dunes, and 2) an overview of sediment transport processes that can incite such geometric changes.

2. BACKGROUND

The growth and decay of dunes in response to changes in flow requires the removal and addition of dunes from the population, which occurs through merger and splitting (Fig. 1 A&B). Merger and splitting can create new dunes with significantly different height-length characteristics and volumes compared to dunes that are in equilibrium with the flow (Fig. 1 A&B; Yalin 1964; Jackson, 1976; Ashley 1990). Thus, these new dunes create defects within the dune pattern:

local excesses and deficiencies of sediment. Experimental investigations illustrate that such defect patterns can change the dynamic feedbacks between flow and morphology because bed morphology controls time-averaged flow and turbulence characteristics (e.g. Fernandez et al., 2006), sediment transport rates, and morphological development (Reesink et al., 2014).

2.1. Sediment dispersal processes

Deformation of dunes and enhanced deformation under disequilibrium conditions require sediment to be redistributed over and among dunes (see summary in Figure 1) Bedload sediment can be suspended temporarily and therefore bypass one, or several, dunes (Fig. 1C; e.g. Naqshband et al., 2014). In cases where regions of high velocity and high-turbulence exist within the flow over the dunes (Hardy et al., 2014), sediment transport paths are likely spatially unequal. Sediment dispersal can also be achieved through differential migration of dunes (Fig. 1D; Martin and Jerolmack, 2013), or the introduction and storage of extra sediment by differential scour (Fig 1E; Gabel, 1993). Superimposition of bedforms (Fig. 1F; Best, 2005; Reesink et al., 2014) has been described as the mechanism by which sediment moves over host dunes (Venditti, 2005a), but is also inherent to bedform adaptation in the onset of splitting (Warmink et al., 2014), and as a prerequisite for through-passing of superimposed bedforms (Fig. 1G; Venditti et al., 2005b). Through-passing of superimposed bedforms may redistribute sediment as bedload when the host dunes approach a stable geometry. Dune volume can also be modified by changing dune geometry from a triangular to a humpback profile. Such changes are not captured by simple metrics such as bedform height and wavelength, but do change the flow field over the dunes (Fig. 1H; Reesink and Bridge, 2009). Finally, cross-stream sediment transfer as a consequence of three-dimensional geometry and flow (Fig. 1I; Allen, 1982; Parsons et al., 2005) can also be an important factor in sediment dispersal. These different processes span a range of temporal and spatial scales, and can be expected to result in different ‘geometrical signatures’ in the deformation of dunes.

3. METHODS

Repeat profiles of sand-bed dunes ($D_{50}=239\ \mu\text{m}$) were measured in a 2 m wide x 12 m long flume at 5 minute intervals, using an Aquascap acoustic backscatter sensor (2MHz) that was mounted on a 5 m long automatic traverse (See Reesink et al., 2013 for details). The downstream and vertical height resolutions were 5 mm and 2.5 mm respectively. Data analysis involved cross-correlation of temporally consecutive streamwise bed profiles, with the maximum correlation being used to determine the mean shift of the dune profile. After removal of this shift, the difference between consecutive profiles represents the deformation of the dunes (Fig. 2; McElroy and Mohrig, 2009). This deformation, reflected by local excess deposition or excess erosion relative to the mean profile shift, is an indication of local sediment dispersal and transfer between dunes.

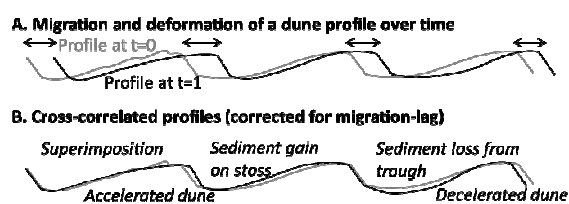


Figure 2. A) Two cross-correlated dune profiles (t_0 and t_1). B) Systematic deviations from the overall migration indicate that sediment has been dispersed among dunes.

4. PRELIMINARY RESULTS

Figure 3 shows a series of profiles that are coloured by the increase or decrease of erosion relative to the principal profile shift, which can be interpreted as local production or storage of sediment (Fig 2). Labels a and b indicate stoss slopes that act as sinks or sources of sediment relative to the main dune migration (cf. Fig. 1D; Martin and Jerolmack, 2013). Label c indicates an example of the persistence of sediment production in an area where a dune is overtaken and reduced. (Fig. 1A). Label d indicates that subsequent development of a train of superimposed bedforms (Fig. 1F) on the long stoss slope is located in a zone of sediment storage. Neither these superimposed bedforms, nor the zone of deposition of sediment, persists over time. Thus, these

relatively large superimposed bedforms are unlikely to be a standard mechanism by which sediment moves across dunes (see Venditti et al., 2005a) and are more likely a signature of local disequilibrium morphology.

5. DISCUSSION

The results show that cross-correlation can be used to visualise the geometric signature of dune deformation. The persistence of zones of erosion and deposition over time, relative to the main migration identified by cross-correlation (Fig. 3), indicates that individual dunes can act as local sources and sinks of sediment within the dune field. Such variability in erosion and deposition affects dune tracking analyses (Ten Brinke et al., 1999), applications of the Exner equation (Paola and Voller, 2005), and interpretations of measured bedload transport rates (e.g. Frings and Kleinhans, 2008).

Dune deformation can only occur when sediment is redistributed over and between dunes. As such, dune adaptation, growth, and decay are the combined characteristic of a population of dunes, and cannot be fully described by a geometric change of a *single* dune.

The dune deformation pattern can be used to interpret sediment transport processes. The outcome of this analysis will depend on the temporal and spatial resolution of the dune profiles and the profile length. At the 5 minute resolution used herein, deformation is dominated by differential migration of lee slopes and stoss slopes that act as local sources and sinks. At larger temporal intervals, an increasing amount of local detail on the change in bed geometry is lost.

The simultaneous operation of multiple processes brings into question the idea that a single relationship can describe the adaptation of dunes to changes in flow. Differential migration and superimposition are known to change between growth and decay, as well as over time (Martin and Jerolmack, 2013). Deformation is known to change between systems, likely in response to grain size (McElroy & Mohrig, 2009). The relative magnitudes of different sediment dispersal processes are not static, but vary in time and space.

Only a few sediment transport processes are currently explicitly captured in predictions of dune development (e.g. Giri et al., 2006; Paarlberg et al., 2009; Warmink et al., 2014). The method presented herein can be used to compare the magnitude and spatial signature of deformation between such predictive models and the natural dunes they represent.

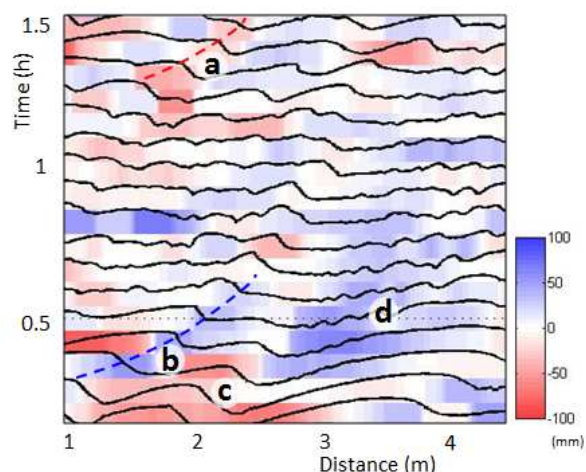


Figure 3. Successive experimental dune profiles, which were sampled at 5-minute intervals, which are coloured according to their difference in elevation after they have been corrected for dune migration (migration lag in a cross-correlation). The difference between the profiles represents excess erosion (red) and deposition (blue) relative to the overall shift of the profile. Flow depth was changed at 0.5 hours from 0.18 to 0.23m, velocity decreased from 0.66 to 0.53 m/s. See text for explanation of labels.

6. CONCLUSIONS

Dunes deform because sediment is eroded locally and dispersed across the dune field to local zones of deposition. Cross-correlation can be used effectively to visualize local dune deformation, and the geometric patterns that are revealed can be used to identify sediment dispersal processes. A review of sediment dispersal processes highlights that not all natural dune dynamics are captured in our models. This study therefore provides a method and the theoretical background to interpret dune deformation, dune adaptation, and variability in sediment transport over dunes.

7. ACKNOWLEDGMENTS

This investigation was funded by NERC grant NE/I014101/1. The authors are grateful to Brendan Murphy, Stuart McLelland, and Chris Unsworth, for their assistance in the project and with data collection.

8. REFERENCES

- Allen, J.R.L., and Collinson, J.D. (1974). The superimposition and classification of dunes formed by unidirectional aqueous flows. *Sedimentary Geology*, 12(3), 169-178.
- Allen, J.R.L. (1982) *Sedimentary structures, their character and physical basis* Vol.1: Amsterdam, Elsevier Scientific Publishing Company, Developments in Sedimentology 30A, 593 pp.
- Ashley, G.M. (1990) Classification of large-scale subaqueous bedforms: a new look at an old problem-SEPM bedforms and bedding structures. *Journal of Sedimentary Research*, 60(1), 160-172.
- Best, J. (2005) The fluid dynamics of river dunes: A review and some future research directions. *Journal of Geophysical Research – Earth Surface*, 110, F4.
- Fernandez, R., Best, J., and Lopez, F., (2006) Mean flow, turbulence structure, and bed form superimposition across the ripple–dune transition. *Water Resources Research*, 42(5), 948–963
- Frings, R.M., and Kleinhans, M.G. (2008) Complex variations in sediment transport at three large river bifurcations during discharge waves in the river Rhine. *Sedimentology*, 55(5), 1145-1171.
- Gabel, S.L., (1993) Geometry and kinematics of dunes during steady and unsteady flows in the Calamus River, Nebraska, USA. *Sedimentology* 40, 237–269.
- Giri, S., and Shimizu, Y. (2006) Numerical computation of sand dune migration with free surface flow. *Water Resources Research*, 42(10).
- Hardy R.J., Marjoribanks T.I., Parsons D.R., Reesink A.J., Murphy B. Ashworth P.J., and Best J.L. (2014) Modelling time dependent flow fields over three dimensional dunes. *River Flow 2014*, 1045-1052.
- Jackson, R.G. (1975) Velocity–bed-form–texture patterns of meander bends in the lower Wabash River of Illinois and Indiana. *Geological Society of America Bulletin*, 86(11), 1511-1522.
- Martin, R.L. and Jerolmack D.J. (2013) Origin of hysteresis in bed form response to unsteady flows. *Water Resources Research* 49(3), 1314-1333.
- McElroy, B., and Mohrig, D. (2009). Nature of deformation of sandy bed forms. *Journal of Geophysical Research: Earth Surface*, 114(F3).
- Naqshband, S., Ribberink, J.S., Hurther, D., & Hulscher, S.J.M.H. (2014) Bed load and suspended load contributions to migrating sand dunes in equilibrium. *Journal of Geophysical Research: Earth Surface*, 119(5), 1043-1063.
- Nittrouer, J.A., Allison, M.A., and Campanella, R. (2008) Bedform transport rates for the lowermost Mississippi River. *Journal of Geophysical Research: Earth Surface*, 113(F3).
- Paarlberg, A.J., Dohmen-Janssen, C.M., Hulscher, S.J., and Termes, P. (2009) Modeling river dune evolution using a parameterization of flow separation. *Journal of Geophysical Research: Earth Surface*, 114(F1).
- Paola, C., and Voller V.R. (2005) A generalized Exner equation for sediment mass balance. *Journal of Geophysical Research*, 110, F04014
- Parsons, D.R., Best, J.L., Orfeo, O., Hardy, R.J., Kostaschuk, R., and Lane, S.N. (2005) Morphology and flow fields of three-dimensional dunes, Rio Paraná, Argentina: Results from simultaneous multibeam echo sounding and acoustic Doppler current profiling. *Journal of Geophysical Research: Earth Surface*, 110(F4).
- Reesink, A.J.H, and Bridge, J.S. (2009) Influence of bedform superimposition and flow unsteadiness on the formation of cross strata in dunes and unit bars—Part 2, further experiments. *Sedimentary Geology*, 222(3), 274-300.
- Reesink A.J.H., Parsons D., Ashworth P., Hardy R., Best J., Unsworth C., McLelland S. and Murphy B. (2013) The response and hysteresis of alluvial dunes under transient flow conditions. *Marine and River Dunes 2013, Conference Proceedings*, 215-220.
- Reesink A.J.H., Parsons D.R. and Thomas R.E. (2014) Sediment transport and bedform development in the lee of bars: Evidence from fixed- and partially-fixed bed experiments. *River Flow 2014, Conference Proceedings*
- Rubin, D.M., and McCulloch, D.S. (1980). Single and superimposed bedforms: a synthesis of San Francisco Bay and flume observations. *Sedimentary Geology*, 26(1), 207-231.
- Ten Brinke, W.B.M., Wilbers, A.W.E., and Wesseling, C. (1999) Dune Growth, Decay and Migration Rates during a Large-Magnitude Flood at a Sand and Mixed Sand–Gravel Bed in the Dutch Rhine River System. *Fluvial Sedimentology* VI, 15-32.
- Unsworth, C.A., Parsons D.R., Reesink A.J.H., Best J.L., Ashworth P.J., and Hardy R.J. (2013) Flow structures over fixed 2D bedforms in transient states. *Proceedings of the Marine and River Dunes Conference 2013*, Bruges, Belgium
- Venditti, J.G., Church, M.A. and Bennett, S.J. (2005a) Morphodynamics of small-scale superimposed sandwaves over migrating dune bedforms. *Journal of Geophysical Research* 110, F01009

Venditti, J.G., Church, M.A. and Bennett, S.J. (2005b) On the transition between 2D and 3D bedforms, *Sedimentology*, 52, 1343–1359

Warmink J.C., Dohmen-Janssen M., Lansink J., Naqshband S., Duin O.J.M., Paarlberg A.J., Termes P., and Hulscher S.J.M.H. (2014) Understanding river dune splitting through flume experiments and

analysis of a dune evolution model. *Earth Surface Processes and Landforms* 39 (9) 1208-1220.

Yalin M.S. (1964) Geometrical properties of sand waves. *Journal of the Hydraulics Division*, American Society of Civil Engineers 90(5), 105-119.

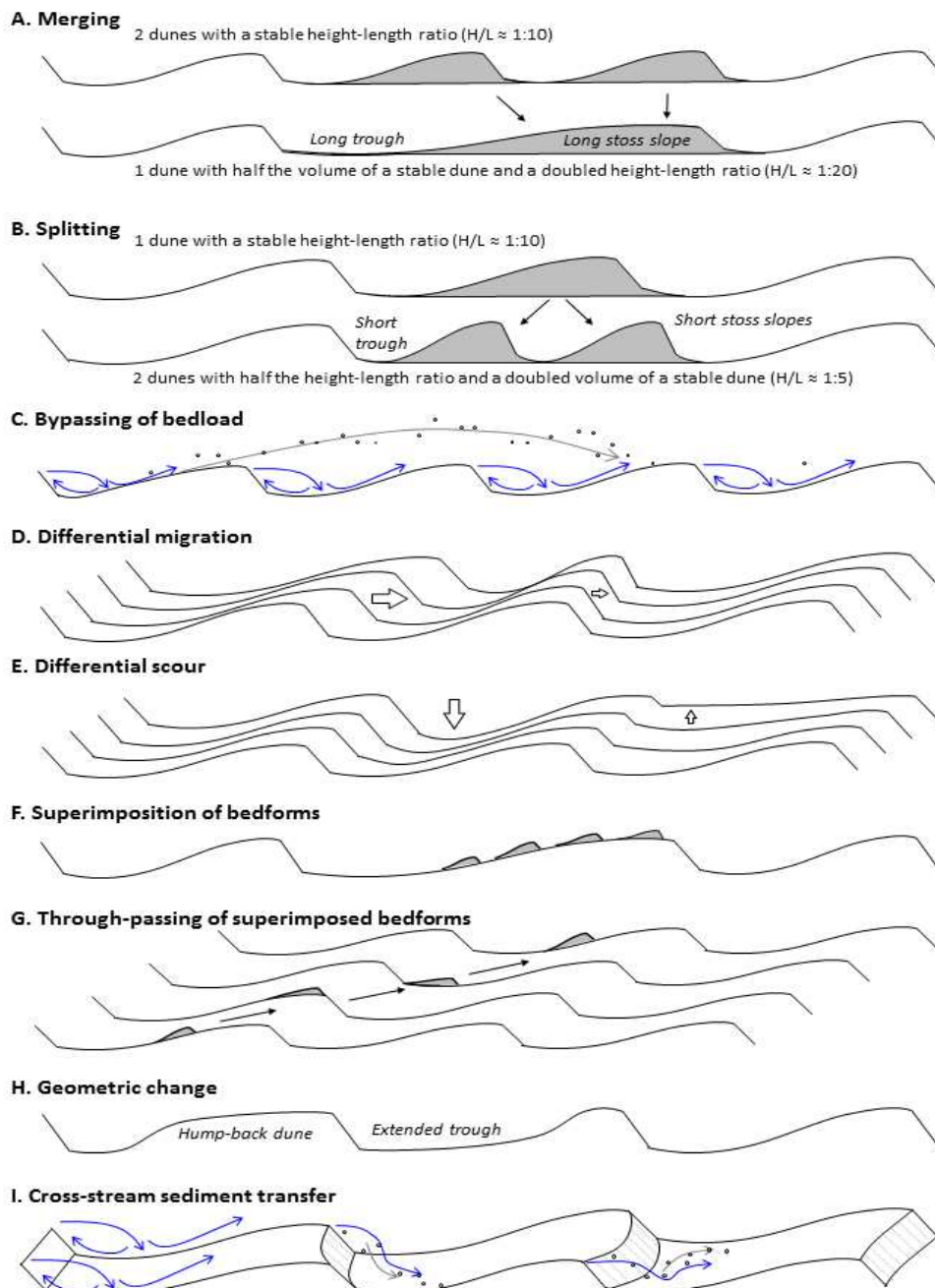


Figure 1. Processes of sediment dispersal over successive dunes. Shaded areas are bedform volumes. Blue arrows are flow. Grey arrows are sediment transport paths.

KEYNOTE: Managing the issue of seabed sediment in offshore renewable energy projects

J.M. Reynolds *North Wales Tidal Energy & Coastal Protection Co. Ltd, Holywell, North Wales, UK – john.reynolds@northwalestidalenergy.com and, Reynolds International Ltd, Mold, North Wales, UK – jmr@reynolds-international.co.uk.*

ABSTRACT: The offshore renewable energy sector requires information about the types and behaviours of sediments at and below the seafloor for: structure foundations; inter-array and export cables corridors; scour and depositional processes post-construction. Identification of the so-called ‘stable seafloor surface’ is also required along with an indication of seabed sediment mobility. Challenges associated with these issues will be discussed in relation to wind farm projects from around UK coastal waters.

Lessons learned from these previous and ongoing investigations are helping to inform the situation with regard to the North Wales Tidal Energy and Coastal Protection Project. This is a proposed 2.5 GW energy generation project with a 30+km long seawall enclosing an impoundment with an area of ~157 km². It will be necessary to understand much more clearly the processes affecting sediment mobility off the North Wales Coast in order to manage sediment and related issues successfully.

1. INTRODUCTION

The offshore renewable energy sector requires information about the types and behaviours of sediments at and below the seafloor for: structure foundations; inter-array and export cables corridors; and scour and depositional processes post-construction. The nature of these materials affects the design and selection of foundation types (monopiles, piled jackets, gravity bases, caissons, *etc.*) and influences the choice of cable routing and subsequent cable installation methods. Understanding the susceptibility of sediments around structures to scour at the seabed or excessive deposition is critical to the ongoing performance of the installed facilities. Identification of the so-called ‘stable seafloor surface’ is also required in order to be able to determine the amplitudes and directions of movement of various types of seabed bedforms as well as to indicate the lowest possible level of scour. Challenges associated with these issues will be discussed in relation to wind farm projects from around UK coastal waters.

2. CONSIDERATIONS FOR SEABED SEDIMENT MOBILITY ANALYSES

When considering seabed sediment mobility, it is commonly assumed that the reference surface over which seafloor bedforms move is level and smooth. This is frequently not the case. There may be a palaeo-topography associated with a landscape that has been formed by late Pleistocene or earlier processes that has subsequently become submerged as sea level has risen since the last ice age. An example of this from the now-abandoned Rhiannon Offshore Wind Farm Project, Irish Sea Zone is shown in Figure 1. The seismic expression of former moraines or drumlin ridges can be seen poking through the contemporary seafloor on this extract from a seismic section. These features, which comprise over-consolidated glacial sands and clays, have a characteristic darker seismo-acoustic expression compared with that of overlying fluvio-glacial deposits that are normally-consolidated and which appear with a light, more open-texture, seismo-acoustic character.

With respect to contemporary seabed bedforms, a consideration is the source of sediments, whether

from elsewhere in the Irish Sea or from erosion of the substrate.

3. SEABED SEDIMENT-SUBSTRATE RELATIONSHIPS

There is a growing body of evidence from detailed geophysical investigations associated with offshore wind farms to suggest that the base level of seafloor in parts of UK coastal waters is being deflated by erosion (Figure 2). This is in part apparently as a consequence of scour into sandy sub-members that contributes material towards bedform development. The role of reworked substrate sediments in the mass balance of mobile sediments within the Irish Sea needs further consideration. There is also evidence that more cohesive components of the substrate, such as clay bands, can resist a degree of scour and can form a flatter surface across which sediments can be moved or/ or winnowed relatively easily. As a consequence of this erosion of the seafloor, the seafloor surface can become more irregular in form. What is not understood is how this irregular topography can influence how sediment migrates across the seafloor and form different styles of bedforms, and affects current flow at a more localised scale to form secondary bedforms. There are clearly scale effects at play. How these can be included in seabed sediment mobility analyses is the subject of ongoing discussion.

4. NORTH WALES TIDAL ENERGY & COASTAL PROTECTION PROJECT

The maximum tidal range along the North Wales coast is one of the highest around the UK and outside of the Severn Estuary, with potential for substantial electricity generation. The North Wales coast has also suffered from major historical coastal flooding that has resulted, for example in 2010, in inundation of >10 km² of land, homes, businesses and vital infrastructure, costing more than £100 million in insured losses. As a result of the coastal flood risk, there has been a reluctance to invest in the region, where there are several areas of significant economic deprivation.

Over the last two years significant work has been undertaken by North Wales Tidal Energy &

Coastal Protection Co. Ltd (NWTE) to develop the vision of a major tidal range power generation project off the North Wales coast with tripartite benefits: (a) predictable generation of clean electricity; (b) coastal flood protection; and (c) economic regeneration.

Nominally, the proposed power generation scheme will include:

- A 32+ km long sea wall providing protection from storm surges within the Irish Sea;
- An impounded area of around 157 km²;
- Up to 100 power turbines with a total installed capacity in excess of 2 GW, potentially generating more than 3 TWh per year;

Low-lying areas along the coast are increasingly at risk of flooding, the more so when sea level rise from changing climate is taken into account. Vital communications links, such as the strategically important North Wales Main Line railway that connects London and Holyhead on Anglesey, and the A55 North Wales Expressway, which forms part of the Trans-European Networks programme (Euro-route E22), will be defended.

The design, construction and support of a tidal impoundment of the size and scale envisaged will be one of Wales' and the UK's largest infrastructure projects, providing employment for many years. Mitigation of the threat of coastal and fluvial flooding will help to reduce insurance premiums and flood-related blight to property values. It will also save local authorities and insurance companies from the costs of repairing flood damage that would most likely occur if the scheme does not proceed, estimated notionally in excess of £500 million over the next hundred years. The improved investment environment will also allow extensive business and property development in areas that are currently an insurance risk. Furthermore, by having such a major impoundment scheme in place it will provide a canvas on which new businesses can be developed to exploit the protected area of water (*e.g.* water sports activities and other visitor amenities), as well as associated enhanced support services within the coastal hinterland.

5. MANAGING SEDIMENT OFF THE NORTH WALES COAST

Before the specific design of the civil engineering structure and power generation units can be completed, there is a need to understand much more fully the hydro-dynamic processes in the southern part of the Irish Sea off the North Wales coast. At present it is evident that there is a generally-eastward migration of sediment along the shoreline, culminating in accretion at the Talacre sand dune system. However, what are unclear are the boundary processes that transport sediment between the coastline and several kilometres offshore. It is evident from satellite imagery of sediment plumes as well as from bathymetry information that there are possibly different scales of gyres operating. These may vary from gyres of the order of two hundred metres length rotating clockwise east of Colwyn Bay but counter-clockwise between Llandulas and Llandudno. These in turn may feed into and be related to three counter-clockwise gyres, of the order to 8 km long, orientated roughly WNW-ESE but south of the existing wind farms and the Constable Bank sand ridge. There are also questions as to why Constable Bank exists where it does with its particular orientation, which is parallel to that of other linear seabed features across the coastal offshore region.

There are questions perhaps of a more academic basis as to processes that might be related to deglaciation and isostatic rebound changing the base levels over millennia compared with the apparent lack of understanding of processes dominated by contemporary influences. The former, due to the very long time scale, may have little significance in relation to processes that

impact offshore renewable energy projects with their short project durations in contrast to the latter that might have greater and more direct impact. It is important to be able to determine the sensitivities within the offshore marine environment in order to know how large engineering structures will impact on these processes and what their consequences will be and where.

6. CONCLUSIONS

It is clear from both the previous investigations undertaken as part of the Rhiannon Wind Farm Project and from other projects elsewhere in UK coastal waters that substrate appears to play a part in influencing bedform development and affecting local current flow. It is also apparent from initial work as part of the North Wales Tidal Energy and Coastal Protection Project that the interaction between large scale hydro-dynamic processes within the Irish Sea and the near-shore coastal environment is complex and very poorly understood. This has been identified as an important component of the research to be undertaken as part of the project's Environmental Impact Assessment baseline studies.

7. ACKNOWLEDGEMENTS

Thanks are due to the RIL seismic team (Dr Lucy Catt, Dr Gwen Salaün and Ms Ana Branco Fernandes) for their work on the various offshore wind farm projects. Thanks are also due to colleagues in NWTE for their input to the early stages of the North Wales Tidal Energy and Coastal Protection Project.

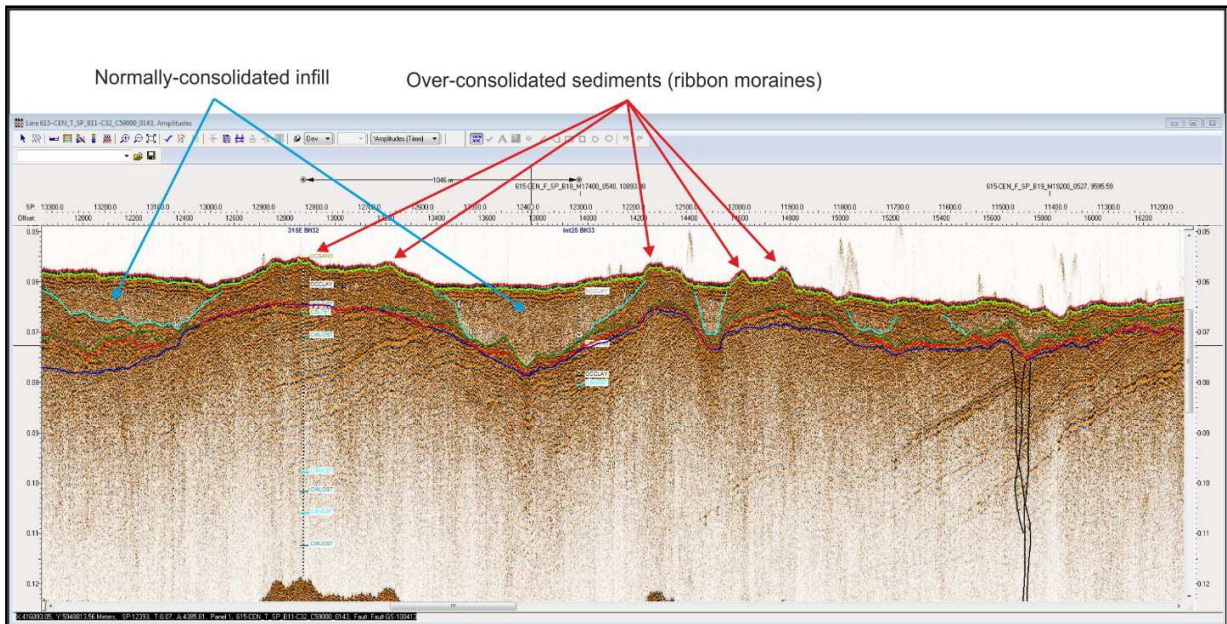


Figure 1. Example of seismic data from the Rhiannon Offshore Wind Farm, Irish Sea Zone, indicating protrusion of over-consolidated glacial sediments through the seabed.

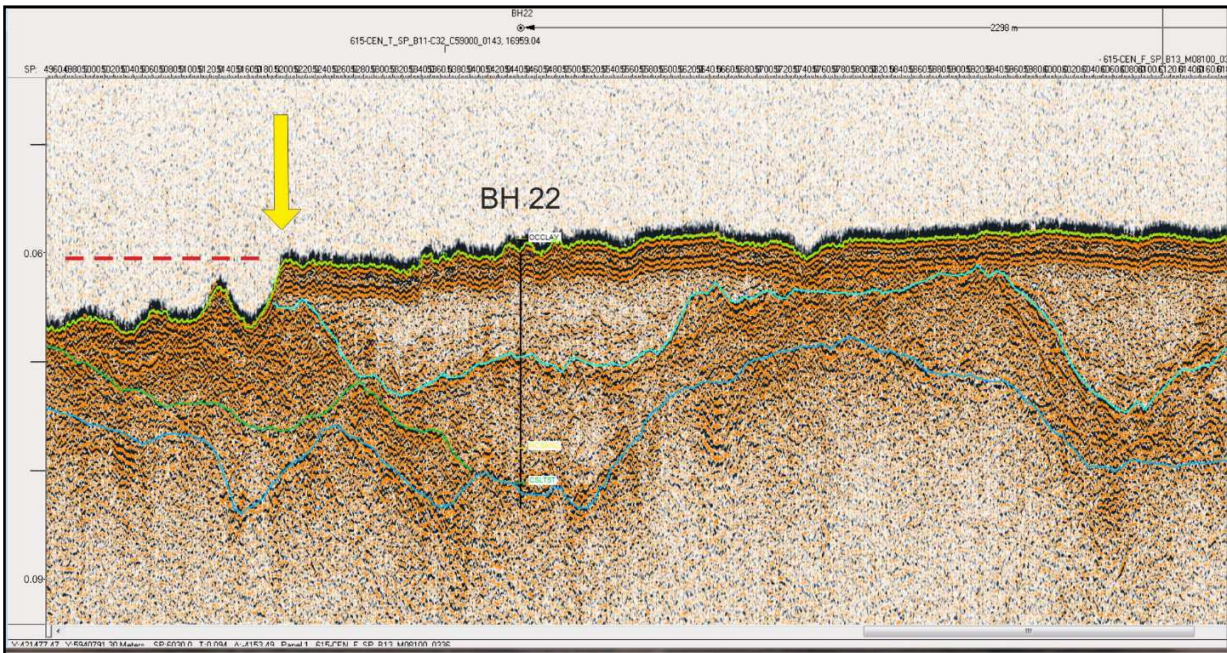


Figure 2. Example of seismic data from the Rhiannon Offshore Wind Farm, Irish Sea Zone, indicating erosion of normally-consolidated sediments and deflation (red dashed line) of the seabed left of the nick point highlighted by the yellow arrow.

Physical modeling of fluvial obstacle marks at a sediment layer of limited thickness

O. Schloemer *Department of Geography, University of Bonn, Germany – oschloem@uni-bonn.de*

J. Herget *Department of Geography, University of Bonn, Germany – herget@giub.uni-bonn.de*

ABSTRACT: A series of 36 clear-water flume experiments were conducted to investigate the influence of a limited layer of uniform medium sand on the morphometry of obstacle marks at a cylindrical pile. The focus was particularly on the scour hole morphometry. Regarding systematical analyzation constant flow conditions and two diameters of cylindrical piles (0.01 m and 0.02 m) were chosen. The thickness of the sedimentary layer ranged from 0.08 m to 0.005 m and was continuously reduced. Results showed that scour hole morphometry differed at a limited sediment layer. While scour depth was greatly reduced, other characteristic parameters (e.g. scour width, scour length) still achieved large parts of their steady state dimensions due to sediment transport induced by the hydraulic processes around the piles.

1. INTRODUCTION

Obstacle marks are sedimentary bedforms induced by an obstacle exposed to a current. As consequence of the variety of potential obstacles in nature like blocks, boulders and woody riparian plants, they are integral components of the fluvial and marine systems (e.g. Breusers & Raudkivi, 1991; Melville & Coleman, 2000). Such obstacles cause the flow to separate, resulting in a complex and high turbulent vortex system around the obstacle, denoted as “horseshoe vortex” (e.g. Muzzammil & Gangadhariah, 2003; Dey & Raikar, 2007). The approaching flow is pushed downwards in front and gets accelerated at the lateral parts of the obstacle resulting in rotating vortex system, which increases bed shear stress and induce sediment mobilization in front and around the obstacle. The legs of the vortex system are stretching around the obstacle base in a horseshoe-like pattern and transport eroded sediment out of the scour hole into the wake. In addition to that, detached shear layers interact with these extended legs causing the formation of trailing vortices, which have the potential to generate sediment accumulations with lengths up to several tenths of the obstacle diameter (Herget et al., 2013). These sediment accumulations are termed as “sediment ridge” (Euler & Herget, 2011,

2012). The sediment ridge and the adjacent frontal, crescent-shaped scour hole are forming a typical obstacle mark (c.f. Fig.1), (e.g. Allen, 1982). A dynamic interaction between hydraulic and sedimentary processes causes a non-linear development towards a steady state (e.g. Melville & Coleman, 2000). Actually this interaction is characterized by positive feedback mechanisms between scour hole incision and horseshoe vortex action, where sliding due to gravity and the angle of repose related to grain size of the sediments are the main processes for scour hole enlargement (Euler & Herget, 2011, 2012). Obstacle mark dimensions are variable and depend on flow, obstacle and sediment characteristics as well as on temporal dynamic (e.g. Breusers & Raudkivi, 1991; Melville & Coleman, 2000). A unique aspect of obstacle marks is their development even when the mean flow velocity is well below the critical threshold for general particle movement (Euler & Herget, 2012).

1.1. Outline for the present research

The formation of obstacle marks is controlled by a variety of independent variables. Many of these variables have been investigated systematically (e.g. Breusers & Raudkivi, 1991; Melville & Coleman, 2000; Arneson et al., 2012). According to recent investigations by flume experiments several morphometric variables could be

determined as order parameters of the obstacle mark topography at steady state conditions. These include maximum scour depth, width of the frontal scour hole, length of the frontal scour hole and width of the sediment ridge, (c.f. Fig. 2), (Euler & Herget, 2011, 2012).

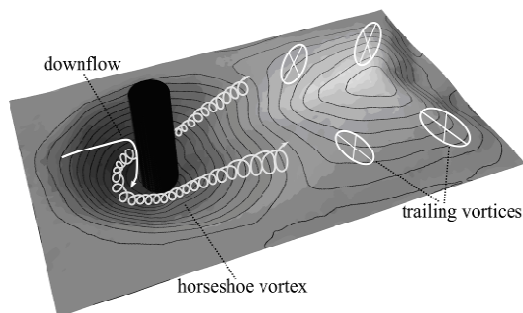


Figure 1. Simplified flow field around an emergent cylinder with frontal scour hole and sediment ridge in the wake. Direction of flow is from left to right (modified from Herget et al., 2013: 304).

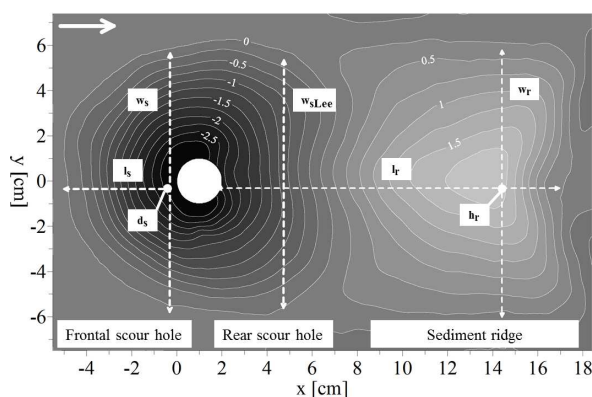


Figure 2. Contour plot of an obstacle mark at a cylindrical pile. Dashed lines indicate locations of morphometric order parameters and topographical profiles (d_s – frontal scour depth; l_s – frontal scour length; w_s – frontal scour width; w_{sLee} – rear scour width; w_r – ridge width; h_r – ridge height; l_r – ridge length. Arrow indicates direction of flow (modified after Euler & Herget, 2012: 40).

The unique characteristic of these variables is their interdependent relationship to each other (Herget et al., 2013). The parameters sediment ridge width and length are not suited for correlation, as they strongly vary with time (Euler & Herget, 2012).

In contradiction to these idealized morphological patterns, obstacle marks in the field are often not fully developed or preserved. This is especially valid for giant obstacle marks generated by Pleistocene megafloods (e.g. Herget 2005).

Especially the scour holes are often very wide, but not very deep (e.g. Herget et al., 2013).

The formation of clear and fully developed structures and forms might be inhibited by numerous factors. One of those is a depth-limited cover of erodible sediments in front of an obstacle.

2. METHODOLOGY

To systematically investigate the influence of a limited sediment layer on the morphology of obstacle marks, 18 flume experiments under constant boundary conditions in regard to flow, obstacle and sediment characteristics were carried out. Each run was repeated to avoid coincidences, leading to a total number of 36 experimental runs. To predict the potential maximum scour depths under given boundary conditions the HEC-18 pier scour equation was used (cf. Arneson et al., 2012). Limited sediment thickness was in this context defined as condition, in which the depth of the sediment layer was less than the potential maximum scour depth. Starting with a sufficient depth of sediment in front of the obstacle, the sediment thickness was continuous reduced after each run. The experiments were not prototype-based and no similarity criterions were applied.

2.1 Experimental setup

The physical modelling experiments were conducted at rectangular flume of 5 m length, 0.32 m width and 0.27 m high working section. The slope was fixed at 0.003 m/m. Cylindrical piles of diameters 0.01 m and 0.02 m and heights of 0.18 m served as obstacles and were mounted in the middle of the working section at the plane of symmetry. Water depth (0.08 m) and mean flow velocity (0.24 m/s) were kept constant during the experiments leading to a stationary discharge (0.00614 m³/s). The obstacles were emergent (water depth < obstacle height). Froude and Reynolds numbers were 0.27 and ~ 12,000 respectively. The experiments were conducted over 24 hours to reach steady state conditions of the morphometric order parameters (e.g. Melville & Chiew, 1999). Uniform sand with median grain size 0.055 mm was used in the experiments. The natural angle of repose of the particles is 30°. Bed shear stress was equal to 57 % of the critical bed shear stress so that clear-water conditions prevailed and no general particle movement occurred.

As distinguished from the previously mentioned parameters the depth of the sedimentary layer was not constant and ranged from 0.005 m up to 0.08 m. For bathymetric surveys along topographical profiles during and at the end of the runs, an ultrasonic punctual distance meter (UltraLab UWS, General Acoustics) was used. Additionally an Acoustic-Doppler Velocimeter (ADV) (Vectrino, Nortek) was used for analysing the flow field around the obstacles, applying the turbulent kinetic energy approach (e.g. Stapelton & Huntley, 1995). Further details on the measurement techniques are given in Euler & Herget (2011, 2012)

3. EXPERIMENTAL RESULTS

3.1 General obstacle mark evolution

Despite the variable sediment layer thickness, obstacle marks developed during each experimental run. The erosion of the scour hole started immediately while reaching the desired flow conditions at the frontal face of the cylindrical pile. The particle-transport out of the developing scour hole into the wake region was driven by the processes of saltation and sliding. At the end of the experimental runs the scour holes completely surrounded the cylinder, while the sediment ridges consisted of a central crest and two lateral flanks with a slight depression in the lee.

3.2 Morphometry

Figure 3 shows the normalized dimensions of the scour hole parameters in relation to normalized sediment thickness. At sufficient sediment thickness the order parameters reached a constant steady state and were general larger at larger obstacle diameter. The observed maximum scour depths corresponded well to predicted values at both obstacle diameters and served as “critical depth” in regard to the thickness of the sedimentary layer.

Below this critical depth the obstacle mark dimensions gradually decreased and did not reach their steady state dimensions under given boundary conditions. While not surprising that the scour depth was reduced significant, the other order parameters still reached a large part of their potential steady state dimensions.

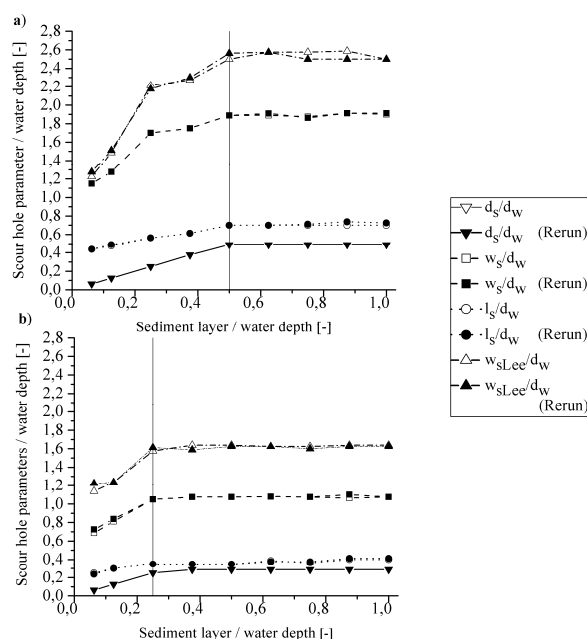


Figure 3. Normalized scour hole parameters in relation to normalized sediment layer thickness (all runs considered). Vertical lines represent maximum scour depths under given boundary conditions. a) obstacle diameter 0.02 m. b) obstacle diameter 0.01 m. d_w denotes water depth (= 0.08 m). Other abbreviations: see Figure 2.

These development resulting in unproportional morphometry of obstacle marks at limited sediment layer (cf. Table 1). This finding was supported by bathymetric surveys during the runs showing that maximum scour depth was already reached in the initial phase of obstacle mark development (< 2 min), whereas slight enlargement of the frontal scour width (w_s) and rear scour width (w_{sLee}) could be observed at subsequent measurements.

Table 1. Obstacle mark parameters at limited sediment thickness in relation to steady state dimensions at obstacle diameter 0.02 m. Sediment layer thickness is in m.

Sediment layer	Scour depth	Scour length	Scour width	Ridge height	Ridge width	Ridge length
0.03	0.77	0.86	0.92	1.00	0.98	0.95
0.02	0.51	0.79	0.89	1.00	0.98	0.93
0.01	0.26	0.67	0.67	0.75	0.66	0.76
0.005	0.13	0.61	0.61	0.38	0.50	0.66

Furthermore, slope calculations from topographical profiles show that sliding was not a major process in scour hole enlargement at limited sediment thickness, because slopes were mostly below the angle of repose. However, ADV measurements revealed that the flow field around the obstacle was characterized by high values of turbulent kinetic energy, indicating the action of the horseshoe vortex system even for a thin sedimentary layer (< 0.001 m). Therefore the horseshoe vortex system has to be considered as partial driving force in scour hole enlargement (especially scour width) through sediment erosion.

4. CONCLUSION

The results show that limited sediment thickness is a critical boundary condition in the evolution of fluvial obstacle marks. At a first view this is not really a surprising result, but it becomes evident that scour hole parameters (depth, width, length) are not decreasing proportional. As a consequence the significance of linear relationship in comparison to steady state dimensions weakens. From this perspective additional experiments are necessary to identify potential regularities as well as to up-scale these regularities to field boundary conditions (e.g. giant obstacle marks formed by Pleistocene megafloods).

Furthermore, new insights in process dynamics and sediment transport processes of fluvial obstacle marks could be obtained. However, the results of the present study are limited to steady flow, clear-water conditions, sub-critical flow conditions and non-cohesive sediments.

5. ACKNOWLEDGEMENTS

The experiments and results were part of the Master thesis of Oliver Schloemer.

6. REFERENCES

- Allen, J.R.L. 1982. Sedimentary structures. Their character and physical basis. Volume 2. Developments in Sedimentology 30B. Amsterdam: Elsevier.
- Arneson, L.A., Zevenbergen, L.W., Lagasse, P.F. & Clopper, P.E. 2012. Evaluating scour at bridges. Hydraulic Engineering Circular No. 18. Virginia: U.S. Department of Transportation.
- Breusers, H.N.C. & Raudkivi, A.J. 1991. Scouring. Hydraulic Structures Design. Manual Series Vol. 2. Rotterdam: CRC Press.
- Dey, S & Raikar, R.V. 2007. Characteristics of horseshoe vortex in developing scour holes at piers. *Journal of Hydraulic Engineering* 133(4): 399-413.
- Euler, T. & Herget, J. 2011. Obstacle-Reynolds-number based analysis of local scour at submerged cylinders. *Journal of Hydraulic Research* 49(2): 267-271.
- Euler, T. & Herget, J. 2012. Controls on local scour and deposition induced by obstacles in fluvial environments. *Catena* 91: 35-46.
- Herget, J. 2005. Reconstruction of Pleistocene ice-dammed lake outburst floods in the Altai Mountains, Siberia. Geological Society of America Special Publication 386. Boulder: Geological Society of America.
- Herget, J., Euler, T., Roggenkamp, T. & Zemke, J. 2013. Obstacle marks as palaeohydraulic indicators of Pleistocene megafloods. *Hydrology Research* 44(2): 300-317.
- Melville, B. & Chiew, Y.M. 1999. Time scale for local scour at bridge piers. *Journal of Hydraulic Engineering* 125(1): 59-65.
- Melville, B. & Coleman, S.E. 2000. Bridge scour. Highlands Ranch: Water Resources Publication
- Muzzammil, M. & Gangadhariah, T. 2003. The mean characteristics of horseshoe vortex at cylindrical pier. *Journal of Hydraulic Research* 41(3): 285-297.
- Stapelton, K.R. & Huntley, D.A. 1995. Seabed stress distribution using the interial dissipation method and the turbulent kinetic energy method. *Earth Surface Processes and Landforms* 20(9): 807-815.

Multibeam survey of a tidal banner bank: morphology of dunes in eroding partially compacted sands?

T. Schmitt *SHOM, Brest, France* – thierry.schmitt@shom.fr

N.C. Mitchell *University of Manchester, UK* – Neil.Mitchell@Manchester.ac.uk

Sand transport simulations often make no allowance for compaction, but even modest compaction significantly increases threshold of movement. Nash Sands, a banner bank in the Bristol Channel, was surveyed in 2002 with multibeam sonar, following a decade of single-beam monitoring. The monitoring data reveal an area that declined by 5-10 m over the prior 11 years and thus where partially compacted sands are likely to have been excavated. In this area, a southerly promontory of the bank retreated by 900 m over the 11 years in the ebb-current direction. Based on dune migration rates, which nearby average 184 m y^{-1} , the 11-year of 900 m retreat is only half that expected. Morphologies of dunes in the multibeam data vary, with some showing superimposed megaripples, indicating mobile surface sand, but other areas lacking such megaripples and having a smoother morphology. We question whether the latter morphology marks less mobile compacted sand.

1. INTRODUCTION

The effect of compaction on sand mobility remains poorly characterized. Modest compaction of a sand surface by pre-stressing it with a current can lead to 27% increase in the shear velocity associated with threshold of motion (Paphitis and Collins, 2005). Monteith and Pender (2005) found that bedload flux decreased with increasing durations of pre-stressing. According to Ockelford and Haynes (2013) resistance to erosion arises because the pre-stressing current causes vertical settlement of particles, which increases hiding effects and grain pivot angles, and because of re-orientation of surface particles. Other indirect evidence would suggest that compaction could lead to greater erosional resistance. Craig (1978) summarizes the results of shear tests on sands under drained conditions. Compacted sands remain incohesive but develop greater shear strengths (friction angles of 35° and 45° for uniform rounded and angular sand, respectively) compared with loose sand (27° and 33° , respectively). Although seabed erosion by tidal currents does not usually involve shear failure, these results also hint that particles have become more closely packed and resistant to erosion by the

mechanisms discussed by Ockelford and Haynes (2013).

We study here Nash Sands, a banner bank in the Bristol Channel, where strong ebb currents (Uncles, 1983) have drawn out the sand from a promontory of the coastline (Figure 1). Banner banks are tidal sand banks emanating from near headlands in the direction of dominant tidal sand transport (e.g., Ferentinos and Collins, 1980; Pingree, 1978). Historical charts reveal that Nash Sands has changed shape and position, movements exposing earlier deposited sand that offer the potential to study how compaction has influenced bedform morphology and migration rates.

2. DATA AND METHODS

Over Nash Sands, multibeam data were collected in late summer 2002 in two phases (the full survey over three days, 16-18 August, and some repeat measurements on 4 September) and single-beam data collected by a local survey company for us in May 2003. Where the different surveys cover the same areas, the two phases of multibeam data show seabed change over ~19 days, while comparison with the single beam show change over 263 days.

The multibeam data were collected with a 101-beam Reson Seabat 8101 240 kHz sonar, with a spatial resolution of around 1 m constrained here by the precision of differential GPS broadcasts from Nash lighthouse. Sounding data were processed by manually removing erroneous soundings using CARIS/HIPS software (such as caused by detections of water-borne noise) and combining with sound velocity and tidal height data from a locally-installed tide gauge before gridding at 1 m resolution. The data are presented as depths relative to Chart Datum (Lowest Astronomical Tide). An overview of these data is shown as a depth-coded colour map with shaded relief in Figure 1, along with two years of the single-beam monitoring data. Figure 2 shows the multibeam data with colours provided by elevation changes in the single beam data. An enlargement of part of the data that declined over that period is shown in Figure 3.

These data were interpreted using methods similar to those described by Schmitt and Mitchell (2014). Sand dunes were identified between successive surveys using their shapes in both cross-section and plan-view (Schmitt and Mitchell, 2014; Schmitt et al., 2007). While migrating, dunes preserved their shapes between the two multibeam surveys and were generally easy to track between the 2002 multibeam and 2003 single-beam surveys except in Nash Passage, where the dunes smoothed out and were too weakly defined for tracking on an annual basis.

Processing of the single-beam monitoring data is summarized by Lewis et al. (2015). Surveys were carried out each year from 1991 to 2002 (excluding 1999-2000) in grid patterns. The data from each survey year were interpolated onto a 20 m x 20 m regular grid using a nearest neighbour scheme. The resulting bathymetry grids for years 1991 and 2002 are shown in the insets to Figure 1. The grids were then differenced to produce elevation changes, which are shown in Figure 2 along with shading from the multibeam data to help in locating morphologic features. Overlain contours in Figure 2 represent the 1991 and 2002 depths as indicated in the lower-left key.

Further data available to us include sediment texture data from a grid of grab samples, which show median grain size (D_{50}) varies from 0.2 to 0.5

mm over East Nash (one sample within the eroded area has 0.5 mm D_{50}). Data from current meter CM2 (Figure 1) collected over one neap-spring cycle show almost rectilinear currents (ellipticity 0.02) with a maximum current of 1 m s^{-1} at 1 m above bottom.

3. OBSERVATIONS

Nash Sands has a curvilinear shape with 'cat back' rounded dunes on its south flank with a sense of asymmetry suggesting ebb dominance (transport to the west). Dune tracking between surveys revealed an average celerity of the dunes along south East Nash of 184 m y^{-1} . The monitoring data show that the crest of the bank advanced southwards and the promontory farther west retreated during this period. In Figure 2, these are shown as areas of accumulation and erosion, respectively. The apparent retreat is 910 m. If this were simply due to dune translation at 184 m y^{-1} , retreat over 11 years would be twice as large.

Within the eroded area (Figure 3), the multibeam sonar data reveal a curious variation in surface texture. Many dunes have typical superimposed megaripples, though here with multiple crest-line orientations, suggestive of varied current directions acting on mobile sand. However, the dunes marked C2, C5 and northerly parts of C6 and C7 have a smoother texture (smaller ripples). These lie at similar elevations to the dunes with superimposed megaripples.

If the dunes migrated perpendicular to their crestlines without changing elevation (i.e., the erosion in Figure 2 were a result of simple retreat of the whole slope), the elevations of the troughs would mark the levels above which the sand has recently been mobile. Projecting these trough levels 'upstream' to where they intersect the modern seabed suggests where (below these levels) the sand has only recently been exposed. A selection of these elevations is marked in Figure 3. The projection 'upstream' of these elevations is shown by the black dots shown. Although some examples have been reported of megaripples changing morphology towards troughs into smaller heights and wavelengths (so this pattern could be unremarkable), there are some changes across this boundary, such as for dune C6, with larger megaripples above the boundary.

Overall, although we cannot claim to have found unequivocal evidence for compaction effects on sand morphology, we find the variations in dune morphology here curious and prompt the question of whether compaction can affect the rate and dynamics of sand transport.

2. CONCLUSIONS

Dunes in an area of Nash Sands that declined by 5-10 m over a decade curiously have either superimposed megaripples or smoother texture with much smaller megaripples. We speculate these differences may reflect varied compaction effects. Further study may provide practical indications for how compaction can be accounted for in transport simulations.

3. ACKNOWLEDGMENT

These multibeam data were originally collected with funding from Hanson Aggregates, RMC Aggregates and United Marine Dredging.

4. REFERENCES

Craig, R.F., 1978. Soil Mechanics, 2nd Ed. Van Nostrand Reinhold, New York, 318 pp.

Ferentinos, G. and Collins, M.B., 1980. Effects of shoreline irregularities on a rectilinear tidal current and their significance in sedimentation. *J. Sed. Petrol.*, 50: 1081-1094.

Lewis, M.J., Neill, S.P. and Elliott, A.J., 2015.

Interannual variability of two offshore sand banks in a region of extreme tidal range. *J. Coastal Res.*, 31: 265-275.

Monteith, H. and Pender, G., 2005. Flume investigations into the influence of shear stress history on a graded sediment bed. *Water Resour. Res.*, 41: Paper W12401.

Ockelford, A.-M. and Haynes, H., 2013. The impact of stress history on bed structure. *Earth Surf. Proc. Land.*, 38: 717-727.

Paphitis, D. and Collins, M.B., 2005. Sand grain threshold, in relation to bed 'stress history': an experimental study. *Sedimentology*, 52: 827-838.

Pingree, R.D., 1978. The formation of the shambles and other banks by tidal stirring of the seas. *J. the Marine biological Association of U.K.*, 58: 211-226.

Schmitt, T. and Mitchell, N.C., 2014. Dune-associated sand fluxes at the nearshore termination of a banner sand bank (Helwick Sands, Bristol Channel). *Cont. Shelf Res.*, 76: 64-74.

Schmitt, T., Mitchell, N.C. and Ramsay, A.T.S., 2007. Use of swath bathymetry in the investigation of sand dune geometry and migration around a near shore 'banner' tidal sandbank. In: P.S. Balson and M.B. Collins (Eds.), *Coastal and shelf sediment transport*, Geol. Soc. Lond., Spec. Pub. 274. pp. 53-64.

Uncles, R.J., 1983. Modelling tidal stress, circulation and mixing in the Bristol Channel as a prerequisite for ecosystem studies. *Can. J. Fish. Aqua. Sci.*, 40 (Suppl. 1): 8-19.

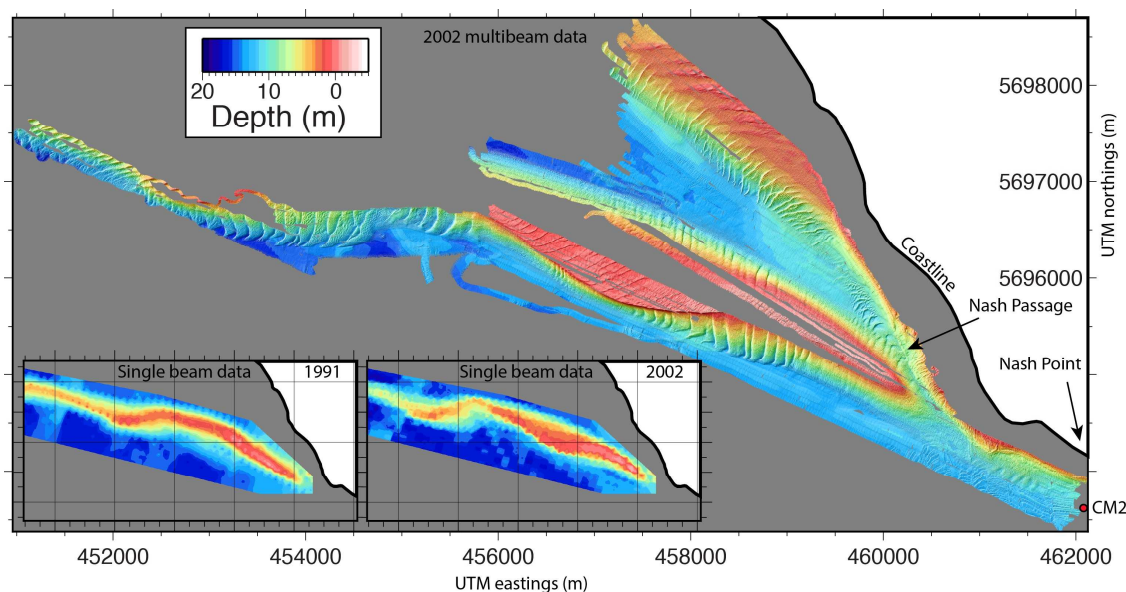


Figure 1. Overview of the multibeam echo-sounder data collected in 2002 over Nash Sands. Coordinates are Universal Transverse Mercator projection metres (zone 30). Lower-left insets show the single-beam data collected in 1991 and 2002 as part of the monitoring efforts (same colour depth scale and extent as the main panel).

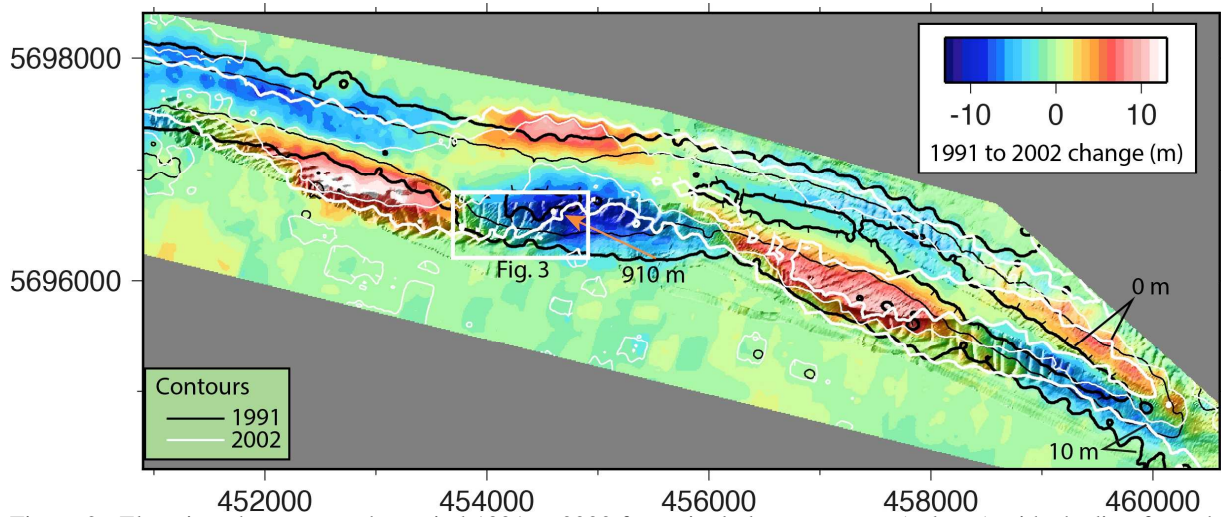


Figure 2. Elevation change over the period 1991 to 2002 from single-beam surveys (colours) with shading from the 2002 multibeam sonar survey. In the colour key, positive values imply deposition, negative values erosion. Also shown are 5-m depth contours of the 1991 and 2002 single-beam surveys (10 m intervals in bold, as annotated lower-right, and tick marks indicating down-direction for the closed contours). Orange arrow in centre marks the 910 m movement in the 10 m depth contour over this period.

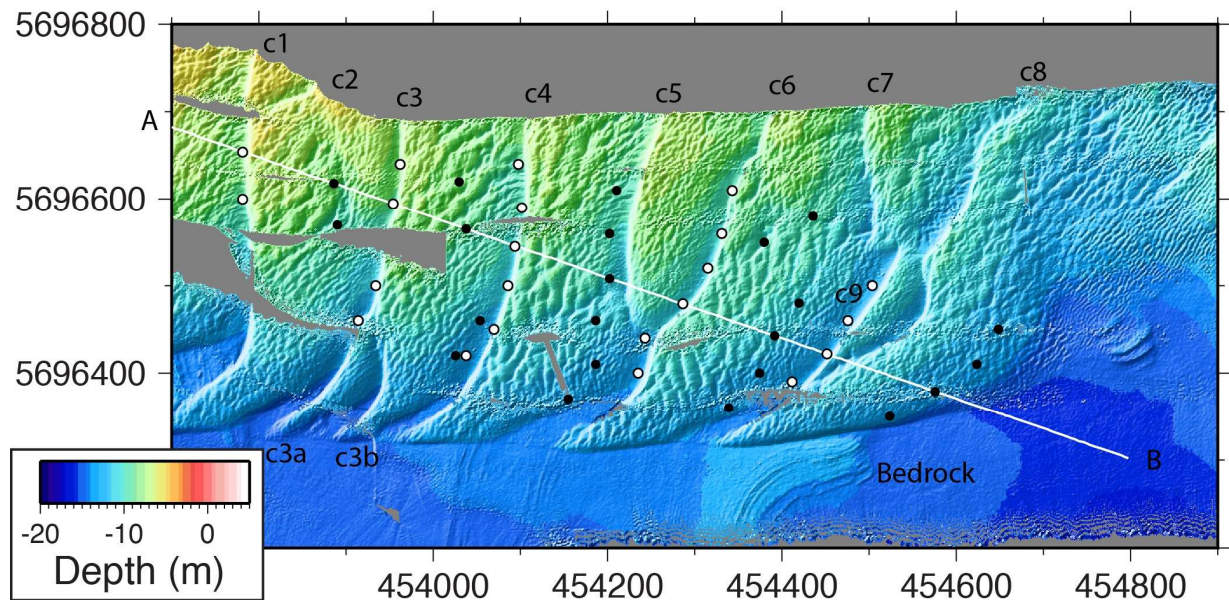


Figure 3. Enlargement of the multibeam data located in Figure 2. Black dots locate where the elevations of minima in troughs (open circles) intersect the surface where projected along the line shown.

Depositional character of submarine dunes on a Pleistocene distally steepened carbonate ramp (Favignana Island, Italy)

A. Slooman, *Department of Earth and Environmental Sciences, University of Geneva, Switzerland – arnoud.slooman@unige.ch*

M.J.B. Cartigny, *National Oceanography Centre, Southampton, UK*

P.L. de Boer, *Faculty of Geosciences, Utrecht University, The Netherlands*

A. Moscarello, *Department of Earth and Environmental Sciences, University of Geneva, Switzerland*

ABSTRACT: Distally steepened carbonate ramps are characterised by a steep proximal slope that passes basinwards into a gentle distal toe-of-slope. Such systems are controlled by clastic depositional processes and may host deposits formed by the migration and progradation of submarine dunes. This study documents the differences in depositional character and preservation potential of large-scale composite bedforms as a function of the location on the ramp slope. Such bedforms migrated as a result of the migration of small-scale parasitic dunes over their stoss-side and the subsequent deposition of compound cross-beds on their lee-side. The proximal slope zone is characterised by thick packages of compound cross-bedded sets that formed by the down-slope migration of composite dunes. The distal toe-of-slope zone is composed of form-sets that preserved the original outline of composite dunes, including the small-scale dunes on their stoss-side. Such preservation occurred by the rapid burial of large, but only marginally erosive, sediment gravity flows.

1. INTRODUCTION

Distally steepened carbonate ramps are gently inclined sea floors with a marked break in slope immediately basinwards of the carbonate factory (Fig. 1). Progradation occurs in particular through deposition on the ramp slope giving rise to the formation of seismic-scale clinofolds up to tens of metres in height.

In temperate waters such as the present-day Mediterranean Sea, non-tropical biological associations generate sand- and gravel-sized material. Such skeletal debris remains loose on the sea bed in the absence of the early cementation and coral build-ups that characterise tropical settings. Consequently, under the influence of shallow-marine unidirectional currents, subaqueous dunes ranging from small- to large-scale (*sensu* Ashley, 1990) may develop on carbonate ramps (e.g. Fornos & Ahr, 2006). Their preservation is most likely in the ramp slope zone. The sedimentary record contains numerous examples of biocalcarenite and -calcirudite bodies that formed by the lateral stacking of submarine dunes on

distally steepened carbonate ramps (e.g. Pomar et al., 2002).

Here, we report on the depositional character and preservation potential of submarine dunes on the Pleistocene distally steepened carbonate ramp of Favignana Island, Italy (Fig. 2). We focus in particular on the differences between the proximal slope zone and the distal toe-of-slope zone.

2. RESULTS

2.1. Clinofold couplets: Dune deposits and event beds

The Pleistocene Favignana carbonate ramp succession is composed of clinofold couplets, which consist of repeated alternations of stacked dune deposits (ca. 50% of the succession) and up to several metres-thick gravity-flow deposits, or event beds (constituting the remaining 50%). The up to 50 metres high clinofolds dip up to 10 degrees in the proximal ramp slope zone, where event beds indicate significant basal erosion, and pass basinwards into the up-to-a-few-degrees-inclined to near-horizontal units of the distal toe-of-slope zone, in which event beds are highly

aggradational and only of limited erosional nature. Dune deposit character also markedly change from the proximal slope zone to the toe-of-slope zone.

2.2. Composite dunes generating sets of compound cross-bedding

The large-scale dunes that generated the clinofomed dune deposits of the ramp slope were composite bedforms up to 4 metres high, generated by the climbing of small-scale dunes not exceeding 40 cm in height. The stoss-side of such parent bedforms were thus covered by parasitic bedforms, both types of dunes advancing in approximately the same direction. Cross-beds were formed as small-scale dunes prograded down the lee-side of a large-scale dune. Such cross-beds are contained within compound cross-beds, the lateral stacking of which resulted in the migration of large-scale dunes and the formation of sets. (See Figs. 3, 4, 5 for visual examples of terminology.) Sediment was largely derived from the carbonate factory occupying the shallow region of the ramp. However, in situ carbonate production also occurred and is responsible for the presence of coarse lags between and within (compound) cross-beds.

2.3. Proximal ramp slope zone

In the proximal ramp slope zone, preservation occurred through the lateral stacking of compound cross-bedded sets as large-scale composite dunes, which were generated on the vast area of the carbonate factory (Fig. 1), migrated down the ramp slope. This process mimics the down-slope migration of parasitic small-scale dunes over the lee-side of larger parent bedforms. Extensive skeletal production in the carbonate factory resulted in high rates of net sediment supply that allowed for slope progradation over a few kilometres length for the entire Pleistocene carbonate ramp succession. Event beds demonstrate significant truncation of dune deposits, locally reaching to the base of containing clinofoms. Nevertheless, in most places in the proximal slope zone several metres-thick (rarely exceeding 15 metres) stacked sets of compound cross-bedding are preserved. Sets have a variable thickness, are composed of variably dipping tabular to trough cross-beds and compound cross-beds, and contain numerous reactivation surfaces and different degrees of bioturbation (Fig. 3).

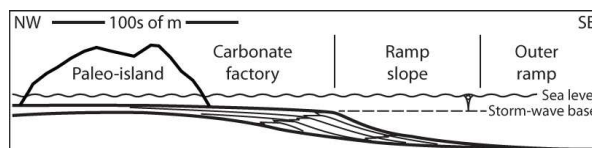


Figure 1. Conceptual cross-section through the Pleistocene distally steepened carbonate ramp of Favignana Island. The carbonate ramp consisted of a near-horizontal carbonate factory, where most of the skeletal material was produced, that connected distally to a ramp slope. The latter is subdivided into a relatively steep (up to 10°) proximal zone and a gently inclined toe-of-slope zone. The outer ramp comprises the area basinwards of the ramp slope. See Fig. 2 for location.

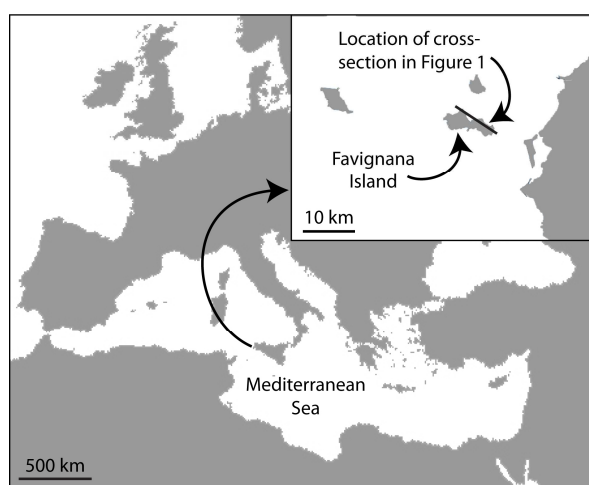


Figure 2. Favignana Island, located on the westward continuation of the Sicilian shelf in the Central Mediterranean Sea.

2.4. Distal toe-of-slope zone

The toe-of-slope zone, located basinwards of the proximal ramp slope and farther away from the carbonate factory, received significantly less sediment than the proximal ramp slope zone. As a result, large-scale composite dunes in the toe-of-slope zone were migrating with stoss-side erosion being equal to lee-side deposition, instead of becoming laterally and vertically stacked due to the climbing of such bedforms. Dip direction of cross-beds in the toe-of-slope zone is more variable, although compound cross-beds generally dip conform the direction of the containing set, which itself follows the dip of the clinofom. The preservation of (fields of) such migrating large-scale composite dunes is rare in the sedimentary record due to a common lack of aggradation. In the Pleistocene carbonate ramp succession of

Favignana Island, however, the frequent occurrence of very large sediment gravity-flow events repeatedly blanketed the entire toe-of-slope zone with no or limited erosion taking place. This resulted in the ‘freezing’ of large-scale composite dunes and the parasitic bedforms on their stoss-side, which have been preserved as large-scale form-sets that are covered with fields of small-scale subordinate form-sets (Fig. 4, 5).

3. DISCUSSION AND CONCLUSIONS

Progradation of the distally steepened carbonate ramp occurred in two ways: (1) lateral stacking of composite dune deposits, and (2) event bed deposition. The near vicinity of the proximal ramp slope to the carbonate factory resulted in higher rates of sediment supply relative to the amount of sediment delivered to the toe-of-slope zone. Consequently, thick packages of compound cross-bedded sets, generated by the lateral stacking of large-scale composite dunes, characterise the proximal ramp slope, which locally display major truncation by event beds. In contrast, the distal toe-of-slope zone was formed under limited aggradation. Under conditions of no net sediment supply, stoss-side erosion equalled lee-side deposition and composite dunes merely migrated. Such dunes were preserved by the rapid burial under a thick gravity-flow deposit, which was accompanied by marginal basal erosion.

The presence of lags of large skeletal remains, indicative of in situ produced carbonate material, suggests that long periods of tranquillity separated times of active dune migration and progradation. This inference is in line with the occurrence of numerous reactivation surfaces and different degrees of bioturbation that characterise (compound) cross-beds. We propose that submarine dunes on the studied carbonate ramp migrated solely during storm-induced bottom currents. Consequently, the sediment gravity flows correspond to events of extreme energy that were capable of delivering vast amounts of material to the ramp slope where excess-density generated short-lived underflows.

4. REFERENCES

- Ashley, G.M. 1990. Classification of large-scale subaqueous bedforms: A new look at an old problem. *Journal of Sedimentary Petrology*, 60(1): 160-172.
- Fornos, J.J. & Ahr, W.M. 2006. Present-day temperate carbonate sedimentation on the Balearic Platform, western Mediterranean: compositional and textural variation along a low-energy isolated ramp. In H.M. Pedley & G. Carannante (eds), *Cool-Water Carbonates: Depositional Systems and Palaeoenvironmental Controls*. Geological Society, London, Special Publications, 255: 71-84.
- Pomar, L., Obrador, A. & Westphal, H. 2002. Sub-wavebase cross-bedded grainstones on a distally steepened carbonate ramp, Upper Miocene, Menorca, Spain. *Sedimentology*, 49: 139-169.

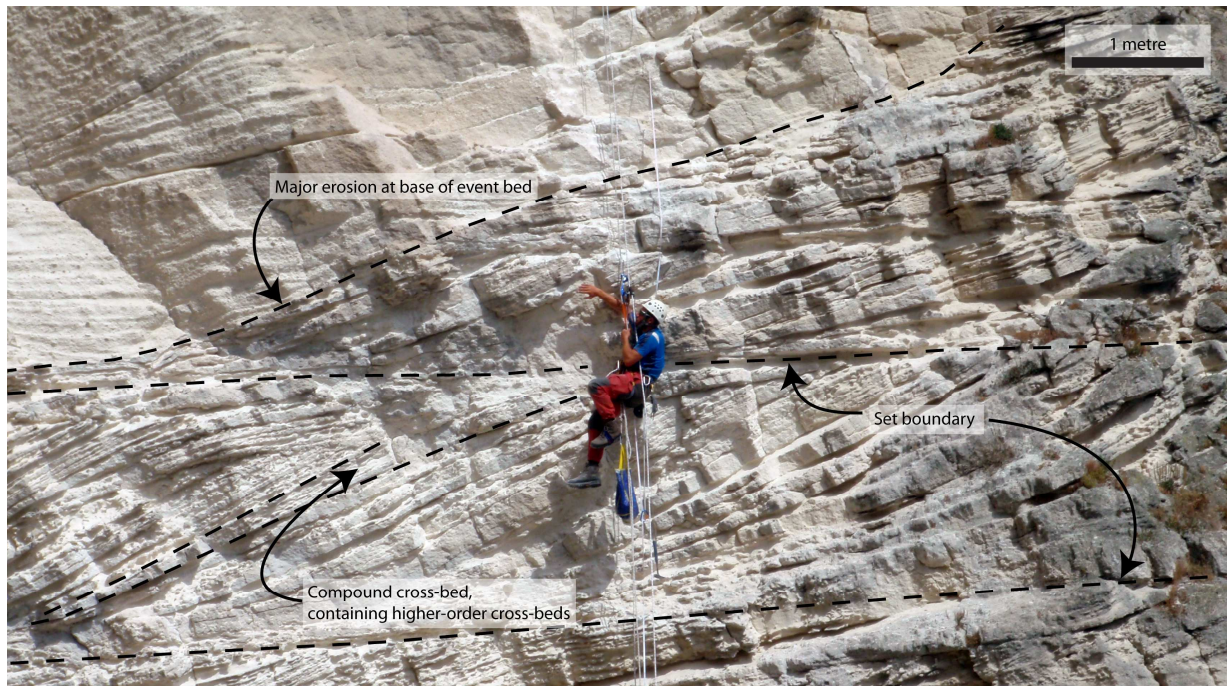


Figure 3. Stacked compound cross-bedded sets, which formed by the down-slope superposition of large-scale composite dunes in the proximal ramp slope zone. Set boundaries truncate the top of compound cross-beds, suggesting that the formative large-scale dunes were slightly higher than the preserved sets. Preservation occurred by the continual burial of large-scale dune sets by younger ones as they migrated down the slope and the carbonate ramp prograded. Note the major erosion at the base of the event bed, truncating deeply into the stacked large-scale dune sets.

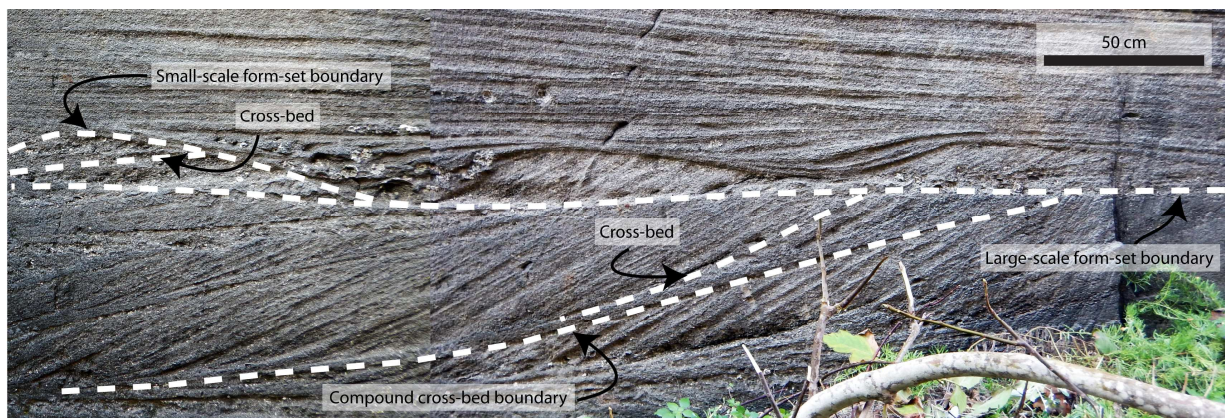


Figure 4. Detail of erosion-based small-scale form-sets on top of a large-scale compound cross-bedded form-set in the toe-of-slope zone, representing a geological snapshot of a train of small-scale parasitic dunes that migrated over the gentle stoss-side of a large-scale composite dune. The large-scale parent dune and small-scale parasitic dunes were preserved by the rapid burial by an event bed (gravity-flow deposit).

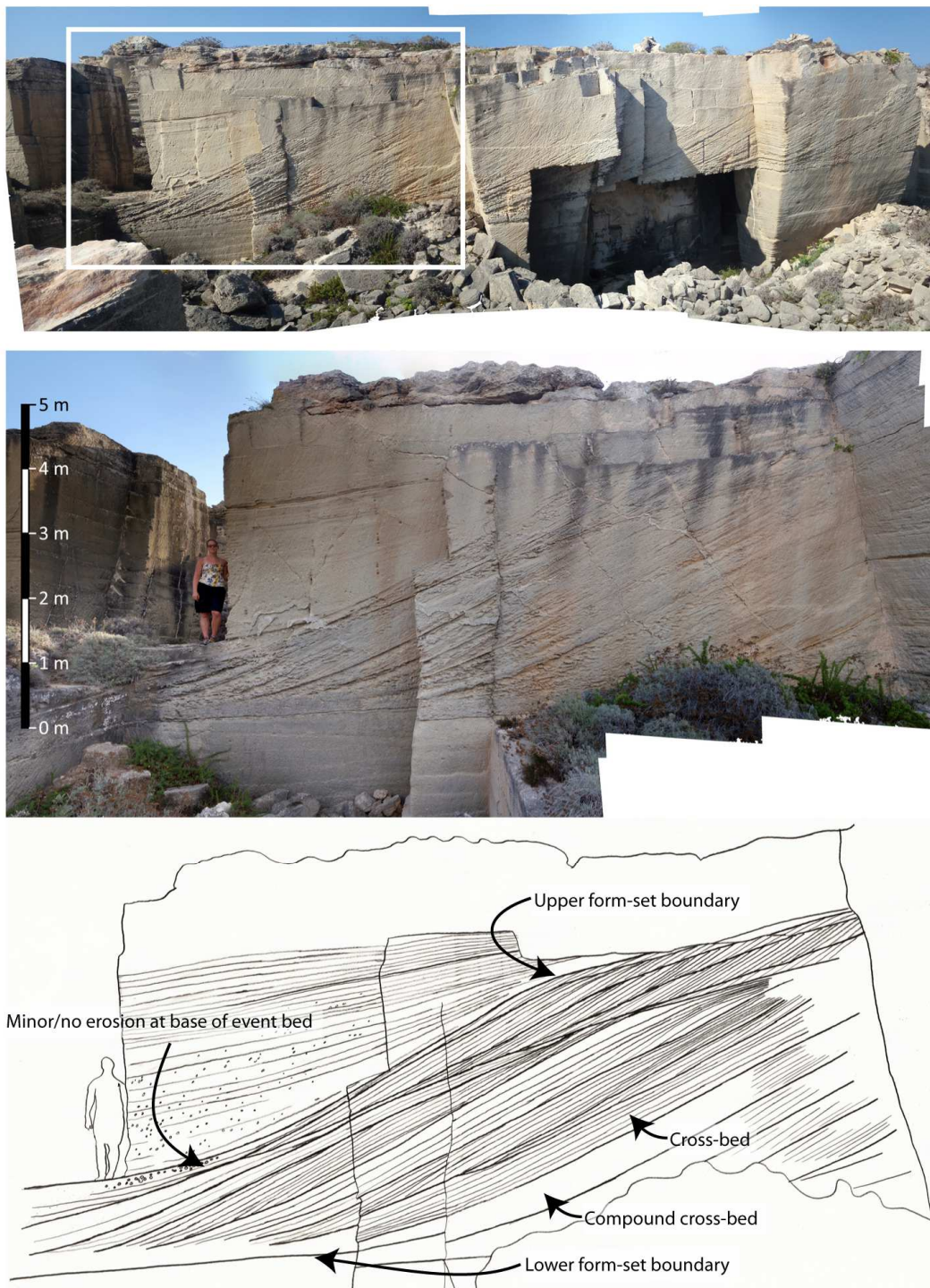


Figure 5. Large-scale compound cross-bedded form-set in the toe-of-slope zone. Cross-beds were formed by small-scale parasitic dunes that migrated over the stoss-side and were ultimately deposited in a compound cross-bed on the lee-side of a large-scale parent dune. The large-scale dune migrated over an event bed (gravity-flow deposit) and became preserved when it was rapidly blanketed during deposition of the subsequent event bed. Note the limited erosion at the top of the large-scale form-set.

Dynamics of very-large dunes in sandbank areas subjected to marine aggregate extraction, Belgian continental shelf

N. Terseleer *Operational Directorate Natural Environment, Royal Belgian Institute of Natural Sciences, Belgium – nathan.terseleerlillo@naturalsciences.be*

K. Degrendele *Continental Shelf Service, Federal Public Service Economy, S.M.E.s, Self-Employed and Energy, Belgium – Koen.Degrendele@economie.fgov.be*

M. Roche *Continental Shelf Service, Federal Public Service Economy, S.M.E.s, Self-Employed and Energy, Belgium – Marc.Roche@economie.fgov.be*

D. Van den Eynde *Operational Directorate Natural Environment, Royal Belgian Institute of Natural Sciences, Belgium – dries.vandeneynde@naturalsciences.be*

V. Van Lancker *Operational Directorate Natural Environment, Royal Belgian Institute of Natural Sciences, Belgium – vera.vanlancker@naturalsciences.be*

ABSTRACT: Dynamics of very-large dunes were investigated over sandbanks subdued to marine aggregate extraction in the Belgian continental shelf. In the Flemish Banks, six areas were regularly monitored with a multibeam echosounder (MBES) providing high resolution bathymetric data. An optimization procedure was set up to estimate the dune migration distance and direction between successive campaigns. These dune migration data were compared to simulated hydrodynamic forces and indicated that dune migration was mostly driven by tidal currents, with the direction and magnitude of migration being dependent on the relative position of the dunes on the sandbanks. Closer investigation in a heavily extracted area suggested a local reorganization of sediments in the area: an accretional trend in the extraction pit is observed at the expense of the surrounding very-large dunes which presented an erosive and flattening pattern.

1. INTRODUCTION

In the Belgian continental shelf, marine aggregate extraction occurs in legally defined areas over sandbanks. These sandbanks are covered with bedforms including very-large dunes (> 3 m height). Beyond human extraction, which can cause seabed depressions up to several meters in depth in intensively exploited sites (Degrendele et al., 2010), the migration of these very-large dunes is the main source of variability in the seabed morphology. In this study, high resolution bathymetric data are exploited in the period 2003-2013 in order to investigate the dynamics of these very-large dunes and to assess whether the extraction activity affected this natural variability. Approximating the dune migration within each area by a homogenous translation of the whole seabed, an optimization process was implemented to extract the migration distance and direction between successive monitoring campaigns over the 2003-2013 period in six exploited areas. The

resulting migration data were compared to simulated hydrodynamic data (currents), and the seabed evolution in a recent extraction hotspot was more closely examined.

2. METHODS

2.1. Study area

In this study, data are exploited from the Flemish Banks area, located 20-30 km offshore the Belgian coast. In this region (Fig. 1), three extraction zones (red polygons) are present along different SW-NE-oriented sandbanks. In these extraction zones, six monitoring areas (black rectangles) are regularly surveyed: Monitoring zone A of the Oostdyck (ODMA); Monitoring zone A, B and C of the Buiten Ratel (BRMA, BRMB and BRMC respectively); and Monitoring zone A and B of the Kwintebank (KBMA and KBMB respectively).

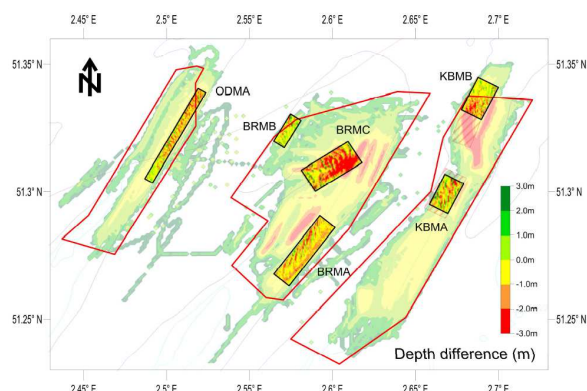


Figure 1. Study area in the Flemish Banks, Belgian continental shelf. Red polygons: marine aggregate extraction zones. Black rectangles: monitoring zones. Background color scale: extraction density. Color scale in monitoring zones: depth difference between recent surveys and a reference bathymetry.

2.2. Bathymetric data

High resolution depth measurements over the monitoring zone were acquired with a MBES (see Roche et al., 2011). Monitoring data started between 2003 (KBMA, KBMB) and 2010 (BRMC). The monitoring intensity ranged from 1 to 4 surveys per year.

2.3. Extraction data

Aggregate extraction activity was recorded through an Electronic Monitoring System (EMS) which was placed onboard of the extraction vessels. The EMS stored the time and location of the ship as well as the extraction activity and was used to build a spatio-temporal dataset of marine aggregate extraction (see Roche et al., 2011).

2.4. Analysis

The MBES data provided a succession of bathymetries for each monitoring zone. Two main sources of variation in the seabed were observed: the human extraction and the migration of the very-large dunes. Despite some peculiarities in the individual movements of the latter, they followed a motion close to a general translation. In order to estimate this dune migration between two campaigns (MBES₁ and MBES₂ for the earlier and later stage, respectively), an optimization procedure has been implemented as follows: (1) the sediments extracted during the period were restored to MBES₂ in order to build a state closer to MBES₁ without extraction; (2) MBES₁ was

shifted laterally with different intensities and directions; (3) the best shift was selected as the one producing the highest log likelihood between the shifted MBES₁ and the reconstructed MBES₂, assuming a normal distribution of the residuals. This workflow was applied to the successive campaigns from all monitoring zones. The obtained migration distance between two campaigns was converted into a migration rate expressed per Spring-Neap cycle (SN) of 15 days. Dune migration data were compared to simulated tidal currents in the monitoring zone produced with the hydrodynamic model COHERENS under tidal and wind forcing (see Van den Eynde et al., 2010).

3. RESULTS AND DISCUSSION

3.1. Migration rates and directions

The migration rates and directions obtained by the optimization procedure are shown for each area in Fig. 2 (y and x axis, respectively).

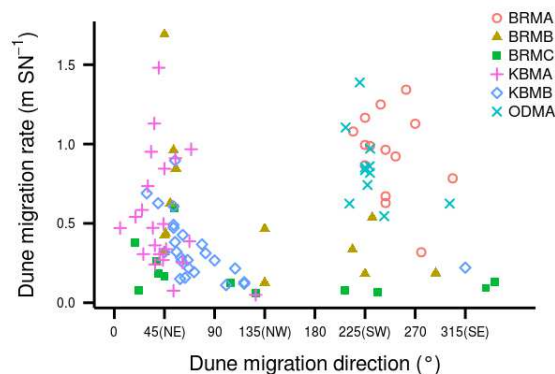


Figure 2. Dune migration rate vs direction.

Out of the six areas, BRMC was characterized by the smallest dune migration rates ($< 0.6 \text{ m SN}^{-1}$). In contrast, BRMA and ODMA showed high migration rates (up to 1.4 m SN^{-1}). These two areas were also the only ones to exhibit a dominant SW-directed dune migration. These areas are indeed located on the SE flank of their sandbanks (Fig. 1), where ebb currents (directed towards the SW) predominate. On the contrary, KBMA and KBMB, which are located on the NW flank of the Kwintebank (Fig. 1), only experienced dune migration towards the NE (flood direction, with the exception of one observation towards the SE for KBMB; Fig. 2). Dune migration along the Buiten Ratel was less obvious. This is due to the

peculiar shape of the head of the sandbank (Fig. 1): dune migration of BRMB, located at the NW edge of this head, displayed the fastest migration towards the NE, but also in the opposite direction (albeit at a lower rate). In the middle kink part of this head (BRMC), dunes migrated both in the flood- and ebb direction with generally lower rates.

3.2. Current-driven dune migration

In shallow marine environments, dune migration, and sediment transport in general, is mostly driven by tidal currents. To test this hypothesis, dune dynamics in the formerly defined areas were compared to the corresponding simulated residual currents. Fig. 3 shows the dune migration direction as a function of the simulated residual current direction. The diagonal dashed line marks the exact agreement between both (i.e. dune migration occurs in the same direction as residual currents). The size of the symbols in Fig. 3 is proportional to the dune migration rate, giving an indication of the migration intensity for each observation.

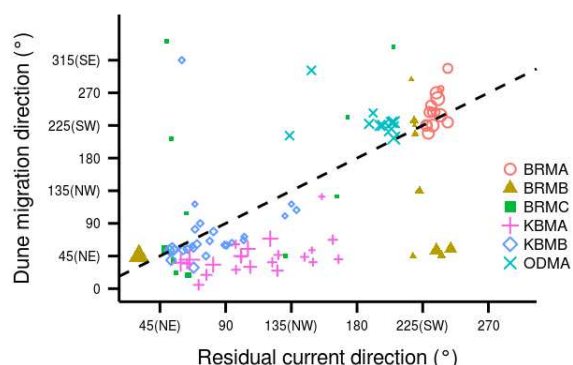


Figure 3. Dune migration direction vs residual currents direction.

BRMA and ODMA occupy a relatively narrow area in the upper right corner (SW-directed) around the diagonal, suggesting that the simulated residual currents explained the migration direction to a large extent. Similarly, but in the opposite direction (NE), the agreement between the direction of dune migration and residual currents was also high for KBMB, while residual currents in KBMA (towards the NE and NW) were more spread than the dune migration (mainly towards the NE). Finally, the agreement between dune migration direction and residual current direction was less good for BRMB and BRMC, indicating

that the model was less able to simulate currents in this peculiar area (head of the Buiten Ratel). Preliminary investigations suggested that the dune migration rate was also positively related to the magnitude of simulated residual currents (not shown), and that winds alone were not able to explain dune migration rate and direction (not shown). Consequently, these results indicate that dune migration over the sandbanks was mainly driven by currents, which essentially have a tidal origin. The agreement between simulated currents and estimated migration parameters also suggests that both approaches produce valid results.

3.3. The effect of aggregate extraction

The optimization procedure set up to determine the dune migration can be used to remove most of the variability in the seabed due to these dune movements in order to examine the remaining pattern. This application was exploited here for the BRMC area, which was a hotspot of aggregate extraction from 2009 to 2014. A comparison was made between the oldest (early 2010) and latest (late 2013) campaigns as follows (Fig. 4): the optimal dune migration was applied as a general translation to the original bathymetry which was then subtracted from the recent bathymetry to produce a difference map showing the evolution of the seabed over this nearly 4-year period; in order to keep the natural accretion and erosion signal, human extraction during this period was removed (Fig. 4). This resulted in a global difference map between late 2013 and early 2010 showing areas where accretion (in blue) or erosion (in red) occurred (Fig. 5).

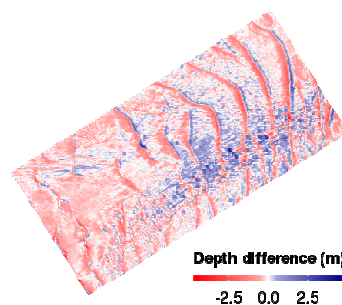


Figure 5. Seabed dynamics in the BRMC area shown as a difference map between late 2013 and early 2010. Note that accretion is observed where extraction took place, whilst the surrounding very-large dunes have flattened.

Overall, in BRMC, the dune migration between 2010 and 2013 occurred in the NE direction. Some remaining patterns indicate that the dune migration effect was not entirely removed: especially at the northern corner of the map, positive accretion fronts (blue bands) showed that the actual position of the new dune crests is further to the East. This effect was sensibly more pronounced and ubiquitous when the dune migration was not accounted for (not shown). Another pattern related to these very-large dunes can be observed: the difference map show wide negative bands over them (red bands in Fig. 5), revealing a global erosional pattern. Indeed, a comparison of the 2010 and 2013 transects across the dunes located in the northern half of the area showed that, in addition to migration towards the NE, they decreased in height over time (not shown). In parallel, the zone where extraction was concentrated in BRMC, located at the East of the map (see Fig. 4), showed a general accretion trend (Fig. 5). The extraction pit (locally deepened with 5 m compared to the reference level) thus experienced a possible refilling while the neighboring dunes exhibited a general flattening.

4. CONCLUSION

The optimization procedure, set up to automatically determine the dune migration, generated valid and valuable data to investigate dune dynamics in different locations over sandbanks. Comparison with simulated currents showed that dune migration over these sandbanks was mostly driven by tidal currents with the position of the dunes over the sandbank determining whether they shifted in an ebb- or flood direction. In a heavily exploited area, there was a general erosive pattern over the very-large dunes surrounding the intensively extracted site,

which on the contrary showed an accretional trend. From this, there seems to be a local reorganization of the sediments in the area at the expense of the very-large dunes which are decreasing in height over time. This calls for further investigation to determine whether this affects the behavior of the sandbank, the hydrodynamics in the surrounding area, and the sustainability of the extraction activity.

5. ACKNOWLEDGMENT

This is a contribution to the Brain-be project TILES (Transnational and Integrated Long-term marine Exploitation Strategies), funded by Belgian Science Policy (Belspo) under contract BR/121/A2/TILES. The research is fully supported by the ZAGRI project, a federal Belgian program for continuous monitoring of sand and gravel extraction, paid from private revenues.

6. REFERENCES

- Degrendele, K., Roche, M., Schotte, P., Van Lancker, V. R., Bellec, V. K., & Bonne, W. M. 2010. Morphological evolution of the Kwinte Bank central depression before and after the cessation of aggregate extraction. *Journal of Coastal Research*, SI 51: 77-86.
- Roche, M., Degrendele, K., De Mol, L., Schotte, P., Vandenreyken, H., Van den Branden, R., De Schepper, G. 2011. Synthesis of the monitoring of the impact from the aggregate extraction on the Belgian Continental Shelf, in: *Study day: Marine aggregate extraction: needs, guidelines and future prospects*. 17 October 2011, Bredene. pp. 3-45
- Van den Eynde, D., Giardino, A., Portilla, J., Fettweis, M., Francken, F., & Monbaliu, J. 2010. Modelling the effects of sand extraction, on sediment transport due to tides, on the Kwinte Bank. *Journal of Coastal Research*, SI 51: 101-116.

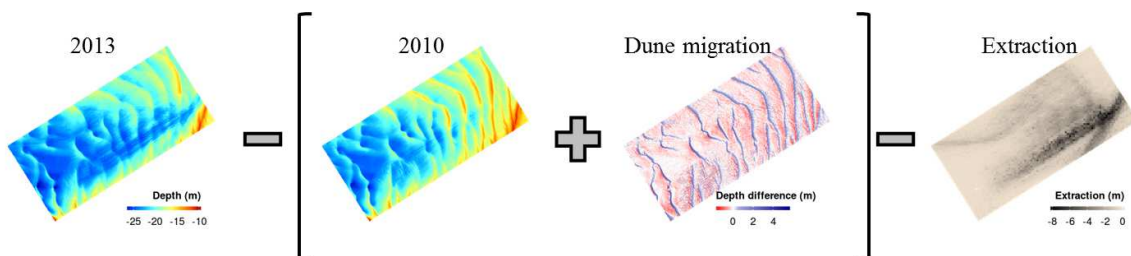


Figure 4. Workflow to produce the difference map in Figure 5. See text for explanations.

Measurements and analysis of suspended sediment particle size sorting above bedforms under waves

P. D. Thorne *NOC, 6 Brownlow Street, Liverpool, L3 5DA U.K. – pdt@noc.ac.uk*

A. G. Davies *CAMS, Bangor University, LL59 5AB, U.K. – a.g.davies@bangor.ac.uk*

ABSTRACT: The relationship between the grain size distribution of the sediment on the bed and that found in suspension, due to wave action above bedforms, is assessed using pumped sample measurements for beds of fine and medium sand. The pumped samples were sieved into multiple grain size fractions and represented by an exponential concentration profile. The analysis of these profiles was carried out in two stages to determine: i) the relationship between the size distribution of the sediment on the bed and that found in the reference concentration, and ii) the behavior of the exponential decay length scale of the concentration profiles. From this analysis inferences are made about the relative roles of diffusion and convection in the upward flux of sediment.

1. INTRODUCTION

To examine the relationship between the bed size distribution and that of the entrained suspended sediments, the present study reports on detailed pumped sample measurements over ripples, under waves. Above ripples under waves the entrainment mixing processes are often referred to as diffusive or convective depending on the steepness of the bedforms (Nielsen 1992, Davies and Thorne 2008, Davies and Thorne 2015). Normally if the ripple slopes, η/λ , (η and λ are the ripple height and wavelength respectively) are less than about 0.12 the dominant process is considered to be diffusive and it is the turbulent fluctuations in the vertical velocity component that give rise to the upward mixing process. Alternatively if the ripples have a slope greater than 0.12, the mixing close to the bed is considered to be dominated by convective coherent vortex processes involving the ejection of a sediment-laden vortex at flow reversal, carrying sediment to several ripple heights above the bed. If the sediment entrainment process is considered to be diffusive then the slope of the logarithmic concentration plotted against linear height above the bed should be inversely proportional to the settling velocity of the grains in suspension. For the case of convective processes it has been

suggested that the slope will remain constant with entrainment essentially independent of settling velocity.

2. MEASUREMENTS

The observations reported here were collected in the Deltaflume of Deltares, Delft Hydraulics, the Netherlands (Thorne et al, 2002). This full scale wave flume facility 230m long, 5m wide and 7m deep allows field scale processes to be studied under controlled conditions. Measurements were carried out above two sand beds, where the median bed diameters were $d_{50}=162 \mu\text{m}$, fine, and $d_{50}=329 \mu\text{m}$, medium. A number of tests were conducted using regular and irregular waves, with periods in the range of 4-6 s and wave heights between 0.4 – 1.3 m. Pumped samples of the suspended sediments were collected at ten heights above the bed nominally between 0.05-1.55 m and particle size analysis carried out on these data sets. The pumped sampling usually lasted for about 15 min, nominally covering 180 wave periods, when 10 litres of suspended fluid was collected at each height above the bed. The samples were dried and sieved into $1/4\phi$ size fractions resulting in profiles of suspended sediment concentration above the bed for up to 15 different size fractions. An

acoustic backscatter system, ABS, adjacent to the pumped samples was used to identify their local precise height above the rippled bed. To interpret the suspended sediment size profiles co-located concurrent measurements of the bedforms and the hydrodynamics were collected. The ripple dimensions were obtained using an acoustic ripple profiler, ARP, which measured a 3 m transect along the bed approximately every 60 s during the tests. Wave flow velocity was obtained using electromagnetic current meters, ECMs, at 0.30, 0.6 and 0.9 m above the bed and sampled at 5 Hz.

3. ANALYSIS

To analyse the $\frac{1}{4}\phi$ size fraction profiles of suspended sediment concentration, C_i , an exponential fit for the i th fraction of the form

$$C_i = C_{ir}e^{-z/L_{si}} \quad (1)$$

was applied to the measurements. This provided reference concentration, C_{ir} , at $z=0$ defined as the crest of the ripples and a decay length scale, L_{si} for the i th grain size fraction. There were 10 tests, 4 on the fine sand and 6 on the medium, resulting in 117 values of both parameters for the whole study.

3.1. Transfer function: T_r

To analyse the values for C_{ir} a transfer function was formed which related the cumulative %-distribution of the reference concentration particle sizes, C_{cr} , to the cumulative %-distribution of bed sediment sizes, C_{cb} . The transfer function was expressed as

$$T_r = \frac{100-C_{cr}}{100-C_{cb}} \quad (2)$$

T_r represents the broad trends in the relationship between the reference suspended sediment and bed size distributions. In figure 1a T_r is plotted against d/d_c , where d is the sediment grain size and d_c the critical grain size in suspension. d_c is the largest grain size expected in suspension based on solely diffusive processes entraining sediment into suspension. A commonly used criterion to determine d_c is that of Fredsøe and Deigaard (1992) who suggested that a particle should be able to remain in suspension provided that its settling velocity, w_s , is sufficiently small compared with the near-bed vertical turbulent velocity

fluctuations, the magnitude of which are of the order of the (skin friction) shear velocity u'_* . Davies and Thorne (2002) used this criterion to define the maximum allowable, or critical, d_c to be that having settling velocity $w_{sc} = 0.8 u'_{*w}$ where u'_{*w} is the peak wave-induced skin-friction shear velocity; this criterion is used here.

All tests show sediment in suspension for $d/d_c > 1$ suggesting that a convective mechanism, as well as turbulent diffusion, is responsible for the upward flux of sediment. The presence in suspension of grains having $d > d_c$ is far more pronounced for the medium sand than the fine sand cases, with the steeper ripples formed in the medium sand, $\eta/\lambda = 0.13 \pm 0.01$, being more capable than the low ripples, $\eta/\lambda = 0.07 \pm 0.02$, in the fine sand of suspending coarser fractions. This reinforces the suggestion of a convective transfer mechanism associated with vortex shedding from the steeper ripple crests supporting the entrainment of the larger size fractions.

To try and bring out the underlying behavior of the measurements presented in figure 1a a number of non-dimensional scaling parameters were investigated. One of the more successful approaches was to include both bed stress and rippled bed effects into the abscissa parameterization. This led to the following expression

$$T_r = 0.5[1.05 - \tanh(b_1(X - b_2))] \quad (3)$$

$$X = \frac{d}{d_c} \frac{\theta'^{0.5}}{\eta/\lambda}$$

θ' is the skin friction Shields parameter. Comparison of this function in figure 1b, the dashed lines, with the measured fine and medium transfer functions averaged over all the regular and irregular wave cases separately, the solid lines, show good agreements. The values of the constants (b_1, b_2) corresponding to the dashed curves in figure 1b are (0.4, 4.5) for the regular waves and (0.35, 7.5) for the irregular waves.

3.2. Decay length scale: L_s

After some assessment of the normalization for the ordinate, the decay length scales L_{si} for each test

were non-dimensionalised by L_{st} , the decay length scale for the aggregated concentration profile corresponding to the sum of all the grain fractions for that test. Again the abscissa uses X given in equation (3). Plots of L_{si}/L_{st} against X are given in figure 2.

Figure 2a shows that with the results plotted logarithmically the curves are reasonably well clustered together with a change of slope in L_{si} / L_{st} at about $X=7$. The results from each L_{si} / L_{st} test have been interpolated linearly with increment 0.1 in X , and have then been averaged together to yield the black bold line shown. The average curve for L_{si}/L_{st} is repeated in Figure 2b together with a simple representative two-part, power law, curve fit:

$$\frac{L_S}{L_{ST}} = c_3 X^{c_4} \quad (4)$$

with the coefficients (c_3, c_4) equal to (3.63, -1.1) for $X < 7$ and (0.82, -0.3) for $X > 7$. The bulk of the grain fractions fall within Hallermeier's (1981) transitional settling range and using this it can be shown (Davies and Thorne, 2015) that the line slope (-1.1) for the smaller grain fractions corresponds to a diffusive behaviour. In contrast, the line slope (-0.3) for the larger fractions suggests an additional, convective, component in the upward sediment flux. Had the line slope become zero for $X > 7$, there would have been a suggestion of 'pure convection' as in the model of Fredsøe and Deigaard (1992) and the similar model of Van Rijn (1989). As it turns out the present Deltaflume data lies between these two extremes, with the slope -0.3 suggesting a combined convective + diffusive sediment flux for $X > 7$.

4. CONCLUSIONS

The relationship between the grain size distribution of the sediment on the bed and that found in suspension has been assessed. The transfer function, T_r , showed a consistent pattern of grains being found in suspension with sizes greater than the critical size d_c . This suggests that the

suspension is caused in part by convective effects that supplement diffusion and this becomes particularly important for the coarser fractions. The variation of L_{si}/L_{st} has been compared with equation (4) from which it has been concluded that, for finer fractions in suspension having $X < 7$, the C_i -profiles are characteristic of a purely diffusive process. In contrast, for fractions having $X > 7$ a combined convective + diffusive upward transfer of grains is suggested. The separate findings for T_r and the L_{si}/L_{st} present supporting evidence of diffusion affecting the finer grain fractions in suspension and combined diffusion + convection affecting the coarser fractions.

5. REFERENCES

- Davies A.G. and P.D. Thorne, 2002. 1DV-model of sand transport by waves and currents in the rippled bed regime. Proceedings of 28th International Conference on Coastal Engineering, Cardiff, World Scientific, 2599-2611.
- Davies A.G. and Thorne P.D., 2008. Advances in the Study of Moving Sediments and Evolving Seabeds. Surveys in Geophysics, 29,1-36. DOI 10.1007/s10712-008-9039-x.
- Davies A.G. and Thorne P.D. 2015. On the suspension of graded sediment by waves above ripples: Inferences of convective and diffusive processes. CSR. <http://dx.doi.org/10.1016/j.csr.2015.10.006>
- Fredsøe J. and R. Deigaard, 1992. Mechanics of Coastal Sediment Transport. Advanced Series on Ocean Engineering, Volume 3. World Scientific, Singapore, 369 pp.
- Hallermeier R.J., 1981. Terminal settling velocity of commonly occurring sand grains. Sedimentology, 28, 6, 859-865.
- Nielsen P, 1992. Coastal Bottom Boundary Layers and Sediment Transport. Advanced series on ocean engineering, volume 4. World Scientific, Singapore, 324 pp.
- Thorne P.D., Williams J.J. and A.G. Davies, 2002. Suspended sediments under waves measured in a large-scale flume facility. Journal of Geophysical Research (Oceans), 107 (C8), 10.1029/2001JC000988, 16pp.
- Van Rijn L.C., 1989. Handbook of sediment transport by currents and waves. Delft Hydraulics, The Netherlands, Report H 461.

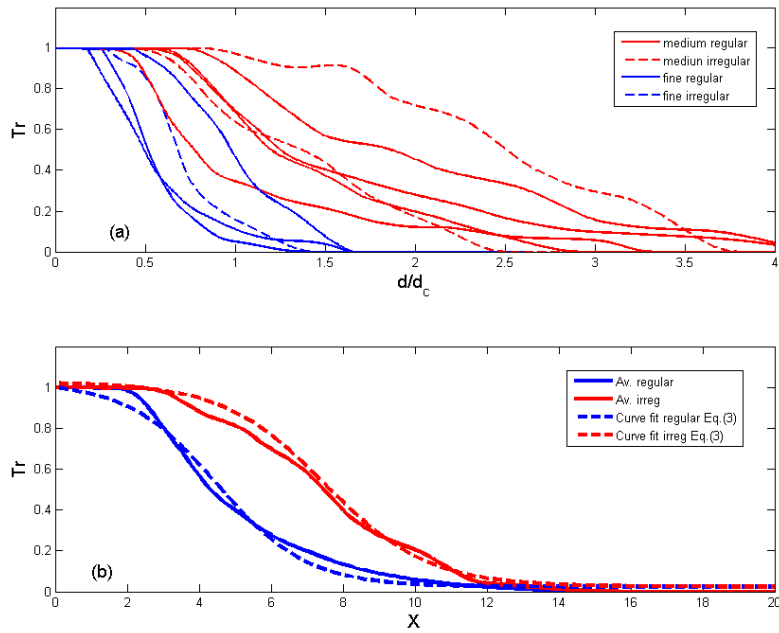


Figure 1. a) Transfer function, T_r , plotted against the normalised grain diameter, d/d_c , for all tests. b) Measured and modelled T_r plotted against X , (see equation (3)) for all tests, with averaged regular wave cases shown in blue and irregular in red.

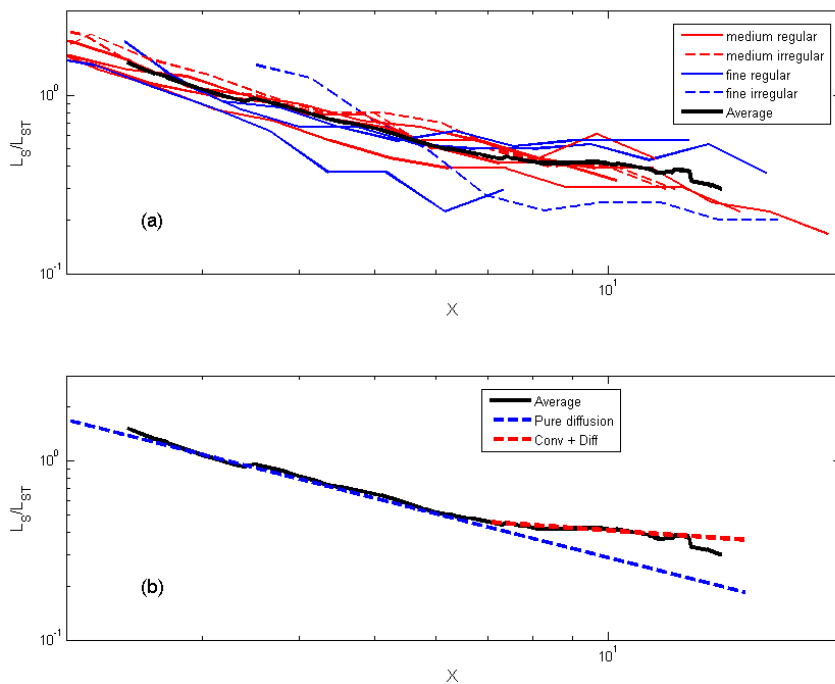


Figure 2. Normalised decay length scale L_s/L_{st} plotted against X . a) Results for all tests with the averaged behaviour indicated by the full black line. b) The averaged curve compared with equation (4) showing a diffusive behaviour for $X < 7$ and diffusive+convective for $X > 7$.

First steps towards developing a risk-based hydrographic surveying policy.

R.Toodesh *Geoscience and Remote Sensing, Delft University of Technology – R.Toodesh@tudelft.nl*

S.Verhagen *Geoscience and Remote Sensing, Delft University of Technology –*

A.A.Verhagen@tudelft.nl

ABSTRACT: Developing a risk-based hydrographic surveying policy requires predicting depths with available bathymetric data. Previous research used the methods of Inverse Distance Weighting (IDW) and kriging using a regular grid for interpolation. The aim of this paper is to investigate the use of quadtree decomposition applied to bathymetric data to define a new grid as the basis for improved interpolation and risk assessment. The quadtree approach allows to adapt the resolution of the grid depending on the variability and data availability such that grid sizes may vary with location. A case study will be tested where the seafloor is relatively flat or sloping versus an area where sandwaves are present. The resulting grid will be the basis for developing a risk-based probability map for which the accuracy of the interpolated depths is important for assigning resurvey frequencies for the Netherland Continental Shelf (NCS).

1. INTRODUCTION

For purposes of safe navigation and in keeping with the Safety of Life at Sea convention (SOLAS) developed by International Maritime Organisation (IMO), there is a need for hydrographic surveys to be managed efficiently and kept up-to-date. The two entities responsible for conducting hydrographic surveys are the Netherlands Hydrographic Office and the Rijkswaterstraat (RWS). They work together and abide by the S44 standards but also developed their own Hydrographic Survey Policy and as such added to the S44 International Standard for the NCS. The current Hydrographic Survey Policy assigns survey frequencies of areas of the NCS which are not based on a comprehensive risk-based assessment.

In addition to the busy shipping lanes, the NCS is characterized as having a shallow seafloor with dynamic seabed formations, especially sandwaves that vary temporally and spatially. This is a concern since the navigable depths have to be maintained and managed efficiently to account for the factors that affect the seafloor depths and hence maritime safety. This research will aim to create an automatic tool which can be used to assign

resurvey frequencies more efficiently using geostatistical analysis. It is essential to be able to make a risk-based assessment focused on expected depths and grounding risks due to sandwave dynamics, objects on the seafloor (such as wrecks and unknown objects), human intervention activities (such as maintenance dredging, sand mining, construction on the seabed, laying of pipelines and cables and land reclamation projects) and extreme storm events.

This paper therefore focuses on the preparation step in the development process to create a dynamic digital elevation model (DEM), which covers the complete NCS (except areas where no hydrographic data is available) with homogeneous accuracy. The single beam echosounding (SBES) and multibeam echosounding (MBES) datasets will be the input for the spatial interpolation analysis procedures. The dynamic DEM should also include for each grid cell, the variability in time, such that predictions of depth changes can be made. For those predictions an elaborate approach based on deformation analysis as described by Dorst (2009) will be explored. Once new hydrographic survey data becomes available for certain areas, the dynamic DEM must be

automatically updated using the new survey data. The dynamic DEM will at first only consider data-based predictions assuming certain hypotheses for the dynamics of the sand waves. In a later stage, additional factors such as human intervention activities, storm events and objects on the seafloor will be considered to assess grounding risks.

2. BACKGROUND

Differences in mapping techniques such as single beam echosounding and multibeam echosounding to map the seafloor of the NCS results in data being heterogeneous in time and space: previously some areas were mapped using only SBES, other areas longer records of both SBES and MBES surveys.

In VanDijk (2011) a 25x25 meter grid was chosen to guarantee sufficient data density in all areas and was considered to be sufficient resolution to reveal the bedforms at the scale of sandwaves. However, the trade-off is that in areas with much higher data density it would be possible to obtain higher resolution results with high accuracy. This would be the areas that are also most interesting in terms of sand wave dynamics. VanDijk (2011) used the deterministic interpolation method inverse distance weighting (IDW) which is simpler and claims more consistency. This method is based on the theory that closer data points have more correlation and similarities than further data points and hence this interpolation method depends on the distance and closeness of the neighbouring data points.

Dorst (2009) used Kriging interpolation technique which considers the distance and direction between all the pairs of observation data points and uses these values to compute the variability in the sandwave field. It is assumed that for sandwave fields, anisotropy in scale can be assumed that maximum variability is orthogonal to minimum variability. Maximum variability is defined as the direction perpendicular to the sandwave crest and minimum variability as the direction which is assumed to be perpendicular to the direction of maximum variability. This method as compared to the IDW, provides better weighting of the data but is more complex and requires blocks of homogenous sandwave characteristics. To provide an accurate, continuous and homogenous

bathymetric map of the entire NCS there is a need for a robust interpolation method that can solve the problems presented above, that is to provide a grid that is small enough to detect the variability in the sandwaves (scale of the sandwaves) without compromising the processing speed of the data for the complete NCS. The aim of this contribution is to solve these issues by considering the potential of the quadtree grid structure as the basis for interpolation of the bathymetry with appropriate data weighting and the foundation for creating the probabilistic map for the NCS.

3. METHOD

3.1 Quadtree Approach

Quadtree decomposition methods have been demonstrated before using bathymetric observations and other related applications such as in Borthwick (2001), Welstead (1999), Mixon (2011) and IDON Technologies (2010). However for this application the quadtree algorithm is designed specifically for the purposes of creating a dynamic DEM as the first step towards creating a probabilistic map which will determine the hydrographic survey frequencies for the NCS. The Quadtree decomposition method will be applied to bathymetric data observations to guarantee homogeneous accuracy and variability. This approach will guarantee higher resolution in areas of large variability and at the same time allowing for data reduction in cases of very high density MBES data in areas of low variability.

The quadtree algorithm is based on initially subdividing an area into four equal quadrants; for each of these quadrants the data density over time and signal variability will be assessed. If both are exceeding a certain predefined threshold, the quadrant will be split into four new sub quadrants recursively, until convergence or until a certain minimum grid size is reached. This will lead to a decomposition of the DEM into blocks, with each having a low standard deviation. Hence each newly subdivided quadrant will have more or less equal variation.

Depending on the application, the algorithm is flexible in terms of the criteria for splitting the quadrants and choice of associated thresholds. For this specific application the variability (depth variations with respect to a fitted plane) will be the

most important criterion. Therefore this algorithm is specifically designed to investigate the best way for which the variability can be computed and represented. In some areas of the NCS, the availability and data density of the depth observations are very low. It is assumed that in these areas depths do not reach a critical value where it affects the safety of navigation and also exhibits the least dynamic behaviour. Therefore in these areas where variability is not critical, a larger grid size is acceptable here for interpolation, especially if the dynamic depth is set equal to the shallowest depth in the corresponding area. Figure 1. shows an example of how the quadtree decomposition may work. Note however, that in reality the decomposition would have continued until an even finer resolution, for example 5 meters.

The added value of the quadtree algorithm will be shown based on a case study for a specific area, with different sea floor characteristics which includes flat or sloping seabed versus areas where sandwaves are present, represented by different data densities. The case study also comprises an analysis of the interpolation results for the depths based on the newly defined grid produced from the quadtree decomposition approach. For the weighting function of kriging, the same variability measure will be used as for the quadtree decomposition. The results are compared to those obtained with the interpolation methods from the previous studies by Dorst (2009) and Van Dijk (2011), to show that the new approach resolves the issue of data availability versus requested accuracy and computation time. Furthermore the results of the quadtree approach can be used as a GIS (Geographic Information System) tool where the newly developed grid can be integrated with the dynamic bathymetric DEM. The time series of bathymetric data sets can be stored in each grid cell for further analysis.

The approach will first use synthetic data for the interpolation. The resulting interpolated values will be compared with the ground truth data which is already known since the simulated dataset is based on the known bathymetry. Subsequently, real data will be used for cross validation which is possible to some extent by comparing the interpolated values at locations where observations are also available. MBES data can also be used where a

subset of data is selected at a track spacing similar to SBES data in order to have same data density as the SBES.

4. CONCLUSION

This quadtree decomposition approach provides optimal use of the available bathymetric data for the NCS. Depending on the seafloor characteristics for example areas with sandwaves, the variability is accounted for by improving the sampling density of the data points which leads to better weighting for interpolation of the depths. Appropriate weighting for accurate interpolation will improve the creation of a dynamic DEM as the basis for developing a probabilistic map which assigns the hydrographic survey frequencies of the NCS.

5. ACKNOWLEDGEMENTS

This project is part of the larger multidisciplinary SMARTSEA project entitled “Safe Navigation by optimizing sea bed monitoring and waterway maintenance using fundamental knowledge for seabed dynamics” which is supported by the Dutch Technology Foundation STW, which is part of the Netherlands Organisation for Scientific Research (NWO). The data used for this research was provided by the Netherlands Hydrographic Office, Rikswaterstraat and Deltares.

6. REFERENCES

- Borthwick, A. G. L., Cruz Leon, S., & Józsa, J. 2001. The shallow flow equations solved on adaptive quadtree grids. *International Journal for Numerical Methods in Fluids*, 37(6): 691-719.
- Dorst, L. L. 2009. *Estimating Sea Floor Dynamics in the Southern North Sea to Improve Bathymetric Survey Planning*, Published Ph.D Thesis University of Twente:218
- IDON Technologies Inc. 2010. *Proposed Specification for Auxiliary Information Layer Integration for use with ENC S.10x : 40*
http://www.iho.int/mtg_docs/com_wg/TSMAD/TSMAD20/TSMAD20_DIPWG2-18B_Proposed_Specification_for_S-10x.pdf
- Koning, M. 2007. *The stochastic characteristics of geometric properties of sand waves in the North Sea*. Masters Thesis, University of Twente:122

Mixon, E., Elmore, P., Petry, F., & Duvieilh, K. 2011. Prototype Variable Resolution Bathymetry Toolbox and Right TIN Implementation.

RIKZ (1997). RWS National Institute for Coastal and Marine Management (RWS RIKZ), Gebruikershandleiding, Digipol V1.0, Hoofdstuk 4 Interpolatie procedure. The Hague, The Netherlands.

Van Dijk, T.; Van der Tak, C.; De Boer, W.; Kleuskens, M.; Doornenbal, P.; Noorlandt, R. & Marges,

V.2011. The scientific validation of the hydrographic survey policy of the Netherlands Hydrographic Office, Royal Netherlands Navy, Deltares Report, Utrecht (NL):165

Welstead, S. T. (1999). Fractal and Wavelet Image Compression Techniques. SPIE Opt. Eng. Press. Bellingham, Wash: 232

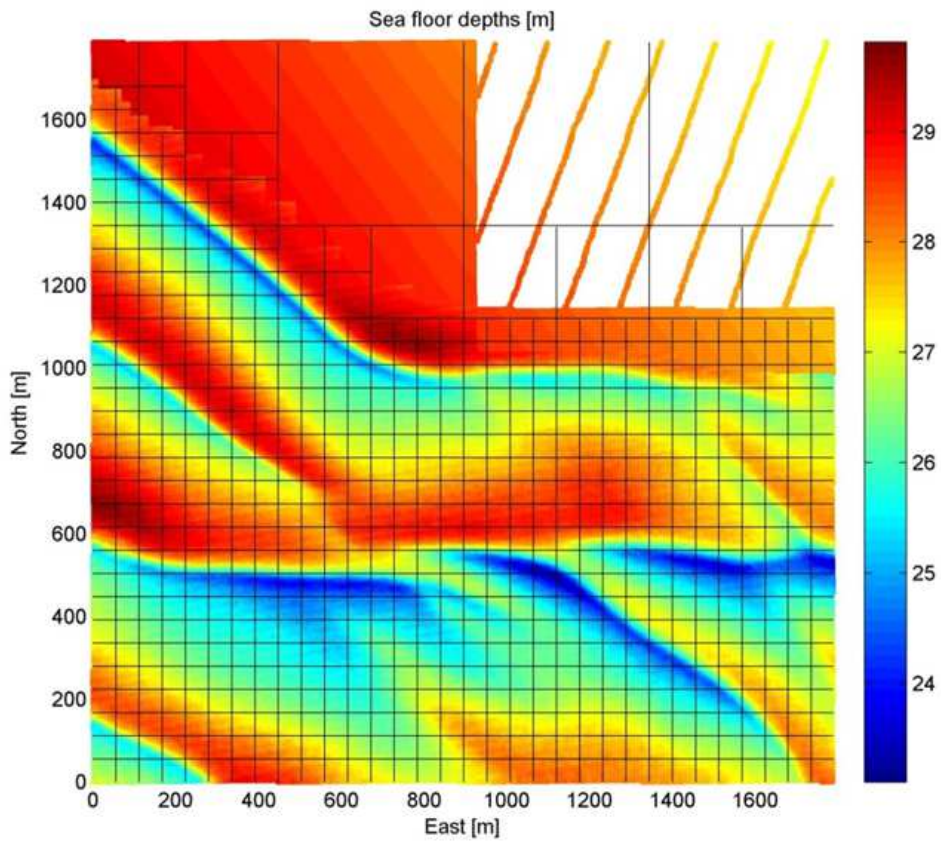


Figure 1. Example of quadtree decomposition for bathymetric data.

Changes in migration of intertidal dunes: from observation to modelling. Case of Somme Bay (NW France).

I. Turki *CNRS, UMR 6143 M2C, F-76821 Mont-Saint-Aignan, France - imen.turki@univ-rouen.fr*

S. Le Bot *CNRS, UMR 6143 M2C, F-76821 Mont-Saint-Aignan, France – sophie.lebot@univ-rouen.fr*

N. Kakeh *Department of Applied Physics, Universitat Politècnica de Catalunya-Barcelona Tech, Barcelona, Spain – nabil.kakeh@gmail.com*

C. Michel *CNRS, UMR 6143 M2C, F-76821 Mont-Saint-Aignan, France – charlotte.michel2@univ-rouen.fr*

R. Lafite *CNRS, UMR 6143 M2C, F-76821 Mont-Saint-Aignan, France – robert.lafite@univ-rouen.fr*

ABSTRACT: Intertidal dune dynamic was investigated in the Somme bay (NW France) using a series of field surveys during a neap-spring tidal cycle: bed level measurements provided by Lidar techniques and energy conditions records of waves, tides and currents. Such observations have been used to quantify the dune migration and the sediment transport rates. The total dune migration can be decomposed into a simple translation component representing approximately 80% of the total movement and a rotation component which increases with the wave obliquity in respect to the coastline. Then, the net sediment transport was quantified from the observed migration rate and compared to the predicted bedload transport. The discrepancies between results suggest the sensitivity of dunes to the convolution between their morphological characteristics of height, length and asymmetry and the energy conditions. This convolution is addressed in a simple model that quantifies the dune response to hydrodynamic variables.

1. INTRODUCTION

Intertidal dunes largely cover sandy estuaries and coastal zones, and play an important role in their morphodynamic. Dune dynamic is very complex since they are sensitive to many sediment parameters and energy conditions. Previous studies have explored the dependence between the sediment transport and the dune migration rates (e.g. Masselink et al., 2009). This research uses field surveys conducted on intertidal dune fields to gain insight in their migration dynamic and the associated sediment transport fluxes under various energy conditions. Understanding this mobility was also explored to develop a simple model for dune response.

2. STUDY AREA

The Bay of Somme is a macrotidal estuary of the eastern English Channel (NW France) with an intertidal sandy area (excluding salt marshes and channels) of 42.5 km² (Figure 1). The bay is classified as a mixed wave-tide dominated estuary since it displays both wave-dominated (beach, dunes, tidal delta) and tide-dominated features (meandering tidal channels, salt marshes). Offshore waves are coming from SW quadrant (mainly swell) and NE quadrant (mainly sea). The area is characterized by semi-diurnal tides with mean neap and spring tidal ranges of 4.9 m and 8.5 m respectively; they can exceed 10 m during exceptional spring tides. The study dune field consists of a core of sinuous mean to large dunes with height and spacing varying between 0.2 and 0.6 m and 6 and 22 m respectively (Figure 1).

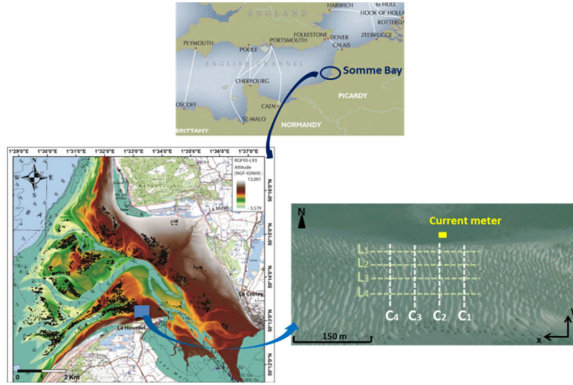


Figure 1. Location map of Somme bay and study dune field. Left: aerial LIDAR, April 2013. Right : Aerial photograph showing the survey lines in x direction (L1, L2, L3 and L4) and y direction (C1, C2, C3 and C4).

2.1 Field Survey

A survey was carried out during a neap-spring tidal cycle in January-February 2014. The maximum and the minimum tidal ranges were 11,1 and 8,3 m respectively.

Topographic measurements were conducted approximately every 3 days from 28/01 to 09/02 along a superficie of 2500 m², using a terrestrial laser scanner (TLS) with a high degree of accuracy. A digital elevation model (DEM) was produced with a 10-cm resolution (Figure 2). Lines were extracted from the DEM in the orthogonal (C1-C4; Figure 1) and parallel (L1-L4) directions with respect to the coastline. Dune morphological parameters were computed over the total data window. Dune migration rates have also been calculated.

Hydrodynamic conditions were measured during the whole neap-spring tidal cycle using punctual current meter and an ADCP instrument, to record the water sea level, flow velocities and wave conditions (height, direction and period) with a time resolution of 1 minute.

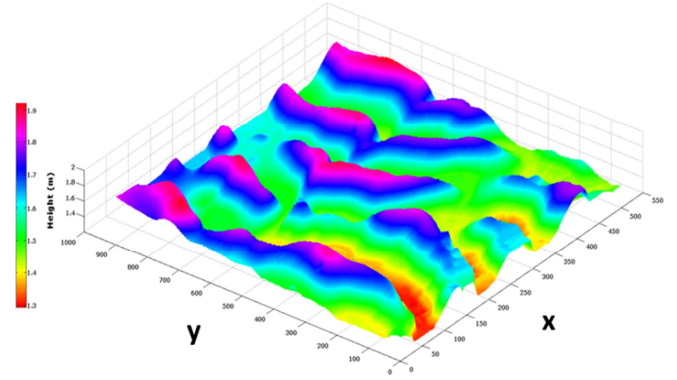


Figure 2. 3-D digital elevation model (DEM) of the intertidal dune field provided by Lidar (09/02/2014); x and y axis are orthogonal and parallel to the coast, respectively. Dune height varies between 1.3 m and 1.9 m (x and y axis are in pixels; 1 pixel =0.1 m)

2.2 Dune migration and sediment transport rates

The survey lines in X (L₁-L₄) and Y directions (C₁-C₄) were analyzed in order to investigate the spatial and temporal variability of dune morphological characteristics: orientation, height η , length λ and dune asymmetry. Then, the migration distance between the different surveys was calculated using a mathematical approach in order to determine the dune migration rates and its local gradient. In this method, the degree of change for every point of the topographic surface, based on local gradients in time and 2D space, is approximated. The objective is to calculate the migration vector M_r in two dimensions (x and y).

For any point of the topographic surface. Then, the migration rate V_{mr} can be approximated as:

$$V_{mr} = \frac{M_r}{\Delta t} = \left(\frac{\Delta Z}{M_r} \right)^{-1} \cdot \frac{\Delta Z}{\Delta t} \quad 1$$

where M_r is the migration vector; V_{mr} is the migration rate and $M_r / \Delta Z$ is the local gradient. In this study, the gradient in space $\Delta Z / M_r$ is expressed in both dimensions X and Y as shown below:

$$\left(\frac{\Delta Z}{M_r}\right)_{n,i,i+1} = \left(\left\{ \frac{Z_{n+1} - Z_{n-1}}{X_{n+1} - X_{n-1}} \right\} + \left\{ \frac{Z_{n+1} - Z_{n-1}}{Y_{n+1} - Y_{n-1}} \right\} \right)_i$$

for any point X_n in two successive surveys at times t_i and t_{i+1} which is illustrated in Figure 3.a (1D case). Then, the local time gradient $\Delta Z/\Delta t$ is:

$$\frac{\Delta Z_{n,i,i+1}}{\Delta t_{i,i+1}} = \frac{Z_{n,i} - Z_{n,i+1}}{t_{i+1} - t_i} \quad 3$$

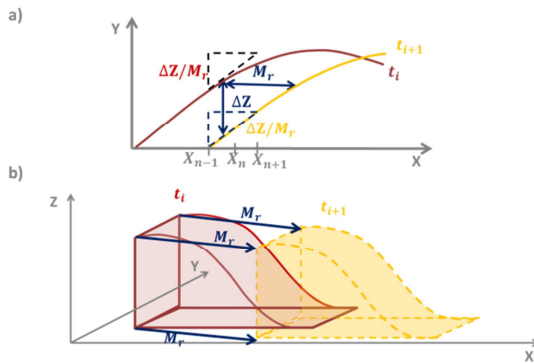


Figure 3. Approximation of the local gradient approach (a) to calculate the migration distance M_r , between t_i and t_{i+1} , which is decomposed in the two directions X and Y (b).

The migration distance was converted to migration rate per tide by considering the number of tides between successive surveys. In reality, this distance can be expressed in two directions and decomposed into 2 movements (Figure 3.b): a simple translation in the x direction of dune migration (parallel to the coastline) and a shift on the y direction orthogonal to the coastline. Both movements were investigated over the different field surveys together with the hydrodynamic conditions.

Finally, the rate of the sediment transport was calculated: (1) from the dune migration previously obtained (volumetric analysis), and (2) from measurements of the current velocities and sediment grain-size, using Soulsby's (1997) procedures. Here, only the component of the bedload transport is considered.

3. RESULTS

The dune migration has been computed in x-direction between the different surveys function of

the local gradients $\left(\frac{\Delta Z}{\Delta t}\right)$ and $\left(\frac{M_r}{\Delta Z}\right)$. Results have shown that the total migration vector M_r is expressed by a component of translation, ΔR , and a shift component, ΔY . A statistical analysis of both components indicates that Δr ranges between 75-90% of the total migration vector and an amount between 10 and 22% describing the dune shift Δy which seems to be more important during the surveys with high wave direction obliquity. An example of dune movement can be displayed in Figure 4. Using the migration and dune parameters (length and height), the rate of the 1-D net sediment transport was calculated between successive surveys. Computed values vary from 0.2m^2 to 0.6m^2 (per unit meter width) during 3 days between the surveys of 03/02 and 06/02 associated to eight spring tide cycles. Maximum values are recorded in the offshore direction where dunes are more dynamic and the energy is higher. Such values range between 0.03m^2 and 0.09m^2 (per unit meter width) between the 28/01 and 03/02 during eight neap tide cycles. The decrease of dune migration in x-direction from offshore (down-bay) to onshore (up-bay) was evaluated approximately to 0.03m/tide during spring tide cycles. Similarly, the sediment transport rate decreases in the onshore direction.

Results suggest that the sediment transport responsible for the dune migration depends on the temporal variability of dune parameters for steady wave and tide conditions. When these conditions are changing, the two main factors, controlling the dune response between successive surveys, are the currents velocities and also the number of tides and the water level.

Measured transport rates have been compared to predicted values estimated from the application of Soulsby's (1997) procedures, function of current velocities, water level and tide range of tidal cycles.

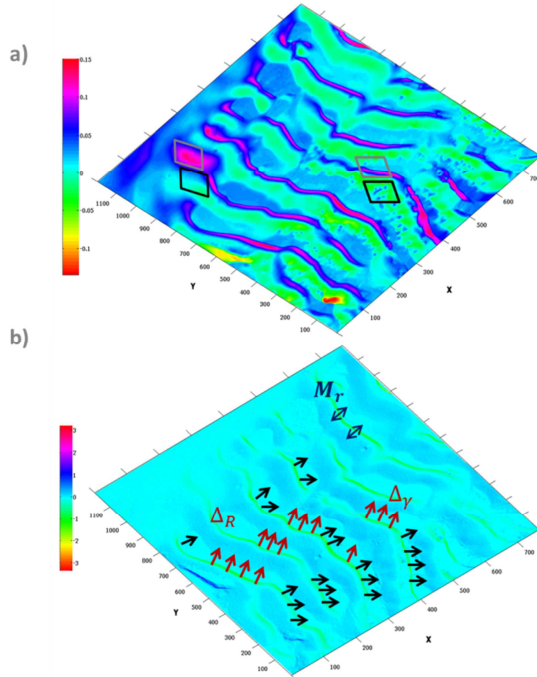


Figure 4. The local gradient shows the fluxes of erosion (black rectangle) and deposition (grey rectangle) between 03/02 and 06/02 (a). The migration vector M_r is composed of a translation ΔR and the shift component $\Delta \gamma$ in the clockwise (black quivers) and counter-clockwise (red quivers) directions (b).

Such comparison has shown discrepancies between both approaches which increases for spring tide cycles. Predicted transport rates, relying only on tides, underestimates the observed transport, obtained by dune migration records, by a mean percentage of 20-30%. This underestimation is less significant if the measured transport rate would be calculated from a dune migration based only on the translation movement without the consideration of the dune shift which is strongly related the incident wave angle. Such results suggested the response of intertidal dunes dune (migration, sediment transport), in macrotidal coasts, is sensitive to: (1) morphological characteristics of dunes (height length, slope, sediment grain size) and (2) wave conditions, in particular the incident wave angle in the surf zone. In this context, a new model is being developed basis on different physical approaches with the aim to calculate the dune migration $V_{mr}(t)$ as a function of the hydrodynamic conditions and the morphological characteristics of the dune. The model uses the convection equation

$$\frac{\partial \eta}{\partial t} = V_{mr} \frac{\partial \eta}{\partial x}. \quad 4$$

The temporal change of the surface is calculated as the result of the local change of the sand flux which can be expressed as a function of energy conditions and the sediment grain size D_{50} . The variability η of is described by both components of rotation and translation. The dune height is related to the length λ and the slopes of dune faces α and β . Therefore mass conservation leads to:

$$\frac{\partial \eta}{\partial t} = \frac{1}{\rho_{sand}} \frac{\partial q}{\partial x} \quad 5$$

Such approaches will be used also to characterize the equilibrium state of the dune.

4. CONCLUSIONS

The findings of this research have shown that the dynamic of intertidal dunes of the Somme bay is strongly related to energy conditions of tide cycles and coastal waves. They are also sensitive to their morphological parameters. Modelling dune migration, in particular its shift component is useful to understand the temporal dune evolution and its relation with the neighbor dunes (e.g. branching).

5. ACKNOWLEDGMENT

The authors are grateful to CNRS-INSU (EC2CO FORSOM), the DGA, the Regional Council of Haute-Normandie and “SFR SCALE” for their supporting to the research, and the members of the laboratory M2C involved in field measurements, in particular Julien Deloffre and Michel Simon.

6. REFERENCES

- Masselink, G., Cointre, L., Williams, J., Gehrels, R., Blake, W. (2009). Tide-driven dune migration and sediment transport on an intertidal shoal in a shallow estuary in Devon, UK. *Marine Geology*, 262, 82–95.
- Soulsby, R.L., 1997. *Dynamics of Marine Sands*. Thomas Telford, London.

Large dunes hosting hotspots of biodiversity: Testing proxies of occurrence and habitat change

V. Van Lancker *Operational Directorate Natural Environment, Royal Belgian Institute of Natural Sciences, Belgium – vera.vanlancker@naturalsciences.be*

F. Francken *Operational Directorate Natural Environment, Royal Belgian Institute of Natural Sciences, Belgium – ffrancken@naturalsciences.be*

L. Kint *Operational Directorate Natural Environment, Royal Belgian Institute of Natural Sciences, Belgium – lkint@naturalsciences.be*

G. Montereale-Gavazzi *Operational Directorate Natural Environment, Royal Belgian Institute of Natural Sciences and Renard Centre of Marine Geology, Ghent University, Belgium – gmonterealegavazzi@naturalsciences.be*

N. Terseleer *Operational Directorate Natural Environment, Royal Belgian Institute of Natural Sciences, Belgium – nterseleerlillo@naturalsciences.be*

D. Van den Eynde *Operational Directorate Natural Environment, Royal Belgian Institute of Natural Sciences, Belgium – dvandeneynde@naturalsciences.be*

ABSTRACT: The interaction of geomorphological and ecological landscape elements is complex. In the case of dunes, not only their shape and dimensions design the habitat, but also the way in which the morphology interacts with the currents. The resulting sedimentary processes will further depend on the in situ sediments, but also on the geological substratum in terms of longevity of biological communities. However in soft substrata, hotspots of biodiversity are mostly observed where coarse substrates combine with deposition of fine-grained sediments. The influx of such fines can originate both from natural and human-induced sources.

In this study, hotspots of biodiversity in dune fields are revisited to define new proxies for the prediction of occurrence, and potential habitat changes. Therefore, several databases are combined: primarily related to geology and sediments, but also to sediment dynamics, including results from cumulative sediment plume dispersal models. The ultimate goal is to facilitate stratification and prioritization of areas that require monitoring of good environmental status (Europe's Marine Strategy Framework Directive).

1. INTRODUCTION

Bedforms as benthic habitats are studied increasingly as acquisition and analyses of acoustic data improve in capturing, visualizing and quantifying benthic and terrain variables on various scales. However, feedback mechanisms between geomorphology and benthos are not always clear (Van Lancker et al., 2012) and complexity increases where the benthos-landscape relationship is also affected by humans.

Based on results from research-oriented seabed mapping and measurements along the Belgian part of the North Sea (BPNS), in combination with large geological and sediment transport databases,

new proxies are tested for the prediction of high-biodiversity bedform areas. Additionally, it is aimed at identifying areas with a high potential of habitat change. Such studies are critical within Europe's Marine Strategy Framework Directive, targeting good environmental status of marine waters by 2020. Cost-efficient monitoring programmes are needed covering impacts of all anthropogenic stressors. The BPNS is a good laboratory for such studies since it is one of world's busiest continental shelf areas, including 30-yr of active disposal of dredged material and extraction of aggregates, as well as more than 150-yr of bottom disturbing fisheries.

2. METHODS

1.1 Study area

The BPNS is a siliciclastic macro-tidal environment (range of 4.5 m), comprising several groups of sandbanks. Depths range from 0 to - 50 m Mean Lowest Low Water at Spring (MLLWS). Mean grain-sizes range from fine to medium sands varying along a subtle gradient. Sediment transport is mainly driven by tidal currents (max. 1.5 m s^{-1}), though wind-induced currents may have a direct effect on sediment resuspension and bedform morphology. Bedform patterns are simple to complex, with varying rates and directions of migrating sand dunes (on average 20 m yr^{-1} and oscillating) with heights being on average 4-6 m in the offshore zone (Lanckneus et al., 2001). Human activities on the BPNS influence natural sediment fluxes, for example through dispersion and deposition of plumes originating from the disposal of dredged material, marine aggregate extraction, wind mill farms, or fishing activities.

1.2 Methodology

Results from very-high resolution acoustic seabed mapping are revisited to spot dense occurrences of species aggregations (following Van Lancker et al., 2012). This imagery was mostly derived from multibeam echosounders (RV Belgica Kongsberg EM1002/95 kHz; EM3002D/300 kHz; RV Simon Stevin Kongsberg EM2040/300 kHz), and contains both depth and backscatter data. At some biodiversity hotspots areas data were also available from current and backscatter profiling (Acoustic Doppler Current Profiling, ADCP) in the water column, in combination with vertical profiling of oceanographic parameters and water sampling.

Information on geology, sediments and their dynamics is now revisited systematically in a research network building a 4D voxel-based resource model of the Belgian and southern Netherlands part of the North Sea up to -30m below the seabed (Van Lancker et al., *subm.*). Focus was on the compilation of long-term datasets and model hindcasts to reflect spatial and temporal variation. For biological validation, several case study areas existed with sufficient ground-truthing and where the link with the physical habitat was studied (e.g. Degraer et al., 2008; Rabaut et al., 2009; Houziaux et al., 2012).

Complementary information is available through international data portals (e.g. EMODnet-Biology; <http://www.emodnet-biology.eu/>).

3. RESULTS

The first part of the study focused on synthesizing the knowledge on where biodiversity increases were depicted in association with bedforms. Simplified, such zones were found: (1) in the lee side of topzones of sandbanks, in combination with large to very-large dunes, and (2) along dune areas where complex sediment transport pathways prevail (e.g. shear zones). In both cases the trapping of an additional naturally or anthropogenically-induced influx of fine-grained sediment was critical. Along those areas sediment distribution is often highly patchy and varying in composition, with a coarser geological substratum.

For this study, key databases that are further exploited relate to: (1) grain-size distribution curves, to maximize parameterization of sediment heterogeneity, and allowing for detailed change detection; and (2) hydrodynamics and sediment transport for which a 16-year hindcast modelling was performed (Francken et al., 2014), from which parametrization of bedload convergence zones is targeted. Additionally, results from cumulative plume dispersion models will be used and confronted to the other datasets.

In the mapping exercises, focus is on the construction of probability models of the underlying parameters. So far, data grids are mostly produced statically, where only one parameter (e.g. mean, percentiles) is mapped. On the contrary, probability mapping includes a measure of interpolation-related uncertainty by making 100 interpolations on each dataset, hence reflecting heterogeneity in the underlying data. Finally, results are confronted with bathymetric datasets to find relationships with occurrences of dune fields. Ultimately, the goal is to find a predictor that can be applied on existing digital terrain models, and that, in combination with intensity maps of human activities, can be used to stratify and prioritize areas for further monitoring of good environmental status of marine waters (Europe's Marine Strategy Framework Directive).

4. ACKNOWLEDGMENT

Paper contributes to the Belspo (www.belspo.be) projects TILES (BR/121/A2/TILES) and INDI67 (BR/143/A2/INDI67), as well as to MOZ4, and ZAGRI, respectively from the Agency of Maritime and Coastal Services (211.177), and from private revenues. Officers and crew of RV Belgica and RV Simon Stevin are particularly acknowledged. Shiptime was provided by Belspo and the Royal Belgian Institute of Natural Sciences, and Flanders Marine Institute.

5. REFERENCES

- Degraer, S., Moerkerke, G., Rabaut, M., Van Hoey, G., Du Four, I., Vincx, M., Henriët, J.P. & Van Lancker, V. 2008. Very high resolution side-scan sonar mapping of biogenic reefs of the tube-worm *Lanice conchilega*. *Remote Sensing of Environment* 112, 3323-3328.
- Francken F., Van den Eynde, D., & Van Lancker, V. (2014). On-demand assessment of spatial and temporal variability of sediment transport parameters, Belgian and southern Dutch part of the North Sea. In: L. De Mol & H. Vandenreyken (Eds.), *Which future for the sand extraction in the Belgian part of the North Sea?* Proceedings of the Study Day Sand Extraction (pp. 73-80). Blankenberge, Belgium: FOD Economie
- Houziaux, J.-S., Craeymeersch, J., Merckx, B., Kerckhof, F., Van Lancker, V., Courtens, W., Stienen, E., Perdon, K.J., Goudswaard, P.C., Van Hoey, G., Virgin, L., Hostens, K., Vincx, M., Degraer, S. 2012. 'EnSIS' - Ecosystem Sensitivity to Invasive Species. Final Report. Belgian Science Policy Office: Brussels. 105 pp.
- Lanckneus, J., Van Lancker, V.R.M., Moerkerke, G., Van den Eynde, D., Fettweis, M., De Batist, M., Jacobs, P. 2001. Investigation of the natural sand transport on the Belgian Continental shelf: BUDGET (Beneficial usage of data and geo-environmental techniques). Scientific Support Plan for a Sustainable Development Policy (SPSD I). Federal Office for Scientific, Technical and Cultural Affairs (OSTC): Brussel. 104 + 87 p. annexes pp.
- Rabaut, M., Du Four, I., Nakas, G., Van Lancker, V.R.M., Degraer, S., Vincx, M. 2009. Ecosystem engineers stabilize sand bank systems: *Owenia fusiformis* aggregations as ecologically important microhabitat, pp. 273-297. In: Rabaut, M. (2009). *Lanice conchilega, fisheries and marine conservation: Towards an ecosystem approach to marine management*. Ghent University, PhD Thesis.
- Van Lancker, V., Moerkerke, G., Du Four, I., Verfaillie, E., Rabaut, M. & Degraer, S. 2012. Fine-scale geomorphological mapping for the prediction of macrobenthic occurrences in shallow marine environments, Belgian part of the North Sea, in: Harris, P. and E. Baker (Eds.) 2012. *Seafloor Geomorphology as Benthic Habitat: GeoHab Atlas of seafloor geomorphic features and benthic habitats*: 251-260. Elsevier Insights.
- Van Lancker, V., Francken, F., Kint, L., Tersleer, N., Van den Eynde, D., De Mol, L., De Tré, G., De Mol, R., Missiaen, T., Chademenos, V., Bakker, M., Maljers, D., Stafleu, J., van Heteren, S. (subm.). Building a 4D Voxel-Based Decision Support System for a Sustainable Management of Marine Geological Resources. In: Diviacco, P., Leadbetter, A. & Glaves, H. (eds.). *Oceanographic and Marine Cross-Domain Data Management for Sustainable Development*. IGI Global.

Methane-rich glacial clays on top of a large sediment wave?

K. J.J. Van Landeghem *School of Ocean Sciences, Bangor University, North Wales, UK*
k.v.landeghem@bangor.ac.uk

H. Niemann *Institute for Environmental Geosciences, Universität Basel, Switzerland*
helge.niemann@unibas.ch

P. F. Croker *The M Horizon (UK) Limited, UK – peter.f.croker@gmail.com*

D. G. Huws *School of Ocean Sciences, Bangor University, North Wales, UK, d.g.huws@bangor.ac.uk*

L. Steinle *Institute for Environmental Geosciences, Universität Basel, Switzerland*
lea.steinle@unibas.ch

S. S. O'Reilly *Department of Earth, Atmospheric and Planetary Sciences, Massachusetts Institute of Technology, Cambridge MA 02139, USA – oreillys@mit.edu*

ABSTRACT: The Quaternary glacial history of our shelf seas influences the distribution and mobility of the marine sediments today, and thus the formation of sediment waves. Here we explore other ways the glacial legacy can influence sediment wave dynamics in the presence of methane seeps. A link between methane seeps and the formation of unusually large, trochoidally shaped sediment waves observed on continental shelves world-wide is deemed unlikely. However, clay-rich muds with high concentrations of methane were observed on top of very large sediment waves in a seafloor trench in the Irish Sea. It suggests that methane gas percolating upwards through sediment waves may be capped by these clay-rich glacial sediments. From sub-bottom evidence, seepage of shallow gas is seemingly guided by the underlying glacial geology and sedimentology. These processes may thus influence sediment wave dynamics and warrant further investigation.

1. INTRODUCTION

The sediments overlying bedrock in the Irish Sea are largely of reworked glacial origin, as the last British and Irish Ice sheet covered the entire Irish Sea during the Last Glacial Maximum at least as far south as the Isles of Scilly (Scourse and Furze 2001).

The Irish Sea also has many potential sources of both microbial and thermogenic methane (Croker 1994; Croker et al. 2005; Judd et al. 2007). Some of these sources are found in deep seafloor trenches. One of these seafloor trenches is called “Jürgen's Nightmare”, and has a particularly steep western wall, exposing glacially derived sediments and with well-documented high concentrations of methane (Judd, 2005). This trench also hosts exceptionally high sediment waves relative to the global maximum height trend suggested by Flemming (1988) and are thus referred to as

“anomalously high”. They are trochoidally shaped and on top clay-rich muds with high concentrations of methane. It is this observation that leads to further explore the link between the seafloor's glacial legacy, sediment wave formation/dynamics and the seepage of methane.

2. OBSERVATIONS

2.1. Clays on top of sediment waves.

The sediment in the Jürgen's Nightmare trench contains up to 94% mud (Figure 1) and contained enhanced methane concentrations up to 7,354 nM, the highest measured in sediments recovered during the AmSedIS survey. The mud was further analysed and with a median grain size d₅₀ of 3 µm was found rich in clay. The trench at the bottom of the cliff hosts a suite of very large trochoidally shaped sediment waves, the flank of one of which had mud contents between 30% and 85% and with

methane concentrations reaching 4,193 nM. By contrast, sediments retrieved from other sediment wave flanks elsewhere in the Irish Sea all had negligible mud contents, including the samples from a large sediment wave in the Harvey's Trench located east of Jürgen's Nightmare (Figure 1b) which is not associated with a steep trench wall. Bottom water methane concentrations in Jürgen's Nightmare varied from 1.44–4.64 nM (Figure 1c), whereas no methane was recorded in the sediments from Harvey's Trench.

2.2. Gas seepage influenced by Quaternary sedimentary history

Whereas in Liverpool Bay the glacial character of the seafloor sediments is evident from the preserved palaeo-glacial landscape (Van Landeghem et al. 2009), the legacy of ice advance and retreat in the Central Irish Sea seems to be largely masked. In 2012, a seismic profile from the "Croker Carbonate Slabs" Special Area of Conservation in the Central Irish Sea seems to compare well with the seismic structure interpreted by Judd et al. (2007) as a prograding late Pleistocene facies of the Western Irish Sea Formation (the latter also described by Jackson et al. 1995). A high-amplitude reflector displays an intermittent inversion in the acoustic impedance, which could be due to the presence of gas in the overlying sediments consisting of relatively smaller gas bubbles. Where this reflector pinches out within ca. 1 m of the seafloor, a small carbonate mound is observed, around which the sediments are over-saturated with methane (Figure 2).

2.3. MDAC enabling enhanced sediment wave growth?

A study by targeting sediment waves within and outside areas of active gas seepage has determined that the large sizes of some sediment waves are not related to past or present gas seepage (Van Landeghem et al. 2015). In the literature, the theory of syndepositional stabilisation of the seafloor via methane seepage was tentatively applied to explain the very large size of some sediment waves (Hovland 1993; Judd et al. 2007), but our data does not support this theory.

3. INTERPRETATIONS

The nature of potential seepage of shallow gas is seemingly guided by the subsurface (glacial) geology and is discontinuous due to the intermittent presence of mud-rich layers in the sediments. Shallow gas in unconsolidated seafloor sediments is common in the NW European shelf seas (e.g. Schroot and Schüttenhelm 2003), and has caused concerns for safety during the many offshore developments currently ongoing worldwide (e.g. drilling operations and construction of wind turbine parks; Chivers 2013). The ability of (1) to understand which geological settings favour the build-up of shallow gas, and (2) to remotely identify the presence of shallow methane in the offshore environment is thus desirable and can be aided by a better understanding of the subsurface geology.

In Jürgen's Nightmare trench, any gas derived from the underlying Westphalian Coal Measures or the Dinantian/Namurian Holywell Shale would migrate through the overlying stiff diamictons (Judd 2005), which was found to be very rich in mud (up to 94%) and containing a significant clay fraction. Within the late Pleistocene Western Irish Sea Formation, this intermittent muddy layer may indeed have trapped the gas seeping from underlying sands and gravels. The stiff mud appears to have been eroded from the cliff and draped over some of the very large and trochoidally shaped sediment waves at the bottom of the trench. It is difficult to invoke any other mechanism in this high-energy environment to explain the presence of muddy sediments on top of very large sediment waves.

4. ACKNOWLEDGMENT

This scientific survey (CV12007) was funded for 8 days offshore, including all the shipment and travel, by the European Commission (EC Grant agreement nr. 228344) through the EUROFLEETS Project, a EU project funded through the EU FP7 Capacities/Research Infrastructures Programme, aiming at creating an alliance of European research fleets, bound to the general EC terms for project funding.

An extra 2 days offshore were funded by the Petroleum Affairs Division, which is part of the Department of Communications, Energy and

Natural Resources that regulates, protects and develops the Natural Resources of Ireland. The project partners at Bangor University, the University of Liverpool, University Basel and Università degli Studi di Genova funded 1 supplementary day on the RV Celtic Voyager. Helge Niemann was funded through a COST Short Term Scientific Mission (COST-STSM-ECOST-STSM- ES0902-190312-016289), Lea Steinle through the Swiss National Science Foundation (project 138057).

5. REFERENCES

- Chivers A. 2013. Dogger Bank Creyke Beck Health and Safety Statement. Document nr. F-HSC-RP-001 prepared for Forewind by PMSS Consultancy Services.
- Crocker P.F. 1994. Shallow gas in the Irish Sea and associated seafloor morphology. In: NIOZ, 3rd International Conference on Gas in Marine Sediments, Texel, The Netherlands, 25–28 September, 1994.
- Crocker P.F., Kozachenko M. & Wheeler A.J. 2005. Gas-related seabed structures in the Western Irish Sea (IRL-SEA6). Technical report produced for Strategic Environmental Assessment of the Irish Sea (SEA6), UK Department of Trade and Industry, London
- Flemming B.W. 1988. Zur Klassifikation subaquatischer, strömungstransversaler Transportkörper. *Boch geol & geotech Arb* 29: 44–47
- Hovland M. 1993. Submarine gas seepage in the North Sea and adjacent areas. In: Parker JR (ed), *Petroleum Geology of Northwest Europe: 4th Conference on, 29 March–1 April 1992*, London, Proceedings: 1333–1338
- Jackson D.I., Jackson A.A., Evans D.J.A., Wingfield R.T.R., Barnes R.P. & Arthur M.J. 1995. United Kingdom offshore regional report: the geology of the Irish Sea. BGS UK Offshore Regional Rep, HMSO, London
- Judd A.G. 2005. The distribution and extent of methane-derived authigenic carbonate. *Strategic Environmental Assessment of the Irish Sea (SEA6)*. UK Department of Trade and Industry, Tech Rep, London
- Judd A.G., Crocker P.F., Tizzard L. & Voisey C. 2007. Extensive methane-derived authigenic carbonates in the Irish Sea. *Geo-Mar Lett* 27: 259–267
- Schroot B.M., Schüttenhelm R.T.E. 2003. Expressions of shallow gas in the Netherlands North Sea. *Netherlands J Geosci/Geol Mijnb* 82(1): 91–105
- Scourse J.D. & Furze F.A. 2001. A critical review of the glaciomarine model for Irish Sea deglaciation: evidence from southern Britain, the Celtic shelf and adjacent continental slope. *J Quat Sci* 16: 419–434
- Van Landeghem K.J.J., Wheeler A.J., Mitchell N.C. (2009) Seafloor evidence for palaeo-ice streaming and calving of the grounded Irish Sea Ice Stream: implications for the interpretation of its final deglaciation phase. *Boreas* 38: 119–131
- Van Landeghem, K.J.J., Niemann, H., Steinle, L.I., O'Reilly, S.S., Huws, D.G. & Crocker, P.F. (2015) Geological settings and seafloor morphodynamic evolution linked to methane seepage. *Geo-Marine Letters*, 35 (4): 289–304

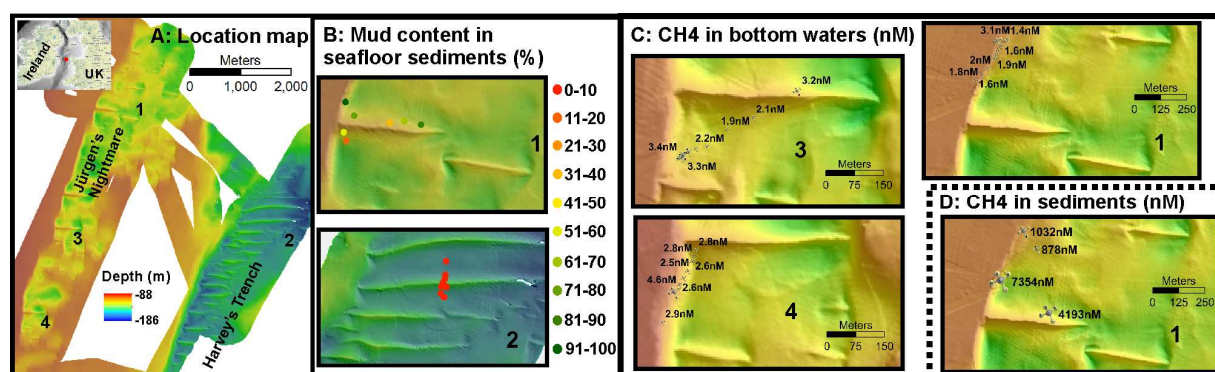


Figure 1. A: Seafloor bathymetry of Jürgen's Nightmare and Harvey's Trench. B: Mud content in seafloor sediments. C: Methane concentrations (nM) in bottom waters. D: Methane concentrations (nM) in seafloor sediments. From Van Landeghem et al., 2015

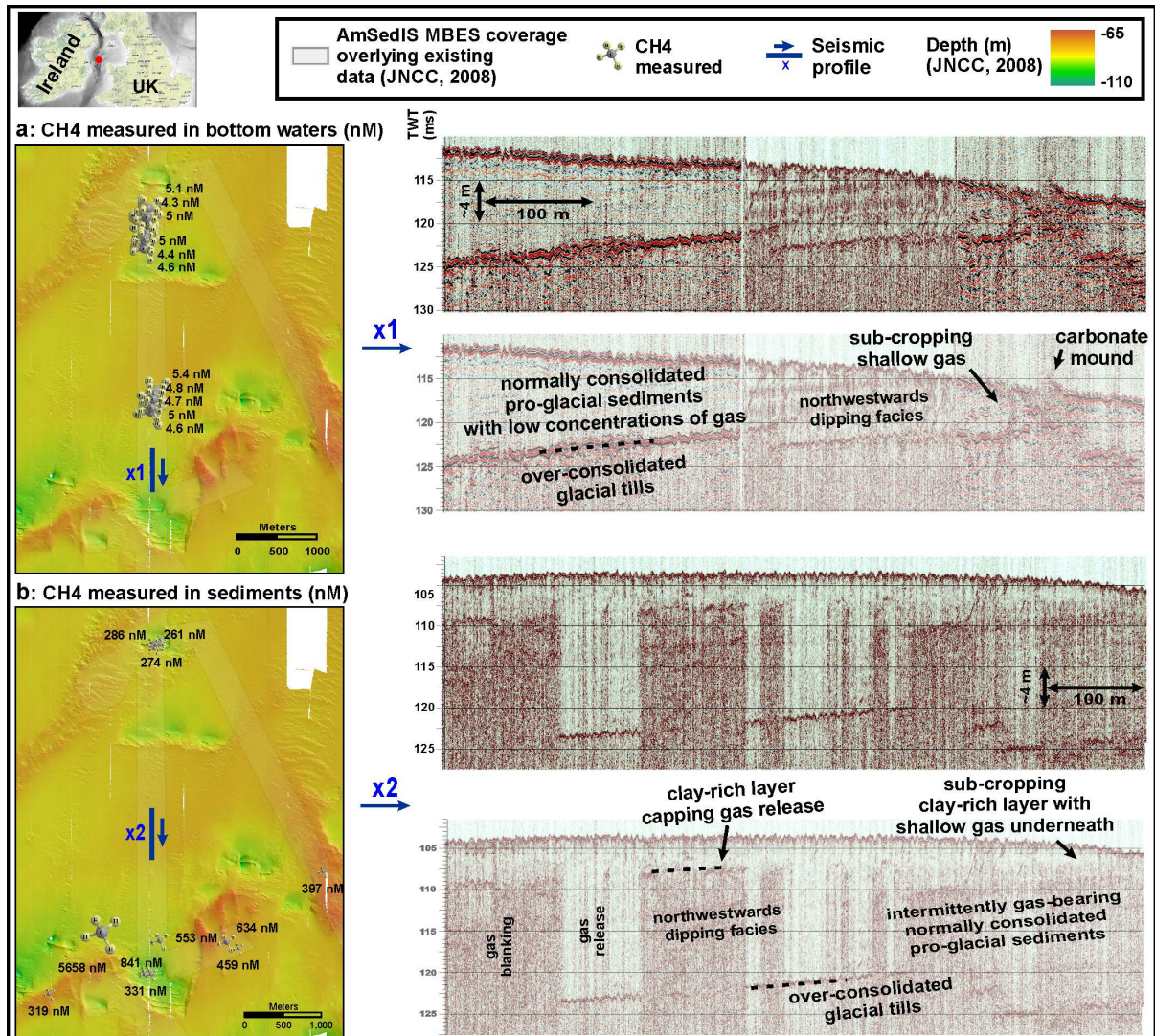


Figure 2. Methane concentrations (nM) in (A) bottom waters and (B) sediments seafloor of the Croker Carbonate Slabs SAC. Swath bathymetry data was collected during the AmSedIS project and by the JNCC in 2008 (©Copyright JNCC 2008). The blue lines locate the seismic profiles presented in cross-sections x1 and x2. From Van Landeghem et al., 2015

Adapting the Coleman et al. (2005) time-lag approach for application under unsteady discharge

J. J. Warmink *Marine and Fluvial Systems Department, Twente Water Centre, University of Twente, The Netherlands* – j.j.warmink@utwente.nl

ABSTRACT: The Coleman et al. (2005) time-lag approach for prediction of bed form dimensions in rivers was originally developed for steady discharge. In this study, the time-lag approach was adapted for application under discharge waves. The application on a discharge wave in a flume experiment shows that including the time-lag approach, enhances the amount of hysteresis between discharge and roughness and may improve the prediction of peak water levels in an operational water level prediction model.

1. INTRODUCTION

River dunes are the dominant bed forms in many rivers. The height is in the order of 10 - 30% of the water depth and their length in the order of 10 times their heights. Under flood conditions the bed is highly dynamic; dunes grow and decay as a result of the changing flow conditions. River bed forms act as roughness to the flow, thereby significantly influencing the water levels. Accurate and fast computer models are required to predict daily water level forecasts for operational flood management and forecasting. It is essential to predict the time evolution of bed forms and assess their influence on the hydraulic roughness.

Coleman et al. (2005) used an analytical time-lag approach to predict dune evolution in a flume experiment with discharge steps. They showed that their approach provides reliable predictions of dune dimensions under step varying discharge. The objective of this study was to extend the Coleman et al. (2005) approach for a discharge wave experiment in a flume. Following Paarlberg & Schielen (2012), we couple this dune evolution model to a 1-D Sobek model to predict the water levels during a discharge wave in a flume (results not presented in this abstract). We used data from two flume experiments of a discharge wave of

Wijbenga & Van Nes (1986): experiment T43 with a duration of 3.5 h and experiment T44 with a duration of 7 h ($T_{\text{wave}} = 3.5$ and 7 h, respectively), see figures 1 and 2.

2. METHOD

Coleman et al. (2005) adopted the common scaling relationship for sand-wave development from an initially flat bed from Nikora & Hicks (1997):

$$\frac{P}{P_e} = \left(\frac{t}{t_e}\right)^\gamma \quad \text{for } 0.01 < \frac{t}{t_e} < 1 \quad [1]$$

where P is the average value of dune length or height, P_e is the equilibrium value, t is time, t_e is the time to achieve P_e , and γ is a growth rate parameter. Coleman et al. (2005) derived a relation for γ , based on many flume experiment with a discharge step. They showed that growth rate was different for dune height, γ_H , and dune length, γ_L , and only depended on sediment size, D :

$$\gamma_H = 0.22D^{0.22} \approx 0.37 \quad [2]$$

$$\gamma_L = 0.14D^{0.22} \approx 0.32 \quad [3]$$

Furthermore, the Coleman approach requires an estimate of the time-to-equilibrium, t_e , and the equilibrium dune dimensions. In this study $H_{\text{eq}} =$

$0.3h$ and $L_{eq} = 2\pi h$ were chosen following Yalin (1992).

Coleman et al. (2005) derived an equation to predict t_e , based on shear velocity, u_{*s} , water depth, h , the Shields number, θ , and critical Shields number, θ_{cr} :

$$t_e \left[\frac{u_{*s}}{D_{50}} \right] = 2.05 * 10^{-2} \left[\left(\frac{D_{50}}{h} \right)^{-2.5} \right] \left[\left(\frac{\theta}{\theta_{cr}} \right)^{-1.12} \right] \quad [4]$$

Note that this equation is highly empirical and shows a large scatter.

The Coleman approach is not directly applicable for discharge waves, because the equilibrium water depth is unknown in case of unsteady discharge. Therefore, the time step to compute the equilibrium state affects the growth rate (due to non-unity of the γ , which describes the adaptation speed).

In the new approach the growth rate is assumed to be independent of γ and instead included in the prediction of t_e , thereby assuming linear growth from the dune dimension at t_0 to the dimension at t_e . This assumption has a negligible effect if the time step is much smaller than the duration of the discharge wave. Additionally, the time to equilibrium, t_e , was adapted to correct the growth rate. A separate t_e value was adopted for dune height and dune length, which is feasible because dune height adapts faster to the flow than dune length.

3. RESULTS

Figures 1 and 2 show the predicted dune dimensions using time-lag, which are now independent of the chosen interval to determine equilibrium conditions (for $dt \ll T_{wave}$) and bed form dimensions are predicted well. Using Van Rijn (1993) to transform dune dimensions to roughness, Figure 3 illustrates that the Coleman predicted hysteresis is more pronounced than the hysteresis using the water depth based equilibrium predictors.

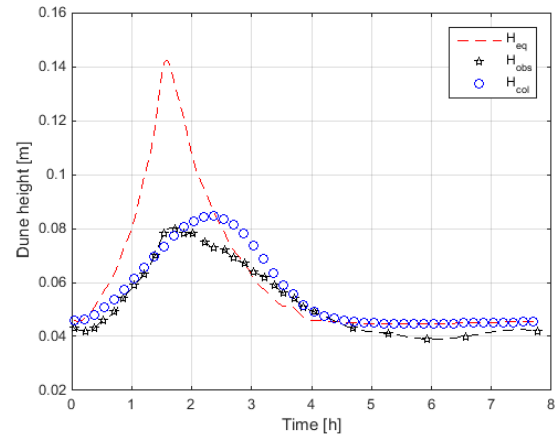


Figure 1. Dune height. The pentagrams represent the observations from experiments from Wijnbenga & Van Nes (1986), the dashed lines show the equilibrium predictions using Yalin (1992) and the open circles show the Coleman predicted dune heights.

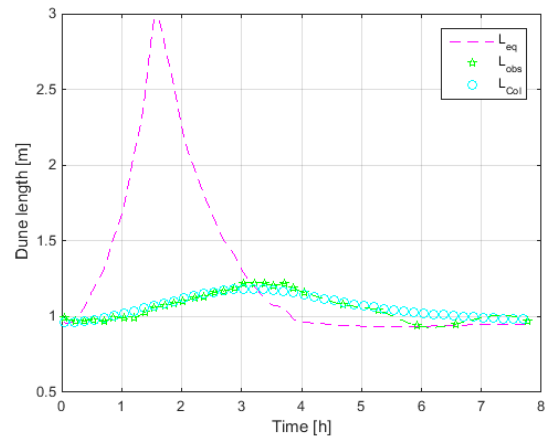


Figure 2. Dune length. The pentagrams represent the observations from experiments from Wijnbenga & Van Nes (1986), the dashed lines show the equilibrium predictions using Yalin (1992) and the open circles show the Coleman predicted dune lengths.

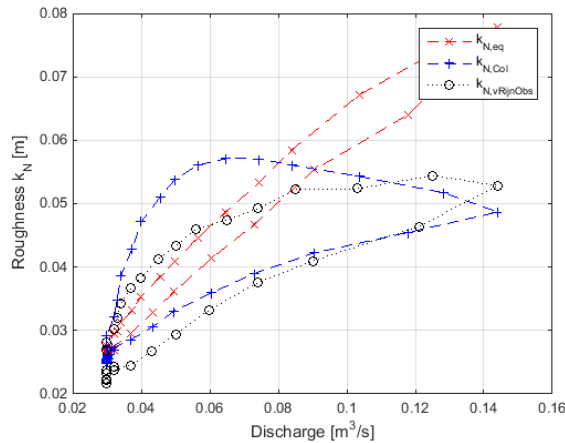


Figure 3. Hysteresis curves between discharge and roughness (k_N), based on dune dimensions from equilibrium predictors (x), adapted Coleman (+) and observed dune dimensions (o).

4. CONCLUSIONS

The Coleman et al. (2005) time-lag bed form model was successfully adapted for application on gradually varying discharge waves. This approach is applicable for the prediction of hysteresis due to bed form roughness the prediction of water levels. The advantages of the time-lag approach compared to more detailed physically based modelling strategies is that it is fast and captures the essential process to predict hysteresis. The results show that replacing the main channel roughness by the time-lag predicted roughness may improve the prediction of water levels.

The time-lag approach proved highly sensitive for the prediction of the equilibrium bed form dimensions. For reliably using this method in the field, future work is required to improve the

equilibrium bed form predictors for field situations. The presented approach is limited to lower regime bed forms and not valid for transitions to upper stage flow regimes. Extending the approach, by including transitions to other regimes in the equilibrium predictor needs further study.

5. ACKNOWLEDGMENT

This study is carried out as part of the project ‘BedFormFlood’, supported by the Technology Foundation STW, the applied science division of NWO and the technology programme of the Ministry of Economic Affairs.

6. REFERENCES

- Coleman S.E., Zhang M.H., Clunie T.M. 2005. Sediment-wave development in subcritical water flow *Journal of Hydraulic Engineering*, 131, 106-111, doi: 10.1061/(ASCE)0733-9429(2005)131:2(106).
- Paarlberg A.J., Schielen R.M.J. 2012. Integration of a dune roughness model with a large-scale flow model. In: Murillo (Ed.) *Proc. of River Flow 2012*, Costa Rica, pp. 155-161.
- Van Rijn L.C. 1993. *Principles of sediment transport in rivers, estuaries and coastal areas*. Aqua Publications, The Netherlands.
- Wijbenga J.H.A. & Van Nes A.R. 1986. Flow resistance and bedform dimensions for varying flow conditions; results of flume experiments with flood waves. WL/Delft Hydraulics research report. R657, M1314 Part XIII.
- Yalin M.S. 1964. Geometrical properties of sand waves. *Journal of the Hydraulics Division*, HY5, 105-119.

New strategy for predictions bedform migration

Th. Wever *WTD 71/FWG, Berliner Str. 115, 24340 Eckernförde, Germany –*

ThomasWever@Bundeswehr.org

S. Papili *Marinebasis Zeebrugge, Graaf Jansdijk 1, 8380 Zeebrugge, Belgium – Sonia.Papili@mil.be*

ABSTRACT: Since early reports of bedforms in rivers and the open sea large efforts were made to understand their formation and migration. Much is understood on their geometrical evolution as well as on the migration in response to hydro-meteorological forcing. The fast developments in positioning system technology and seafloor sensing methods in the last 15 years led to a focus on analyses of bathymetrical data and the quantification of individual bedform migration. Implying several initial assumptions these results are only locally valid and limited the portability to other areas. This too narrow perspective led to the loss of a general understanding. One proposed new strategy is based on simple experiments in which uncertainties are ruled out. Another strategy is proposed to make use of existing data and GIS systems. This can also account for uncertainty and variability in space and time.

1. BEDFORM RESEARCH

Although bedform dynamics is thoroughly investigated, the achieved knowledge is often only locally valid and cannot be generalized.

Moreover discrepancies between the bedform observations and the hydrodynamic predictions are commonly found (Duffy & Clarke, 2005) mostly due to simplifications in a pre-modelling phase.

Researchers try to predict bedform dimensions and evolution using mathematical equations. Those equations were derived from individual experiments in the last decades mostly trying to explain observed data sets and phenomena, see, e.g., previous MARID Conferences. They fail, however to predict properties correctly in other locations.

The actual need for better prediction capabilities of bedform evolution and movement on the seafloor in unmapped areas is an expression of the growing use of the seas for offshore engineering or installations. It is important for safety and environmental impact of drill rigs, wind farms and related pipelines or cables. Reliable predictions of seafloor stability are nowadays a necessity. New strategies are required to respond to permanently growing societal requirements.

1.1 Prediction difficulties

Bedforms are the equilibrium expression of physics controlled by water depth, water flow, and sedi-

ment properties. Early predictions of bedform properties used simple mathematical equations combining those parameters (e.g., Flemming, 2000, and references therein). The equations implicitly assumed ideal conditions. Especially variability and inhomogeneity were and still are not considered (Papili & others, 2013, Duffy & Clarke, 2012).

One simplification of this approach is the use of only one single sand grain size neglecting the spectrum or variability in space as, e.g., along sand dune flanks (for a summary see Wever, 2004).

A regular seasonal variability of sediment supply is not accounted for. This leads to imperfect bedform-related predictions, especially when measurements from different situations are used.

Borsje & others (2013) recently highlighted the problem of bedform stabilization and dimension changes due to a seasonal biological colonization. Also this factor demands time-dependent prediction models.

One of the unanswered questions relates to the problem of sufficient sediment supply which controls the development of bedforms reliefs. It remains unclear whether or not the observed bedforms achieved their equilibrium dimensions. Only in that case physics-based equations have relevance. Among the first to raise this problem were Anthony & Leth (2002). They assumed that a

shortage of sand did not allow bedforms to reach optimum dimensions. An example for such a condition is shown in Figure 1. Nonetheless it is generally assumed that the condition of sufficient sediment supply is fulfilled. This opens the door for miscalculations in case that this assumption is not fulfilled by the nature.



Figure 1. Side scan sonar images from the Jade area (Germany). Individual (starving) megaripples are separated by large gaps in which underlying glacial till and coarse sediment shows a high backscatter due to a lack of sediment. In an area at 10 nm distance with sufficient sediment supply this is not observed.

Most modelling approaches assume for simplicity 2-D flows across 2-D bedforms. Currents in bedforms fields are, however, absolutely 3-D and turbulent and less stationary than mostly assumed. Figure 2 shows a rotary sonar scan during accelerating ebb current. At slow currents megaripples (marked by the ellipse) develop. At higher current speeds (1 kn) they are flattened. The circle of Figure 2 marks sand ripples, oriented perpendicular to the main current. They also change during the tidal phase, including temporary disappearance. They are a clear sign for a corkscrew-like 3-D water movement within the sand dune field.

To the standard simplifications mentioned so far other uncertainties have to be added. They are introduced by small-scale seafloor relief variations and by non-stationary water movement across bedform fields.

Examples for the impact of uncertain parameters on calculated results have been given by Wever & Stender (2000).

1.2 Technology developments

The technological development continuously supported progress in underwater bedform research. It allowed to map more details than before with a better resolution and accuracy.

Considerable progress was made first for position determination which started with bearings. Electronic navigation aids such as DECCA and nowadays satellite-based positioning almost eliminates position uncertainties and thus reduced error bars in calculations.

A second big step forward was made possible were acoustic devices (ADCPs and ADVs) to determine current–depth distributions. They operate for long periods and record current–depth profiles instead of current speed at one fixed depth. The results are necessary for an understanding of sediment transport.

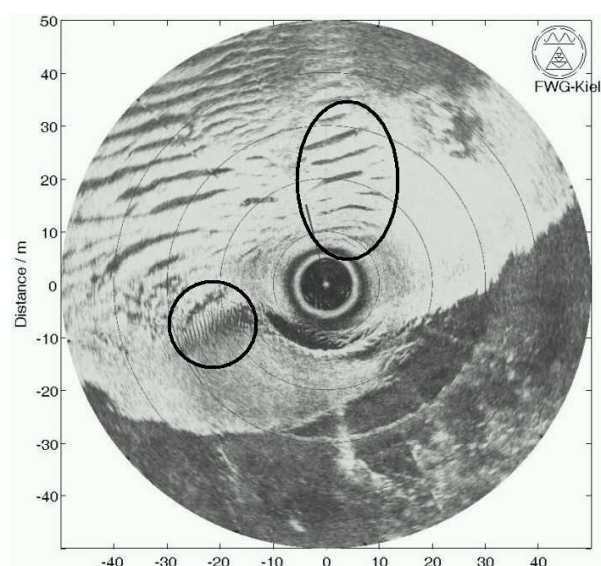


Figure 2. Rotary sonar image during ebb current, shortly after ebb slack water. The radius of the circle is 50 m, every 10 m a marker ring is shown. The dark area in the lower part represents the shadow zone of a sand dune with a curved crest. The light patches within this area result from backscatter from suspended sediment. The tidal currents move up and down the displayed area (no tidal ellipse). For more explanations see text.

The third important technological advance is the development of acoustic systems for mapping the seafloor and bedforms (side scan sonars and multi-beam echo sounders). They replaced simple depth echosounder recordings along profiles with considerable spacing. The implementation of such sonars on Autonomous Underwater Vehicles diminishes the impact of wave motion on the sonars.

The improved technologies revealed more details. The concentration on explaining those details reduced the efforts for a general understanding of bedforms.

1.3 Prediction Capability

The recently increased data quantity and detail of single mappings led scientists to focus on explaining the observed data. This de-focused from the necessary predictive capability of where, when and what kind of bedforms will develop.

This disappointing situation was noticed by offshore engineers during the actual planning for offshore wind farms and cable routes to land.

Equations derived from experiments often require an additional adjustment of parameters to local conditions. This restricts the general use and transportability to other areas.

We see a central difficulty in the voluntary concentration on single data sets and subsequent limitation of results.

Assumptions and simplifications are necessary for modelling the complex seafloor. However, they come along with a reduction of available information and an increase of uncertainty in the results.

1.4 New Strategy

In view of these limitations, a new strategy is needed to answer the recurrent questions and societal needs. The goal must be the development of a general concept for the prediction of (a) bedform existence in unmapped areas, and (b) their dimensions and behavior. Lessons learned for different local conditions are an important supplement. The aim is a more general vision and treatment of seafloor bedform dynamics.

Different approaches are needed to reach the goal of a universal reliable bedform prediction based on validated equations.

As important obligatory step is a mathematic description of fully developed bedforms. This must be achieved for different combinations of the easily observable parameters depth, current, grain size under sufficient sediment supply.

A supplementary thrust should be the mapping of bedforms and correlation with other data using GIS (Geographical Information System) technology to integrate different information layers. They can and should include statistical information instead of only one single value.

We think, e.g., not of only a grain size layer but also a grain size spectrum layer in a GIS. Other layers can display sample density and related uncertainty, and many similar parameters as variability of bedform migration speed or give information about flow conditions (direction, turbulence,

3-D flow, interaction with waves) and variability (tidal and non-tidal).

2. DISCUSSION

In view of the disappointment of civil engineers involved in offshore engineering as soon as information about bedforms is needed in unmapped areas, new approaches are necessary. This is especially true for their distribution, dimensions or behavior.

Experiments can be designed to analyze bedform dimensions under ideal conditions, i.e., when they reach their (site dependent) equilibrium dimensions. Nasner (1983) made such observations in Elbe river. He determined the time for restoration of original bedform dimension after crest-capping. Additional upstream sediment supply could be used to rule out sediment shortage. In a different approach filling the upstream trough of a bedform with sediment could be used to monitor the bedform's response. A rotating sonar with regular scanning intervals installed on a small tower (Wever et al., 2008) can resolve changes in time, even in intervals of a few minutes.

On a larger scale experiments based on regular bedform mapping and monitoring of the water climate (waves, currents, tides) could help to understand controlling processes and factors.

The intense mapping of shelves and rivers for navigational purposes has led to the accumulation of large data sets. Their synoptic analyses should offer insight into the long-term development and help to distinguish those from short-term reactions to changes of forcing parameters. GIS technology offers very good tools to implement that. Additional ADCPs within the research area would be a useful addition for understanding processes.

Bedform research seemingly remains anchored on a hindcast level without making the appropriate advancement into predictive applied science. The reasons are multifold. They arise from the topic's complexity and the need of simplifications. The topic's complexity is illustrated by the discussion about the value of bedform classification schemes in contrast to continuous dimensions (e.g., Fleming, 2000 and references therein).

The proposed practical approaches can help to tackle the actual difficulties and find answers.

Difficulties arising from contrasting observations (e.g., grain size distributions along bedforms) leave scientists puzzled with the escape route to concentrate on and deliver the best possible explanation of measured data sets.

Baas & Malarkey (2013) analyzed the grain size distribution's impact and biological factors that influence sediment transport, thus making steps in the direction of a wider understanding.

Any new approach should be planned to understand the general picture first and then to explore and explain details within the broad picture. Necessary simplifications can be carefully chosen and kept under control.

3. CONCLUSIONS

The results of bedform research are not successfully applied in offshore engineering.

A strong focus on the explanation of existing observations led to a loss of the general picture. This, however, needs to be understood before the details can be predicted (top-down approach).

Simplifying assumptions and lacking information limit the value of data-derived solutions in terms of their transportability to other locations.

We propose as one step towards a better bedform related predictions dedicated and well planned experiments to achieve a basic understanding of how the controlling forces interact to form bedforms and how they control their dimensions.

A different proposed tactic makes use of existing data is the summary and integration of all data and their variations. GIS-based approaches offer the necessary tools.

We propose the identification of a suitable bedform dominated area which is thoroughly analyzed. This includes dense sediment sampling, wave/current climate monitoring, and repeated bathymetric surveys in a joint effort of different labs and various nations. Such a test field will offer ideal conditions to test and validate concepts, especially when displayed with a GIS.

It is important to switch from a focus on explaining existing (historic) data to a "forward looking" prediction of future data.

4. REFERENCES

Anthony, D. & Leth, J.O. 2002. Large-scale bedforms, sediment distribution and sand mobility in the

Eastern North Sea off the Danish west coast, *Marine Geology* 182, 247-263.

Baas, J. & Malarkey, J. 2013. Physical and Biological Cohesion Within Mixed Sand-Mud Beds: Implications for Erosion and Bedform Development, *Marine and River Dune Dynamics – MARID IV*, 15-17 April 2013, Bruges, V. Van Lancker & T. Garlan (eds.), 23.

Borsje, B.W., Hulscher, S.J.M.H., Herman, P.M.J. & Degraer, S., 2013. Biogeomorphological self-organization in sandy shelf seas. *Marine and River Dune Dynamics – MARID IV*, 15-17 April 2013, Bruges, V. Van Lancker & T. Garlan (eds.), 53-58.

Duffy, G.P. & Clarke, J.E.H., 2005. Application of spatial cross correlation to detection of migration of submarine sand dunes. *Journal of Geophysical Research*. V.110, F04S12. 1-11.

Duffy, G.P. & Clarke, J.E.H., 2012. Measurement of bedload transport in a coastal sea using repeat swath bathymetry surveys: assessing bedload formulae using sand dune migration. *International Association of Sedimentologists. Special Publication*. V.44, 249-272.

Flemming, B.W. 2000. The role of grain size, water depth and flow velocity as scaling factors controlling the size of subaqueous dunes, *Marine Sandwave Dynamics, International Workshop*, March 23-24, 2000, University of Lille 1, Proceedings, A. Trentesaux & T.E. Garlan, (eds.), 55-61.

Nasner, H. (1983). Dredging of tidal dunes, *International Harbour Conference*, Antwerp, Belgium.

Papili S., Baeye M. & Van Lancker V. 2013. Deciphering Mega-Ripple variability in an anthropogenically-steered environment: implications for mine burial studies. *Marine and River Dune Dynamics – MARID IV*, 15-17 April 2013, Bruges, V. Van Lancker & T. Garlan (eds.), 207-208

Wever, Th.F. 2004. Bedforms and Bedform Migration: A Data Review, *Marine Sandwave & River Dune Dynamics II*, 1-2 April 2004, Enschede, S.J. M.H. Hulscher, T. Garlan & D. Idier (eds.), 330-338.

Wever, Th.F. & Stender, I.H. 2000. Strategies for and results from the investigation of migrating bedforms in the German Bight, *Marine Sandwave Dynamics, International Workshop*, March 23-24, 2000, University of Lille 1, Proceedings, A. Trentesaux & T.E. Garlan, (eds.), 221-226.

Wever, Th., Voß, H., & Lühder, R. (2008). High-resolution observation of small-scale variability in a bedform field, *Marine Sandwaves and River Dynamics III*, *International Workshop*, April 1-3, 2008, Leeds University, Proceedings, D. Parsons, T. Garlan, & J. Best (eds), 331-335.

KEYNOTE: Properties of active tidal bedforms.

C. Winter *Center for Marine Environmental Sciences, MARUM, Bremen, Germany, cwinter@marum.de*

A. Lefebvre *Center for Marine Environmental Sciences, MARUM, Bremen, Germany*

M. Becker *Center for Marine Environmental Sciences, MARUM, Bremen, Germany*

Y. Ferret *Center for Marine Environmental Sciences, MARUM, Bremen, Germany*

V.B. Ernstsen *Dpt of Geosciences & Natural Resource Management, Univ. of Copenhagen, Denmark*

J. Bartholdy *Dpt of Geosciences & Natural Resource Management, Univ. of Copenhagen, Denmark*

E. Kwooll *Department of Geography, Simon Fraser University, Burnaby BC, Canada*

B. Flemming *Senckenberg am Meer, Wilhelmshaven, Germany*

ABSTRACT: Bedforms of various shapes and sizes are ubiquitous in tidal channels, inlets and estuaries. They constitute a form roughness which has a large scale effect on the hydrodynamics and sediment transport of coastal environments. It has been shown that this form roughness can be expressed in terms of the lee side slope of bedforms. This study compiles data on the topography and hydraulics of compound dunes from different settings in the German Bight to discuss implications of a critical lee slope in tidal environments with reversing flow. Data from the Weser estuary is used to exemplify and quantify these effects.

1. INTRODUCTION

The German Bight is a prominent example for the dynamic interaction of different coastal ocean elements such as the shallow shelf sea, estuaries, tidal channels, barrier islands and tidal flats under a wide range of forcing conditions. This zone features extensive human uses (shipping lanes, ports, windparks, constructions, fishing, etc.) in close proximity of precious ecosystems as in the natural World heritage Wadden Sea (Winter & Bartholomä, 2006; Reise et al., 2010). Large scale morphodynamics of this area have been described by the annual bed elevation range (Winter, 2011), and respective drivers were differentiated into wave, wind and tidal forcing (Kösters & Winter, 2014). The highest morphodynamic activity is observed in the outer estuaries and tidal inlets of the Wadden Sea (Herrling & Winter, 2014; 2015). Predominately at these locations which are characterized by strong tidal currents a variety of mainly flow transverse subaqueous bedforms, are found (Ulrich, 1971; Winter et al., 2016). These morphological elements have been explored for long times (e.g. Flemming, 1988; Nasner, 1978,

Davis & Flemming, 1991; Flemming & Davies 1992), and the availability of observation techniques like multibeam echosounders (MBES) with precise positioning and correction for ship motion (Ernstsen et al., 2006), has triggered a multitude of process-based studies on the stunning complexity of these bedforms (Ernstsen et al., 2005, 2006b), their formation and development (Ernstsen et al., 2005, 2006b, 2008, 2010, 2011; Svenson et al., 2008), and their interaction with the hydrodynamics (Lefebvre et al., 2011), suspended sediments (Kwooll et al., 2013), micro-biology (Ahmerkamp et al., 2015), bed fauna and flora, and coastal constructions (Noormets et al., 2006).

Besides their aesthetic nature, their role as prominent transport agents, their frequently addressed hazard for coastal constructions and navigation, it is the bedforms cross-scale impact that make them a prominent field of applied and fundamental research: These (individually) small scale elements of short term dynamics have a large scale and long term effect on whole coastal systems. The hydraulic effect of bedforms needs to be considered in the development, set-up and application of numerical models on coastal

settings. Bedforms are ubiquitous and thus their effect on flow and transport patterns acts on large spatial scales, i.e. they constitute a hydraulic roughness influencing the overlying current structure, and thus the transport of sediments, and other biogeochemical properties throughout the whole coastal domain (Bartholdy et al, 2010).

Compound dunes in the outer tidal channels and estuaries of the German Bight are bedform assemblages of large (length $O(100)$ meters), heights $O(\text{meters})$) primary dunes which are superimposed by smaller (lengths $O(10\text{m})$, height $O(\text{dm})$) secondary dunes, and occasionally by small scale ripples, which however often are below the resolution of ship mounted MBES observations and out of the scope of this study.

In this contribution *active bedforms* are defined as subaqueous flow transverse features which significantly influence the flow field and in turn develop (grow, migrate, decay) as an effect of the governing flow conditions.

2. RELEVANCE OF SCALES

The superimposed primary and secondary dunes dynamics feature different temporal behavior and can be separated by spectral methods into components of high and low celerity (Winter & Ernstsens, 2008). Secondary bedforms share geometric properties of dunes known from common laboratory flume experiments (Guy et al., 1966) and tend to adjust to the oscillating tidal currents, thus changing their asymmetric shape and migration according to the instantaneous flow direction. Reported secondary bedform celerity can be up to several meters per tide, although residual migration over a tidal cycle may be very low (Ernstsens et al., 2011). Primary bedforms develop at larger timescales, and follow in shape and migration the direction of residual tidal forcing, thus do not adapt to the reversing tidal directions. Recognition of individual bedforms in successive annual measurements have revealed slow migration celerities in the order of 10-20m per year in a tidal inlet (Ernstsens, 2006) 25 m in the estuaries of Weser (Nasner, 1974) and Elbe (Zorndt et al., 2010).

3. SUSPENDED SEDIMENTS

Bedforms interact with the flow in that turbulent wakes and coherent flow structures behind the crests of bedforms are formed, which depend in size and characteristics on the direction of the flow (Best, 2005; Kwooll et al., 2014). In estuarine tidal environments two separate transport regimes may be observed: Fine, cohesive sediments settle predominately in the troughs of dunes at slack water, with subsequent erosion and resuspension at rising tidal currents. The dunes are formed in coarser sediments and develop and migrate at higher flow stages, until the next slack water, when dune migration comes to a halt, and subsequently fines subsequently settle out at the next slack water, forming distinct mud deposits in the troughs of the dunes (Becker et al., 2013, Kwooll et al., 2013).

4. HYDRAULIC RELEVANCE

Double averaging of measured velocity profiles along dunes had revealed how the hydraulic effect of large asymmetric compound dunes differs according to the tidal stage. Lefebvre et al. (2011), calculated that the hydraulic effect of primary dunes can be an order of magnitude larger when the flow and bedform shape (gentle stoss side, steep lee side) are in line, thus the large bedforms may be called active or hydraulically relevant only if the flow is in the direction of dominant currents. The effect of secondary bedforms does not vary much over the tidal cycle, which is explained by the fast adaptation of bedform shape according to the instantaneous flow. The hydraulic effect of bedforms is mainly depending on the turbulent characteristics and energy turnover behind bedforms. The latter is highly dependent on the lee slope of bedforms (Best & Kostaschuk, 2002; Kwooll et al., 2016) at which flow separation may or may not occur, a simple descriptor can be found, which reduces common bedform descriptors depending on the lee slope (Lefebvre & Winter, 2016).

5. OBSERVATIONS

A compilation of MBES data from the Jade Bay, and the Weser and Elbe estuaries has produced about 40,000 individual datasets on bedform

geometry. These bedforms range in heights from 0.05 to 8.9m and lengths from 4 to 490m. Only 4.2% of all identified bedforms meet the criterion of being active, or hydraulically relevant (here simplified to a lee slope $>10^\circ$). These scale with $H=0.1665 L^{0.6672}$ ($R^2=0.53$) when taking into account weighted bedform heights (generalized extreme value method). The majority of this subset falls in between predicted mean and maximum H/L relationship by Flemming (1988).

Classic bedform predictors reveal very limited skill in reproducing bedform shapes based on sedimentary and flow conditions. An adjusted polynomial model fit on all active bedform data results in a goodness of fit $R^2=0.66$.

For different areas of the Weser estuary the evolution of bedform geometry and migration is related to different drivers. Significant correlations to Weser fresh water discharge are shown.

6. ACKNOWLEDGMENTS

The different studies were carried out in cooperation between mentioned home institutions and the relevant authorities Federal Waterways and Shipping Institute (BSH) and Federal Waterways and Engineering Institute (BAW).

7. REFERENCES

- Ahmerkamp S, Winter C, Janssen F, Kuypers MMM, Holtappels M (2015) The impact of bedform migration on benthic oxygen fluxes, *J. Geophys. Res. Biogeosci.*, 120.
- Bartholdy J, Flemming BW, Ernstsens VB, Winter C, Bartholomä A, 2010. Hydraulic roughness over simple subaqueous dunes. *Geo-Marine Letters*, 30(1): 63-76.
- Becker M, Schrottke K, Bartholomä A, Ernstsens VB, Winter C and Hebbeln D (2013) Formation and entrainment of fluid mud layers in troughs of subtidal dunes in an estuarine turbidity zone. *Journal of Geophysical Research-Oceans*, 118(4). 2175-2187
- Best, J. (2005), The fluid dynamics of river dunes: A review and some future research directions, *J. Geophys. Res.*, 110(F4), F04S02
- Best, J., and R. A. Kostaschuk (2002), An experimental study of turbulent flow over a low-angle dune, *J. Geophys. Res.*, 107(C9), 3135
- Davis, R.A., Jr., Flemming, B.W. 1991. Time-series study of mesoscale tidal bedforms, Martens Plate, Wadden Sea, Germany. *Canadian Society of Petroleum Geology Memoir* 16: 275–282.
- Ernstsens VB, Noormets R, Winter C, Hebbeln D, Bartholomä A, Flemming BW, Bartholdy J (2005). Development of subaqueous barchanoid-shaped dunes due to lateral grain size variability in a tidal inlet channel of the Danish Wadden Sea. *Journal of Geophysical Research*, 110(F04S08), DOI: 10.1029/2004JF000180.
- Ernstsens VB, Noormets R, Hebbeln D, Bartholomä A, Flemming BW (2006a). Precision of high-resolution multibeam echo sounding coupled with high-accuracy positioning in a shallow water coastal environment. *Geo-Marine Letters*, 26: 141-149, DOI: 10.1007/s00367-006-0025-3.
- Ernstsens VB, Noormets R, Winter C, Hebbeln D, Bartholomä A, Flemming BW, Bartholdy J (2006b). Quantification of dune dynamics during a tidal cycle in an inlet channel of the Danish Wadden Sea. *Geo-Marine Letters*, 26: 151-163, DOI: 10.1007/s00367-006-0026-2.
- Ernstsens VB, Becker M, Winter C, Bartholomä A, Flemming BW, Bartholdy J (2008). Bedload transport in an inlet channel during a tidal cycle. In: Dohmen-Janssen CM, Hulscher SJMH (eds) *River, Coastal and Estuarine Morphodynamics: RCEM 2007*. Taylor & Francis Group, London, pp. 351-358, ISBN: 978-0-415-45363-9.
- Ernstsens VB, Winter C, Becker M, Bartholdy J (2010). Tide-controlled variations of primary- and secondary-bedform height: Innenjade tidal channel (Jade Bay, German Bight). In: Vionnet C, Perillo G, Latrubesse E, Garcia M (eds) *River, Coastal and Estuarine Morphodynamics: RCEM 2009*. Taylor & Francis Group, London, pp. 779-786, ISBN: 978-0-415-55426-8.
- Ernstsens VB, Lefebvre A, Bartholdy J, Bartholomä A, Winter C (2011). Spatiotemporal height variations of large-scale bedforms in the Grådyb tidal inlet channel (Denmark): a case study on coastal system impact. *Journal of Coastal Research*, SI64: 746-750, ISSN: 0749-0208.
- Flemming, B.W. 1988. Zur Klassifikation subaquatischer, strömungstransversaler Transportkörper. *Bochumer geologische und geotechnische Arbeiten* 29: 44–47.
- Flemming, B.W., Davis, R.A. Jr. (1992). Dimensional adjustment of subaqueous dunes in the course of a spring-neap semicycle in a mesotidal backbarrier channel environment (German Wadden Sea, southern North Sea). *Courier Forschungs-Institut Senckenberg* 151: 28–30.
- Fraccascia S, Hebbeln D, Winter C, 2011. Bedform evolution in a tidal inlet inferred from wavelet analysis. *Journal Coastal Research*, SI 64.

- Guy HP, Simons DB, Richardson EV (1966) Summary of Alluvial Channel Data from Flume Experiments, 1956-61. In: *Sediment Transport in Alluvial Channels*, Geological Survey Professional Paper. U.S. Department of the Interior, Washington, p 104
- Herrling G, Winter C (2014) Morphological and sedimentological response of a mixed-energy barrier island tidal inlet to storm and fair-weather conditions. *Earth Surf. Dynam.* 1, 745-782. doi:10.5194/esurf-2-363-2014
- Herrling G, Winter C (2015) Tidally- and wind-driven residual circulation at the multiple-inlet system East Frisian Wadden Sea. *Continental Shelf Research*, 106, 45–59. doi:10.1016/j.csr.2015.06.001
- Kösters F, Winter C (2014) Exploring German Bight coastal morphodynamics based on modelled bed shear stress. *Geo-Marine Letters* 34: 21-36
- Kwoll E, Becker M, Winter C (2014). With or against the tide: the influence of bedform asymmetry on the formation of macroturbulence and suspended sediment patterns. *Water Resources Research* 50, 1-16,
- Kwoll E, Venditti JG, Bradley R, Winter C (2016) Flow structure of high and low angle dunes. *Journal of Geophysical Research – Earth Surface* 10.1002/2015JF003637
- Kwoll E., Winter C. and Becker M (2013). Intermittent suspension and transport of fine sediment over natural tidal bedforms. In: *Coherent Structures in Flows at the Earth's Surface*. Venditti, J. G., Best, J., Church, M. and R. J. Hardy (eds.). Wiley-Blackwell, London
- Lefebvre A, Ernstsens VB, Winter C, 2011. Influence of compound bedforms on hydraulic roughness in a tidal environment. *Ocean Dynamics*.
- Lefebvre A, Ernstsens VB and Winter C (2013) Estimation of roughness lengths and flow separation over compound bedforms in a natural-tidal inlet. *Continental Shelf Research*, 61-62. 98-111.
- Lefebvre A, Paarlberg A, Winter C (2013) Flow separation and shear stress over angle of repose bedforms: A numerical investigation. *Water Resources Research* 50, 2, 986-1005
- Lefebvre A, Winter C (2016) The influence of bed form lee angle to hydraulic roughness. Accepted for publication *Geo Marine Letters*, on Jan 17, 2016
- Nasner H (1978) Time-lag of dunes for unsteady flow conditions. In: 16th International Conference on Coastal Engineering (ICCE), ASCE. Hamburg, Germany, 1801-1817
- Noormets R, Ernstsens V, Bartholomä A et al. (2006) Implications of bedform dimensions for the prediction of local scour in tidal inlets: a case study from the southern North Sea. *Geo-Marine Letters* 26:165-176
- Reise, K., Baptist, M., Burbridge, P., Dankers, N. M. J. A., Fischer, L., Flemming, B., Smit, C. (2010). *The Wadden Sea-a universally outstanding tidal wetland. The Wadden Sea 2010. Common Wadden Sea Secretariat (CWSS); Trilateral Monitoring and Assessment Group: Wilhelmshaven. (Wadden Sea Ecosystem; 29/editors, Harald Marencic and Jaap de Vlas), 7.*
- Svenson C, Ernstsens VB, Winter C, Bartholomä A, Hebbeln D, 2009. Tide-driven sediment variations on a large compound dune in the Jade tidal inlet channel, Southeastern North Sea. *Journal of Coastal Research*, SI 56: 361-365.
- Winter C, 2011. Macro scale morphodynamics of the Southern German Bight, North Sea. *Journal of Coastal Research*, SI 64.
- Winter C, Bartholomä A., 2006. Coastal dynamics and human impact in the south-eastern North Sea: An introduction. *Geo-Marine Letters*, Pages 121-124.
- Winter C, Becker M, Ernstsens VB, Hebbeln D, Port A, Bartholomä A, Flemming BW, Lunau M, 2007. In-situ observation of aggregate dynamics in a tidal channel using acoustics, laser-diffraction and optics. *Journal of Coastal Research* SI 50, 1173-1177
- Winter C, Ernstsens VB, 2007. Spectral Analysis of Bedforms, In: C. Dohmen-Janssen and SJMH Hulscher (Ed) *River, Coastal and Estuarine Morphodynamics*. 907-912
- Winter C, Lefebvre A, Benninghoff M, Ernstsens V. (2015) Die Verteilung und Eigenschaften von Bodenformen in der Deutschen Bucht, eine Rekonstruktion der Karten von Ulrich (1973). *Die Küste* 83, 65-76
- Winter C, Vittori G, Ernstsens VB, Bartholdy J, 2008. On the superimposition of bedforms in a tidal channel. In: Parsons, D., T. Garlan and J. Best (eds) *Marine and River Dune Dynamics*, p. 337-344.
- Zorndt, A. Wurpts, A., Schlurmann, T., Ohle, N., Strotmann, T. 2010. Dune migration and sand transport rates in tidal estuaries: the example of the River Elbe. *Proc. Sediment* 38, ICCE 32.

Wave-induced ripples development in mixed clay-sand substrates

X. Wu *University of Hull, Hull, UK – X.Wu@2013.hull.ac.uk*

J.H. Baas *University of Bangor, Bangor, UK*

D.R. Parsons *University of Hull, Hull, UK*

D. Mouazé *University of Caen, Caen, France*

S. Mclelland *University of Hull, Hull, UK*

L. Amoudry *National Oceanography Centre, Liverpool, UK*

J. Eggenhuisen *University of Utrecht, Utrecht, Netherland*

M. Cartigny *National Oceanography Centre, Southampton, UK*

G. Ruessink *University of Utrecht, Utrecht, Netherland*

ABSTRACT: A large-scale flume experiment was conducted in the Total Environment Simulator, University of Hull. Run 01 was a control experiment with pure sand bed, and clay fraction increased gradually from 4.2% in Run 03 to 7.4% in Run 06. The experimental results demonstrate the significant influence of the amount of cohesive materials in the substrate on ripples evolution under regular surface waves. Most importantly, the cohesive clay added into sand bed dramatically slowed down the rate of bed erosion. Consequently, with the addition of a larger cohesive fraction, the equilibrium time of each run increased exponentially. The paper discusses the slower ripple growth rates with higher cohesive fractions, via an influence on critical shear, but highlights that the equilibrium size of ripples is found to be independent of increasing substrate clay fraction. The suspended particles mass (SPM) concentration indicates that clay particles were efficiently suspended and winnowed by wave action.

1. INTRODUCTION

Wave-induced ripple size is related with the sediment characteristics including sediment particles size and flow properties, such as maximum near-bed orbital velocity (Nielson, 1981; van Rijn, 1993; Nelson et al., 2013 ;). Previous studies, however, focused on the dynamics of bedforms only composed of well-sorted sand. This restrictive sediment type is far from being a realistic representation of natural sediment size distributions, particularly in European coastal and estuarine environments, where mixed sediments with and without fine cohesive components are common (Flemming, 2002). In particular cohesive mixed sediments (mud-sand) influence bedform characteristics (Bass et al., 2011, 2013) and, in turn, the near-bed boundary conditions for turbulence and sediment transport within dynamic models. Bass et al. (2013) highlighted that cohesive clay particles added into sand bed slowed the rate of current ripples development. Particularly, ripples

dimensions decrease with increase clay content under unidirectional flow (Bass et al., 2013). Therefore, the present paper concentrates on the influence of cohesive clay on the ripples development under regular wave conditions. The aims can be concluded as following: (1) identifying the relationship between the rate of wave ripple development and initial bed clay fraction; (2) determining the equilibrium height and length of the wave ripples as a function of initial bed clay fraction.

2. METHODS

The main experimental parameters see table 1. 7 bedform elevation profiles (BEPs) were recorded by the acoustic bed scanner URS for each scanning time. These raw data of BEPs were processed by the method based on bedform tracking tool (BTT) that is a numerical code in Matlab (Van der Mark, 2008; Van der Mark, 2009). Van der Mark *et al.* (2008) method was used to determine the locations of wave ripple crests and troughs in a measured

bed elevation profile and then to determine the geometric properties of individual bedforms. The equilibrium conditions could be established by the Bass *et al.* (2013) method, where the ripples development by the following equations:

$$\frac{Lt-L_0}{Le-L_0} = 1 - (0.1)^{\frac{t-t_f}{T_L-t_f}} \quad (1)$$

$$\frac{Ht}{He} = 1 - (0.1)^{\frac{t-t_f}{T_H-t_f}} \quad (2)$$

where Lt and Ht are wave ripples length and height derive from BTT at time t after experiment start, t_f is the delay time of wave ripples appearance, Le and He denote equilibrium wave ripple length and height, L_0 is the wave ripple length of the first appearance of wave ripple, and T_L and T_H are the equilibrium time for length and height. A non-linear fit using the Curve Fitting Tool in Matlab was used to find the best solution for Equations 1 and 2, therefore obtaining Le , He , L_0 , T_L and T_H . In present study, T_L and T_H are defined as 90% of wave ripples get equilibrium.

Table 1. Experimental parameters

Run	Duration (min)	f_0 (%)	Salinity (‰)	U_m (m/s)	d_o (m)	H_s (m)
1	290	0	17.8	0.32	0.26	0.16
2*	270	0	19.5	-	-	-
3	300	4.2	19.2	0.33	0.26	0.22
4	250	6.2	17.2	0.31	0.25	0.22
5	510	7.2	20.4	0.30	0.23	0.24
6	630	7.4	19.1	0.30	0.23	0.21

f_0 = initial clay fraction

U_m = maximum near-bed orbital velocity

d_o = maximum near-bed orbital diameter

H_s = significant wave height

*Run 02 was conducted under irregular wave conditions and is not discussed in present paper.

3. RESULTS

3.1 Ripples development

The typical 2D wave ripples were developed during each runs. The ripples evolution of Run 06 with the highest clay fraction is an example. At $t=30$ min, most of the bed still remained flat, but a nucleus of wave ripples had formed at the edge below the URS transverse. The

nucleus expanded towards centre of scanning section by growth of existing ripples and by addition of new ripples, until the ripples occupied most of the bed after 2 hours of experiment start (Fig. 1).

3.2 Equilibrium state

Equilibrium time of ripple length increased exponentially with increasing clay fraction from 66 min of Run 03 to 346 min of Run 04 (fig. 2). Similarly, the equilibrium time of ripple height experienced a sharp increase from 31 min of Run 03 to 120 min of Run 06 (Fig. 2). But the increase rate was relatively slower than that of equilibrium length, which indicates ripple length needs more time to get equilibrium. The equilibrium wave height and length appeared to be independent of initial bed clay fraction for the applied experimental conditions as shown in Figure 2. Equilibrium length remained level from Run 01 to Run 04 and slightly increased to 150 mm of Run 06. Equilibrium height basically kept around 20 mm for all the runs.

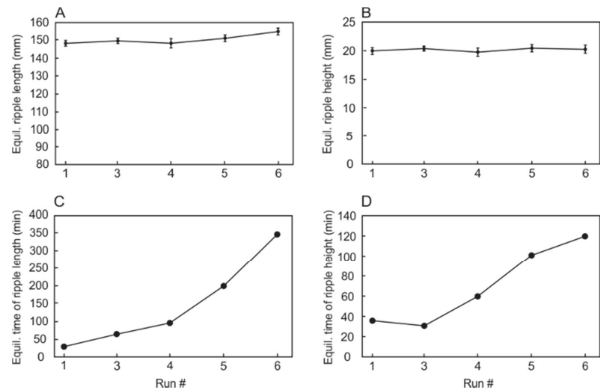


Fig. 2. Equilibrium time and equilibrium ripple length and height against initial bed clay fraction.

4. DISSCUSION

The results of the present experiments above suggest that the cohesive clay reduce wave ripples development rate. The scanning section were covered by 2D wave ripples at beginning of Run 01. In Run 03, all of 7 probes of URS scanned wave ripples at $t=15$ min. The expanding rate of wave ripples decreased dramatically in subsequent experiments, with first time of whole bed width covered by ripples reaching to 70 min of Run 04,

and to 120 min of Run 05 and 06. Besides that, the equilibrium time for both ripple length and height

increased exponentially with clay increasing from Run 01 to 06 (Fig. 2). Therefore, the wave ripple growth progressively declined with clay fraction increasing of each run. Mitchener and Torfs (1996) found that the erosion rate under wave condition of pure sand bed was an order of magnitude higher than the 20% and 40% sand bed. Panagiotopoulos et al. (1997) highlighted that bed erosion rate decreases when the clay fraction is higher than 11% under oscillatory flow condition. Therefore, the increase clay fraction of experiments plays a significant role on decreasing bed erosion rate, as a result wave ripple growth rate decreased dramatically from Run 01 to Run 06. Particularly, this paper highlights that the bed erosion rate decreases with a relatively small increase in bed fraction (4.2% to 7.4%), which further narrows down clay content with the influence on the bed erosion rate under wave conditions based on previous studies of Mitchener and Torfs (1996), and Panagiotopoulos et al. (1997).

Visual observation of clean flow water transforming to turbid fluid during experiments indicates that clay particles were suspended from the pores in between sand grains. Grain size analysis reveals that there are pure sand layer at the top of sediment cores collected from ripples crests. This may be explained by the high winnowing efficiency that the waves highly pump amount of clay particles from crests. The waves winnowed clay from the ripple troughs as well, but with a lower winnowing efficiency compare with that of crests because lack of 100% sand layer at top cores. The reason for a relatively lower winnowing efficiency from ripples troughs is possibly higher protection from near-bed oscillatory flow at ripple troughs. The experiments of Bass et al. (2013) also showed current ripples crest comprising clean sand. But the wave winnowing efficiency was presumably higher than that of current, because the pure sand crest only dominated in the highest clay content (18%) experiments of study of Bass et al. (2013).

5. CONCLUSIONS

1. Relatively small increase of clay fraction from 4.2% to 7.4% in present experiments stabilised the

flume bed and dramatically slowed down the bed erosion rate.

2. Both equilibrium time of wave ripples length and height exponentially increased with clay content increase.

3. Equilibrium dimensions of wave ripples were independent with clay fraction.

4. Highly efficient winnowing of clay particles from bed presumably contributed to constancy of equilibrium wave ripple length and height.

6. ACKNOWLEDGMENT

This COHWAVE project has been supported by European Community's Seventh Framework Programme through the grant to the budget of the Integrating Activity HYDRALAB IV within the Transnational Access Activities, Contract no. 261520.

7. REFERENCES

- Baas, J.H., 1999. An empirical model for the development and equilibrium morphology of current ripples in fine sand. *Sedimentology*, 46(1), pp.123–138.
- Baas, J.H., Best, J.L. & Peakall, J., 2011. Depositional processes, bedform development and hybrid bed formation in rapidly decelerated cohesive (mud-sand) sediment flows. *Sedimentology*, 58(7), pp.1953–1987.
- Baas, J.H., Davies, A.G. & Malarkey, J., 2013. Bedform development in mixed sand–mud: The contrasting role of cohesive forces in flow and bed. *Geomorphology*, 182, pp.19–32.
- Nelson, T.R., Voulgaris, G. & Peter, T., 2013. Sticky stuff: Redefining bedform prediction in modern and ancient environments. *Journal of Geophysical Research*, 118, pp.3202–3220.
- Nielsen, P., 1981. Dynamics and geometry of wave-generated ripples. *Journal of Fluid Mechanics*, 86, pp.6467–6472.
- Panagiotopoulos, I., Voulgaris, G. & Colh, M.B., 1997. The influence of clay on the threshold of movement of fine sandy beds. , 32, pp.19–43
- Van der Mark, C.F., Blom, A., & Hulscher, S.J.M.H., 2008. Quantification of variability in bedform geometry.pdf. *Journal of Geophysical Research*, 113.
- Van Rijn, L. C., 2007. Unified view of sediment transport by currents and waves. I: Initiation of motion, bed roughness, and bed-load transport.

Journal of Hydraulic Engineering, 133(June), pp.649–667.

Van Rijn, L.C. et al., 1993. Transport of fine sands by currents and waves. Journal of Waterway, Port, Coastal, and Ocean Engineering, 119(2), pp.123–143.

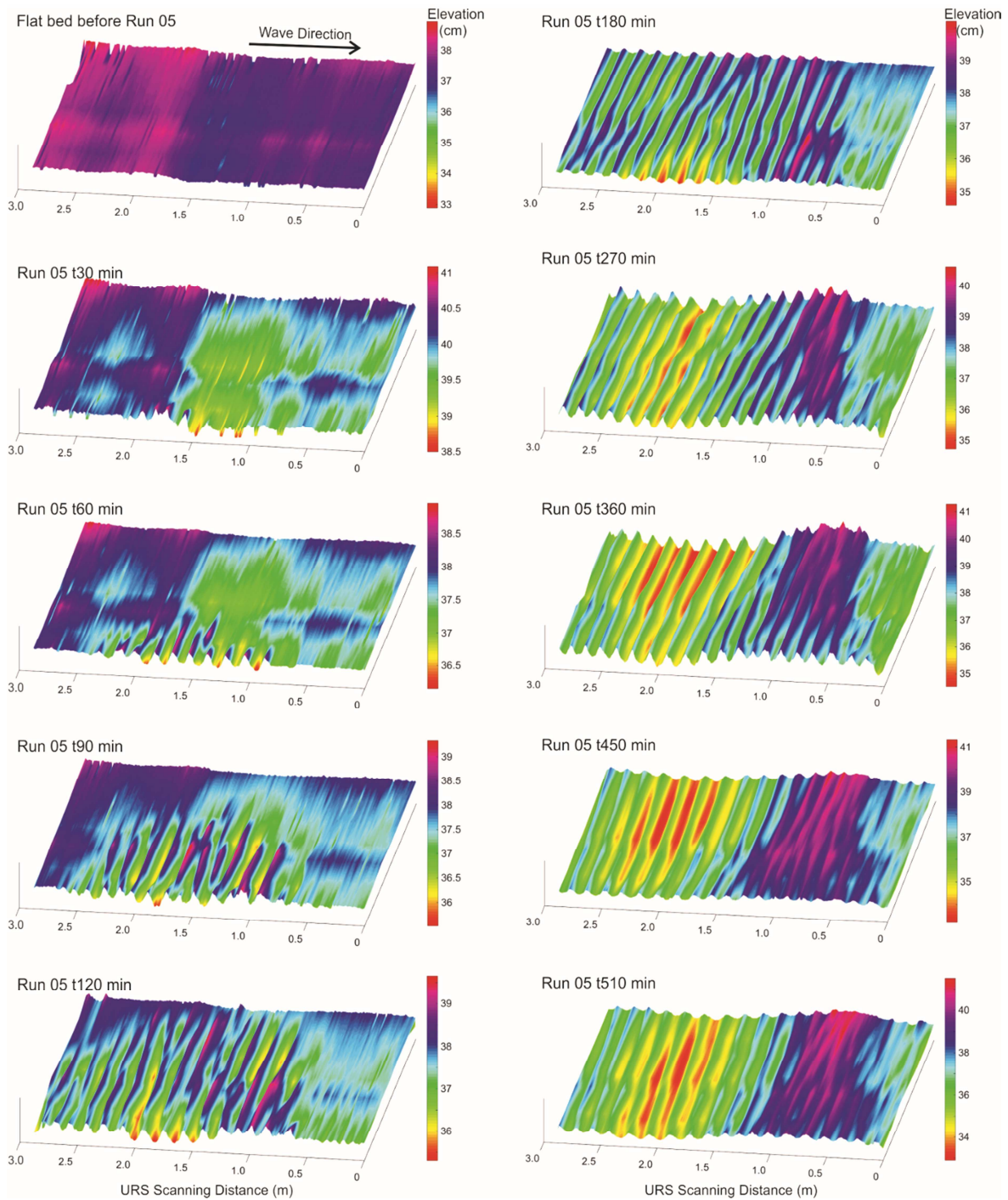


Fig. 1. 3D image of wave ripples evolution of Run 05 with initial clay fraction of 7.2%.

Bedform development and morphodynamics in mixed cohesive sediment substrates: the importance of winnowing and flocculation

L. Ye *University of Hull, Hull, UK. – yeleiping37@gmail.com*

D.R. Parsons *University of Hull, Hull, UK. – D.Parsons@hull.ac.uk*

A.J. Manning *HR Wallingford, Wallingford, UK. – andymanning@yahoo.com*

COHBED Project Team (J. Baas, J. Malarkey & A. Davies (Bangor U.); J. Peakall (U. Leeds); S. Simmons (U. Hull); P. Thorne, I.D. Lichtman (NOC Liverpool); S. Bass, R.J. Schindler (U. Plymouth); D. Paterson, J. Hope, R. Aspden (U. St Andrews).

ABSTRACT: There remains a lack of process-based knowledge of sediment dynamics within flows over bedforms generated in complex mixtures of cohesionless sand and biologically-active cohesive muds. The work presented here forms a part of the UK NERC “COHesive BEDforms (COHBED)” project which aims to fill this gap in knowledge. Herein results from a set of large-scale laboratory experiments, conducted using mixtures of non-cohesive sands, cohesive muds and Xanthan gum (as a proxy for the biological stickiness of Extracellular Polymeric Substances (EPS)) are presented. The results indicate the significance of biological-active cohesive sediments in controlling winnowing rates and flocculation dynamics, which contributes significantly to rates of bedform evolution.

1. INTRODUCTION

Understanding and quantifying sediment dynamics within flows over bedforms generated in complex mixtures of cohesionless sand and biologically-active cohesive muds, is a key to parameterizing physical processes in natural estuarine systems. Such processes ultimately control morphodynamics at local and regional scales (French, 2010). Moreover, understanding sediment movement is also significant for monitoring water quality, fate of pollutants, and even for the success of coastal dredging operations (Rao et al., 2011). Fine sediments, which commonly exist in natural estuarine flow systems and are composed of fine silts and clays, with biological agents that have cohesive properties that modulate the complex interactions between flow, sediment transport and morphological evolution (Baas and Best, 2008). In morphodynamic investigations, the properties and influence of the substrate has largely been ignored but can significantly impinge on the behaviour and dynamics of sediment transport, which ultimately influences and interacts with the form and the size of bedforms.

2. METHODS

2.1. Flume and substrates

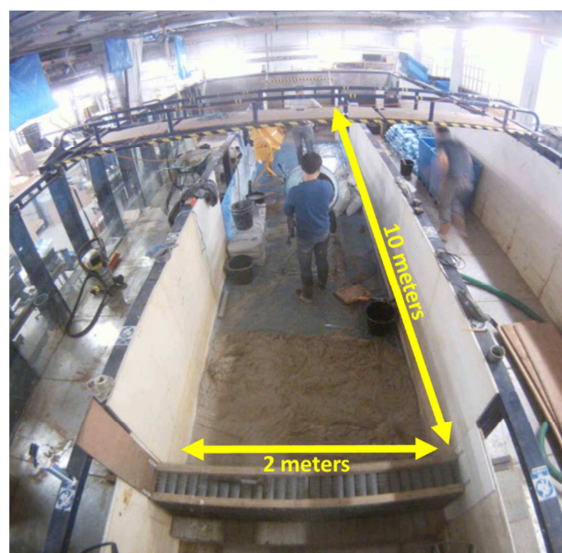


Fig.1. Flume lab set-up

Experiments were undertaken at the University of Hull's Total Environment Simulator flume/wave

tank facility (Fig.1). The tank was a recirculating flume channel, 10 m long and 2 m wide, and filled with homogeneously mixed substrata with varying ratios of sand, clay and EPS (Xanthan gum was used as a proxy for EPS found in natural sediment (e.g. Tolhurst et al.,2002)). Flow depth was set at $d = 0.38$ m. Depth-mean flow velocity (U) over the initial flat bed set to a zero slope was 0.80 m/s, yielding a Froude number $Fr = U/(gd)^{0.5} = 0.40$ and a Reynolds number $Re = Ud/\nu = 212,000$, where g is the acceleration due to gravity and ν is the kinematic viscosity. The salinity was 15–17 PSU, approximating estuarine conditions, and temperature was kept as constant as possible, varying between 16 and 19 °C. A total of 14 experimental runs were performed that included a series with mixed substrata of (1) fine sand with a median diameter, D_{50} , of 239 μm and kaolin clay with a D_{50} of 3.4 μm in run A1 to run A6, and (2) varying ratios of fine sand, clay and EPS in run B series (B1-3, three runs with low EPS % and various clay %) and run C series (C1-3, high EPS % and various clay). Three series of experimental runs were conducted. Run A1 to A6 (section 1) and run B1 to 3, and C1 to C3 (section 2), were prepared by incrementally increasing initial substratum mud (kaolin clay) content respectively (1.9 % < m < 14.1 % in section 1 runs and 2.8 % < m < 17.7 % in section 2 runs, both in dry weight). The detailed percentages of clay and EPS in initial bed of each run is shown in fig.2).

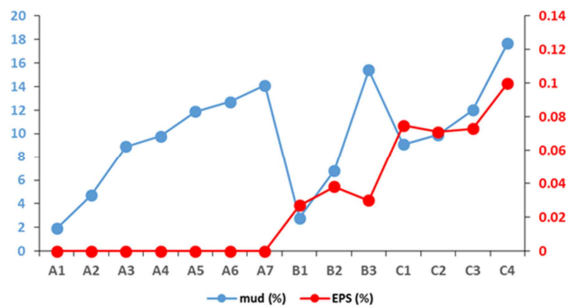


Fig.2. The percentages of clay and EPS in initial substrates of each experimental runs.

2.1. Instrument settings

Various instruments were set to collect bedform, suspension and flow properties. Bed topography of each run was measured with ultrasonic probes driven by and automatic traverse across a swathe of the channel bed during and at the end of each

experiment. Suspended sediment dynamics were measured through: (1) ABS (Acoustic backscatter profiling sensors) that obtains profiles at 1, 2 and 4 MHz (throughout all runs); (2) vertically spaced OBS (Optical backscatter point sensor); (3) LISST-100X (bulk samples taken every 30 mins of each run); (4) physical water samples used for both gravimetrically derived suspended sediment concentrations and grain size distributions (every 30 mins of each run). Water samples also were analyzed using LabSFLOC (e.g. Manning et al., 2002) every half an hour for selected runs, facilitating the measurement of the size, settling velocities and thus densities of suspended particulates and flocs. Consequently, the effects of varying suspended sands, clays and EPS on flocculation were monitored throughout each run. Flow velocity was monitored by four vertically-stacked 10 MHz Acoustic Doppler Velocimeters (ADV), located close to the flume centreline, at an acquisition rate of 25 Hz throughout each experiment run.

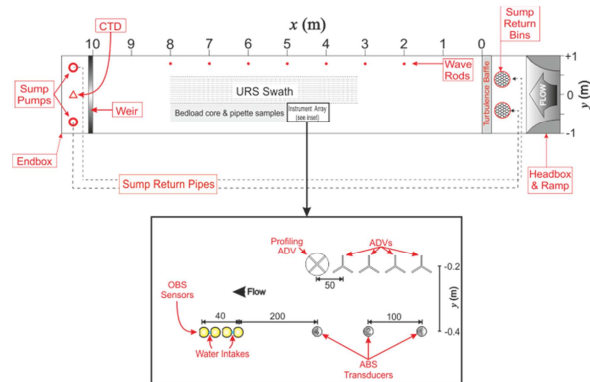


Fig.3. Instruments settings in the experimental flume channel

3. RESULTS

3.1. Bedform morphology

The experimental results reveals that higher mud fraction in initial bed leads to slower bedform growth and larger bedform size. The existence of EPS in the initial bed results in a significantly more stable bed and a dramatic reduction in bedform size. At very high concentrations the bed remains flat with no bedforms generated.

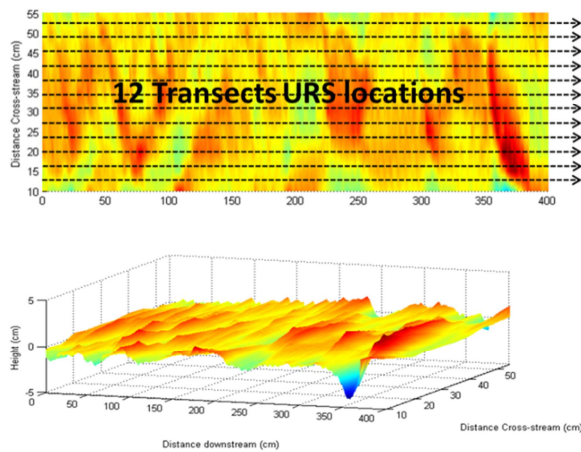


Fig.4. 3D bedform rendering example

3.2. Flow turbulence

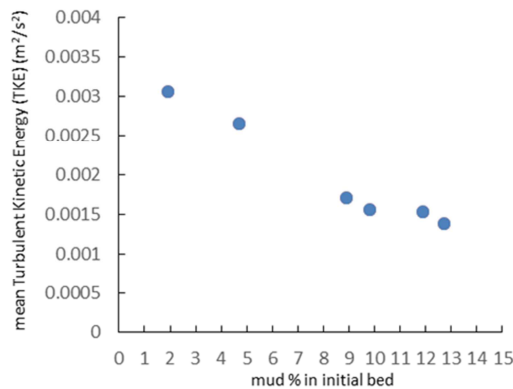


Fig.5. The relationship between Turbulence Kinetic Energy (TKE).

The results of near-bed turbulence kinetic energy (TKE) (Figure 5), which were obtained from the ADV data shows strong correlation with mud.

3.3. Flocculation and winnowing efficiency

The LabSFLOC camera results indicate both mud and EPS fractions in initial bed can form flocculation in the flow and the existence of EPS component in initial bed significantly increases floc size and slows down the mean settling velocity of the grains as a result (Fig.6. a & b).

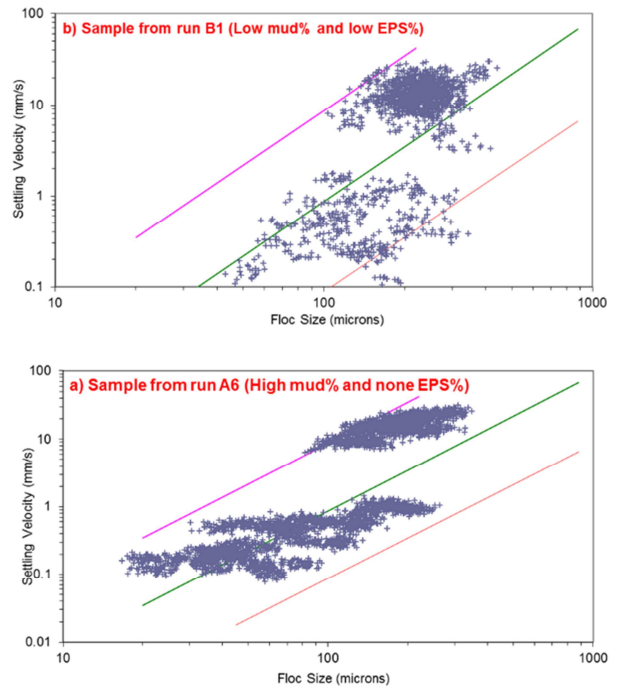


Fig.6. Typical floc samples analysis of typical sand-mud run A6 and sand-mud-EPS run B1, using LabSFLOC floc camera (A.J. Manning, 2006)

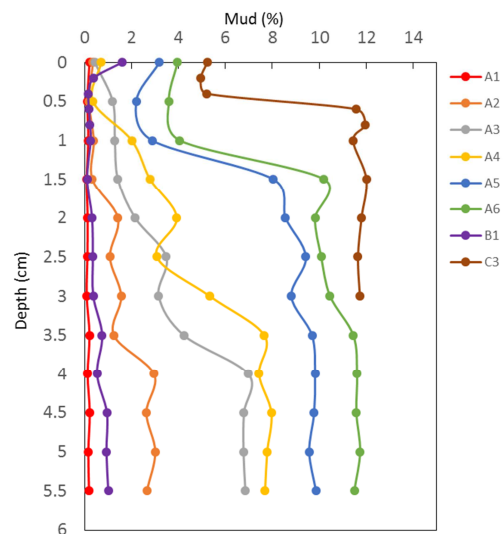


Fig.7. Mud percentages in depth of selected bedform crest of some experimental runs.

Winnowing occurs when fine sediments are systematically removed from the bed over time. Particle size analysis taken through substrates using small push cores taken at the end of the experiments indicate that existence

of mud and EPS in bed surface both decreases the rate at which fine sediments winnow from bed, this is especially so for high EPS fractions that stabilize the bed significantly (Fig.7).

4. CONCLUSIONS

Both clay and EPS fractions in the initial bed conditions have a significant influence on the sediment transport over mobile beds. Higher clay and EPS fractions in substrates decrease bedform size, increase bedform evolution time and generally impedes the development of bedforms.

Winnowing and flocculation occur commonly in any flow condition with cohesive substrates (mud or EPS). Mud and EPS fractions in the initial bed decreases the winnowing efficiency, enhances the floc size and thus effect the grain settling velocity of the suspended material.

EPS has a higher efficiency in stabilizing the bed and enhancing the flocculation than clay alone, which highlights the necessity of including biological factors in sedimentological research in estuaries and coastal seas, particularly when considering morphodynamic rates of adjustment.

5. ACKNOWLEDGMENT

This work was funded by the UK Natural Environment Research Council (NERC) under the COHBED project (NE/1027223/1). Brendan Murphy, Karen Scott, Mark Anderson, Arjan Reesink, Claire Keevil, Chris Unworth, Robert Thomas, Xuxu Wu, and Stuart McLelland are thanked for their help in running the laboratory experiments.

6. REFERENCES

Baas, J.H., Davies, A.G. and Malarkey, A.G., 2013. Bedform development in mixed sand-mud:

the contrasting role of cohesive forces in flow and bed. *Geomorphology*, 182, 19–32.

Liu, Y., and Fang, H.H.P., 2003. Influences of extracellular polymeric substance (EPS) on flocculation, settling, and dewatering of active sludge. *Environmental Science and Technology*, 33:237-273.

Manning, A.J. (2008). The development of algorithms to parameterise the mass settling flux of flocculated estuarine sediments. In: T. Kudusa, H. Yamanishi, J. Spearman and J.Z. Gailani, (eds.), *Sediment and Ecohydraulics - Proc. in Marine Science 9*, Amsterdam: Elsevier, pp. 193-210, ISBN: 978-0-444-53184-1.

Manning, A.J., Langston, W.J. and Jonas, P.J.C. (2009). A Review of Sediment Dynamics in the Severn Estuary: Influence of Flocculation. *Marine Pollution Bulletin*, 61, 37–51, doi:10.1016/j.marpolbul.2009.12.012.

Paterson, D.M., 1997. Biological mediation of sediment erodibility: ecology and physical dynamics. In *Cohesive Sediments*, N. Burt, R. Parker and J. Watta eds., John Wiley, Chichester, UK, 215-229.

Tolhurst, T.J.; Gust, G. and Paterson, D.M. , 2002. The influence of an extracellular polymeric substance (EPS) on cohesive sediment stability, in: Winterwerp, J.C. et al. (ed.), 2002. *Fine sediment dynamics in the marine environment*. *Proceedings in Marine Science*, 5: pp. 409-425 ICFS10

van den Berg and van Gelder, 1993. A new bedform stability diagram, with emphasis on the transition of ripples to plane bed in flows over fine sand and silt. *IAS Spec. Publ.*, 17, 11-21.

van Rijn (1993) *Principles of Sediment Transport in Rivers, Estuaries and Coastal Seas*. Aqua Publ., Amsterdam.

Schindler, R.J., D.R. Parsons, L. Ye, J.A. Hope, J.H. Baas, J. Peakall, A.J. Manning, R.J. Aspden, J. Malarkey, S. Simmons, D.M. Patterson, I.D. Lichtman, A.G. Davies, P.D. Thorne and S.J. Bass, 2015. Sticky stuff: redefining bedform prediction in modern and ancient environments. *Geology*, 43(5), 399-402.

Malarkey, J., J.H. Baas, J.A. Hope, R.J. Aspden, D.R. Parsons, J. Peakall, D.M. Paterson, R.J. Schindler, L. Ye, I.D. Lichtman, S.J. Bass, A.G. Davies, A.J. Manning and P.D. Thorne, 2015. The pervasive role of biological cohesion in bedform development. *Nature Comms.*, 6:6257.

Service hydrographique et
océanographique de la marine
Imprimé par nos soins
CS 92803
29228 BREST CEDEX 2
Mars 2016

Dépôt légal premier trimestre 2016
Numéro d'éditeur : 2921

